

# NOTE TO USERS

This reproduction is the best copy available.

**UMI**<sup>®</sup>



**STRUCTURE-FUNCTION STUDIES OF THE SEROTONIN TYPE-3  
RECEPTOR LIGAND-BINDING DOMAIN**

**A**

**THESIS**

**Presented to the Faculty  
of the University of Alaska Fairbanks**

**in Partial Fulfillment of the Requirements**

**for the Degree of**

**DOCTOR OF PHILOSOPHY**

**By**

**Prasad Ramesh Joshi, M.D.**

**Fairbanks, Alaska**

**May 2005**

UMI Number: 3167009

### INFORMATION TO USERS

The quality of this reproduction is dependent upon the quality of the copy submitted. Broken or indistinct print, colored or poor quality illustrations and photographs, print bleed-through, substandard margins, and improper alignment can adversely affect reproduction.

In the unlikely event that the author did not send a complete manuscript and there are missing pages, these will be noted. Also, if unauthorized copyright material had to be removed, a note will indicate the deletion.

**UMI**<sup>®</sup>

---

UMI Microform 3167009

Copyright 2005 by ProQuest Information and Learning Company.

All rights reserved. This microform edition is protected against unauthorized copying under Title 17, United States Code.

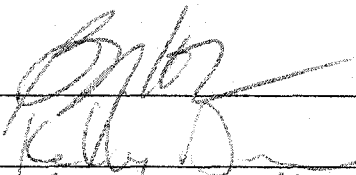

ProQuest Information and Learning Company  
300 North Zeeb Road  
P.O. Box 1346  
Ann Arbor, MI 48106-1346

**STRUCTURE-FUNCTION STUDIES OF THE SEROTONIN TYPE-3  
RECEPTOR LIGAND-BINDING DOMAIN**

By

**Prasad Ramesh Joshi**

RECOMMENDED:

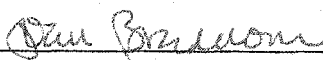
  
\_\_\_\_\_  
Kelly D. Thomas  
\_\_\_\_\_  
Thomas Kelly  
\_\_\_\_\_  
  
\_\_\_\_\_

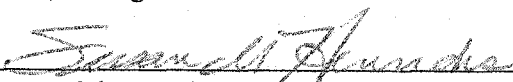
Advisory Committee Chair

  
\_\_\_\_\_

Department Head

APPROVED:

  
\_\_\_\_\_  
Dean, College of Natural Science & Mathematics

  
\_\_\_\_\_  
Dean of the Graduate School

  
\_\_\_\_\_  
Date

## ABSTRACT

The serotonin type-3 receptor (5-HT<sub>3</sub>R) is widely distributed in peripheral and central nervous systems. This pentameric protein is a member of the Cys-loop superfamily of ligand gated ion channels and plays a role in mediating physiological processes in nervous, cardiovascular, and digestive systems. The ligand-binding domain of this receptor is extracellularly located and is composed of multiple putative loop structures. Based on structural and sequence homology with other members of the superfamily, it has been proposed that at least six such loops (loops A to F) contribute to the ligand-binding domain. Binding of agonist initiates a conformational change which is transduced to the channel, leading to channel opening (gating). The aim of this study was to elucidate the contribution of residues in loops B and E to the mechanism of channel gating in the 5-HT<sub>3</sub>R. To this end, the three critical tyrosine residues in the loop E region were characterized employing site-directed mutagenesis, electrophysiological studies as well as radio-ligand binding assays involving two structural classes of 5-HT<sub>3</sub>R agonists. In addition, structure/function analysis of the loop B region was carried out alanine-scanning mutagenesis. Experimental data were correlated with molecular modeling studies. These studies show that the hydroxytryptamine and phenylbiguanide class of compounds utilize different mechanisms of ligand binding and gating in the 5-HT<sub>3</sub>R. Studies involving the loop B reveal that this region plays a critical role in ligand binding and channel gating. Data obtained from comparison of ground state and agonist-bound models of the 5-HT<sub>3</sub>R was correlated with biochemical data. Taken together, these data suggest that agonist interaction with loop B region probably initiates a conformational

wave that results in intra- and inter- subunit hydrogen bonding interactions. Our data suggest that these interactions play a critical role in agonist-induced channel opening.

## Table of contents

Signature Page.....	i
Title Page.....	ii
Abstract.....	iii
Table of Contents.....	v
List of Figures.....	xvi
List of Tables.....	xxi
Acknowledgements.....	xxii
 <b>CHAPTER 1: INTRODUCTION.....</b>	 <b>1</b>
<b>1.1 Historical perspective .....</b>	<b>1</b>
<b>1.2 A brief classification of ion channels according to the mechanism of gating .....</b>	<b>2</b>
<b>1.3 Physiological role of ligand-gated ion channels: Fast synaptic transmission at the neuro-muscular junction.....</b>	<b>3</b>
<b>1.4 5-HT<sub>3</sub> receptor is a member of ‘Cys-loop’ superfamily of ligand-gated ion channel receptors. ....</b>	<b>5</b>
<b>1.5 Primary, secondary, tertiary and quaternary structure of 5-HT<sub>3</sub>R .....</b>	<b>8</b>
<b>1.6 Assembly, trafficking and cell-surface localization of the 5-HT<sub>3</sub>R .....</b>	<b>8</b>



	Page
<b>1.7 Central and peripheral distribution of the 5-HT<sub>3</sub>R.....</b>	<b>10</b>
<b>1.8 Gating and desensitization kinetics of LGIC coupled receptors including 5-HT<sub>3A</sub>R.....</b>	<b>12</b>
1.8.1 Stochastic behavior of the 5-HT <sub>3</sub> R and its relationship to the macroscopic events .....	13
1.8.2 Kinetic parameters of inward currents produced by 5-HT <sub>3A</sub> R .....	16
1.8.3 A possible mechanism of gating in the 5-HT <sub>3</sub> R: .....	19
<b>1.9 Discovery of AChBP and it's impact on studies pertaining to ligand-binding domain of LGIC receptors .....</b>	<b>20</b>
<b>1.10 Characterization of ligand-binding site of the 5-HT<sub>3A</sub> receptor.....</b>	<b>22</b>
1.10.1 Role of loop A residues.....	23
1.10.2 Role of loop B residues.....	24
1.10.3 Role of loop D residues.....	25
1.10.4 Role of loop E residues .....	26
<b>1.11 Medicinal chemistry of 5-HT<sub>3</sub>R ligands.....</b>	<b>26</b>
<b>1.11.1 5-HT<sub>3A</sub>R Agonists.....</b>	<b>27</b>
<b>1.11.2 5-HT<sub>3A</sub>R antagonists .....</b>	<b>28</b>
<b>1.12 Modulators of 5-HT<sub>3</sub>R function.....</b>	<b>29</b>

	<b>Page</b>
1.12.1 Interaction of binding site with ions .....	29
1.12.2 Interaction of 5-HT <sub>3</sub> R with atypical ligands .....	29
1.12.2.1 Steroids .....	29
1.12.2.2 Neuroleptic drugs.....	30
1.12.2.3 Forskolin .....	30
1.12.2.4 Toxin.....	31
1.12.2.5 Alcohol and other drugs of abuse .....	31
1.12.2.6 Interaction with anesthetics.....	33
<b>1.13 Clinical (current and potential) uses of 5-HT<sub>3</sub>R antagonists .....</b>	<b>33</b>
<b>References.....</b>	<b>43</b>
<b>CHAPTER 2: HYPOTHESES, RESEARCH DESIGN AND DATA ANALYSIS... 55</b>	
<b>2.1 Introduction.....</b>	<b>55</b>
<b>2.2 Gaps in the knowledge of murine 5-HT<sub>3A</sub>R structure-function correlations.....</b>	<b>55</b>
2.2.1 5-HT <sub>3A</sub> R ligand-binding domain .....	55
2.2.2 5-HT <sub>3A</sub> R agonist specificities .....	56
2.2.3 5-HT <sub>3A</sub> R mechanism of activation and desensitization.....	57
2.3 Scope for improvement in methodologies pertaining to <i>Xenopus</i> oocyte electrophysiology .....	57

	Page
<b>2.4 Protein homology in structure-function studies.....</b>	<b>58</b>
<b>2.5 General hypothesis.....</b>	<b>59</b>
<b>2.6 Specific hypotheses.....</b>	<b>60</b>
2.6.1 Antagonist action of lerisetron is mediated mainly by the interaction of its terminal amine with the binding site. This interaction is probably a cation-pi interaction. ....	60
2.6.2 Different classes of 5-HT <sub>3A</sub> R ligands mediate their action through distinctly different interactions with loop E amino acid residues.....	60
2.6.3 Different classes of 5-HT <sub>3A</sub> R agonists mediate their action through distinctly different modes of receptor gating.....	61
2.6.4 Amino acids T179 to I190 of 5-HT <sub>3A</sub> R constitute a region of the protein that corresponds to the purported loop B region of the nicotinic acetylcholine receptor. This region plays a critical role in mediating agonist action. ....	61
<b>2.7 Research design.....</b>	<b>61</b>
<b>2.8 Mutagenesis .....</b>	<b>64</b>
2.8.1 Replacement of a structurally/functionally important amino acid causes major changes to protein structure/function, while replacement of an unimportant amino acid causes minor/ no changes to protein structure/function.....	64

	<b>Page</b>
2.8.2 Alanine scanning mutagenesis can be used to identify structurally/ functionally important amino acids of a protein. ....	66
<b>2.9 Radio-ligand binding assays using mammalian cells.....</b>	<b>66</b>
<b>2.10 Electrophysiology .....</b>	<b>67</b>
2.10.1 Electrophysiology using mammalian cells .....	68
2.10.2 Electrophysiology using <i>Xenopus laevis</i> oocytes .....	68
2.11 Molecular modeling.....	69
<b>References.....</b>	<b>70</b>
<b>CHAPTER 3: STRUCTURE-ACTIVITY RELATIONSHIP STUDY OF LERISETRON, A COMPETITIVE ANTAGONIST AT THE 5-HT<sub>3A</sub>R. ....</b>	<b>71</b>
<b>3.1 Summary.....</b>	<b>71</b>
<b>3.2 Introduction.....</b>	<b>72</b>
<b>3.3 Materials and Methods.....</b>	<b>75</b>
3.3.1 Materials .....	75
3.3.2 Site-directed mutagenesis .....	75
3.3.3 <i>Xenopus laevis</i> oocyte two-electrode voltage-clamp assay .....	75
3.3.4 <i>Xenopus laevis</i> oocyte two-electrode voltage-clamp assay .....	76

	<b>Page</b>
<b>Results .....</b>	<b>78</b>
<b>Discussion.....</b>	<b>80</b>
<b>References.....</b>	<b>84</b>
<b>Appendix.....</b>	<b>87</b>
<b>CHAPTER 4: MUTATIONS AT LOOP E TYROSINE RESIDUES</b>	
<b>DIFFERENTIALLY MODULATE GATING OF THE <i>MURINE</i> 5-HT<sub>3A</sub></b>	
<b>RECEPTOR .....</b>	<b>88</b>
<b>4.1 Summary.....</b>	<b>88</b>
<b>4.2 Introduction.....</b>	<b>90</b>
<b>4.3 Materials and Methods.....</b>	<b>93</b>
4.3.1 Materials: .....	93
4.3.2 Receptor modeling:.....	93
4.3.3 Site-directed Mutagenesis:.....	95
4.3.4 Cell culture and transient transfection: .....	95
4.3.5 <i>Xenopus laevis</i> oocyte two-electrode voltage-clamp assay .....	97
4.3.6 Whole-cell Patch-clamp assay:.....	98
4.3.7 Data analysis: .....	99

	<b>Page</b>
<b>4.4 Results</b> .....	<b>101</b>
4.4.1 Results from molecular modeling studies:.....	101
4.4.2 Results from biochemical assays: .....	102
<b>4.5 Discussion</b> .....	<b>111</b>
<b>References</b> .....	<b>141</b>
<b>Appendix</b> .....	<b>146</b>
<b>CHAPTER 5: THE ROLE OF LOOP B AMINO ACID RESIDUES IN THE STRUCTURE AND FUNCTION OF THE 5-HT<sub>3A</sub>R</b> .....	<b>147</b>
<b>5.1 Summary</b> .....	<b>147</b>
<b>5.2 Introduction</b> .....	<b>148</b>
<b>5.3 Materials and Methods</b> .....	<b>150</b>
5.3.1 Materials: .....	150
5.3.2 Methods: .....	150
5.3.2.1 Site-directed Mutagenesis.....	150
5.3.2.2 Cell culture and transient transfection .....	150
5.3.2.3 <i>Xenopus laevis</i> oocyte two-electrode voltage-clamp assay .....	151
5.3.2.4 Radio-ligand Binding Assays .....	152

	<b>Page</b>
5.3.3 Data analysis .....	153
5.3.4 Receptor modeling .....	153
<b>5.4 Results .....</b>	<b>156</b>
5.4.1 Electrophysiological characterization of loop B mutant receptors .....	156
5.4.1.1 Electrophysiological profile of loop B mutant receptors: 5-HT .....	157
5.4.1.2 Electrophysiological profile of loop B mutant receptors: <i>m</i> CPBG .....	158
5.4.1.3 Differential effects of the loop B mutations on action of 5-HT and <i>m</i> CPBG .....	159
5.4.2 Granisetron binding to loop B mutant receptors .....	161
5.4.3 Maximal binding ( $B_{Max}$ ) values for the loop B mutant receptors .....	161
5.4.4 Displacement of granisetron binding to loop B mutant receptors by 5-HT and <i>m</i> CPBG .....	162
5.4.5 Results of the molecular modeling studies .....	163
5.4.5.1 Results form the ligand-docking studies using 5-HT <sub>3A</sub> R homology model. .....	163
5.4.5.2 Results form structural predictions obtained from 5-HT <sub>3A</sub> R homology models .....	164
<b>5.5 Discussion .....</b>	<b>166</b>
5.5.1 Loop B region plays a role in proper receptor expression .....	166
5.5.2 Ligand-receptor interactions .....	167

	<b>Page</b>
5.5.3 Ligand-specific mechanisms mediated through loop B region.....	168
5.5.4 Desensitization.....	168
5.5.5 Gating mechanism of the 5-HT <sub>3A</sub> R.....	169
<b>References.....</b>	<b>189</b>
<b>Appendix.....</b>	<b>191</b>
<b>CHAPTER 6: CONCLUSIONS.....</b>	<b>192</b>
<b>6.1 An overview.....</b>	<b>192</b>
<b>6.2 Methodological advancement.....</b>	<b>193</b>
<b>6.3 The ligand binding domain.....</b>	<b>194</b>
<b>6.4 5-HT<sub>3A</sub>R ligand specificities.....</b>	<b>196</b>
<b>6.5 Mechanism of activation and desensitization.....</b>	<b>197</b>
<b>APPENDIX 1: MECHANISTIC MODELS OF THE 5-HT<sub>3</sub> RECEPTOR FUNCTION.....</b>	<b>203</b>
<b>A1.1 Concerted model of receptor action.....</b>	<b>203</b>
<b>A1.2 A concerted model of 5-HT<sub>3</sub>R function.....</b>	<b>206</b>
<b>A1.2.1 Alternate model of 5-HT<sub>3</sub>R function-1.....</b>	<b>207</b>



	<b>Page</b>
A1.2.3 Alternate model of 5-HT <sub>3</sub> R function-2 .....	207
<b>A1.3 Sequential model of receptor action .....</b>	<b>209</b>
<b>References .....</b>	<b>211</b>
 <b>APPENDIX 2: A VERTICAL FLOW CHAMBER FOR XENOPUS OOCYTE ELECTROPHYSIOLOGY AND AUTOMATED DRUG SCREENING .....</b>	
<b>A2.1 Abstract.....</b>	<b>214</b>
<b>A2.2 Introduction.....</b>	<b>216</b>
<b>A2.3 Materials and Methods.....</b>	<b>218</b>
A2.3.1 Materials: .....	218
A2.3.2 Methods.....	218
A2.3.2.1 Chamber construction .....	218
A2.3.2.2 Harvesting and maintenance of <i>Xenopus laevis</i> oocytes .....	222
A2.3.2.3 Electrophysiological recordings.....	222
<b>A2.4 Results .....</b>	<b>227</b>
<b>A2.5 Discussion.....</b>	<b>231</b>
<b>References.....</b>	<b>246</b>

**Appendix..... 247**

## List of Figures

<b>Figure 1.1: Structural features of the 5-HT<sub>3A</sub>R .....</b>	<b>38</b>
1.1 A: A single subunit of 5-HT <sub>3A</sub> R .....	38
1.1 B: Pentameric assembly of the 5-HT <sub>3R</sub> pentamer .....	39
<b>Figure 1.2: Structure of the acetylcholine binding protein (AChBP) .....</b>	<b>40</b>
<b>Figure 1.3: 5-HT<sub>3A</sub> R homology model based on acetylcholine binding protein (AChBP).....</b>	<b>41</b>
<b>Figure 3.1 Parent compound, lerisetron .....</b>	<b>82</b>
<b>Figure 4.1 Results from molecular modeling and ligand-docking studies.....</b>	<b>120</b>
4.1.A Movements of the 5-HT <sub>3A</sub> R regions surrounding the ligand-binding domain associated with activation: .....	120
4.1.B Docking of 5-HT to ligand-bound 5-HT <sub>3A</sub> R receptor model:.....	121
4.1.C Docking of <i>m</i> CPBG to ligand-bound 5-HT <sub>3A</sub> R receptor model: .....	121
<b>Figure 4.2 Electrophysiological characterization of wt 5-HT<sub>3AS</sub> receptors expressed in <i>Xenopus laevis</i> oocytes.....</b>	<b>123</b>
4.2.A Characteristics of inward currents elicited by application of agonists at supra- maximal concentration.....	123
4.2.B Concentration-response curves for four agonists .....	123
4.2.C A comparison of efficacy values for agonists .....	123
<b>Figure 4.3 Electrophysiological characterization of Y141A 5-HT<sub>3AS</sub> receptors expressed in <i>Xenopus laevis</i> oocytes.....</b>	<b>125</b>

	Page
4.3.A Characteristics of inward currents elicited by application of agonists at supra-maximal concentration.....	125
4.3.B Concentration-response curves for four agonists.....	125
4.3.C A comparison of efficacy values for agonists 5-HT, <i>m</i> CPBG and PBG.....	125
4.3.D Inhibition of 5-HT induced responses by co-application of d-TC.....	125
<b>Figure 4.4 Electrophysiological characterization of Y143F 5-HT<sub>3AS</sub> receptors expressed in <i>Xenopus laevis</i> oocytes.....</b>	<b>127</b>
<b>4.4.A Characteristics of inward currents elicited by application of agonists at supra-maximal concentration.....</b>	<b>127</b>
4.4.B Concentration-response curves for four agonists.....	127
4.4.C Comparison of efficacies of 5-HT, <i>m</i> CPBG, PBG and 2-Me5HT.....	127
4.5.A Currents elicited by application of increasing concentrations of 5-HT to oocytes expressing Y153A mutant receptors.....	129
4.5.B Characteristics of inward currents elicited by application of agonists at supra-maximal concentration.....	129
4.5.C Comparison of efficacies of 5-HT, <i>m</i> CPBG, PBG and 2-Me5HT.....	129
<b>Figure 4.6 Whole-cell patch-clamp recording from tSA 201 cells transfected with wt and Y15<sub>3A</sub> cDNA.....</b>	<b>130</b>
<b>Figure 4.7 Electrophysiological characterization of Y153F 5-HT<sub>3AS</sub> receptors expressed in <i>Xenopus laevis</i> oocytes.....</b>	<b>132</b>

	Page
4.7.A Characteristics of inward currents elicited by application of agonists at supra-maximal concentration.....	132
4.7.C Comparison of efficacies of 5-HT, <i>m</i> CPBG, PBG and 2-Me5HT.....	132
<b>Figure 4.8 Sequence alignment of the purported loop E region of the 5-HT<sub>3A</sub> receptor.....</b>	<b>133</b>
<b>Table 4.1 Results from ligand-docking studies.....</b>	<b>134</b>
<b>Figure 5.1 Amino acid sequence alignment of murine 5-HT<sub>3A</sub>R with other members of the superfamily, with a focus on the predicted loop B region.....</b>	<b>172</b>
<b>Figure 5.2: A comparison of EC<sub>50</sub> values for 5-HT and <i>m</i>CPBG.....</b>	<b>173</b>
<b>Figure 5.3: A comparison of Hill number values for 5-HT and <i>m</i>CPBG .....</b>	<b>174</b>
<b>Figure 5.4: Electrophysiological characterization of S182A mutation .....</b>	<b>176</b>
5.4.A Comparison of 5-HT and <i>m</i> CPBG induced responses from S182A mutant receptor .....	176
5.4.B Comparison of 5-HT induced responses from WT and S182A mutant receptor .....	176
5.4.C Comparison of <i>m</i> CPBG induced responses from WT and S182A mutant receptor .....	176
<b>Figure 5.5 [3H] granisetron binding to loop B mutant receptors.....</b>	<b>178</b>
<b>Figure 5.6 A comparison of BMax values of loop B mutant receptors.....</b>	<b>179</b>
<b>Figure 5.7 Displacement of bound radio-ligand by 5-HT<sub>3A</sub>R agonists .....</b>	<b>181</b>

	Page
5.7.A Displacement of [ <sup>3</sup> H] granisetron binding to loop B mutant receptors by 5-HT .....	181
5.7.B Displacement of [ <sup>3</sup> H] granisetron binding to loop B mutant receptors by <i>m</i> CPBG .....	181
<b>Figure 5.8 Intra-subunit and inter-subunit contacts of the loop B region formed in the agonist-bound state of the receptor.....</b>	<b>182</b>
<b>Figure 6.1: Loop B-Cys loop-loop E connection .....</b>	<b>201</b>
<b>Figure 6.2: Interactions formed during activation of the homomeric 5-HT<sub>3A</sub>R. 202</b>	
<b>Figure A1.1: Mechanistic models of 5-HT<sub>3</sub>R function .....</b>	<b>213</b>
A1.1.A A Concerted model for cooperative behavior of pentameric 5-HT <sub>3</sub> R .....	213
A1.2.B Sequential model for cooperative behavior of pentameric 5-HT <sub>3</sub> R .....	213
<b>Figure A2.1: A schematic diagram of <i>X. laevis</i> oocyte perfusion chamber.....</b>	<b>236</b>
<b>Figure A2.2: The chamber design .....</b>	<b>239</b>
A2.2.A The vertical flow chamber.....	239
A2.2.B An experiment demonstrating non-turbulent flow in the vertical flow system .....	239
A2.2.C Inward currents elicited from a single oocyte using (a) the conventional chamber and (b) vertical-flow chamber, using 30 micromolar 5-HT.....	239
<b>Figure A2.3: The schematic arrangement of elements comprising the automated oocyte perfusion system.....</b>	<b>240</b>
<b>Figure A2.4: Validation of the apparatus.....</b>	<b>242</b>

	Page
A2.4.A Currents elicited by rapid application of various concentrations of 5-HT to <i>Xenopus laevis</i> oocytes expressing human 5-HT <sub>3AB</sub> receptors.....	242
A2.4. B. Dose-response curves for 5-HT <sub>3AB</sub> R obtained from exposure to agonist 5-HT.....	242
A2.4.C. Current-voltage (I-V) relationship curve generated from oocytes expressing human 5-HT <sub>3A</sub> receptor.....	242
<b>Figure A2.5: 5-HT induced traces recorded from single oocyte expressing human 5-HT<sub>3A</sub>R, over a period of 10.5 hours. ....</b>	<b>243</b>
<b>Figure A2.6: Validation of the automated drug perfusion system .....</b>	<b>244</b>
A2.6. A Currents elicited from an oocyte expressing human 5-HT <sub>3A</sub> receptors by exposure to agonists 5-HT and <i>m</i> CPBG utilizing the automated oocyte perfusion system. ....	244
A2.6. B Dose response relationship curves obtained from automated drug perfusion experiments (human 5-HT <sub>3A</sub> R).....	245

## List of Tables

Table 3.1 IC <sub>50</sub> values obtained for the series of N-substituted lerisetron analogs	83
Table 4.1 Results from ligand-docking studies .....	134
Table 4.2 Heteroatomic distances (Y141, Y143, Y153, W183 and their H-bonding partners) in ligand-bound and ligand-free receptor models.....	136
Table 4.3 Characteristics of wt and mutant receptors expressed in tSA201 cells. .....	137
Table 4.4 Electrophysiological characterization of wt and mutant receptors expressed in <i>Xenopus laevis</i> oocytes. ....	138
Table 4.5 I <sub>Max</sub> values measured from oocytes expressing wt and mutant receptors .....	140
Table 5.1 Electrophysiological characterization of loop B receptors, data obtained using agonists 5-HT and mCPBG.....	183
Table 5.2 Radio-ligand binding to loop B receptors, data from saturation and competition assays.....	184
Table 5.3 Results from the ligand-docking studies using 5-HT <sub>3A</sub> R homology model .....	185
Table 5.4 A comparison of the H-bonding interactions of the loop B region in molecular models of the relaxed and ligand bound state of 5-HT <sub>3A</sub> R. ....	187
Table 5.4.1: Loop B H-Bonds in the ground state .....	187
Table 5.4.2: Loop B H-Bonds in the ligand-bound open/desensitized state.....	188



### Acknowledgements

I would like to sincerely thank my parents Shailaja and Ramesh Joshi for their life-long love, support and encouragement. I would also like to thank my wife Asha Suryanarayanan whose help and support made everything possible. I would like to thank my major advisor Dr. Marvin Schulte for his guidance over the last five years. I would also like to thank Ms. Mary Von Mulken for all her help with writing. I thank Alaska INBRE and Dr. George Happ for funding my research at the University of Alaska. I also thank Dr. Zsolt Bikadi for providing molecular models. I am grateful to my advisory committee members and Dr. Tom Clausen who had to take time out of their busy schedules in order to help me with my dissertation. I am also grateful to the wonderful people of the University of Alaska Fairbanks for providing me with the amazing experience of living and studying in this beautiful State of Alaska.

## Chapter 1: Introduction

Ionic concentrations inside and outside of cells, not only maintain the physiological homeostasis but also mediate the dynamics of various biological functions. Ion channels are complex membrane proteins that allow ions to flow in and out of cells in a controlled fashion. Literally, thousands of different ion channels from various species, including bacteria, have been identified and most of the physiological processes involve ion channels directly or indirectly. As expected, malfunction of specific type ion channels leads to distinct pathological states. Importance of ion channel research is amply illustrated by their special relevance to clinical cardiology, clinical nephrology, and clinical neurology.

### 1.1 Historical perspective

The history of ion channel research dates back to the early 18<sup>th</sup> century. Luigi Galvani demonstrated in 1792 that an isolated muscle from frog leg could be made to spasm with electric stimulation. He coined the term bioelectricity for this phenomenon. In 1902, Julius Bernstein proposed the membrane hypothesis. Using the Nerst equation, he suggested that nerves are surrounded by semi-permeable membrane, which allows selective passage of  $K^+$  out of the neuron, in turn generating the resting membrane potential. He also suggested that temporary changes in this potential, as a result of loss of selective  $K^+$  permeability, causes action potential. It was later revealed that not only  $K^+$  but other ions such as  $Na^+$ ,  $Ca^{++}$  and  $Cl^-$  play a role in this phenomenon. The era of classical biophysics started with the work of John Young (1937), when he first attempted

the use of giant squid axon to measure ionic currents. In classical studies, which used the same experimental model of giant squid axon, Hodgkin, Huxley and Katz were able to show that  $\text{Na}^+$  and  $\text{K}^+$  indeed move across the neuronal membrane to produce currents responsible for generating the action potential. These studies were made possible due to the development of voltage-clamp by Kenneth Cole in 1949. However, it was not until 1974 that it was first demonstrated that ion channels exist as discrete protein molecules and conduct currents across the membrane. Using a muscle membrane preparation containing nicotinic acetylcholine receptor, Neher and Sakmann were able to demonstrate ionic currents through single nicotinic acetylcholine receptor ion channel. This remarkable feat was achieved through development of a novel electrophysiological technique called patch-clamp. Almost 70 years after the receptor hypothesis was first published (John Langley, 1907), it was shown conclusively that ion channels are an integral part of certain surface receptors (in this case for acetylcholine).

## 1.2 A brief classification of ion channels according to the mechanism of gating<sup>1</sup>

- 1) Voltage-gated ion channels: These ion channels have a voltage sensor in the transmembrane region, which directs the opening and closing of the channel gate. Members of this family include sodium, potassium, calcium, proton and anion conducting channels.
- 2) Mechano-sensitive ion channels (Stretch-Activated ion Channels; SAC): This class of ion channels responds to mechanical stress, such as stretch. These types of ion channels are involved in mediating pressure and sound sensation. CLC group of

---

<sup>1</sup> This classification is a modified version of ion channel classification published on the World Wide Web at CFTR review page at <http://opal.msu.montana.edu/cftr/default.htm>

mechano-sensitive chloride channels are activated by hyperpolarization and changes to cell volume.

- 4) Ligand-gated ion channels: These ion channels are gated by agonist molecules interacting with a binding domain, which is usually located away from the actual channel gate. Extracellular ligand-gated ion channels, with the exception of glutamate receptors, are pentameric. The prototype of this superfamily is nicotinic acetylcholine receptor. GABA<sub>A</sub> and GABA<sub>C</sub>, Glycine and 5-HT<sub>3</sub> receptors constitute other members of this superfamily.
- 5) Intracellular ligand-gated ion channels: Chloride conducting cystic fibrosis transmembrane conductance regulator (CFTR), members of ABC (ATP Binding Cassette) family of transporters, Amiloride-sensitive sodium channels, Calcium-activated Chloride Channels (ClCAs) and several members of ASIC family form this group of ion channels. These ion channels are stimulated indirectly through G-protein coupled receptor stimulation. These ion channels can also be activated by intracellular entities such as ions (calcium), nucleotides (ATP, GMP, cyclic AMP) and phospholipid derivative phosphatidyl inositol (PI).

### **1.3 Physiological role of ligand-gated ion channels: Fast synaptic transmission at the neuro-muscular junction.**

The physiological role of the two major classes of ion channels (i.e., voltage- and ligand-gated ion channels) can be described using the model system of muscle nicotinic acetylcholine receptor (muscle nAChR) mediated neuro-transmission at the nerve-muscle junction. The neuro-muscular junction is formed by the axon of the stimulatory motor

neuron that arises in the spinal cord. The cell-body of the motor neuron is located in the anterior horn of the spinal gray mater. The dendrites of the motor neuron form central synapses with axons of central motor neurons. Action potential is generated in the central synapse and travels down the cell body and the axon towards the nerve-muscle junction. The action-potential generated by the transmission of impulse through the motor neuron is mediated by voltage-sensitive sodium channels. Under resting conditions, the cell membrane of the dendrite is held at approximately -90 mV. A local electrical disturbance, usually in the form of a change towards positive in the membrane potential, at the central synapse causes activation of voltage-sensitive sodium channels. The opening of these channels leads to movement of the sodium ions into the dendrite, which causes further changes to membrane potential. This sets into motion a train of events where the local electrical change in the membrane potential is propagated through the end of the axon, into the pre-synaptic terminal of the neuro-muscular junction. This is achieved by a wave of openings of voltage-sensitive sodium channels located mainly at the nodes of Ranvier. At the neuro-muscular junction, the arrival of an action potential leads to opening of calcium channels that cause a rise in the local calcium concentration. The raised calcium levels cause the endogenous neuro-transmitter acetylcholine (ACh) filled vesicles to dump large amounts of ACh in the synapse. Muscle nAChRs are hetero-pentameric complexes of proteins with a ligand-binding region that binds ACh. Ion channels are expressed on the muscle cell surface and are clustered near the post-synaptic terminal. The binding site for neurotransmitter the ACh is located in the extra-cellular domain, which probably allows easy contact with the neuro-transmitter released in the synapse.

The binding of the neurotransmitter is followed by opening of the ion channel pore that allows a rush of cations, such as calcium and sodium, through the open ion channels into the interior of the sarcoplasm of the muscle cell. These events again lead to local changes in membrane, called 'end-plate potentials'. The resulting change in the membrane potential leads to a further release of calcium from the intra-cellular calcium depots, causing an interaction between actin and myosin filament through complex steps, ultimately resulting in muscle contraction.

#### **1.4 5-HT<sub>3</sub> receptor is a member of 'Cys-loop' superfamily of ligand-gated ion channel receptors.**

The 5-HT<sub>3A</sub> receptor shows high degree of sequence and structural homology with the nicotinic acetylcholine receptor and other members of the Cys-loop family. A sequence alignment of all members of this family suggests that 5-HT<sub>3A</sub> receptor subunit has a large extracellular N-terminal domain, four transmembrane domains (TM 1-4) and a small extracellular C-tail. The N-terminal domain continues as the first transmembrane domain (TM1). The N-terminal domain also contains the signature Cys-loop, which is a stretch of 11 amino acids marked at both ends by a cysteine (C161-C174 in mature protein). Two small cytoplasmic and one small extracellular loops connect four transmembrane domains. Five such subunits come together to form the homopentameric receptor. The ion channel is an integral part of the protein and is lined by one side of five TM-2 domains.

Seven types (5-HT<sub>1</sub> to 7) and 14 subtypes of serotonin (5-HT) receptors have been discovered over last five decades. However, the realization that 5-HT<sub>3</sub> receptor is an

ion channel is relatively recent. All other members of this family are G-protein coupled receptors and mediate slower forms of neuronal and non-neuronal signal transmission. The possibility of the existence of a neuronal type 5-HT receptor was suggested as early as 1957 by Gaddum and Picarelli (Gaddum and Picarelli, 1957). They suggested the existence of serotonin-M receptor, which was sensitive to Morphine inhibition and insensitive to inhibition by LSD. Although several later studies suggested the presence of a specific 5-HT receptor in the peripheral neuronal tissue, specific information was unavailable. In 1986, Bradley and colleagues renamed the serotonin-M receptor as 5-HT<sub>3</sub>R. Detailed pharmacological characterization of 5-HT<sub>3</sub>R had to await the development of specific ligands, such as antagonists tropisetron, zacopride, granisetron, MDL-72222 and agonists 2-methyl 5-HT, phenylbiguanide and *m*-chloro phenylbiguanide (Costall and Naylor, 2004). In the late 80's and the early 90's, interest in 5-HT<sub>3</sub>R research was rejuvenated by the discovery that 5-HT<sub>3</sub>R antagonists were potent anti-emetics, especially for post-chemotherapy nausea and vomiting. In 1989, 5-HT<sub>3</sub>R was shown to be a cell membrane bound, cation-specific, ligand-gated ion channel. Using patch-clamp assay, Derkach et al. showed that 5-HT induced single-channel currents from membrane patches of guinea pig sub mucosal plexus. These unitary currents could be specifically blocked by 5-HT<sub>3</sub> receptor antagonists (Derkach et al., 1989). The full nucleotide and deduced protein sequence of mature *murine* 5-HT<sub>3A</sub> receptor was published in 1991 (Maricq et al., 1991). Since then, 5-HT<sub>3</sub>R sequences for multiple species e.g. *porcine* (Lankiewicz et al., 1998) and *human* (Belelli et al., 1995) have been reported. Splice variants of 5-HT<sub>3A</sub> subunit have also been reported (for review, see

(Reeves and Lummis, 2002). For the studies described in this thesis, we have used the short splice variant of *murine* 5-HT<sub>3A</sub> receptor. The short form is termed 5-HT<sub>3AS</sub> receptor, and is six amino acids shorter than the long form (termed as 5-HT<sub>3AL</sub>). The missing amino acids (G385-L390) are from the second cytoplasmic loop, which connects M3 and M4 regions. The two splice variants show differences only in relative efficacy values (relative to 5-HT) for 2-methyl 5-HT and *m*CPBG (Niemeyer and Lummis, 1998). In a mutagenesis study involving the aforesaid 6 amino acids, no clear conclusion about their specific role in the efficacy of 2-methyl 5-HT and *m*CPBG could be drawn. In this regard, it is interesting to note that the second cytoplasmic loop plays a role in determining ionic conductance through the homomeric 5-HT<sub>3AR</sub> ion channel. Three arginine residues at positions 432, 436 and 440 in the second intracellular loop (a region called the HA stretch) cause an inhospitable ionic environment for cation conduction in the homomeric receptors. The absence of such a stretch in heteromeric 5-HT<sub>3AB</sub> receptors is thought to be responsible for the higher conductance of the 5-HT<sub>3AB</sub> receptor (Kelley et al., 2003). It is possible that the lack of amino acids G385-L390 causes structural changes in the HA stretch, which may cause 2-methyl 5-HT and *m*CPBG mediated channel opening to be modulated differently compared to the 5-HT<sub>3AL</sub> isoform.

For both mouse and human, the sequence of the 5-HT<sub>3B</sub> subunit has also been reported (Davies et al., 1999; Stewart et al., 2003). Recent studies have identified the presence of 5-HT<sub>3C</sub>, D and E subunit-like genes in *human* genome (Karnovsky et al., 2003; Niesler et al., 2003). It has been suggested that 5-HT<sub>3</sub> receptors in the peripheral



nervous system are mostly 5-HT<sub>3AB</sub> heteropentamers, while those in central nervous system are 5-HT<sub>3A</sub> homopentamers (Morales and Wang, 2002).

### **1.5 Primary, secondary, tertiary and quaternary structure of 5-HT<sub>3</sub>R**

Mature single subunit of 5-HT<sub>3</sub> receptor is ~480 amino acids long and weighs ~50 kDa (~65 kDa when glycosylated) (Hovius et al., 1998; McKernan et al., 1990). N-terminal domain, which is predicted to exist mostly as  $\beta$ -strands, is extra-cellular. Similar to the nAChR, the binding site is contained at the subunit interface at the N-terminal (Arias, 2000; Brejc et al., 2001; Eisele et al., 1993). Secondary structure of the 5-HT<sub>3A</sub>R N-terminal domain is predicted to be very similar to that of the nAChR (Brejc et al., 2001; Karlin, 2002; Reeves and Lummis, 2002). These assumptions have been confirmed through the use of a downscaled version of Fourier transform infrared spectroscopy (FTIR) for both 5-HT<sub>3A</sub>R and nAChR under identical conditions (Rigler et al., 2003). The results of these studies predict that both receptors are 36%  $\alpha$ -helix, 33%  $\beta$ -strand, 15%  $\beta$ -turn, and 16% non-regular structures. These results complement computational models based on the structure of the AChBP. 5-HT<sub>3</sub>R assembles as a homo- or hetero-pentamer (Brejc et al., 2001; Green et al., 1995; Hovius et al., 1998; Lummis and Martin, 1992). Using a purified receptor preparation, electron micrographs of the *murine* 5-HT<sub>3A</sub> receptor were obtained (Boess et al., 1995; Green et al., 1995), which show the receptor as a doughnut shaped pentamer of size ~70X140 Å with a ~20 Å central pore.

### **1.6 Assembly, trafficking and cell-surface localization of the 5-HT<sub>3</sub>R**

Studies using immunocytochemistry have shown that subunit A of the 5-HT<sub>3</sub> receptor can assemble as a homo-pentamer in neuronal cells as well as immortalized cell lines. This

assembly takes place in the endoplasmic reticulum with the help of a variety of chaperon proteins. Binding sites on homopentameric receptors are probably formed during the assembly process in the endoplasmic reticulum. The 5-HT<sub>3</sub>B subunit alone cannot assemble into functional ion channels at the endoplasmic reticulum level; it can only co-assemble with 5-HT<sub>3</sub>A subunit as a hetero-pentamer (Boyd et al., 2002). The 5-HT<sub>3</sub>B subunit, when expressed alone, gets trapped in the endoplasmic reticulum, and is degraded therein. A sequence of amino acids in the first cytoplasmic loop of 5-HT<sub>3</sub>B subunit may be responsible for this retention. Within the endoplasmic reticulum, chaperone proteins, BiP and calnexin interact with 5-HT<sub>3</sub>R and probably aid in its assembly. These 'helper' proteins may also be involved in degradation of partially formed subunits (Boyd et al., 2002).

Both 5-HT<sub>3A</sub> and 5-HT<sub>3AB</sub> receptors become N-glycosylated at 3 putative sites of glycosylation: N109, N174; and N190 (Quirk et al., 2004). N-glycosylation adds to the molecular weight of the mature protein (Green et al., 1995). Early studies suggested that N-glycosylation does not play a role in receptor assembly or ligand-binding. However, Quirk et al., using site-directed mutagenesis and Tunicamycin treatment (which inhibits glycosylation), have shown that N109 is involved in correct receptor assembly. These studies also suggest a role of glycosylation at N109, N174 and N190 in membrane targeting of the 5-HT<sub>3</sub> receptor as well as receptor-ligand interaction. After assembly 5-HT<sub>3</sub>Rs are transported to the neuronal cell surface, where they cluster at high concentrations at functionally important areas, such as micropodia in HEK293 cells (a

non-neuronal cell-line) and dendritic spines of hippocampal neurons (Grailhe et al., 2004).

### **1.7 Central and peripheral distribution of the 5-HT<sub>3</sub>R**

Early studies examining distribution of 5-HT<sub>3</sub>R in rat brains utilized high affinity, specific binding of the antagonist [<sup>3</sup>H]GR65630. These studies suggested that 5-HT<sub>3</sub>Rs are widely distributed in rat cortical and limbic areas (Kilpatrick et al., 1987). The distribution of 5HT<sub>3</sub>R in rat brain was also studied using immunocytochemistry. In studies reported by the Bloom group, various polyclonal antibodies raised against synthetic peptides based on the primary sequence of the 5HT<sub>3</sub>R were utilized (Morales et al., 1998). The 5HT<sub>3</sub>R-immunoreactive neurons could be detected in the forebrain (layers II-III of the neocortex, anterior olfactory nucleus, hippocampal formation, amygdala, caudate putamen, nucleus accumbens), brainstem (nuclei for cranial nerves trigeminal motor (V) and facial (VII) ) and dorsal and the ventral horn of the spinal cord. A similar study indicated that 5-HT<sub>3</sub>R is distributed in forebrain (isocortex, olfactory regions, hippocampal formation and amygdala), brainstem (sensory and motor nuclei and nuclei of the reticular formation) and spinal cord (dorsal and ventral horn) of the rat central nervous system (Morales et al., 1996). In rat neocortex and hippocampus, the majority of 5-HT<sub>3</sub>R are expressed on GABAergic neurons, suggesting a modulatory role of 5-HT<sub>3</sub>R in release of GABA and it's mediation of inhibitory neurotransmission (Morales et al., 1996). Such a wide distribution is suggestive of a broad role played by 5-HT<sub>3</sub>R in synaptic transmission. In the peripheral nervous system, 5-HT<sub>3</sub>Rs are expressed in dorsal root and nodose ganglia, vagus nerve and intestinal submucosal plexus. In rat

gastrointestinal system, 5-HT<sub>3</sub>Rs are localized to neurons of the myenteric and submucosal plexus, fibers in the circular and longitudinal muscles, submucosa, and mucosa. 5-HT<sub>3</sub>R immuno-reactivity can also be detected in interstitial cells of Cajal (Glatzle et al., 2002). Interestingly, peripheral 5-HT<sub>3</sub>Rs can be both homomeric and heteromeric, while central 5-HT<sub>3</sub>R are essentially homomeric (Morales and Wang, 2002). These differences in composition probably reflect the differential modulatory role played by these receptors.

In the mouse nervous system, the distribution is very similar to that seen in the rat nervous system. In mouse cerebral cortex, groups of neurons in piriform, cingulate, and entorhinal areas are labeled with 5-HT<sub>3</sub>R specific in-situ hybridization. Areas of the limbic system, such as interneurons of hippocampal formation, posteroventral hippocampal region and the molecular layer of CA1 also contain 5-HT<sub>3</sub>Rs. Based on this distribution in the hippocampal region, it was suggested that 5-HT<sub>3</sub> receptors inhibit pyramidal cell populations via excitation of inhibitory interneurons. 5-HT<sub>3</sub>Rs are also present on neurons of the amygdaloid complex, the olfactory bulb, the trochlear nerve nucleus, the dorsal tegmental region, the facial nerve nucleus, the nucleus of the spinal tract of the trigeminal nerve, and the dorsal horn of spinal cord. In the *murine* peripheral nervous system, 5-HT<sub>3</sub>Rs are also located on the dorsal root ganglion (Tecott et al., 1993).

Quantitative *in vitro* autoradiography in combination with [<sup>3</sup>H] ICS 205-930 (a selective 5-HT<sub>3</sub>R antagonist) was applied to study the distribution of 5-HT<sub>3</sub>R in post-mortem human brain tissue. 5-HT<sub>3</sub>Rs were localized to discrete nuclei of the lower brainstem and the substantia gelatinosa at all levels of the spinal cord (Waeber et al.,

1989). Another study employing [<sup>3</sup>H]Zacopride revealed low levels of binding localized to the limbic system, particularly to amygdala and hippocampus. These receptors were of a single population, probably of 5-HT<sub>3A</sub> type homomeric receptors. 5-HT<sub>3R</sub> were also localized with high densities in the area postrema, a finding which is in accordance with the proposed central mechanism of anti-emetic action of 5-HT<sub>3R</sub> antagonists (Barnes et al., 1989).

### **1.8 Gating and desensitization kinetics of LGIC coupled receptors including 5-HT<sub>3A</sub>R**

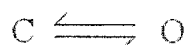
Attempts at functionally isolating 5-HT<sub>3R</sub>s were initially limited by complications arising from a mixture of 5-HT receptors present in neuronal cell lines. Thus, early studies of receptor function were based solely on the use of 5-HT<sub>3R</sub> specific receptor ligands such as the antagonist ICS 205-930 and agonist 2-Methyl 5-HT. Large quantities of nicotinic acetylcholine receptors can be purified from electric organ of Torpedo eel. Before the advent of molecular biology techniques, biochemical studies of the nAChRs utilized these protein preparations. However, no such source of purified protein are available for the 5-HT<sub>3R</sub>s.

Initial studies indicated that 5-HT<sub>3R</sub> caused membrane depolarization in neurons. These studies employed intracellular recordings made from parasympathetic neurons of the rabbit vesical pelvic ganglia. In such neurons 5-HT caused a membrane depolarization that could be competitively antagonized by ICS 205-930, a specific 5-HT<sub>3R</sub> antagonist. These currents were resistant to inhibition by non-specific blocker of non-5-HT<sub>3</sub> 5-HT receptors (e.g., 5-HT<sub>1</sub>, 5-HT<sub>2</sub> etc) methysergide (Akasu et al., 1987).

Membrane depolarization induced by 5-HT<sub>3</sub>R in turn was shown to lead to the generation of action potential and other post-synaptic events (Surprenant and Crist, 1988). A detailed characterization of receptor kinetics was however obtained from whole-cell voltage-clamp studies using cultured hippocampal neurons, which natively express 5-HT<sub>3</sub>R. Rapid application of 5-HT (the natural full agonist) to such cells caused rapid inward currents with rapid desensitization. The rapidity of the response suggested coupling of 5-HT receptor and the ion channel (Yakel and Jackson, 1988).

### **1.8.1 Stochastic behavior of the 5-HT<sub>3</sub>R and its relationship to the macroscopic events**

The macroscopic events of opening and desensitization (waveform of macroscopic currents) are a transition of a *population* of receptors through various states. However, at the level of a single ion channel, such transitions are stochastic (random events governed by probability). These probabilities, however, are distinct entities which can be calculated from experimental observations obtained from single-channel recording. Such calculations are based on certain assumptions. One important assumption is that a single ion channel follows Markovian processes. If it is assumed that a single channel oscillates between a closed and an open state, then the process can be written as:



Where C is closed and O is open state. A Markovian process assumes that a constant probability exists of change in the state of ion channel (e.g. from closed to open) in a short period of time  $dt$ , and such probability does not depend upon how much time

was spent by the channel in the closed state before beginning of  $dt$  and how it reached the closed state (i.e. from either the open or from desensitized state, if desensitized state is assumed). However, at the level of a single ion channel the probability is only predictive. For example, given a 0.3 probability of transition from closed to open state in 0.1 ms, an ion channel has a 3/10 probability of passing from closed to open state if observed for 0.1 ms; which may or may not happen given a single observation. Based on such probabilities, predictions about behavior of a large number of ion channels can be easily made. Given a large population of ion channels, in 0.1 ms 30% of ion channels will pass from closed to open state in 0.1 ms and 70% will be in closed state. In next 0.1 ms the next 30% of closed population will change into open state. Over a period of 10 such periods ( $0.1 \times 10 = 1$  ms), a single exponential describing channel opening is obtained. A similar exponential can be obtained for channel closing. The probability of transition from one state to another is expressed in terms of transition rates when applied to macroscopic system. Such rates have units of frequency (per second,  $s^{-1}$ ). Thus macroscopic currents can be used as a direct reflection of probabilities of various lifetimes.

The functioning of 5-HT<sub>3</sub> receptors can actually be considered in three distinct states; two in equilibrium conditions and one in a non-equilibrium condition. In each of these conditions, the passage of receptor from one state to other follows the law of mass action. The law of mass action states that the rate of a given reaction is proportional to the product of reactant concentrations at any given time. Under equilibrium conditions, the equilibrium constant determines the rate of reaction, since the rate of product formation

and product breakdown is the same. Under non-equilibrium conditions, the forward and backward reaction rates determine the overall reaction rate, which keeps changing exponentially until equilibrium is reached.

The receptor exists in an equilibrium condition under resting conditions, with no contact with agonist molecules. In such conditions, the energy barriers that oppose transformation into the open state cannot be easily overcome, and the protein can only rarely venture into the open state. The receptors also exist in an equilibrium condition in continuous presence of the agonist. Various equilibrium constants determine the proportion of receptors in various states. In a receptor where there are two states; closed and open, continued presence of agonist will result in equilibrium condition where a proportion of receptors remain in the open state. This proportion will be dictated by the equilibrium constant. However, ligand-gated ion channels pass into a second close state in continuous presence of agonist, the desensitized state. Thus, in continued presence of agonist, the receptor population at any given time will be separated into desensitized, open, or closed states. For example, in continuous presence of the agonist 5-HT, 5-HT<sub>3</sub>R prefers the desensitized state, which probably reflects the most stable receptor conformation in presence of agonist.

A non-equilibrium or kinetic state exists when a population of receptors is simultaneously exposed to a quantum of agonist. Under such conditions, the macroscopic currents can be useful in measuring kinetic rates.



### 1.8.2 Kinetic parameters of inward currents produced by 5-HT<sub>3A</sub> R

At supra-maximal concentrations, 5-HT is the most efficacious agonist on wild-type (wt) receptors. At such concentrations, *m*CPBG elicits only 92 ( $\pm$ 1) % of the current produced by 5-HT. Agonists 2-Me5HT and PBG also behave as partial agonists; producing only 12 ( $\pm$ 1) and 87 ( $\pm$ 7) % of 5-HT induced currents. These data suggest that the open conformation of the wild type 5-HT<sub>3A</sub>SR channel is most efficiently stabilized by the endogenous agonist 5-HT, followed by *m*CPBG, PBG and least efficiently by 2-Me5HT. These values were obtained in the course of the study described in chapter 4.

Three major macroscopic states are observed with 5-HT<sub>3</sub>R mediated inward currents; closed, open and desensitized. Upon fast application of agonist to cells expressing *murine* 5-HT<sub>3A</sub>R, a rapid inward current with sharp peak is observed. In continued presence of agonists *murine* 5-HT<sub>3A</sub> receptors desensitize with an apparent biphasic course, a rapid desensitization phase and a slow desensitization phase. A small percentage of the response is non-desensitizing. The response returns to the baseline with removal of agonist. The EC<sub>50</sub> for 5-HT determined for recombinant *murine* 5-HT<sub>3A</sub> receptors ranges from ~2-4  $\mu$ M with Hill slope of 1.7-3 (Barann et al., 1997; Gunthorpe and Lummis, 1999; Hussy et al., 1994; Joshi et al., 2004; Maricq et al., 1991; Mott et al., 2001; van Hooft and Vijverberg, 1996).

Kinetics of activation can be measured by rapid pulses of agonist, where solution exchange is achieved in 1-5 ms. *m*5-HT<sub>3A</sub>R demonstrates slow activation time (mean  $\pm$  s.e.m. 10-90 % rise time 12.5  $\pm$  1.6 ms for 100  $\mu$ M 5-HT). The rising waveform of the response can be fit to a single exponential waveform and yields a time constant ( $\tau$ ) of 7.3

ms. Given the  $\tau$  and the total rise time, the activation rate was calculated to be 136/s (Mott et al., 2001). The slow activation rate is presumably a function of slow conformational changes and not of slow agonist binding rates, since no significant difference in activation time could be detected at 2X  $EC_{50}$  and 20X  $EC_{50}$  concentrations of 5-HT (Yang et al., 2000). Activation rates for *m*CPBG-induced responses are about 2.2 fold slower than those of 5-HT.

Kinetics of deactivation can be measured by ultra-short pulses of agonist (for 2-5 ms). The rate of decay in maximum response amplitude in experiments measuring deactivation probably conveys the measure of agonist unbinding rate, and hence the rate of receptor deactivation. Rate of desensitization is measured simply by using longer agonist perfusions, which allows most of the receptors to reach desensitized state. Interestingly, the time constants ( $\tau$ ) for both desensitization and deactivation of the 5-HT<sub>3A</sub>Rs are almost identical, suggesting that agonist unbinding from the activated receptor occurs at the same rate as transition of activated receptor into the desensitized state (Bartrup and Newberry, 1996; Neijt et al., 1989). Mott et al. (Mott et al., 2001) report slower deactivation rates compared to desensitization rates in a population of patches, indicating that certain biological factors may also be controlling desensitization kinetics. Various studies have described the role of calcium, as well as factors controlling receptor phosphorylation in modulation of desensitization kinetics.

The slow activation and deactivation of the 5-HT<sub>3</sub>R is unique among all the ligand-gated ion channels. With the exception of NMDA receptors (Clements et al., 1998), all other ligand-gated ion channels demonstrate much faster rates of activation and

deactivation i.e., nicotinic acetylcholine muscle receptors at 12000/sec (Liu and Dilger, 1991), GABA<sub>A</sub> receptors at 6000/sec (Maconochie et al., 1994),  $\alpha$ 1-glycine receptors at 2200/sec (Greuer, 1999). AMPA receptors (Mosbacher et al., 1994), kainite receptors and purinergic P2X receptors (Evans et al., 1992) also demonstrate faster activation rates. The 5-HT<sub>3</sub>R is unique among ligand-gated ion channels since it also belongs to the 5-HT class of receptors, which are G-protein coupled receptors. These G-protein coupled receptors are primarily involved in mediating slow synaptic transmission of a modulatory nature. It has been suggested that 5-HT<sub>3</sub>R may also be involved in mediating slower (among ligand-gated ion channels) types of synaptic transmission (Jackson and Yakel, 1995).

In continued presence of agonists 5-HT<sub>3A</sub>Rs desensitize, with the time constant ( $\tau$ ) of ~300 ms (Mott et al., 2001). The biphasic course of desensitization in can be fitted to the sum of two exponential components with time constants  $\tau_{\text{slow}} = 2300\text{--}6000$  ms and  $\tau_{\text{fast}} = 170\text{--}570$  ms (Jones and Yakel, 1998; Mott et al., 2001; Yakel et al., 1991; Yang et al., 1992). Recovery from *m*CPBG-induced desensitization is about 5 times slower than 5-HT induced desensitization.

Various groups have utilized the time-course of recovery from desensitization to predict the number of final desensitization states induced by agonists. In such studies recovery of the receptor population from effects of desensitization is measured using double-pulse approach. The time course of desensitization can be measured by progressively increasing the time between two pulses, and taking the ratio of maximal

currents at pulse 1 and pulse 2. The data obtained is fit to the equation, where  $ND$  indicates number of desensitization steps.

$$\text{Current } (I) = A(1 - \exp(-t/\tau_{\text{recovery}})^{ND}) + \text{offset}$$

In such experiments, the ratios obtained at each time point can be fit to a single exponential waveform when partial agonists are used. However, when full agonists are used, the waveform becomes sigmoid. These results indicate that partial agonists probably induce single desensitized state while full agonists induce 3-4 different desensitization states (van Hooft and Vijverberg, 1996). These results however are not unanimous. Mott et al. (Mott et al., 2001) have reported that recovery from desensitization induced by full agonists (5-HT and *m*CPBG) can be fit to a single exponential waveform, which indicates presence of a single desensitization state. Interestingly, data from kinetic modeling experiment reported by Mott et al. is in agreement with predictions of multiple desensitization steps.

### 1.8.3 A possible mechanism of gating in the 5-HT<sub>3</sub>R:

The mechanism of 5-HT<sub>3</sub>R gating is unknown. Deciphering the gating mechanism of 5-HT<sub>3A</sub>R is one of the questions being addressed in this thesis. Several kinetic models for 5-HT<sub>3</sub>R mechanism have been proposed (for a detailed description, see Appendix 1). However, none of these models deal with molecular dynamics of conformational changes associate with gating.

It is generally accepted that ligand-gated ion channels follow a cyclic path through various conformational stages. Interaction of agonist molecule(s) with the

receptor in resting state leads to activation with stabilization of the open state of the ion channel. The opening of the ion channel is followed by desensitization which is probably accompanied by conformational changes both at the ligand-binding domain and the ion channel. Various molecular processes involved in mediating these effects at the protein level remain unknown.

Auerbach and colleagues have utilized rate-equilibrium free energy relationship (REFER) analysis to map the progression of conformational changes that follow receptor-agonist interaction in nicotinic receptor (Chakrapani et al., 2004). This method utilizes measurements of changes in the energy landscape as a result of various mutations along the suspected path of the conformational wave. These studies have suggested that protein region around the ligand-binding domain first undergoes the conformational change associated with agonist interaction. This conformational change is propelled towards the channel region through  $\beta$  loops 2 and 7. These regions in turn cause conformational changes in the extracellular M2-M3 linker region which is in direct contact with the ion channel. This mode of receptor action suggests that a “conformational wave” passes from the ligand-binding domain to the channel region and opens the ion channel pore.

### **1.9 Discovery of AChBP and its impact on studies pertaining to ligand-binding domain of LGIC receptors**

The acetylcholine binding protein (AChBP) was discovered in 2001 by Sixma's group (Brejc et al., 2002) while investigating mechanisms of glia-mediated synaptic modulation. The protein was isolated from glia of snail *Lymnea stagnalis* by virtue of its

epibatidine (a nicotinic ligand) binding properties. AChBP is a soluble protein and binds nicotinic ligands with high affinity with a pharmacological profile similar to that of homo-pentameric nicotinic  $\alpha 7$  receptor. It is released from glial cells in cholinergic synapses and modulates acetylcholine (ACh) mediated neurotransmission by binding to ACh released in the synapse. The ability of AChBP to bind nicotinic ligands prompted its purification followed by biochemical and crystallographic characterization. These studies revealed that AChBP is a homo-pentameric protein. Each subunit consists of 210 amino acids. There exists about 31% sequence homology with nicotinic  $\alpha 7$  receptor. AChBP also shares ~20% sequence homology with other members of the LGIC superfamily of receptors (including GABA<sub>A</sub> and GABA<sub>C</sub>, the glycine, and the 5HT<sub>3</sub> receptors). Although overall % homology is low, AChBP shares most of the conserved structural elements of the LGIC superfamily, including a 12 amino acid cysteine-cysteine loop. Most of the amino acids thought to be involved in binding to nicotinic ligands are also conserved. The crystal structure of AChBP was resolved at 2.7Å resolution (Figure 1.2). Electron cryo-microscopic images of nAChR show a doughnut-shaped pentameric protein with a barrel-shaped arrangement of  $\beta$ -sheets (Miyazawa et al., 2003). At the macromolecular level, the structure of AChBP shows remarkable similarity to the known structural features of *torpedo eel* muscle nicotinic receptor (Brejc et al., 2001). The ligand-binding domain is located at the subunit interface. The crystal structure of the AChBP with nicotine or carbamylcholine bound was obtained at 2.7Å resolution. The positions and characteristics of the amino acids involved in binding to these ligands are in

good agreement with mutagenesis and biochemical data involving homologous residues from other LGIC family receptors.

The availability of a high resolution structural template has allowed preparation of homology models of extracellular domain of LGIC receptors. In case of 5-HT<sub>3A</sub> receptor, homology models of human, rat and mouse 5-HT<sub>3A</sub> (Maksay et al., 2003; Reeves et al., 2003) as well as 5-HT<sub>3AB</sub> receptor have been prepared. Homology models not only allow interpretation of biochemical data, but also help in formulation of novel hypotheses about receptor structure and function. The studies described here also utilize homology models of *murine* 5-HT<sub>3A</sub> receptor (Figure 1.3). Preliminary homology models have been prepared by our research group while refined models with ligand-docking calculations have been provided by Dr. Zsolt Bikadi from National Academy of Sciences, Hungary.

#### **1.10 Characterization of ligand-binding site of the 5-HT<sub>3A</sub> receptor**

The majority of the studies of the putative ligand-binding site of the 5-HT<sub>3AR</sub> have been conducted using site-directed mutagenesis. Such studies have also employed diverse probe molecules (Venkataraman et al., 2002a; Venkataraman et al., 2002b), including fluorescent (Hovius et al., 1999; Schreiter et al., 2003) and photo-sensitive ligands (Lummis and Baker, 1997). Site-directed mutagenesis studies are the most extensively employed approach used in identification of 5-HT<sub>3R</sub> binding site residues. Early biochemical studies of Cys-loop receptors suggested that the ligand-binding site was at the interface between adjacent subunits and was comprised of at least six binding loops. The discovery of the crystal structure of AChBP showed that six discontinuous loops contribute to the binding site; A-C from the principal face and D-F from the

complementary face. The subsequent development of AChBP-based 5-HT<sub>3</sub>R amino terminal homology models provided a three dimensional framework for the experimentally identified residues. These residues are E129, F130 (loop A) (Boess et al., 1997; Steward et al., 2000), W183 (loop B) (Spier and Lummis, 2000), E225, E236 (loop C) (Schreiter et al., 2003) W89, R91 (loop D) (Yan et al., 1999), Y141, Y143, Y153 (loop E) (Venkataraman et al., 2002b). To date, there are no published studies on the loop F region of the 5-HT<sub>3</sub>R.

#### 1.10.1 Role of loop A residues

Based on radio-ligand binding and electrophysiological studies, E129 (Boess et al., 1997) (E106 according to author's numbering) was proposed to interact with the ammonium group of 5-HT via an ionic or a hydrogen bond interaction. However, according to the 5-HT<sub>3</sub>R homology model, this residue is located distant from the binding site and does not contribute to binding to either agonist or antagonists.

The results of mutational analysis of F130 (Steward et al., 2000) (F107, according to the author's numbering) of the 5-HT<sub>3</sub>R suggest that this residue is critical in determining recognition of the natural agonist 5-HT, and not *m*CPBG. F130 is a unique residue, since mutation at this position specifically altered association rates of 5-HT but not *m*CPBG. It is possible that F130 is involved in early events involved in 5-HT recognition. Docking calculations with 5-HT<sub>3</sub>R homology models suggest that this residue does not form major interactions with any docked ligand. These data suggest that F130 may not be a part of the main binding site, and initial recognition of 5-HT molecule by F130 may be followed by the interaction of 5-HT with the main binding site. The



distinct differences in action of 5-HT and *m*CPBG in context of F130 mutations indicate that structurally distinct agonists may have distinct modes of action, including early events in association.

When mutated to their homologous counterpart in nicotinic acetylcholine receptor (asparagine), F130N receptors, could be activated by acetylcholine. It is possible that the role of residue at homologous position in all ligand-gated ion channels is recognition of specific agonist. Mu et al. have suggested that all members of the LGIC superfamily are activated by cation- $\pi$  interactions involving the principal face and are fairly non-specific (Mu et al., 2003). There also exists a large amount of cross-talk between ligands for nicotinic and 5-HT<sub>3</sub> receptors. In such a scenario, residues such as F130 may be guarding the 'gate' towards the binding site, only allowing the endogenous agonist 5-HT to approach the main binding site. Mutation of F130 to asparagines probably deceives the 5-HT<sub>3A</sub>R into accepting acetylcholine as agonist, leading to channel opening. Interestingly, *m*CPBG does not require any such interaction at F130.

#### **1.10.2 Role of loop B residues**

W183 from loop B region has been shown to be a critical component of the 5-HT<sub>3</sub>R binding site (Spier and Lummis, 2000) Spier et al. utilized site-directed mutagenesis in combination with radio-ligand binding assays and whole-cell patch-clamp assay to decipher the role of W183 in ligand-binding. According to this study, mutation of tryptophan 183 to either tyrosine or phenylalanine resulted in ablation of radio-ligand binding. Although agonists could bind to and activate the mutant receptors, large changes in EC<sub>50</sub> values for both 5-HT as well as *m*CPBG are observed. Using unnatural amino

acid substitutions, it has been postulated that this tryptophan residue forms a cation- $\pi$  interaction with the amino group of 5-HT (Beene et al., 2002). In such an interaction, the charged amino group of the ligand interacts with the  $\pi$  cloud of the aromatic ring. Using the method of non-sense suppression, various unnatural amino acids (modified forms of tryptophan) with substitutions at the aromatic ring of tryptophan, were introduced at position 183. The mutant protein was expressed in *Xenopus* oocytes and assayed using two-voltage electrode clamp using agonist 5-HT. This technique provided a unique approach for examining the structure-activity relationship of a particular amino acid, while maintaining the biologically active form of the protein. The homologous residue in the nAChR has also been shown to form a cation- $\pi$  interaction with acetylcholine, but not nicotine (Beene et al., 2002; Zhong et al., 1998). The homologous residue in GABA receptors is also critical for ligand-binding. The roles of the remaining residues of the loop B region have not been examined in detail, and form the basis of the study described in chapter 5.

### **1.10.3 Role of loop D residues**

In an alanine scanning mutagenesis study of the putative loop D region, it was shown that affinity for *d*-TC was reduced by substitution only at W90, whereas affinity for 5-HT was reduced only by substitution at R92 (Yan et al., 1999). Recent data suggests that *d*-TC may not be directly interacting with loop D residues. Results of a study involving *d*-TC analogs and loop D mutant receptors suggests that the general topology of the loop D region is important for *d*-TC interaction (Yan and White, 2002). On the other hand, affinity for granisetron was reduced by mutations at W90, R92 and Y94. Published

ligand-docked models for the 5-HT<sub>3</sub>R suggest that the tertiary ammonium group of antagonists could interact with W90 via a cation-pi interaction (Maksay et al., 2003). This differential effect of substitutions on ligand affinity suggests that different ligands may have different points of interaction within the ligand-binding pocket. In addition, the 'every-other-residue' periodicity of the effect on affinity for granisetron indicates that this region of the ligand-binding site of the 5HT<sub>3</sub>R adopted a beta-strand conformation; a prediction that was substantiated by structural model based on AChBP homology.

#### **1.10.4 Role of loop E residues**

Based on alanine scanning mutagenesis, three tyrosine residues (Y141, Y143 and Y153) have been shown to significantly alter the binding of 5-HT<sub>3</sub>R ligands (Venkataraman et al., 2002b). A role for the putative E-loop region of the 5-HT<sub>3</sub>R in the binding of 5-HT, *m*CPBG, *d*-TC and lerisetron was investigated using site-directed mutagenesis. 5-HT and *m*CPBG interact with Y143, *d*-TC with Y141 and lerisetron with both Y143 and Y153. This study also provided support for the hypothesis that this region of the receptor is present in a loop structure. Since mutations of loop E tyrosine residues affected binding of competitive antagonists, involvement of these residues in interaction with ligands ('binding') was suggested. On the other hand, results from preliminary electrophysiological assays had suggested a possible role of Y153 in mediating conformational changes that follow agonist binding and produce channel opening.

#### **1.11 Medicinal chemistry of 5-HT<sub>3</sub>R ligands**

The following section briefly describes the medicinal chemistry of 5-HT<sub>3A</sub>R ligands. Structures of ligands used in the studies described here are shown in figure 1.4

### 1.11.1 5-HT<sub>3A</sub>R Agonists

Serotonin or 5-Hydroxytryptamin (5-HT) is a non-selective 5-HT<sub>3A</sub>R agonist. 5-HT is the most efficacious agonist for all types of 5-HT<sub>3A</sub>Rs, irrespective of subclass. 5-HT consists of an indole ring with a hydroxyl group at 5 position. 5-HT purportedly interacts with amino acids in the ligand-binding domain through either cation-pi (terminal secondary amine) or pi-pi interaction (indole). The hydroxyl group is also an important determinant of agonist activity, since tryptamine is a partial agonist at 5-HT<sub>3A</sub>R (van Hooft and Vijverberg, 1997). Other variations of 5-HT (5-HTQ, 2-Me-5HT) also behave as partial agonists. Efficacy of 2-Me-5HT is different for each subclass of the 5-HT<sub>3A</sub>R. 2-Me-5HT is a poor partial agonist with low efficacy (10% compared to 5-HT) at *murine* 5-HT<sub>3AS</sub>R (receptor utilized in studies described here). Partial agonists can be utilized to qualitatively study gating behavior of wild type and mutant receptors (see chapter 4).

Phenylbiguanides (PBG) and phenylguanides (PG) behave as agonists of 5-HT<sub>3A</sub>R. *m*-chloro-phenylbiguanide (*m*CPBG) is a potent agonist at *murine* 5-HT<sub>3AS</sub>R, although its efficacy varies according to the subclass of the 5-HT<sub>3R</sub> (Niemeyer and Lummis, 1998). Available evidence suggests that these agonists interact with the binding site in a fashion similar to that of 5-HT, although interactions at the molecular level may vary. The kinetic parameters of *m*CPBG induced responses including rise-times as well as desensitization are markedly different compared to those of 5-HT. There are marked differences in the structure of *m*CPBG and 5-HT (Figure 1.4). *m*CPBG consists of a phenyl instead of an indole ring and contains a biguanide group with five nitrogens in place of the aminoethyl group in 5-HT. It is conceivable that the differences in action of *m*CPBG and 5-HT arise

from the differences in their chemical nature and their interactions with the ligand-binding domain at the molecular level. However, there are no published studies that address this question. For this reason, *m*CPBG can be a useful tool for investigations of biophysical aspects of 5-HT<sub>3A</sub>R gating. Other classes of ligands, such as piperazinylquinolines, tetrahydrothiazolopyridines and various aminoalkyl- and imidazoloalkyl-indenothiazoles can also behave as agonists at the 5-HT<sub>3A</sub>R.

### 1.11.2 5-HT<sub>3A</sub>R antagonists

Numerous selective and non-selective ligands for the 5-HT<sub>3A</sub>R have been identified. Selective 5-HT<sub>3A</sub>R antagonists generally confirm to the pharmacophoric model proposed by Hibert's group (Hibert et al., 1990). According to this model, a 'typical' antagonist consists of carbonyl group coplanar to an aromatic ring, and a basic center 1.7 Å above the plane of the aromatic ring. lerisetron and its analogs constitute another class of potent 5-HT<sub>3A</sub>R antagonists (Orjales et al., 1997; Parihar et al., 2001; Venkataraman et al., 2002a). In addition to the features described by Hibert's model, lerisetron incorporates a benzimidazole ring structure. Using SAR and mutagenesis studies in tandem, we have demonstrated that the terminal amine is involved in a critical interaction with the ligand-binding domain while the benzimidazole ring structure forms a relatively minor component of binding interaction (Venkataraman et al., 2002a).

(+)-Tubocurarine (*d*-TC) and its analogs are moderately potent (~80 nM K<sub>i</sub>) competitive antagonists at 5-HT<sub>3A</sub>Rs, and form a third structural class of antagonists. Curariform antagonists also inhibit the nicotinic acetylcholine receptor with similar affinity. Amino acids W90 and Y141 at 5-HT<sub>3A</sub>R binding domain are involved in

mediating *d*-TC interaction, however this involvement is probably indirect (see chapter 4) (Venkataraman et al., 2002b; Yan et al., 1999; Yan and White, 2002). *d*-TC may also be mediating binding interactions through the loop C region of the binding site.

### **1.12 Modulators of 5-HT<sub>3</sub>R function**

In addition to specific agonists and antagonists, various non-specific atypical ligands interact with 5-HT<sub>3</sub>R. Certain atypical ligands interact competitively by interacting with the ligand-binding domain, while others interact allosterically in a non competitive manner.

#### **1.12.1 Interaction of binding site with ions**

Available data suggests that divalent cations such as Ca<sup>++</sup> and Mg<sup>++</sup> inhibit 5-HT<sub>3</sub>R function by interfering with agonist binding, probably by binding directly at the agonist binding site (Niemeyer and Lummis, 2001). Zn<sup>++</sup> potentiates 5-HT induced currents and reduces the rate of desensitization and apparent affinity for 5-HT (Gill et al., 1995; Hubbard and Lummis, 2000); 5-HT<sub>3AB</sub> receptors on the other hand, may actually be inhibited by Zn<sup>++</sup> (Hubbard and Lummis, 2000). The effects of Zn<sup>++</sup> on 5-HT<sub>3AR</sub> are dampened by the presence of other divalent cations Ca<sup>++</sup> and Mg<sup>++</sup>, suggesting that these divalent cations may compete with each other at their site of interaction with the receptor.

#### **1.12.2 Interaction of 5-HT<sub>3</sub>R with atypical ligands**

##### **1.12.2.1 Steroids**

Glucocorticoids inhibit 5-HT<sub>3AR</sub>s. These molecules affect receptor function by interacting allosterically with the protein, probably at the receptor-membrane interface (Suzuki et al.,

2004). Glucocorticoid mediated inhibition may aid in the anti-emetic actions of 5-HT<sub>3A</sub>R antagonists when both are co-administered. Gonadal steroids functionally inhibit 5-HT<sub>3A</sub>R in a non-competitive manner. Such antagonism may have a role in pathophysiology of certain pregnancy-related disorders (Oz et al., 2002b; Wetzel et al., 1998).

#### **1.12.2.2 Neuroleptic drugs**

Flupentixol, haloperidol and various phenothiazines antagonize 5-HT<sub>3A</sub>R non-competitively in a voltage-independent manner, while clozapine antagonizes 5-HT<sub>3R</sub> in a competitive manner. Chlorpromazine, also a phenothiazine may be inhibiting 5-HT<sub>3R</sub> competitively (Sepulveda et al., 1994). Fluphenazine and haloperidol also cause a change in membrane anisotropy when applied to the cell, which may also be playing a role in its antagonism at the 5-HT<sub>3R</sub> (Rammes et al., 2004).

#### **1.12.2.3 Forskolin**

Forskolin inhibits 5-HT<sub>3A</sub>R (Oz et al., 2002b). Forskolin acts through adenylyl cyclase to raise intracellular cAMP levels in a variety of cell types. The effect of Forskolin on 5-HT<sub>3A</sub>R is interesting since it suggests the possibility that 5-HT<sub>3A</sub>R function is modulated by Forskolin through cAMP related mechanisms. However, electrophysiological analysis of the Forskolin effects on 5-HT<sub>3A</sub> receptors expressed in *Xenopus* oocytes suggests that Forskolin acts on the extra-cellular domain of the 5-HT<sub>3A</sub>R and inhibits its function through direct non-competitive inhibition (Oz et al., 2002b). Apparently the non-competitive inhibition is not mediated through open-channel block, but through an

interaction with the extra-cellular domain of the closed state of the receptor (Oz et al., 2002b).

#### **1.12.2.4 Toxin**

Final sigma-Conotoxin from venom of a marine snail competitively inhibits 5-HT<sub>3A</sub>R in a selective and competitive fashion (England et al., 1998). Nicotinic AChR is susceptible to several toxins (Arias, 2000). Final sigma-Conotoxin- 5-HT<sub>3</sub>R interaction was reportedly the first instance where 5-HT<sub>3A</sub>R has been described to be the target of a natural toxin.

#### **1.12.2.5 Alcohol and other drugs of abuse**

Alcohols such as ethanol and butanol potentiate agonist-induced responses at the 5-HT<sub>3A</sub>R (Machu and Harris, 1994; Zhou et al., 1998), but do not cause channel opening by themselves. This potentiation is presumably affected by increasing the rate of receptor activation and stabilizing the open state of the receptor and not by blocking desensitization (Yang et al., 2003). Arginine 222 from the pre-M1 region plays a role in gating. Mutation at this position cause spontaneous openings, increase rate of activation, increase the efficacy of full agonist and convert partial agonists into full agonists (Hu et al., 2003). The R222 residue thus seems to be involved in stabilizing the closed state of the wt receptor, presumably through its connection with the M1 region. Mutations at R222 also cause altered sensitivity to effects of ethanol on 5-HT<sub>3</sub>R activation (Zhang et al., 2002).

5-HT<sub>3</sub>R antagonist ICS 205-930 at lower concentration decreases and at higher concentration enhances the discriminative stimulus effects associated with a lower to



moderate dose of ethanol. 5-HT<sub>3</sub> antagonist ICS 205-930 enhances naltrexone's effects on ethanol intake (Mhatre et al., 2004; Mhatre et al., 2001). Ethanol drinking and deprivation shows altered dopaminergic and serotonergic function in the nucleus accumbens of alcohol-preferring rats (McBride et al., 2004). Reduced 5-HT<sub>3</sub> receptor binding in the brain tissue as well as lower baseline plus maze anxiety in the alcohol-preferring inbred fawn-hooded rat were observed by Hensler et al. (Hensler et al., 2004). Subregion-specific down-regulation of 5-HT<sub>3</sub> immunoreactivity in the nucleus accumbens shell during the induction of cocaine sensitization has also been observed (Ricci et al., 2004). These data suggest that 5-HT<sub>3</sub>R physiology can be altered by drugs of abuse such as alcohol and cocaine.

Other potential drugs of abuse also interact with 5-HT<sub>3A</sub>R, suggesting a physiological role of 5-HT<sub>3A</sub>R in mediation of their action. Cocaine inhibits 5-HT<sub>3R</sub> competitively at low micromolar concentrations, probably by competing at the binding site (Carta et al., 2003; Fan et al., 1995). Nicotine and other nicotinic agonists except 3-(2,4)-dimethoxybenzylidene-anabaseine also inhibit 5-HT<sub>3A</sub>R competitively (Gurley and Lanthorn, 1998), also indicating a significant cross-talk between nAChR and 5-HT<sub>3R</sub> systems. Inhaled agents of abuse 1,1,1-trichloroethane, trichloroethylene and toluene potentiate 5-HT induced currents from 5-HT<sub>3A</sub>R (Lopreato et al., 2003b). Endogenous cannabinoid, anandamide (Oz et al., 2002a), as well as other cannabinoid agonists inhibit 5-HT<sub>3A</sub>R non-competitively (Barann et al., 2002; Fan, 1995). The inhibition by cannabinoids is stereo-selective and is probably achieved through an interaction with an allosteric site on the receptor (Barann et al., 2002).

#### 1.12.2.6 Interaction with anesthetics

Halothane, 1,2,2-trifluorocyclobutane and Isoflurane, Enflurane and Chloroform potentiate 5-HT-mediated currents from 5-HT<sub>3A</sub>R (Lopreato et al., 2003a; Machu and Harris, 1994). Interaction of Halothane with 5-HT<sub>3</sub>R may be responsible for mediating some of the effects of Halothane on the spinal sensory systems (Koshizaki et al., 2003). Sevoflurane inhibits 5-HT<sub>3A</sub>R in noncompetitive fashion while nitrous oxide and Xenon competitively inhibit 5-HT-induced currents from 5-HT<sub>3A</sub>R (Machu and Harris, 1994; Suzuki et al., 2002). Lidocaine derivative QX222 also inhibits the receptor in a competitive fashion (Sepulveda et al., 1994). There is some evidence that the action of anesthetics may involve N-terminal domain, (Zhang et al., 1997) although trans-membrane region 2 (TM2) may also be involved (Lopreato et al., 2003a).

#### 1.13 Clinical (current and potential) uses of 5-HT<sub>3</sub>R antagonists

Specific 5-HT<sub>3A</sub> receptor antagonists have been extensively used for treatment of chemotherapy induced emesis. However 5-HT<sub>3</sub> receptor ligands are also being developed for treatment of certain other conditions.

- Ant-emetics: Anti-emetic action is mediated by action of 5-HT<sub>3</sub>R antagonists on central 5-HT<sub>3</sub> receptors located in chemoreceptor trigger zone (CTZ) of Area Postrema.
- Analgesics: possibly mediated by antagonism of 5-HT<sub>3</sub>R located in peripheral pain conducting fibers.
- Irritable bowel syndrome and other intestinal hypermotility disorders: Alosetron is a potent and highly selective 5-HT<sub>3</sub> receptor antagonist that in large randomized

controlled clinical trials has been shown to be clinically efficient in female patients with diarrhea-predominant IBS (Andresen and Hollerbach, 2004). 5-HT<sub>3</sub> receptor in gut may be involved in mediating secretory responses. granisetron, a competitive 5-HT<sub>3</sub>R antagonist attenuates rotavirus diarrhea in mice (Kordasti et al., 2004), suggesting a novel approach to rotavirus therapy. 5-HT<sub>3</sub>R agonists, on the other hand, may prove useful for therapy of constipation, especially the episodic type associated with IBS.

- Anxiolytics: In animal models as well as human trials, 5-HT<sub>3</sub>R antagonists seem to produce anxiolysis. These results however remain largely unsubstantiated.
- Bulimia nervosa: 5-HT<sub>3</sub>R may be involved in development of pathophysiology of bulimia nervosa. According to some clinical studies, Ondansetron can be useful in modifying behavior related with Bulimia (Faris et al., 1998; Faris et al., 2000; Hasler, 2000). Results from large scale clinical trials are however lacking.
- Drug abuse and drug withdrawal (Also see above): 5-HT<sub>3</sub>R system in corticolimbic areas (such as nucleus accumbens) plays a major role in regulation and modulation of dopaminergic neurotransmission. 5-HT<sub>3</sub>Rs located on pre-synaptic terminals to play such a role in dopamine release. Specific 5-HT<sub>3</sub>R agonist *m*CPBG causes release of dopamine from striatal brain slices. While not leading to changes in behavioral patterns in control animals, drug-induced changes in dopamine neurotransmission can be altered by 5-HT<sub>3</sub>R antagonists (Costall et al., 1987). Many of the effects of a variety of drugs of abuse, including cocaine and alcohols, seem to be mediated through modulation of dopamine

neurotransmission in limbic cortex. 5-HT<sub>3</sub>R antagonists can block morphine self-administration in rats. 5-HT<sub>3</sub>R antagonists lead to changes in behavioral and neurochemical expression of cocaine sensitization that follows a period of withdrawal. Administration of Ondansetron with a challenge dose of cocaine in the withdrawal period produces an increase in locomotor activity compared to that produced by challenge dose alone. At the same time, attenuation in extent of *m*CPBG induced dopamine release from striatal brain slices is also observed (King et al., 1997). A recent study suggests that, using Ondansetron, it is possible to permanently block expression of sensitization following cocaine withdrawal (King et al., 2000). In rats, alcohol consumption as well as alcohol related hyperlocomotion can be blocked by 5-HT<sub>3</sub>R antagonist administration (Kostowski et al., 1993; Kostowski et al., 1995). In addition, alcohol induced place preference under stressful conditions, in rats conditioned to fear stress can also be blocked by 5-HT<sub>3</sub>R antagonists (Matsuzawa et al., 1999). In human subjects, Ondansetron moderately reduces alcohol consumption (Naranjo and Bremner, 1993). Ondansetron has been shown to be efficacious in particular for the treatment of early onset alcoholism. The reduction in alcohol consumption seems to be associated with reduction in alcohol craving. The efficacy of the treatment is increased if Naltrexone (an opioid antagonist) is combined with Ondansetron (Johnson, 2003). Interestingly, late onset alcoholism does not seem to benefit from 5-HT<sub>3</sub>R antagonist therapy. Many drugs of abuse directly interact with 5-HT<sub>3</sub>R (see above). While cocaine and cannabinoids competitively inhibit 5-HT<sub>3</sub>R,

alcohol allosterically potentiates the action of 5-HT<sub>3</sub>R agonists. Interestingly, dopamine also directly interacts with 5-HT<sub>3</sub>R as a partial agonist. The 5-HT<sub>3</sub>R system may thus be playing a complex role in effects of drugs of abuse; indirectly through its modulation of dopaminergic neurotransmission and directly through direct interaction with the 5-HT<sub>3</sub>R. In such a scenario, 5-HT<sub>3</sub>R antagonists can be potentially used in pharmacotherapy of addiction. On the other hand, clear clinical efficacy of 5-HT<sub>3</sub>R antagonists for therapy of drug-abuse has not been demonstrated. This is probably a reflection of complex interactions between direct and indirect effects of drugs of abuse on the 5-HT<sub>3</sub>R system.

- Sleep disorders: Stimulation of peripheral 5-HT<sub>3</sub> receptors at the nodose ganglion can cause inhibition of respiration. Incidentally, Ondansetron and Zucopride can suppress sleep-related central apnea associated with 'Obstructive sleep apnea hypopnea syndrome' (OSAHS) in rat and dog models (Carley et al., 2001; Veasey, 2003; Veasey et al., 2001), suggesting a possible pharmaco-therapeutic approach for this disorder.
- Schizophrenia: A small number of studies have suggested a beneficial effect of 5-HT<sub>3</sub>R antagonist ondansetron on schizophrenia outcome, especially the psychotic syndromes and tardive dyskinesia (Sirota et al., 2000).
- Cognitive enhancers: Raised 5-HT function can impair cholinergic function, affecting cognitive processes. Antagonism of central 5-HT<sub>3</sub>Rs can prevent such impairment. A study in rats with deafferentation lesions of cortical cholinergic system was performed to assess effect of concomitant blockade of GABA and 5-

HT<sub>3</sub>Rs. The results suggest that combined therapy of ondansetron and flumazenil (Gil-Bea et al., 2004) treatment probably aids restoration of a diminished cholinergic function. Such a treatment in patients of diminished cholinergic function associated with cognitive disorders may be beneficial (Gil-Bea et al., 2004). In human subjects, 5-HT<sub>3</sub>R antagonists cause improved cognition in patients with age-related impairment and scopolamine induced cognitive impairment in healthy subjects. On the other hand, clear benefits of 5-HT<sub>3</sub>R antagonists in Alzheimer's disease related memory impairment have not been reported (Eid and Rose, 1999).

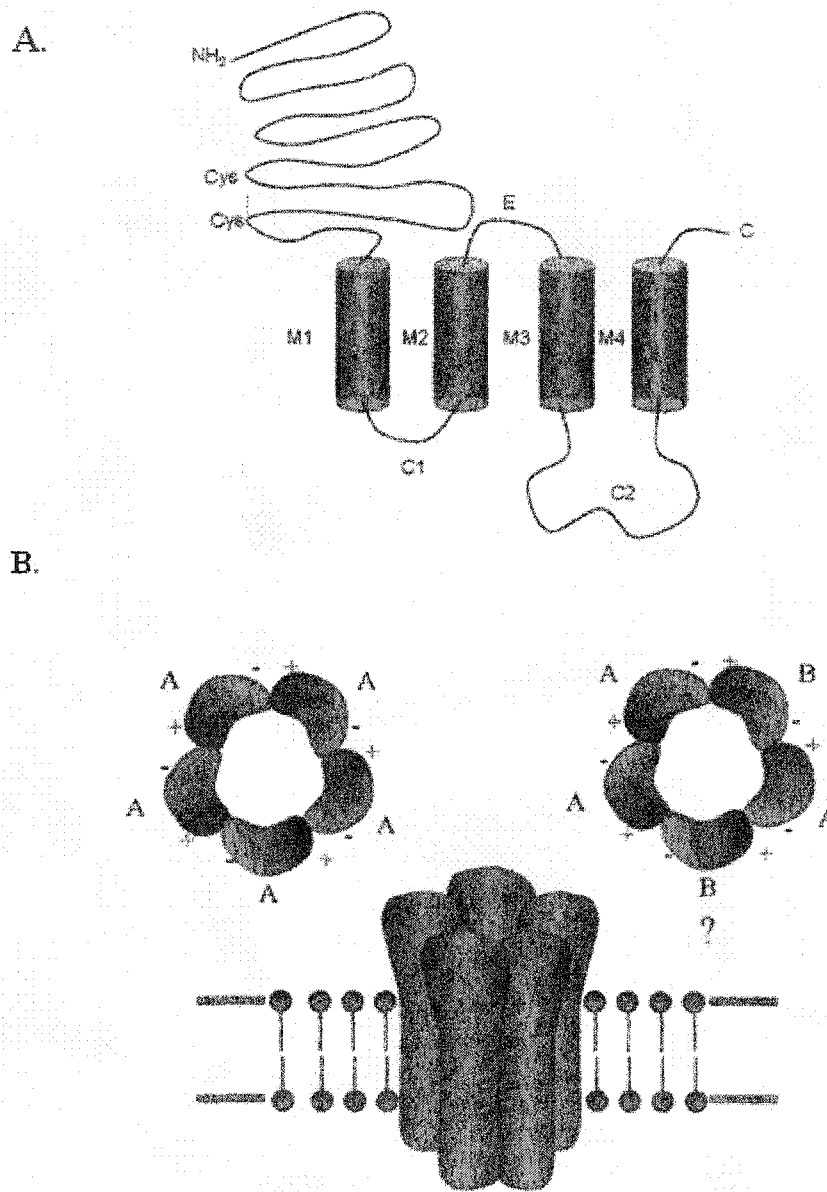


**Figure 1.1: Structural features of the 5-HT<sub>3A</sub>R**

**1.1 A: A single subunit of 5-HT<sub>3A</sub>R**

A large N-terminal is characterized by a disulfide loop (C-C). The four transmembrane regions are marked M1-M4. An extracellular loop (E) connects M2-M3 regions and may be interacting with the cys-loop. Two intracellular loops are marked C1 and C2. C2 is the larger loop and contains the 'HA' stretch of amino acids. Small extracellular C-terminal tail is marked by C.

**1.1 B: Pentameric assembly of the 5-HT<sub>3</sub>R pentamer**

The binding site is marked by at the subunit interface by principal (+) and complimentary (-) sides. The stoichiometric make-up of the 5-HT<sub>3AB</sub> receptor is not known.



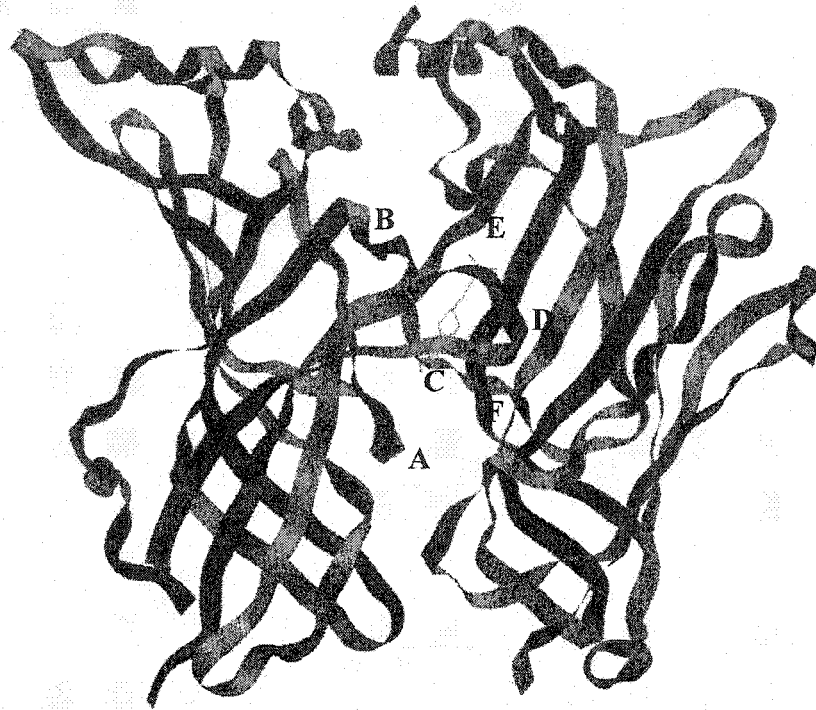


**Figure 1.2: Structure of the acetylcholine binding protein (AChBP)**

Crystal structure of acetylcholine binding protein for two adjacent subunits is shown. The backbone of the AChBP in dimeric ribbon form is displayed. The cleft between two subunits forms the putative binding site, where a HEPES molecule is bound. The gross topology of binding loops is thought to be similar for all the members of the LGIC superfamily. The 'principal' face on left hand side contributes three discontinuous regions ('loops') to the binding site, named A, B and C. On the right hand side, the 'complimentary' face contributes another three discontinuous regions ('loops') to the binding site, named D, E and F.

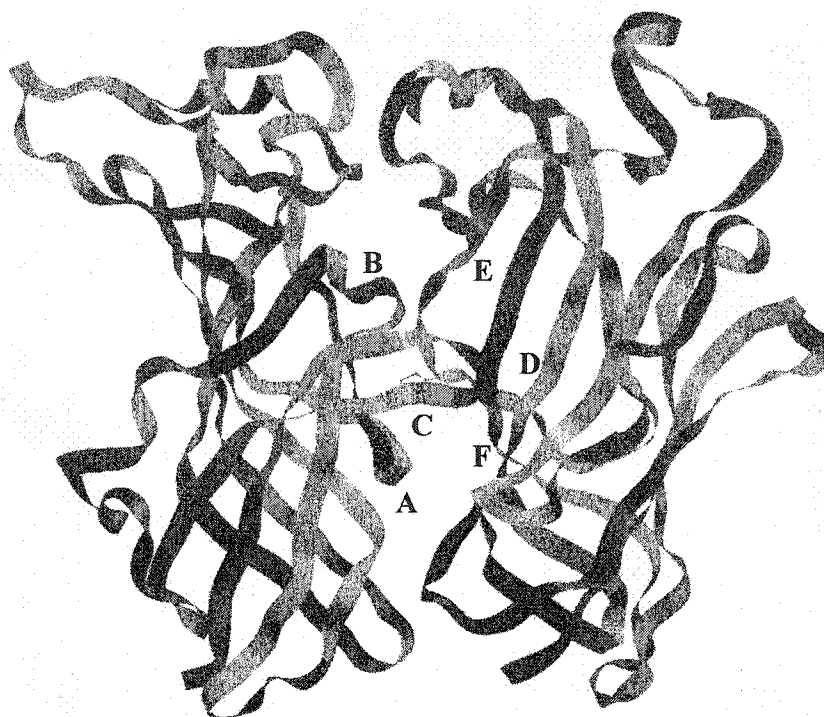


**Figure 1.3: 5-HT<sub>3A</sub> R homology model based on acetylcholine binding protein (AChBP)**

The backbone of the 5-HT<sub>3A</sub>R homology model in dimeric ribbon form is shown. The cleft between two subunits forms the binding site. The 'principal' face on left hand side contributes three discontinuous regions ('loops') to the binding site, named A, B and C. On the right hand side, the 'complimentary' face contributes another three discontinuous regions ('loops') to the binding site, named D, E and F. Role of region F in ligand-binding is yet to be demonstrated.

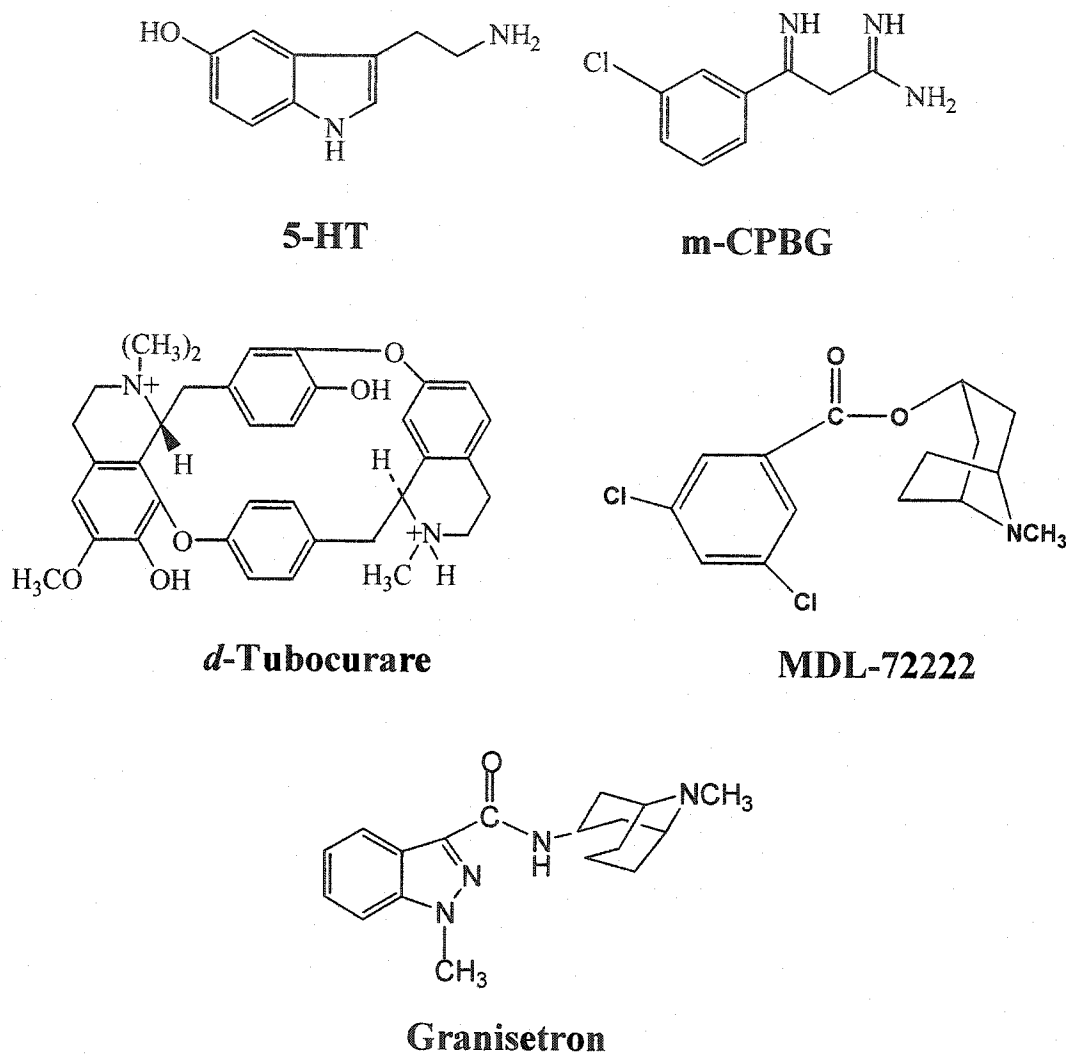


Figure 1.4: 5-HT<sub>3A</sub>R ligands

## References

- Akasu T, Hasuo H and Tokimasa T (1987) Activation of 5-HT<sub>3</sub> receptor subtypes causes rapid excitation of rabbit parasympathetic neurones. *Br J Pharmacol* **91**(3):453-455.
- Andresen V and Hollerbach S (2004) Reassessing the benefits and risks of alosetron: what is its place in the treatment of irritable bowel syndrome? *Drug Saf* **27**(5):283-292.
- Arias HR (2000) Localization of agonist and competitive antagonist binding sites on nicotinic acetylcholine receptors. *Neurochem Int* **36**(7):595-645.
- Barann M, Gothert M, Bonisch H, Dybek A and Urban BW (1997) 5-HT<sub>3</sub> receptors in outside-out patches of N1E-115 neuroblastoma cells: basic properties and effects of pentobarbital. *Neuropharmacology* **36**(4-5):655-664.
- Barann M, Molderings G, Bruss M, Bonisch H, Urban BW and Gothert M (2002) Direct inhibition by cannabinoids of human 5-HT<sub>3A</sub> receptors: probable involvement of an allosteric modulatory site. *Br J Pharmacol* **137**(5):589-596.
- Barnes JM, Barnes NM, Costall B, Ironside JW and Naylor RJ (1989) Identification and characterisation of 5-hydroxytryptamine 3 recognition sites in human brain tissue. *J Neurochem* **53**(6):1787-1793.
- Bartrup JT and Newberry NR (1996) Electrophysiological consequences of ligand binding to the desensitized 5-HT<sub>3</sub> receptor in mammalian NG108-15 cells. *J Physiol* **490** (Pt 3):679-690.
- Beene DL, Brandt GS, Zhong W, Zacharias NM, Lester HA and Dougherty DA (2002) Cation- $\pi$  interactions in ligand recognition by serotonergic (5-HT<sub>3A</sub>) and nicotinic acetylcholine receptors: the anomalous binding properties of nicotine. *Biochemistry* **41**(32):10262-10269.
- Belelli D, Balcerek JM, Hope AG, Peters JA, Lambert JJ and Blackburn TP (1995) Cloning and functional expression of a human 5-hydroxytryptamine type 3A receptor subunit. *Mol Pharmacol* **48**(6):1054-1062.
- Boess FG, Beroukhim R and Martin IL (1995) Ultrastructure of the 5-hydroxytryptamine<sub>3</sub> receptor. *J Neurochem* **64**(3):1401-1405.
- Boess FG, Steward LJ, Steele JA, Liu D, Reid J, Glencorse TA and Martin IL (1997) Analysis of the ligand binding site of the 5-HT<sub>3</sub> receptor using site directed mutagenesis: importance of glutamate 106. *Neuropharmacology* **36**(4-5):637-647.

- Boyd GW, Low P, Dunlop JI, Robertson LA, Vardy A, Lambert JJ, Peters JA and Connolly CN (2002) Assembly and cell surface expression of homomeric and heteromeric 5-HT<sub>3</sub> receptors: the role of oligomerization and chaperone proteins. *Mol Cell Neurosci* **21**(1):38-50.
- Brejc K, van Dijk WJ, Klaassen RV, Schuurmans M, van Der Oost J, Smit AB and Sixma TK (2001) Crystal structure of an ACh-binding protein reveals the ligand-binding domain of nicotinic receptors. *Nature* **411**(6835):269-276.
- Brejc K, van Dijk WJ, Smit AB and Sixma TK (2002) The 2.7 Å structure of AChBP, homologue of the ligand-binding domain of the nicotinic acetylcholine receptor. *Novartis Found Symp* **245**:22-29; discussion 29-32, 165-168.
- Carley DW, Depoortere H and Radulovacki M (2001) R-zacopride, a 5-HT<sub>3</sub> antagonist/5-HT<sub>4</sub> agonist, reduces sleep apneas in rats. *Pharmacol Biochem Behav* **69**(1-2):283-289.
- Carta M, Allan AM, Partridge LD and Valenzuela CF (2003) Cocaine inhibits 5-HT<sub>3</sub> receptor function in neurons from transgenic mice overexpressing the receptor. *Eur J Pharmacol* **459**(2-3):167-169.
- Chakrapani S, Bailey TD and Auerbach A (2004) Gating dynamics of the acetylcholine receptor extracellular domain. *J Gen Physiol* **123**(4):341-356.
- Clements JD, Feltz A, Sahara Y and Westbrook GL (1998) Activation kinetics of AMPA receptor channels reveal the number of functional agonist binding sites. *J Neurosci* **18**(1):119-127.
- Costall B, Domeney AM, Naylor RJ and Tyers MB (1987) Effects of the 5-HT<sub>3</sub> receptor antagonist, GR38032F, on raised dopaminergic activity in the mesolimbic system of the rat and marmoset brain. *Br J Pharmacol* **92**(4):881-894.
- Costall B and Naylor RJ (2004) 5-HT<sub>3</sub> receptors. *Curr Drug Targets CNS Neurol Disord* **3**(1):27-37.
- Davies PA, Pistis M, Hanna MC, Peters JA, Lambert JJ, Hales TG and Kirkness EF (1999) The 5-HT<sub>3B</sub> subunit is a major determinant of serotonin-receptor function. *Nature* **397**(6717):359-363.
- Derkach V, Surprenant A and North RA (1989) 5-HT<sub>3</sub> receptors are membrane ion channels. *Nature* **339**(6227):706-709.
- Eid CN, Jr. and Rose GM (1999) Cognition enhancement strategies by ion channel modulation of neurotransmission. *Curr Pharm Des* **5**(5):345-361.

- Eisele JL, Bertrand S, Galzi JL, Devillers-Thiery A, Changeux JP and Bertrand D (1993) Chimaeric nicotinic-serotonergic receptor combines distinct ligand binding and channel specificities. *Nature* **366**(6454):479-483.
- England LJ, Imperial J, Jacobsen R, Craig AG, Gulyas J, Akhtar M, Rivier J, Julius D and Olivera BM (1998) Inactivation of a serotonin-gated ion channel by a polypeptide toxin from marine snails. *Science* **281**(5376):575-578.
- Evans RJ, Derkach V and Surprenant A (1992) ATP mediates fast synaptic transmission in mammalian neurons. *Nature* **357**(6378):503-505.
- Fan P (1995) Cannabinoid agonists inhibit the activation of 5-HT<sub>3</sub> receptors in rat nodose ganglion neurons. *J Neurophysiol* **73**(2):907-910.
- Fan P, Oz M, Zhang L and Weight FF (1995) Effect of cocaine on the 5-HT<sub>3</sub> receptor-mediated ion current in *Xenopus* oocytes. *Brain Res* **673**(2):181-184.
- Faris PL, Kim SW, Meller WH, Goodale RL, Hofbauer RD, Oakman SA, Howard LA, Stevens ER, Eckert ED and Hartman BK (1998) Effect of ondansetron, a 5-HT<sub>3</sub> receptor antagonist, on the dynamic association between bulimic behaviors and pain thresholds. *Pain* **77**(3):297-303.
- Faris PL, Kim SW, Meller WH, Goodale RL, Oakman SA, Hofbauer RD, Marshall AM, Daughters RS, Banerjee-Stevens D, Eckert ED and Hartman BK (2000) Effect of decreasing afferent vagal activity with ondansetron on symptoms of bulimia nervosa: a randomised, double-blind trial. *Lancet* **355**(9206):792-797.
- Gaddum JH and Picarelli ZP (1957) Two kinds of tryptamine receptor. *Br J Pharmacol* **12**(3):323-328.
- Gil-Bea FJ, Dominguez J, Garcia-Alloza M, Marcos B, Lasheras B and Ramirez MJ (2004) Facilitation of cholinergic transmission by combined treatment of ondansetron with flumazenil after cortical cholinergic deafferentation. *Neuropharmacology* **47**(2):225-232.
- Gill CH, Peters JA and Lambert JJ (1995) An electrophysiological investigation of the properties of a murine recombinant 5-HT<sub>3</sub> receptor stably expressed in HEK 293 cells. *Br J Pharmacol* **114**(6):1211-1221.
- Glatzle J, Sternini C, Robin C, Zittel TT, Wong H, Reeve JR, Jr. and Raybould HE (2002) Expression of 5-HT<sub>3</sub> receptors in the rat gastrointestinal tract. *Gastroenterology* **123**(1):217-226.
- Grailhe R, de Carvalho LP, Paas Y, Le Poupon C, Soudant M, Bregestovski P, Changeux JP and Corringer PJ (2004) Distinct subcellular targeting of fluorescent nicotinic

- alpha 3 beta 4 and serotonergic 5-HT<sub>3A</sub> receptors in hippocampal neurons. *Eur J Neurosci* **19**(4):855-862.
- Green T, Stauffer KA and Lummis SC (1995) Expression of recombinant homo-oligomeric 5-hydroxytryptamine<sub>3</sub> receptors provides new insights into their maturation and structure. *J Biol Chem* **270**(11):6056-6061.
- Grewer C (1999) Investigation of the alpha(1)-glycine receptor channel-opening kinetics in the submillisecond time domain. *Biophys J* **77**(2):727-738.
- Gunthorpe MJ and Lummis SC (1999) Diltiazem causes open channel block of recombinant 5-HT<sub>3</sub> receptors. *J Physiol* **519 Pt 3**:713-722.
- Gurley DA and Lanthorn TH (1998) Nicotinic agonists competitively antagonize serotonin at mouse 5-HT<sub>3</sub> receptors expressed in *Xenopus* oocytes. *Neurosci Lett* **247**(2-3):107-110.
- Hasler WL (2000) 5-HT<sub>3</sub> antagonist therapy of bulimia nervosa: a peripherally active agent for a central nervous system eating disorder? *Gastroenterology* **119**(1):271-272.
- Hensler JG, Hodge CW and Overstreet DH (2004) Reduced 5-HT<sub>3</sub> receptor binding and lower baseline plus maze anxiety in the alcohol-preferring inbred fawn-hooded rat. *Pharmacol Biochem Behav* **77**(2):281-289.
- Hibert MF, Hoffmann R, Miller RC and Carr AA (1990) Conformation-activity relationship study of 5-HT<sub>3</sub> receptor antagonists and a definition of a model for this receptor site. *J Med Chem* **33**(6):1594-1600.
- Hovius R, Schmid EL, Tairi AP, Blasey H, Bernard AR, Lundstrom K and Vogel H (1999) Fluorescence techniques for fundamental and applied studies of membrane protein receptors: the 5-HT<sub>3</sub> serotonin receptor. *J Recept Signal Transduct Res* **19**(1-4):533-545.
- Hovius R, Tairi AP, Blasey H, Bernard A, Lundstrom K and Vogel H (1998) Characterization of a mouse serotonin 5-HT<sub>3</sub> receptor purified from mammalian cells. *J Neurochem* **70**(2):824-834.
- Hu XQ, Zhang L, Stewart RR and Weight FF (2003) Arginine 222 in the pre-transmembrane domain 1 of 5-HT<sub>3A</sub> receptors links agonist binding to channel gating. *J Biol Chem* **278**(47):46583-46589.
- Hubbard PC and Lummis SC (2000) Zn<sup>2+</sup> enhancement of the recombinant 5-HT<sub>3</sub> receptor is modulated by divalent cations. *Eur J Pharmacol* **394**(2-3):189-197.

- Hussy N, Lukas W and Jones KA (1994) Functional properties of a cloned 5-hydroxytryptamine ionotropic receptor subunit: comparison with native mouse receptors. *J Physiol* **481** (Pt 2):311-323.
- Jackson MB and Yakel JL (1995) The 5-HT<sub>3</sub> receptor channel. *Annu Rev Physiol* **57**:447-468.
- Johnson BA (2003) The role of serotonergic agents as treatments for alcoholism. *Drugs Today (Barc)* **39**(9):665-672.
- Jones S and Yakel JL (1998) Calcium influx through voltage-gated calcium channels regulates 5-HT<sub>3</sub> receptor channel desensitization in NG108-15 cells. *Ann N Y Acad Sci* **861**:253-254.
- Joshi PR, Suryanarayanan A and Schulte MK (2004) A vertical flow chamber for *Xenopus* oocyte electrophysiology and automated drug screening. *J Neurosci Methods* **132**(1):69-79.
- Karlin A (2002) Emerging structure of the nicotinic acetylcholine receptors. *Nat Rev Neurosci* **3**(2):102-114.
- Karnovsky AM, Gotow LF, McKinley DD, Piechan JL, Ruble CL, Mills CJ, Schellin KA, Slightom JL, Fitzgerald LR, Benjamin CW and Roberds SL (2003) A cluster of novel serotonin receptor 3-like genes on human chromosome 3. *Gene* **319**:137-148.
- Kelley SP, Dunlop JI, Kirkness EF, Lambert JJ and Peters JA (2003) A cytoplasmic region determines single-channel conductance in 5-HT<sub>3</sub> receptors. *Nature* **424**(6946):321-324.
- Kilpatrick GJ, Jones BJ and Tyers MB (1987) Identification and distribution of 5-HT<sub>3</sub> receptors in rat brain using radio-ligand binding. *Nature* **330**(6150):746-748.
- King GR, Xiong Z, Douglass S and Ellinwood EH (2000) Long-term blockade of the expression of cocaine sensitization by ondansetron, a 5-HT<sub>3</sub> receptor antagonist. *Eur J Pharmacol* **394**(1):97-101.
- King GR, Xiong Z and Ellinwood EH, Jr. (1997) Blockade of cocaine sensitization and tolerance by the co-administration of ondansetron, a 5-HT<sub>3</sub> receptor antagonist, and cocaine. *Psychopharmacology (Berl)* **130**(2):159-165.
- Kordasti S, Sjovall H, Lundgren O and Svensson L (2004) Serotonin and vasoactive intestinal peptide antagonists attenuate rotavirus diarrhoea. *Gut* **53**(7):952-957.



- Koshizaki M, Kawamata M, Shimada SG, Saito Y and Collins JG (2003) 5-HT<sub>3</sub> receptors partially mediate halothane depression of spinal dorsal horn sensory neurons. *Anesth Analg* **96**(4):1027-1031, table of contents.
- Kostowski W, Dyr W and Krzascik P (1993) The abilities of 5-HT<sub>3</sub> receptor antagonist ICS 205-930 to inhibit alcohol preference and withdrawal seizures in rats. *Alcohol* **10**(5):369-373.
- Kostowski W, Sikora J, Bisaga A and Rosnowska E (1995) Effects of 5-HT<sub>3</sub> receptor antagonists on ethanol-induced hyperlocomotion in mice. *Pol J Pharmacol* **47**(4):293-297.
- Lankiewicz S, Lobitz N, Wetzel CH, Rupprecht R, Gisselmann G and Hatt H (1998) Molecular cloning, functional expression, and pharmacological characterization of 5-hydroxytryptamine<sub>3</sub> receptor cDNA and its splice variants from guinea pig. *Mol Pharmacol* **53**(2):202-212.
- Liu Y and Dilger JP (1991) Opening rate of acetylcholine receptor channels. *Biophys J* **60**(2):424-432.
- Lopreato GF, Banerjee P and Mihic SJ (2003a) Amino acids in transmembrane domain two influence anesthetic enhancement of serotonin-3A receptor function. *Brain Res Mol Brain Res* **118**(1-2):45-51.
- Lopreato GF, Phelan R, Borghese CM, Beckstead MJ and Mihic SJ (2003b) Inhaled drugs of abuse enhance serotonin-3 receptor function. *Drug Alcohol Depend* **70**(1):11-15.
- Lummiss SC and Baker J (1997) Radio-ligand binding and photoaffinity labelling studies show a direct interaction of phenothiazines at 5-HT<sub>3</sub> receptors. *Neuropharmacology* **36**(4-5):665-670.
- Lummiss SC and Martin IL (1992) Solubilization, purification, and functional reconstitution of 5-hydroxytryptamine<sub>3</sub> receptors from N1E-115 neuroblastoma cells. *Mol Pharmacol* **41**(1):18-23.
- Machu TK and Harris RA (1994) Alcohols and anesthetics enhance the function of 5-hydroxytryptamine<sub>3</sub> receptors expressed in *Xenopus laevis* oocytes. *J Pharmacol Exp Ther* **271**(2):898-905.
- Maconochie DJ, Zempel JM and Steinbach JH (1994) How quickly can GABA<sub>A</sub> receptors open? *Neuron* **12**(1):61-71.

- Maksay G, Bikadi Z and Simonyi M (2003) Binding interactions of antagonists with 5-hydroxytryptamine<sub>3A</sub> receptor models. *J Recept Signal Transduct Res* **23**(2-3):255-270.
- Maricq AV, Peterson AS, Brake AJ, Myers RM and Julius D (1991) Primary structure and functional expression of the 5HT<sub>3</sub> receptor, a serotonin-gated ion channel. *Science* **254**(5030):432-437.
- Matsuzawa S, Suzuki T, Misawa M and Nagase H (1999) Roles of 5-HT<sub>3</sub> and opioid receptors in the ethanol-induced place preference in rats exposed to conditioned fear stress. *Life Sci* **64**(21):PL241-249.
- McBride WJ, Lovinger DM, Machu T, Thielen RJ, Rodd ZA, Murphy JM, Roache JD and Johnson BA (2004) Serotonin-3 receptors in the actions of alcohol, alcohol reinforcement, and alcoholism. *Alcohol Clin Exp Res* **28**(2):257-267.
- McKernan RM, Gillard NP, Quirk K, Kneen CO, Stevenson GI, Swain CJ and Ragan CI (1990) Purification of the 5-hydroxytryptamine 5-HT<sub>3</sub> receptor from NCB20 cells. *J Biol Chem* **265**(23):13572-13577.
- Mhatre M, Pruthi R, Hensley K and Holloway F (2004) 5-HT<sub>3</sub> antagonist ICS 205-930 enhances naltrexone's effects on ethanol intake. *Eur J Pharmacol* **491**(2-3):149-156.
- Mhatre MC, Garrett KM and Holloway FA (2001) 5-HT<sub>3</sub> receptor antagonist ICS 205-930 alters the discriminative effects of ethanol. *Pharmacol Biochem Behav* **68**(1):163-170.
- Miyazawa A, Fujiyoshi Y and Unwin N (2003) Structure and gating mechanism of the acetylcholine receptor pore. *Nature* **423**(6943):949-955.
- Morales M, Battenberg E and Bloom FE (1998) Distribution of neurons expressing immunoreactivity for the 5HT<sub>3</sub> receptor subtype in the rat brain and spinal cord. *J Comp Neurol* **402**(3):385-401.
- Morales M, Battenberg E, de Lecea L, Sanna PP and Bloom FE (1996) Cellular and subcellular immunolocalization of the type 3 serotonin receptor in the rat central nervous system. *Brain Res Mol Brain Res* **36**(2):251-260.
- Morales M and Wang SD (2002) Differential composition of 5-hydroxytryptamine<sub>3</sub> receptors synthesized in the rat CNS and peripheral nervous system. *J Neurosci* **22**(15):6732-6741.

- Mosbacher J, Schoepfer R, Monyer H, Burnashev N, Seeburg PH and Ruppertsberg JP (1994) A molecular determinant for submillisecond desensitization in glutamate receptors. *Science* **266**(5187):1059-1062.
- Mott DD, Erreger K, Banke TG and Traynelis SF (2001) Open probability of homomeric murine 5-HT<sub>3A</sub> serotonin receptors depends on subunit occupancy. *J Physiol* **535**(Pt 2):427-443.
- Mu TW, Lester HA and Dougherty DA (2003) Different binding orientations for the same agonist at homologous receptors: a lock and key or a simple wedge? *J Am Chem Soc* **125**(23):6850-6851.
- Naranjo CA and Bremner KE (1993) Clinical pharmacology of serotonin-altering medications for decreasing alcohol consumption. *Alcohol Alcohol Suppl* **2**:221-229.
- Neijt HC, Plomp JJ and Vijverberg HP (1989) Kinetics of the membrane current mediated by serotonin 5-HT<sub>3</sub> receptors in cultured mouse neuroblastoma cells. *J Physiol* **411**:257-269.
- Niemeyer MI and Lummis SC (1998) Different efficacy of specific agonists at 5-HT<sub>3</sub> receptor splice variants: the role of the extra six amino acid segment. *Br J Pharmacol* **123**(4):661-666.
- Niemeyer MI and Lummis SC (2001) The role of the agonist binding site in Ca<sup>2+</sup> inhibition of the recombinant 5-HT<sub>3A</sub> receptor. *Eur J Pharmacol* **428**(2):153-161.
- Niesler B, Frank B, Kapeller J and Rappold GA (2003) Cloning, physical mapping and expression analysis of the human 5-HT<sub>3</sub> serotonin receptor-like genes HTR3C, HTR3D and HTR3E. *Gene* **310**:101-111.
- Orjales A, Mosquera R, Labeaga L and Rodes R (1997) New 2-piperazinylbenzimidazole derivatives as 5-HT<sub>3</sub> antagonists. Synthesis and pharmacological evaluation. *J Med Chem* **40**(4):586-593.
- Oz M, Zhang L and Morales M (2002a) Endogenous cannabinoid, anandamide, acts as a noncompetitive inhibitor on 5-HT<sub>3</sub> receptor-mediated responses in *Xenopus* oocytes. *Synapse* **46**(3):150-156.
- Oz M, Zhang L and Spivak CE (2002b) Direct noncompetitive inhibition of 5-HT<sub>3</sub> receptor-mediated responses by forskolin and steroids. *Arch Biochem Biophys* **404**(2):293-301.

- Parihar HS, Suryanarayanan A, Ma C, Joshi P, Venkataraman P, Schulte MK and Kirschbaum KS (2001) 5-HT<sub>3</sub>R binding of lerisetron: an interdisciplinary approach to drug-Receptor interactions. *Bioorg Med Chem Lett* **11**(16):2133-2136.
- Quirk PL, Rao S, Roth BL and Siegel RE (2004) Three putative N-glycosylation sites within the murine 5-HT<sub>3</sub>(A) receptor sequence affect plasma membrane targeting, ligand binding, and calcium influx in heterologous mammalian cells. *J Neurosci Res* **77**(4):498-506.
- Rammes G, Eisensamer B, Ferrari U, Shapa M, Gimpl G, Gilling K, Parsons C, Riering K, Hapfelmeier G, Bondy B, Zieglgansberger W, Holsboer F and Rupprecht R (2004) Antipsychotic drugs antagonize human serotonin type 3 receptor currents in a noncompetitive manner. *Mol Psychiatry*.
- Reeves DC and Lummis SC (2002) The molecular basis of the structure and function of the 5-HT<sub>3</sub> receptor: a model ligand-gated ion channel (review). *Mol Membr Biol* **19**(1):11-26.
- Reeves DC, Sayed MF, Chau PL, Price KL and Lummis SC (2003) Prediction of 5-HT<sub>3</sub> receptor agonist-binding residues using homology modeling. *Biophys J* **84**(4):2338-2344.
- Ricci LA, Stellar JR and Todtenkopf MS (2004) Subregion-specific down-regulation of 5-HT<sub>3</sub> immunoreactivity in the nucleus accumbens shell during the induction of cocaine sensitization. *Pharmacol Biochem Behav* **77**(3):415-422.
- Rigler P, Ulrich WP, Hovius R, Ilegems E, Pick H and Vogel H (2003) Downscaling Fourier transform infrared spectroscopy to the micrometer and nanogram scale: secondary structure of serotonin and acetylcholine receptors. *Biochemistry* **42**(47):14017-14022.
- Schreiter C, Hovius R, Costioli M, Pick H, Kellenberger S, Schild L and Vogel H (2003) Characterization of the ligand-binding site of the serotonin 5-HT<sub>3</sub> receptor: the role of glutamate residues 97, 224, AND 235. *J Biol Chem* **278**(25):22709-22716.
- Sepulveda MI, Baker J and Lummis SC (1994) Chlorpromazine and QX222 block 5-HT<sub>3</sub> receptors in N1E-115 neuroblastoma cells. *Neuropharmacology* **33**(3-4):493-499.
- Sirota P, Mosheva T, Shabtay H, Giladi N and Korczyn AD (2000) Use of the selective serotonin 3 receptor antagonist ondansetron in the treatment of neuroleptic-induced tardive dyskinesia. *Am J Psychiatry* **157**(2):287-289.

- Spier AD and Lummis SC (2000) The role of tryptophan residues in the 5-Hydroxytryptamine(3) receptor ligand binding domain. *J Biol Chem* **275**(8):5620-5625.
- Steward LJ, Boess FG, Steele JA, Liu D, Wong N and Martin IL (2000) Importance of phenylalanine 107 in agonist recognition by the 5-hydroxytryptamine(3A) receptor. *Mol Pharmacol* **57**(6):1249-1255.
- Stewart A, Davies PA, Kirkness EF, Safa P and Hales TG (2003) Introduction of the 5-HT3B subunit alters the functional properties of 5-HT3 receptors native to neuroblastoma cells. *Neuropharmacology* **44**(2):214-223.
- Surprenant A and Crist J (1988) Electrophysiological characterization of functionally distinct 5-hydroxytryptamine receptors on guinea-pig submucous plexus. *Neuroscience* **24**(1):283-295.
- Suzuki T, Koyama H, Sugimoto M, Uchida I and Mashimo T (2002) The diverse actions of volatile and gaseous anesthetics on human-cloned 5-hydroxytryptamine3 receptors expressed in *Xenopus* oocytes. *Anesthesiology* **96**(3):699-704.
- Suzuki T, Sugimoto M, Koyama H, Mashimo T and Uchida I (2004) Inhibitory effect of glucocorticoids on human-cloned 5-hydroxytryptamine3A receptor expressed in *xenopus* oocytes. *Anesthesiology* **101**(3):660-665.
- Tecott LH, Maricq AV and Julius D (1993) Nervous system distribution of the serotonin 5-HT3 receptor mRNA. *Proc Natl Acad Sci US A* **90**(4):1430-1434.
- van Hooft JA and Vijverberg HP (1996) Selection of distinct conformational states of the 5-HT3 receptor by full and partial agonists. *Br J Pharmacol* **117**(5):839-846.
- van Hooft JA and Vijverberg HP (1997) Full and partial agonists induce distinct desensitized states of the 5-HT3 receptor. *J Recept Signal Transduct Res* **17**(1-3):267-277.
- Veasey SC (2003) Serotonin agonists and antagonists in obstructive sleep apnea: therapeutic potential. *Am J Respir Med* **2**(1):21-29.
- Veasey SC, Chachkes J, Fenik P and Hendricks JC (2001) The effects of ondansetron on sleep-disordered breathing in the English bulldog. *Sleep* **24**(2):155-160.
- Venkataraman P, Joshi P, Venkatachalan SP, Muthalagi M, Parihar HS, Kirschbaum KS and Schulte MK (2002a) Functional group interactions of a 5-HT3R antagonist. *BMC Biochem* **3**(1):16.

- Venkataraman P, Venkatachalan SP, Joshi PR, Muthalagi M and Schulte MK (2002b) Identification of critical residues in loop E in the 5-HT<sub>3</sub>ASR binding site. *BMC Biochem* 3(1):15.
- Waeber C, Hoyer D and Palacios JM (1989) 5-hydroxytryptamine<sub>3</sub> receptors in the human brain: autoradiographic visualization using [<sup>3</sup>H]ICS 205-930. *Neuroscience* 31(2):393-400.
- Wetzel CH, Hermann B, Behl C, Pestel E, Rammes G, Zieglgansberger W, Holsboer F and Rupprecht R (1998) Functional antagonism of gonadal steroids at the 5-hydroxytryptamine type 3 receptor. *Mol Endocrinol* 12(9):1441-1451.
- Yakel JL and Jackson MB (1988) 5-HT<sub>3</sub> receptors mediate rapid responses in cultured hippocampus and a clonal cell line. *Neuron* 1(7):615-621.
- Yakel JL, Shao XM and Jackson MB (1991) Activation and desensitization of the 5-HT<sub>3</sub> receptor in a rat glioma x mouse neuroblastoma hybrid cell. *J Physiol* 436:293-308.
- Yan D, Schulte MK, Bloom KE and White MM (1999) Structural features of the ligand-binding domain of the serotonin 5HT<sub>3</sub> receptor. *J Biol Chem* 274(9):5537-5541.
- Yan D and White MM (2002) Interaction of d-tubocurarine analogs with mutant 5-HT<sub>3</sub>(3) receptors. *Neuropharmacology* 43(3):367-373.
- Yang HS, Kim SY, Choi SJ, Kim KJ, Kim ON, Lee SB and Sung KW (2003) Effect of 5-hydroxyindole on ethanol potentiation of 5-hydroxytryptamine (5-HT)<sub>3</sub> receptor-activated ion current in NCB-20 neuroblastoma cells. *Neurosci Lett* 338(1):72-76.
- Yang J, Mathie A and Hille B (1992) 5-HT<sub>3</sub> receptor channels in dissociated rat superior cervical ganglion neurons. *J Physiol* 448:237-256.
- Yang Z, Xu H, Cui N, Qu Z, Chanchevalap S, Shen W and Jiang C (2000) Biophysical and molecular mechanisms underlying the modulation of heteromeric Kir4.1-Kir5.1 channels by CO<sub>2</sub> and pH. *J Gen Physiol* 116(1):33-45.
- Zhang L, Hosoi M, Fukuzawa M, Sun H, Rawlings RR and Weight FF (2002) Distinct molecular basis for differential sensitivity of the serotonin type 3A receptor to ethanol in the absence and presence of agonist. *J Biol Chem* 277(48):46256-46264.
- Zhang L, Oz M, Stewart RR, Peoples RW and Weight FF (1997) Volatile general anaesthetic actions on recombinant nACh alpha 7, 5-HT<sub>3</sub> and chimeric nACh alpha 7-5-HT<sub>3</sub> receptors expressed in *Xenopus* oocytes. *Br J Pharmacol* 120(3):353-355.

Zhong W, Gallivan JP, Zhang Y, Li L, Lester HA and Dougherty DA (1998) From ab initio quantum mechanics to molecular neurobiology: a cation- $\pi$  binding site in the nicotinic receptor. *Proc Natl Acad Sci U S A* **95**(21):12088-12093.

Zhou Q, Verdoorn TA and Lovinger DM (1998) Alcohols potentiate the function of 5-HT<sub>3</sub> receptor-channels on NCB-20 neuroblastoma cells by favouring and stabilizing the open channel state. *J Physiol* **507** (Pt 2):335-352.

## **Chapter 2: Hypotheses, research design and data analysis**

### **2.1 Introduction**

Proteins are complex macromolecules. Investigations into the nature of a protein's ligand-binding site are critical to the understanding protein function. Understanding ligand-binding site interactions leads to better understanding of protein function in general and development of better ligands in particular. The structural and functional diversity of proteins arises mainly from differences in the primary structure, since primary structure is responsible for positioning both the protein backbone and amino acid side chains. The analysis of structure-function relationship of proteins can be achieved through a variety of means. Mutagenesis remains the mainstay method for structure-function analysis of membrane-bound proteins or receptors. Mutagenesis is used to investigate the role of individual amino acids in normal functioning of the protein. While site-directed mutagenesis is the most widely employed method, other methods such as photo-affinity labeling and internal fluorescence measurements can also be utilized.

### **2.2 Gaps in the knowledge of murine 5-HT<sub>3A</sub>R structure-function correlations**

The following section briefly describes some of the gaps in the knowledge of 5-HT<sub>3A</sub>R function at the molecular level. Some of these identified gaps form the basis of research presented in this thesis.

#### **2.2.1 5-HT<sub>3A</sub> R ligand-binding domain**

At the beginning of the studies described here (year 2000), the general topology of the 5-HT<sub>3A</sub>R binding site was unknown. It was however hypothesized that the general topology



of the binding domain is similar to that of the nicotinic acetylcholine receptor. Amino acids in the purported ligand-binding domain had been postulated on the basis of sequence homology with the nicotinic acetylcholine receptor. Although a few select residues had been confirmed by mutagenesis (D89, R91, W183, F129), a systematic analysis of the binding site was not available.

The first attempt at such an analysis was made with an alanine scanning mutagenesis study of the purported loop E conducted in our laboratory. Using a systematic approach, this study identified residues Y141, Y143 and Y153. These studies also defined the involvement of these amino acids in purported interactions with antagonists lerisetron and *d*-TC. However, a detailed analysis of the role played by these amino acids in agonist action and agonist-induced conformational changes was unavailable.

### **2.2.2 5-HT<sub>3A</sub>R agonist specificities**

Structurally distinct agonists of the 5-HT<sub>3A</sub>R display distinct pharmacological (EC<sub>50</sub> obtained from electrophysiological assays, K<sub>i</sub> values obtained from competition radioligand binding assays and maximal efficacy) as well as biophysical parameters (activation and desensitization parameters). The structural basis for these differences remains unexplored. Few studies have explored the biochemical basis of antagonist specificity. Utilizing structurally distinct antagonists along with mutations at the ligand-binding domain, our lab has probed the specificity of granisetron, lerisetron and *d*-TC (Venkataraman et al., 2002a; Venkataraman et al., 2002b). No such study involving structurally distinct agonists of the 5-HT<sub>3A</sub>R had been reported.

### 2.2.3 5-HT<sub>3A</sub>R mechanism of activation and desensitization.

The dynamics of 5-HT<sub>3A</sub>R activation and desensitization were largely unknown. The available data on the ligand-binding site amino acid residues mostly described a static state of receptor-ligand interaction. However, the interaction of agonist with the ligand-binding site is followed by events that produce the conformational changes leading to channel opening. Channel opening is presumably followed by desensitization, which is accompanied by distinct conformational changes. No study had systematically explored the role of purported ligand-binding residues in mediating the conformational changes associated with channel opening and desensitization.

Use of 5-HT<sub>3A</sub>R, a homo-pentameric protein, provides a simple model for explorations into the functional dynamics of a ligand-gated ion channel. Since all five ligand-binding domains are presumably identical, it is simpler to correlate the effect of a mutation at a global level.

### 2.3 Scope for improvement in methodologies pertaining to *Xenopus* oocyte electrophysiology

*Xenopus* oocytes have been used extensively in the studies of ion channels. An exceptional amount of versatility (in terms of types of proteins expressed as well as types of assays performed) is provided by use of this system. In the case of ligand-gated ion channels, *Xenopus* oocytes allow sufficient receptor expression as well as measurement of various parameters such as activation and desensitization rates. Use of two-electrode voltage-clamp and *Xenopus* oocytes to characterize ligand-gated ion channels is relatively easier compared to the use of whole-cell patch-clamp assay and mammalian cells. Use of

oocytes provides yet another advantage. The expression of various mutant proteins is probably better handled by oocytes compared to mammalian cells. In certain cases, it is possible to obtain detectable levels of receptor expression only using *Xenopus* oocytes.

Given the importance of oocyte electrophysiology in 5-HT<sub>3A</sub>R research, it is imperative that the measurements obtained be as accurate as possible. However, conventional methods of oocyte electrophysiology lack required fidelity, with low rates of drug perfusion and unstable environment preventing long term measurements from a single oocyte.

#### **2.4 Protein homology in structure-function studies**

Proteins can be classified on the basis of similarity in primary structure. The similarity in primary structure usually has an evolutionary origin. In course of evolution, structurally important features of the related proteins (such as structurally important amino acids residues proline and glycine) are conserved, since specific function of a protein is closely related to its structure. Such conservation probably ensures that the basic structural scaffold of the protein is maintained. Thus, it can be assumed that proteins sharing primary structure share tertiary and quaternary structure. In structure-function studies of protein of unknown tertiary and quaternary structure, such an assumption can be used to formulate primary protein models.

The structure-function studies of a protein utilizing site-directed mutagenesis as an approach assumes certain general hypotheses. Site-directed mutagenesis in general and alanine scanning mutagenesis in particular, along with molecular modeling can be

used initially as tools to generate a basic map of the protein. Based on the results obtained from the initial studies, specific hypotheses can be formed and tested

When the work described in this thesis was started, how the structure of the presumed 5-HT<sub>3</sub> receptor ligand-binding domain affected interactions with various ligands and how the function was modulated by ligand interactions was largely unknown. Using the techniques described below and based on the general and specific hypotheses described here, we have been able to generate numerous specific hypotheses, which can be tested in future.

## **2.5 General hypothesis**

Members of the ligand-gated ion channel super-family (LGICS) include 5-HT<sub>3</sub>R, nicotinic acetylcholine receptor, GABA A and C receptor and glycine receptor and acetylcholine binding protein (AChBP). This family is also called the Cys-loop family due to presence of a loop of amino acids in the extracellular domain, flanked by cysteines on both sides. The nicotinic acetylcholine receptor is the prototype receptor. All the proteins are pentamers. Moderately high homology (19-31%) exists between all members. All major structural domains (extra-cellular N-terminal, four transmembrane domains and a short C-tail) are conserved. While low resolution electron micrographs are available for the 5-HT<sub>3</sub>A<sub>R</sub>, the structure of the nicotinic acetylcholine receptor has been resolved at 4Å resolution (Unwin, 2005). The crystal structure of AChBP at 2.7Å resolution is also available. Available data suggests that 5-HT<sub>3</sub>A<sub>R</sub>, nicotinic acetylcholine receptor and AChBP all share the pentameric doughnut-shaped structure. In addition, mutagenesis data for all the members of the LGIC superfamily is available.

All the available information suggests that members of the LGIC superfamily share structural and probably functional features. Based on this general hypothesis, we developed a primary model of the 5-HT<sub>3A</sub>R structure based on all available biochemical data and AChBP crystal structure. We have utilized this primary protein model to interpret initial studies and form specific hypothesis.

## **2.6 Specific hypotheses**

**2.6.1 Antagonist action of lerisetron is mediated mainly by the interaction of its terminal amine with the binding site. This interaction is probably a cation- $\pi$  interaction.**

This hypothesis is based on data from studies on both 5-HT<sub>3A</sub>R and nicotinic acetylcholine receptor. For a detailed description, please refer to section 4.1 of chapter 4.

**2.6.2 Different classes of 5-HT<sub>3A</sub>R ligands mediate their action through distinctly different interactions with loop E amino acid residues.**

Structurally distinct agonists and antagonists use distinctly different molecular interactions to mediate specific effects. This hypothesis is based on the results of initial studies of the loop E region (Venkataraman et al., 2002a; Venkataraman et al., 2002b). These studies indicate that mutations in loop E region affect different classes of antagonists differently. For example, a Y141A mutation specifically alters *d*-TC binding but not granisetron or lerisetron binding. For a detailed description, please refer to section 5.1 of chapter 5.

### **2.6.3 Different classes of 5-HT<sub>3A</sub>R agonists mediate their action through distinctly different modes of receptor gating**

5-HT, a hydroxytryptamine, and *m*CPBG, a phenylbiguanide, are structurally distinct classes of 5-HT<sub>3R</sub> agonists. Preliminary electrophysiological studies of 5-HT<sub>3A</sub> Y153A mutant receptor suggest that amino acid Y153 modulates action of 5-HT and *m*CPBG differentially. A Y153A mutant specifically alters characteristics of 5-HT but not *m*CPBG-elicited inward currents. Based on these results, we hypothesize that structurally distinct 5-HT<sub>3A</sub>R agonists differentially mediate conformational changes associated with channel gating. For a detailed description, please refer to section 4.1 of chapter 4.

### **2.6.4 Amino acids T179 to I190 of 5-HT<sub>3A</sub>R constitute a region of the protein that corresponds to the purported loop B region of the nicotinic acetylcholine receptor. This region plays a critical role in mediating agonist action.**

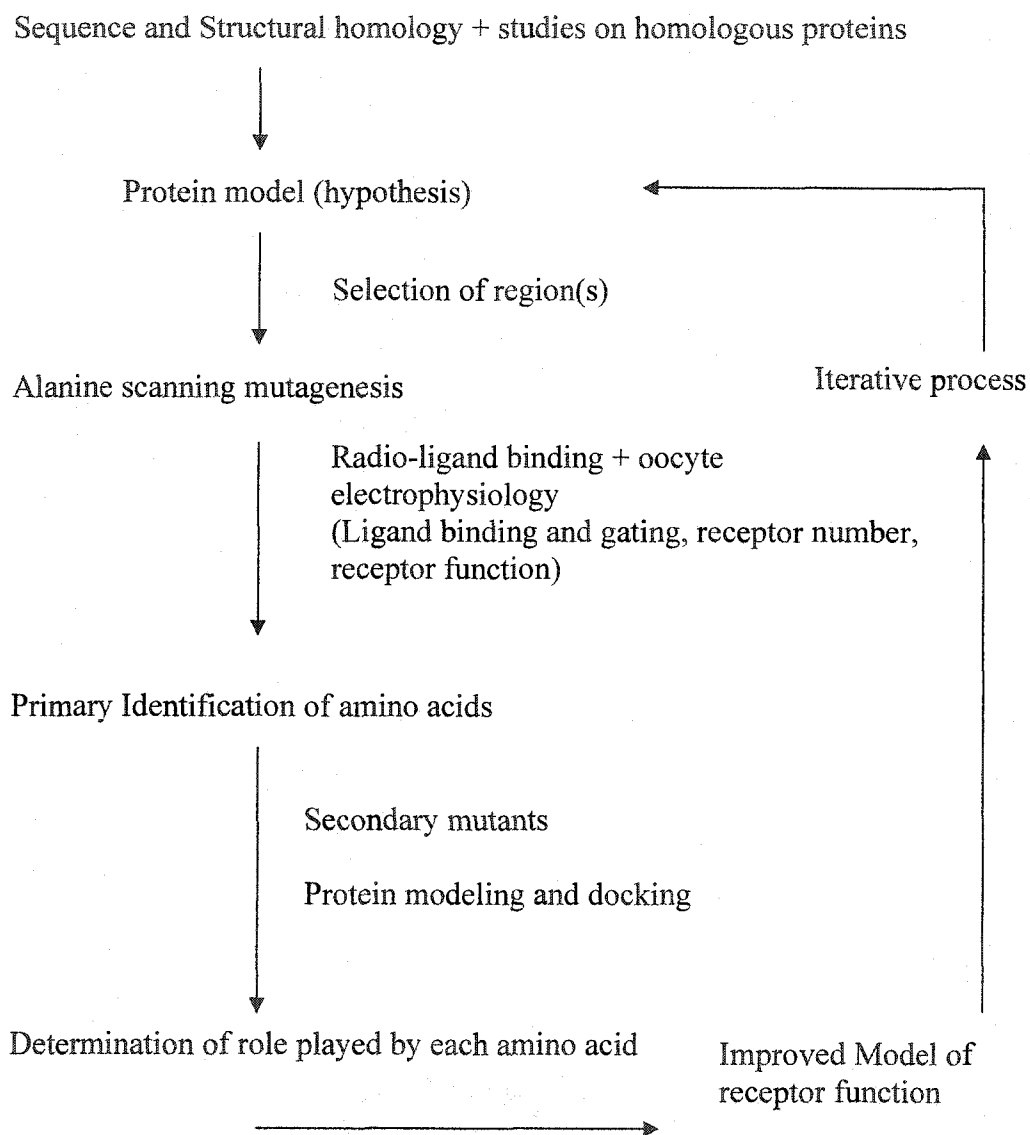
Previous studies support such a hypothesis. W143 of muscle nicotinic acetylcholine receptor and the homologous residue W183 of 5-HT<sub>3A</sub>R have both been shown to be involved in mediating ligand interactions (Beene et al., 2002; Spier and Lummis, 2000). However, detailed analysis of the role of the putative loop B region has not been reported. Using site-directed mutagenesis, we have examined 12 residues of the putative loop B region. For a detailed description, please refer to section 6.1 of chapter 6.

### **2.7 Research design**

The following flow-chart describes an idealized research plan (incorporating basic hypothesis and assumptions) that may be employed in structure-function studies of a protein with unknown structure. The research described in this thesis is designed to test

the hypotheses and in general address the following question: How does the structure of 5-HT<sub>3A</sub>R translate into maintenance of structural integrity, ligand interaction and mediation of conformational changes associated with channel gating?

### Research Design: Binding, Gating, Assembly or a combination?



A detailed description of each of the methods being used follows.



## 2.8 Mutagenesis

Site-directed mutagenesis is widely employed to examine the relationship of structure and function in proteins. Mutagenesis of a defined protein region is termed scanning mutagenesis, e.g. alanine scanning, cysteine scanning etc.

The following assumptions are associated with the use of mutagenesis

### **2.8.1 Replacement of a structurally/functionally important amino acid causes major changes to protein structure/function, while replacement of an unimportant amino acid causes minor/ no changes to protein structure/function**

Site-directed mutagenesis (as opposed to random mutagenesis) involves replacement of a specific amino acid with another. The basic structure of all the amino acids involves a carbonyl group and an amino group bonded to the same carbon atom. Only the R-groups vary between different amino acids. Substitution of the R group of one amino acid with the R group of another amino acid is the basic premise of site-directed mutagenesis. If the R group altered is important for ligand binding then substitution will change the ligand binding characteristics. The mutation can be drastic such as an alanine mutation or can be subtle, for example a tyrosine replaced by phenylalanine. The hypothesis holds that such a replacement will result in a significant change to protein function if the amino acid is important for either ligand binding or functioning of the protein. The mutation of an amino acid can also lead to changes in general to protein backbone. Such structural changes can lead to alteration in protein functioning. Whether the effect of the mutation is a specific effect of the side-chain replacement or a general effect on protein backbone

can sometimes be difficult to determine. However certain guidelines can be used to interpret such data.

1) A specific effect of the side-chain replacement can be verified by using subtle mutation. Subtle mutation does not alter the local environment at the position of the original amino acid. A subtle mutation is thus unlikely to cause any significant change to protein backbone. If both drastic and subtle mutations produce significant changes to the receptor function, then the amino acid in question is probably mediating the effects on ligand binding and/or channel gating through side-chain involvement.

2) If a mutation leads to changes in receptor expression without changes to pharmacological parameters, then the amino acid is probably playing a purely structural role. Mere changes to receptor number will not lead to changes in the pharmacological parameters such as  $K_d$ ,  $K_i$ ,  $EC_{50}$  and  $IC_{50}$  values, while changes to  $B_{Max}$  (using radio-ligand binding) and  $I_{Max}$  (using electrophysiology) will be observed. The structural role played by an amino acid can be mediated either by the virtue of its location in the backbone or intra-/inter-subunit interactions.

3) If a mutation leads to changes in receptor expression and pharmacological parameters, then the amino acid is probably playing a mixed role; both in the structure and function of the protein.

### **2.8.2 Alanine scanning mutagenesis can be used to identify structurally/ functionally important amino acids of a protein.**

Alanine scanning mutagenesis involves sequential replacement of each amino acid (one amino acid at a time) with alanine. This approach is specifically used, when little or no structural information is available. In our studies, we have utilized this approach to verify the structural/functional features of a specific region ("loop B") of the protein. Again, selection of the region is based on information obtained from homologous proteins, generally members of the same protein family. Alanine is an ideal replacement since it can replace amino acids both in the hydrophilic or the hydrophobic environment equally well (Cunningham and Wells, 1989). Alanine mutation causes complete removal of the side chain while maintaining the rigidity of the backbone. In such a scan, important amino acids are quickly identified, while unimportant amino acids are quickly demarcated.

### **2.9 Radio-ligand binding assays using mammalian cells**

Radio-ligand binding is employed to assess the impact of a mutation on the high affinity binding to the competitive antagonist granisetron. The [ $^3\text{H}$ ] labeled granisetron emits beta particles on decay, which can be counted using a scintillation counter. Using saturation binding assays, the affinity of [ $^3\text{H}$ ] granisetron is measured ( $K_d$ ), while the  $B_{\text{Max}}$  allows evaluation of the receptor number. However, radio-ligand binding detects all of the receptors (including the intracellular pool) and no comment can be made about surface expression. A change in the  $K_d$  compared to the wt receptor indicates change in the

affinity for granisetron, while a change in  $B_{Max}$  indicates that mutation has affected receptor assembly.

### 2.10 Electrophysiology

Electrophysiological assays are used to assess the functional integrity of mutant receptors. Detection of electrophysiological responses indicates that the receptors are assembled and expressed on the cell surface. Changes in  $I_{Max}$  values compared to the wt receptor can be indicative of a change in receptor expression. On the other hand, if  $B_{Max}$  data suggests little or no change to receptor assembly, or if the changes are specific to a particular agonist, then changes in  $I_{Max}$  reflect alterations in efficacy of that particular agonist.

A change in  $EC_{50}$  for a mutant receptor indicates a change to in either agonist binding or gating of the receptor-ion channel complex. Changes to receptor number will not cause changes in  $EC_{50}$  values. Whether the changes observed in  $EC_{50}$  are a result of pure change in ligand binding or a pure change in gating or mixed effect can be deciphered by use of partial agonists. For a full discussion of the partial agonist approach, please refer to section 4.3 of this thesis.

Electrophysiological inhibition assays can also be performed.  $IC_{50}$  and  $K_i$  values for competitive antagonists can be obtained from such assays. Assuming that the 5-HT<sub>3A</sub>R follows the cyclic model of receptor function (i.e., closed-open-desensitized-closed), these values probably indicate affinity of the competitive antagonist for the closed state of the receptor.

### 2.10.1 Electrophysiology using mammalian cells

Mammalian cells can be used to record currents using the whole-cell patch-clamp assay. This assay allows rapid drug delivery to the mammalian cell (given the small size of the cell). Using rapid drug delivery, measurements of kinetic parameters such as rise time, slope of the rising phase of the current, peak amplitude, desensitization time constants and the number of macroscopic desensitization phases can be obtained. These measurements allow calculation of rates e.g., ligand on/off rates, desensitization rates, and channel opening/closing rates. In addition to being directly informative, these values can also be used to prepare kinetic models of the receptor function. The whole-cell patch-clamp assay is technically challenging, especially in the case of mutant receptors with low receptor expression levels.

### 2.10.2 Electrophysiology using *Xenopus laevis* oocytes

Although it provides a non-mammalian cellular environment for protein expression, numerous studies have shown the fidelity of *Xenopus laevis* oocytes as an expression system. Stage IV *Xenopus laevis* oocytes are primed for protein expression and faithfully reproduce any protein of which genetic material has been introduced. All the features of the protein assembly and targeting of the protein are preserved. Thus, a membrane-bound receptor is targeted to the cell membrane. The advantages of using this system for protein expression and analysis are two-fold,

- 1) Proteins are expressed in large quantities. Thus in a case where it is difficult to detect currents from a mutant receptor being expressed in mammalian cells, expression in oocytes can make those currents detectable.

2) Oocytes provide a more stable system for electrophysiological recording, allowing prolonged recording sessions.

On the other hand, drug delivery is not as rapid as whole-cell patch-clamp. Also, oocytes may impose certain post-translational modifications, such as glycosylation, which may be different than those taking place in the protein's native environment. Thus the data obtained from oocytes needs to be interpreted more carefully than that obtained from the whole-cell patch-clamp assay.

### **2.11 Molecular modeling**

Homology-based protein modeling and the use of the protein model for ligand docking allows a more systematic interpretation of biochemical data by providing a three-dimensional model. Such a model allows visualization of the inter-relation between various amino acids in the purported ligand-binding domain as well as between various amino acids and the docked ligand molecule. Corroboration of biochemical data with the information obtained from molecular dynamics (MD) calculations can also provide information about the dynamics of the protein between various conformational states. Information obtained from all the molecular modeling studies also aids in formulation of testable hypotheses.

## References

- Beene DL, Brandt GS, Zhong W, Zacharias NM, Lester HA and Dougherty DA (2002) Cation- $\pi$  interactions in ligand recognition by serotonergic (5-HT<sub>3A</sub>) and nicotinic acetylcholine receptors: the anomalous binding properties of nicotine. *Biochemistry* **41**(32):10262-10269.
- Cunningham BC and Wells JA (1989) High-resolution epitope mapping of hGH-receptor interactions by alanine-scanning mutagenesis. *Science* **244**(4908):1081-1085.
- Spier AD and Lummis SC (2000) The role of tryptophan residues in the 5-Hydroxytryptamine(3) receptor ligand binding domain. *J Biol Chem* **275**(8):5620-5625.
- Unwin N (2005) Refined Structure of the Nicotinic Acetylcholine Receptor at 4Å Resolution. *J Mol Biol* **346**(4):967-989.
- Venkataraman P, Joshi P, Venkatachalan SP, Muthalagi M, Parihar HS, Kirschbaum KS and Schulte MK (2002a) Functional group interactions of a 5-HT<sub>3R</sub> antagonist. *BMC Biochem* **3**(1):16.
- Venkataraman P, Venkatachalan SP, Joshi PR, Muthalagi M and Schulte MK (2002b) Identification of critical residues in loop E in the 5-HT<sub>3ASR</sub> binding site. *BMC Biochem* **3**(1):15.

## Chapter 3: Structure-activity relationship study of lerisetron, a competitive antagonist at the 5-HT<sub>3A</sub>R<sup>2</sup>.

### 3.1 Summary

The serotonin type 3 receptor (5-HT<sub>3</sub>R) is a prototypical member of the cysteine-loop family of ligand-gated ion channels. lerisetron (1-phenylmethyl-2-piperizinyl benzimidazole) is a potent 5-HT<sub>3</sub>R antagonist. Functional groups on this compound capable of forming interactions with the receptor are the terminal amino group in 4'-N position, an aromatic imidazole and a benzyl group in the N1 position of the imidazole. The present study explored the importance of the 4'-N nitrogen by utilizing 4'-N substituted analogs of lerisetron. The properties of the analogs were characterized using *murine* 5-HT<sub>3AS</sub>Rs expressed in *Xenopus laevis* oocytes. The apparent affinities of the analogs for 5-HT<sub>3AS</sub>RS were determined using electrophysiological competition assays. The results obtained suggest that the terminal nitrogen of lerisetron is involved in a precise interaction with certain amino acid(S) in the 5-HT<sub>3A</sub>R binding site. Our results also indicate that the partial negative charge on the 4'-N nitrogen as well as its ability to participate in a cation-pi interaction are probably critical to its action as a potent 5-HT<sub>3A</sub>R antagonist.

---

<sup>2</sup> Manuscript in preparation for submission to *Neuropharmacology* (Elsevier publication).



### 3.2 Introduction

The serotonin type 3<sub>AS</sub> receptor (5-HT<sub>3AS</sub>R) is a prototypical member of the cysteine-loop family of ligand-gated ion channels (LGIC) (Belelli et al., 1995; Jackson and Yakel, 1995; Maricq et al., 1991). Other members of this family include the nicotinic acetylcholine receptors (Karlin and Akabas, 1995), the  $\gamma$ -amino butyric acid type A receptor (GABA<sub>A</sub>R) (Schofield et al., 1987) and the glycine receptor (GlyR) (Grenningloh et al., 1987). Comprised of a pentameric quaternary structure with at least two ligand-binding sites present at the subunit interfaces (Arias, 2000; Celie et al., 2004; Miyazawa et al., 1999), this receptor family is characterized by the presence of a critical disulfide loop structure within the binding site and an integral ion selective channel. Like other members of this family, more than one subtype of the receptor can be found in the CNS. Both an A and B subunit have been identified and cloned (Davies et al., 1999). Two splice variants of the A subunit have also been identified (Downie et al., 1994; Hope et al., 1996). While both long and short splice forms are capable of forming functional homomeric receptors, some differences in agonist and partial agonist activity have been observed between the long and short splice variants of this subtype (Niemeyer and Lummis, 1998). A second subtype is formed by combination of the A and B subunits to produce a heteromeric receptor with unknown stoichiometry (Davies et al., 1999). Heteromeric receptors are pharmacologically and functionally distinct from homomeric 5-HT<sub>3A</sub>Rs (Brady et al., 2001). 5-HT<sub>3</sub>Rs are distributed throughout the central and peripheral nervous system, playing a significant role in phenomena such as anxiety, emesis and alcoholism (Ait-Daoud et al., 2001; Gandara et al., 1993). Antagonists to 5-

HT<sub>3</sub>R<sub>s</sub> are clinically efficacious in the treatment of chemotherapy-induced emesis and recent studies on human subjects have suggested they may be useful in treatment of early onset alcoholism (Ait-Daoud et al., 2001).

A model for the antagonist pharmacophore of the 5-HT<sub>3</sub>R was proposed by Hibert et al (Hibert et al., 1990). Although some modifications have been made to this model since that time, the common structural features of 5-HT<sub>3</sub>R antagonists remain essentially the same. All 5-HT<sub>3</sub>R antagonists contain an aromatic ring, a carbonyl oxygen or bioisosteric equivalent and a basic nitrogen. According to Hibert's model, the basic nitrogen is located 5.2Å from the centre of the aromatic ring and approximately 1.7Å above plane of the ring. The carbonyl oxygen and the aromatic ring are coplanar and separated by a distance of 3.3Å. Additional studies have expanded on this model to include another lipophilic region (Clark et al., 1993) and second hydrogen bonding interaction two atoms away from the first. A compound that appears to fit all 4 binding site regions was synthesized by Orjales et al. (Orjales et al., 1997). This compound (1-phenylmethyl-2-piperiziny benzimidazole or lerisetron) is shown in figure 3.1 and is a potent 5-HT<sub>3</sub>R antagonist. Functional groups on this compound capable of forming interactions with the receptor are the terminal amino group, an aromatic imidazole and a benzyl group in the N1 position of the imidazole. While lerisetron contains no carbonyl group, one or both of the imidazole nitrogens could act as bioisosteres of this functional group (Orjales et al., 1997).

Orjales demonstrated the importance of the N1 benzyl group by synthesizing several N1 substituted analogs of lerisetron. Removal of the N-benzyl group produced a

80-fold decrease in affinity, indicating a role for this group in interacting with the 5-HT<sub>3</sub>R. Similar studies involving N1 substituent analogs by Parihar et al. have supported this observation and suggest a more specific charge-charge interaction rather than a general lipophilic interaction (Parihar et al., 2001)

In the present study, we examined the effect of alterations at the 4'-N position (the terminal nitrogen group, see Figure 3.1) of lerisetron. Our results indicate that the terminal nitrogen is involved in a precise interaction with certain amino acid (S) in the 5-HT<sub>3A</sub>R binding site. Our results also indicate that the partial negative charge on the 4'-N nitrogen as well as its ability to participate in a cation- $\pi$  interaction are probably critical to its action as a potent 5-HT<sub>3A</sub>R antagonist.

### 3.3 Materials and Methods

#### 3.3.1 Materials

*Xenopus laevis* frogs and frog food were purchased from Xenopus Express (FL, US). Sigma type II collagenase was purchased from Sigma-Aldrich (MO, US). [<sup>3</sup>H]granisetron was purchased from New England Nuclear (ST, US), 5-HT, 2-Me5HT from Spectrum, and *m*CPBG and *d*-TC from Research Biochemical International (MO, US). All other chemicals were obtained from Fisher Scientific (TX, US).

lerisetron and its 4'-N substituted analogs were kindly provided by Harish Parihar, who is a co-author of this manuscript, and Dr. Karen Kirschbaum at the University of Louisiana at Monroe, Monroe, LA 71203.

#### 3.3.2 Site-directed mutagenesis

Wild-type (wt) m5-HT<sub>3AS</sub> receptor cDNA was derived from N1E-115 neuroblastoma cells as previously described (Yan et al., 1999). All mutant receptors were constructed using the pAlter *altered sites* mutagenesis kit (Promega, CA) as described earlier (Venkataraman et al., 2002). All mutations were confirmed by restriction digests and DNA sequencing (UC Davis, CA).

#### 3.3.3 *Xenopus laevis* oocyte two-electrode voltage-clamp assay

Details of the methodology employed for electrophysiological assays have been described earlier (Joshi et al., 2004). Ovarian lobes were surgically removed from *Xenopus laevis* frogs and washed twice in Ca<sup>+2</sup>-free Barth's buffer [82.5 mM NaCl / 2.5 mM KCl / 1mM MgCl<sub>2</sub> / 5 mM HEPES, pH 7.4], then gently shaken with 1.5mg/ml

collagenase for 1 hour at 20-25 °C. Stage IV oocytes were selected for microinjection. Synthetic cRNAs for wt and mutant m5-HT<sub>3A</sub>Rs were prepared using an mMACHINE mMACHINE™ High Yield Capped RNA Transcription Kit (Ambion, TX). Each oocyte was injected with 50nl cRNA at a concentration of 0.2ng/nl. Oocytes were incubated at 19°C for 2 to 4 days before electrophysiological recording. Electrical recordings were made using conventional two-electrode voltage-clamp at -60 mV employing an OC-725C oocyte clamp amplifier (Warner Instruments, CT, US) coupled to an online, computerized data acquisition system (DataPac 2000, RUN technologies, CA, US). Recording and current electrodes were filled with 3M KCl and had resistances of 1-2 MΩ. Oocytes were held in a chamber of 400μl volume and perfused with ND-96 recording buffer (96mM NaCl / 2mM KCl / 1.8mM CaCl<sub>2</sub> / 1mM MgCl<sub>2</sub> / 5mM HEPES, pH 7.4) at a rate of 15ml/min. All agonists and antagonists were prepared in ND-96 buffer and applied at a rate of 25ml/min using an electrical pump. For competition assays involving lerisetron and its analogs, oocytes expressing *murine* 5-HT<sub>3AS</sub>Rs were pre-exposed to varying concentrations of each antagonist for a period of 30 seconds. After 30 seconds, the oocyte was co-exposed to a mixture of 5-HT and the antagonist. The 5-HT concentration in each case corresponded to the EC<sub>50</sub> value; i.e., 4μM.

#### **3.3.4 *Xenopus laevis* oocyte two-electrode voltage-clamp assay**

Data was analyzed using the equation  $\theta = \frac{1}{(1 + EC_{50}/[A])^n}$  as previously described (Yan et al, 1999), where  $\theta$  is the normalized current at 5-HT concentration  $[A]$ , EC<sub>50</sub> is the concentration of 5-HT required to obtain half-maximal current, and  $n$  is the apparent

Hill slope. Concentration-Response curves were obtained by non-linear regression analysis using GraphPad PRISM. Data were compared for significant differences using student's *t* test.

## Results

*Murine* 5-HT<sub>3AS</sub> receptor expressed using *X. laevis* oocytes produced characteristic inward currents on exposure to agonist serotonin (5-HT). Iterative curve fitting of the doses-response data yielded an EC<sub>50</sub> value of  $3.4 \pm 0.3 \mu\text{M}$  ( $n = 4$ ). The parent compound lerisetron (Figure 1) potently inhibits the inward currents induced by  $4 \mu\text{M}$  5-HT, with concentration of  $10 \text{ nM}$  completely obliterating the response. An IC<sub>50</sub> value  $0.54 \text{ nM}$  was obtained for the wt receptor.

Certain analogs were designed to study the effect of alteration of the position of the terminal amino group on the apparent affinity. lerisetron analog HSP-153 was tested in order to examine the effect of altering the position of the terminal amino group on the piperidine ring structure. The shift of the amino group from 4 to 5 position leads to significant changes to the apparent affinity of the compound, with almost 100-fold reduction in IC<sub>50</sub> (Table 3.1). However, alteration of the position of the terminal amino group addition of a carbon (analog HSP-155) produced only a minor change in the apparent affinity (Table 3.1). Addition of a methyl group to the terminal nitrogen also did not significantly change the apparent affinity of the lerisetron analog (analog HSP 93, Table 3.1).

Effects of the alteration of the characteristics of the terminal amino group itself were examined with the help of another series of analogs (Table 3.1, second group). Replacement of the terminal amino group with a charged quaternary amine led to a small but statistically significant increase in the apparent affinity of lerisetron (HSP-97, Table 3.1). Substitution of the terminal amine by a sulfur (HSP-161) led to complete loss of the

activity. Although substitution with a charged sulfur group (methyl sulfonium) somewhat restored the activity, the apparent affinity was very poor, with almost 400,000 fold reduction in the apparent affinity (HSP-165, Table 3.1). Surprisingly, substitution with oxygen (SAK-8) was better tolerated as compared to substitution with sulfur or positively charged sulfur (methyl sulfonium); with almost 40,000 fold reduction in the affinity. In any case, any substitution at the terminal nitrogen was very poorly tolerated.

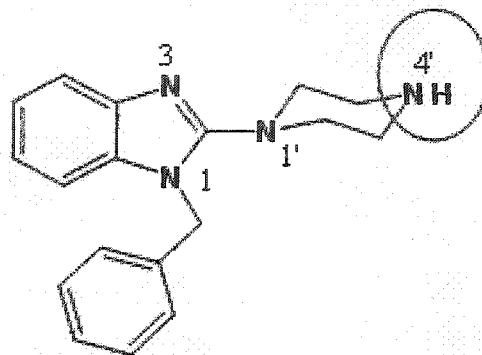


## Discussion

Previous studies have supported a critical role of the terminal amino group in mediating the action of lerisetron, a potent antagonist of the benzimidazole group of 5-HT<sub>3</sub>R antagonists (Orjales et al., 1997; Parihar et al., 2001; Venkataraman et al., 2002). The results described here further support such a role. Our studies also indicate that proper positioning of the nitrogen group also plays an important role in maintaining the potency of lerisetron. In the case of HSP-153 and HSP-155, the terminal secondary amine of lerisetron has been replaced by primary amine. In the case of the secondary amine of lerisetron, the basicity of the terminal amino group may be contributing to the overall interaction with the interacting amino acid. It is conceivable that the minor decrease in the apparent affinity observed with HSP-155 is probably a compound effect of reduction in the distance as well as reduction in basicity as result of replacement with the primary amine. The major decrease in the apparent affinity observed with HSP153 may similarly reflect a compound effect of change in the position of the amino group as well as reduction in basicity resulting from the replacement with the primary amine. Data obtained from analogs HSP 161 (sulfur) and SAK-8 (oxygen) also support the assumption that the basic charge on the terminal group is important for its purported interaction.

Previous studies have indicated that addition of charge to the terminal nitrogen increases potency, an assumption supported by the results obtained for analog HSP-97 (Orjales et al., 1997; Petersson et al., 2002). The terminal amino group is purportedly involved in a cation- $\pi$  interaction, presumably with the aromatic amino acids on the

positive face of the 5-HT<sub>3</sub>R binding site (Beene et al., 2002). Cation-pi interaction involves charge interaction of the positively charged cation with the negatively charged pi electron cloud of an aromatic ring, typically of an aromatic amino acid such as tyrosine or tryptophan (Beene et al., 2002; Zhong et al., 1998). In case of the 5-HT<sub>3A</sub>R, cation-pi interaction of charged terminal nitrogen of ligands with amino acids W183 or Y234 have been proposed (Beene, 2004). The results described here for analogs HSP-97, HSP-161 and HSP-165 (See Table 3.1) support these assumptions. Interestingly, a charged sulfur (as in the case of HSP-165) cannot adequately replace the nitrogen, since it probably does not participate equally well in the purported cation-pi interaction.





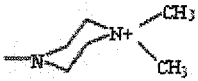





**Figure 3.1 Parent compound, lerisetron**  
The terminal amino group is marked by a circle

**Table 3.1 IC<sub>50</sub> values obtained for the series of N-substituted lerisetron analogs**

The IC<sub>50</sub> values were obtained using *Xenopus laevis* oocytes expressing murine 5-HT<sub>3A</sub> receptor and two-electrode voltage-clamp assay.

The number of experiments is at least 3.  $\pm$  indicates IC<sub>50</sub>  $\pm$  the standard error. All the IC<sub>50</sub> values were significantly different from that obtained for the parent compound lerisetron.

Name	Structure	IC <sub>50</sub> in $\mu$ M
Lerisetron		0.56 $\pm$ 0.19
HSP-153		57.9 $\pm$ 8.9
HSP-155		2.51 $\pm$ 0.52
HSP-93		2.46 $\pm$ 0.3
HSP-97		0.15 $\pm$ 0.04
HSP-161		No Inhibition up to 1 mM
HSP-165		20000 $\pm$ 8000
SAK-8		19650 $\pm$ 3030

## References

- Ait-Daoud N, Johnson BA, Prihoda TJ and Hargita ID (2001) Combining ondansetron and naltrexone reduces craving among biologically predisposed alcoholics: preliminary clinical evidence. *Psychopharmacology (Berl)* **154**(1):23-27.
- Arias HR (2000) Localization of agonist and competitive antagonist binding sites on nicotinic acetylcholine receptors. *Neurochem Int* **36**(7):595-645.
- Beene DL, Brandt GS, Zhong W, Zacharias NM, Lester HA and Dougherty DA (2002) Cation- $\pi$  interactions in ligand recognition by serotonergic (5-HT<sub>3A</sub>) and nicotinic acetylcholine receptors: the anomalous binding properties of nicotine. *Biochemistry* **41**(32):10262-10269.
- Beene DL, Price, K.L., Lester, H.A., Dougherty, D.A., and Lummis, S.C.R.(2004) (2004) *J Neurosci in press*.
- Belelli D, Balcarek JM, Hope AG, Peters JA, Lambert JJ and Blackburn TP (1995) Cloning and functional expression of a human 5-hydroxytryptamine type 3AS receptor subunit. *Mol Pharmacol* **48**(6):1054-1062.
- Brady CA, Stanford IM, Ali I, Lin L, Williams JM, Dubin AE, Hope AG and Barnes NM (2001) Pharmacological comparison of human homomeric 5-HT<sub>3A</sub> receptors versus heteromeric 5-HT<sub>3A/3B</sub> receptors. *Neuropharmacology* **41**(2):282-284.
- Celie PH, van Rossum-Fikkert SE, van Dijk WJ, Brejc K, Smit AB and Sixma TK (2004) Nicotine and carbamylcholine binding to nicotinic acetylcholine receptors as studied in AChBP crystal structures. *Neuron* **41**(6):907-914.
- Clark RD, Miller AB, Berger J, Repke DB, Weinhardt KK, Kowalczyk BA, Eglen RM, Bonhaus DW, Lee CH, Michel AD and et al. (1993) 2-(Quinuclidin-3-yl)pyrido[4,3-b]indol-1-ones and isoquinolin-1-ones. Potent conformationally restricted 5-HT<sub>3</sub> receptor antagonists. *J Med Chem* **36**(18):2645-2657.
- Davies PA, Pistis M, Hanna MC, Peters JA, Lambert JJ, Hales TG and Kirkness EF (1999) The 5-HT<sub>3B</sub> subunit is a major determinant of serotonin-receptor function. *Nature* **397**(6717):359-363.
- Downie DL, Hope AG, Lambert JJ, Peters JA, Blackburn TP and Jones BJ (1994) Pharmacological characterization of the apparent splice variants of the murine 5-HT<sub>3</sub> R-A subunit expressed in *Xenopus laevis* oocytes. *Neuropharmacology* **33**(3-4):473-482.

- Gandara DR, Harvey WH, Monaghan GG, Perez EA and Hesketh PJ (1993) Delayed emesis following high-dose cisplatin: a double-blind randomised comparative trial of ondansetron (GR 38032F) versus placebo. *Eur J Cancer* **29A Suppl 1**:S35-38.
- Grenningloh G, Rienitz A, Schmitt B, Methfessel C, Zensen M, Beyreuther K, Gundelfinger ED and Betz H (1987) The strychnine-binding subunit of the glycine receptor shows homology with nicotinic acetylcholine receptors. *Nature* **328**(6127):215-220.
- Hibert MF, Hoffmann R, Miller RC and Carr AA (1990) Conformation-activity relationship study of 5-HT<sub>3</sub> receptor antagonists and a definition of a model for this receptor site. *J Med Chem* **33**(6):1594-1600.
- Hope AG, Peters JA, Brown AM, Lambert JJ and Blackburn TP (1996) Characterization of a human 5-hydroxytryptamine<sub>3</sub> receptor type A (h5-HT<sub>3</sub>R-AS) subunit stably expressed in HEK 293 cells. *Br J Pharmacol* **118**(5):1237-1245.
- Jackson MB and Yakel JL (1995) The 5-HT<sub>3</sub> receptor channel. *Annu Rev Physiol* **57**:447-468.
- Joshi PR, Suryanarayanan A and Schulte MK (2004) A vertical flow chamber for *Xenopus* oocyte electrophysiology and automated drug screening. *J Neurosci Methods* **132**(1):69-79.
- Karlin A and Akabas MH (1995) Toward a structural basis for the function of nicotinic acetylcholine receptors and their cousins. *Neuron* **15**(6):1231-1244.
- Maricq AV, Peterson AS, Brake AJ, Myers RM and Julius D (1991) Primary structure and functional expression of the 5HT<sub>3</sub> receptor, a serotonin-gated ion channel. *Science* **254**(5030):432-437.
- Miyazawa A, Fujiyoshi Y, Stowell M and Unwin N (1999) Nicotinic acetylcholine receptor at 4.6 Å resolution: transverse tunnels in the channel wall. *J Mol Biol* **288**(4):765-786.
- Niemeyer MI and Lummis SC (1998) Different efficacy of specific agonists at 5-HT<sub>3</sub> receptor splice variants: the role of the extra six amino acid segment. *Br J Pharmacol* **123**(4):661-666.
- Orjales A, Mosquera R, Labeaga L and Rodes R (1997) New 2-piperazinylbenzimidazole derivatives as 5-HT<sub>3</sub> antagonists. Synthesis and pharmacological evaluation. *J Med Chem* **40**(4):586-593.
- Parihar HS, Suryanarayanan A, Ma C, Joshi P, Venkataraman P, Schulte MK and Kirschbaum KS (2001) 5-HT<sub>3</sub>R binding of lerisetron: an interdisciplinary

- approach to drug-Receptor interactions. *Bioorg Med Chem Lett* **11**(16):2133-2136.
- Petersson EJ, Choi A, Dahan DS, Lester HA and Dougherty DA (2002) A perturbed pK(a) at the binding site of the nicotinic acetylcholine receptor: implications for nicotine binding. *J Am Chem Soc* **124**(43):12662-12663.
- Schofield PR, Darlison MG, Fujita N, Burt DR, Stephenson FA, Rodriguez H, Rhee LM, Ramachandran J, Reale V, Glencorse TA and et al. (1987) Sequence and functional expression of the GABA A receptor shows a ligand-gated receptor super-family. *Nature* **328**(6127):221-227.
- Venkataraman P, Joshi P, Venkatachalan SP, Muthalagi M, Parihar HS, Kirschbaum KS and Schulte MK (2002) Functional group interactions of a 5-HT3R antagonist. *BMC Biochem* **3**(1):16.
- Yan D, Schulte MK, Bloom KE and White MM (1999) Structural features of the ligand-binding domain of the serotonin 5HT3 receptor. *J Biol Chem* **274**(9):5537-5541.
- Zhong W, Gallivan JP, Zhang Y, Li L, Lester HA and Dougherty DA (1998) From *ab initio* quantum mechanics to molecular neurobiology: a cation-pi binding site in the nicotinic receptor. *Proc Natl Acad Sci U S A* **95**(21):12088-12093.

**Appendix**

Acknowledgements: This work is supported by the National Science Foundation (NSF CAREER 9985077) and the American Heart Association (AHA 0151065B).

PRJ and AS are both Alaska INBRE pre-doctoral research fellows.



## Chapter 4: Mutations at loop E tyrosine residues differentially modulate gating of the *murine* 5-HT<sub>3A</sub> Receptor<sup>3</sup>

### 4.1 Summary

The 5-HT<sub>3</sub>R belongs to a superfamily of ligand-gated ion channel coupled receptors and shares several structural and functional features with other members including the nAChR, GABA and Gly receptors. Previous mutagenesis & protein modeling studies suggest that three tyrosine residues (Y141, Y143 and Y153) in the putative loop E region of the amino terminal may form part of the ligand-binding site and play a role in ligand-receptor interactions. Results from the molecular modeling studies suggested that tyrosine residues 143 and 153 are part of a dynamic H-bonding pattern and play a role in receptor gating. These studies also suggested that these gating interactions are differentially modulated by 5-HT and *m*CPBG through differential interactions. Mutations at Y143 and Y153 produced significant changes in receptor function. The Y143A mutation resulted in non-functional receptors; while the Y143F mutation produced large changes in EC<sub>50</sub> values for four agonists; 5-HT, *m*CPBG, PBG and 2-Me5HT. In addition, relative efficacies ( $I_{\text{Max}} \text{ Agonist} / I_{\text{Max}} \text{ 5-HT}$ ) of the partial agonists PBG (24% vs. 87% for wt receptor) and 2-Me5HT (1.8% vs. 12% for wt receptor) were altered. The Y153A mutation significantly altered response kinetics for 5-HT but not *m*CPBG and PBG. The Y153A mutation also led to drastic changes in the rank efficacy of four agonists compared to wt (wt: 5-HT > *m*CPBG > PBG >> 2-Me5HT, Y153A:

---

<sup>3</sup> Manuscript in preparation for submission to *Neuropharmacology* (Elsevier publication).

*m*CPBG ≥ PBG >> 5-HT >> 2-Me5HT). The Y153F mutation produced receptors that displayed an efficacy profile similar to Y153A receptors. These results suggest that Y143 is critical in general to channel gating, while Y153 mediates agonist specific gating of the 5-HT<sub>3A</sub> receptor.

## 4.2 Introduction

The serotonin type 3 receptor (5-HT<sub>3</sub>R) is a membrane bound, cation-selective, ion channel coupled, glycoprotein (Derkach et al., 1989; Maricq et al., 1991). The 5-HT<sub>3</sub>R belongs to a superfamily of ligand-gated ion channels (LGICs) and shares several structural and functional features with other members including the nicotinic acetylcholine (nACh), gamma amino butyric acid (GABA) A and C, and glycine (Gly) receptors. The presence of a characteristic loop formed by two cysteine residues ('cys loop') in the extracellular N-terminal of these receptors has led to their designation as the 'Cys-loop' superfamily of receptors. Expressed in both the central and peripheral nervous system (Reeves and Lummis, 2002), the 5-HT<sub>3</sub>R mediates fast synaptic transmission through rapid opening and desensitization of the ion channel (Sugita et al., 1992).

Two subunits of the 5-HT<sub>3</sub>R, A and B (Davies et al., 1999; Hanna et al., 2000) have been characterized, although DNA sequences coding for 5-HT<sub>3</sub>C, D and E are known (Niesler et al., 2003). While the A subunit assembles in a homo-pentameric form, B subunit can assemble into a functional protein only if co-expressed with the A. Two splice variants of the A subunit of the murine receptor (m5-HT<sub>3</sub>R): A<sub>S</sub> and A<sub>L</sub> are also known (Downie et al., 1994; Hope et al., 1993). Receptors composed of different splice variants demonstrate distinct pharmacological characteristics; interacting differentially with 5-HT<sub>3</sub>R agonists (Hope et al., 1993).

The ligand-binding site of the 5-HT<sub>3A</sub>R is located in the extracellular N-terminal domain (van Hooft et al., 1998). Sequence homology with the nACh receptor and acetylcholine binding protein (AChBP) suggests that the ligand binding site is located in

the inter-subunit interface and is formed by at least 6 'loop' structures designated A to F (Brejc et al., 2001). Results from several site-directed mutagenesis studies have so far identified numerous residues from a number of these purported loop structures (Boess et al., 1997; Schreiter et al., 2003; Spier and Lummis, 2000; Steward et al., 2000; Yan et al., 1999). We have previously reported that three tyrosine residues from the loop E region (Y141-Y153) are similarly important to ligand-receptor (L-R) interactions (Venkataraman et al., 2002b). These residues were identified through the use of alanine scanning mutagenesis of a stretch of amino acids from Y141 to K153 of the m5-HT<sub>3A</sub>R. Based on results obtained from radio-ligand binding assays, we have earlier proposed that residues Y143 and Y153 might be important in L-R interactions of both agonists (5-hydroxytryptamine [5-HT] and *m*-chlorophenylbiguanide [*m*CPBG]) and antagonists (lerisetron, its analogs and to a lesser extent, granisetron) (Venkataraman et al., 2002a; Venkataraman et al., 2002b). A role for Y141 in the interaction of *d*-tubocurarine (*d*-TC) with the ligand-binding domain was also proposed. Results from our laboratory and others have suggested that Y153 and Y143 may also be involved in mediating conformational changes in response to agonists (Beene et al., 2004; Price and Lummis, 2004; Venkataraman et al., 2002b); however, no direct evidence has been reported in support of this hypothesis.

*m*CPBG, a selective agonist at the 5-HT<sub>3A</sub> receptor, displays a distinct pharmacological profile. When assayed on murine 5-HT<sub>3AS</sub> and 5-HT<sub>3AL</sub> receptors, *m*CPBG displays lower efficacy compared to 5-HT (Niemeyer and Lummis, 1998) but higher apparent affinity (based on the EC<sub>50</sub>, K<sub>d</sub>, K<sub>i</sub> values) (Joshi et al., 2004; Spier and

Lummis, 2000; Venkataraman et al., 2002b). *mCPBG* also demonstrates higher affinity for the desensitized state of the 5-HT<sub>3A</sub>R (Bartrup and Newberry, 1996; Mott et al., 2001). Earlier studies have indicated that *mCPBG* and 5-HT interact differentially with the loop A and loop C region of ligand binding domain of 5-HT<sub>3A</sub>R (Lankiewicz et al., 1998; Steward et al., 2000). However, the role of loop E region in mediating these differential interactions remains unexplored.

In the present study, comparison of ligand-free and ligand bound models of the 5-HT<sub>3A</sub>R suggested that tyrosine residues 143 and 153 are part of a dynamic H-bonding pattern and play a role in receptor gating. Results from ligand docking studies suggested that these gating interactions are differentially modulated by 5-HT and *mCPBG* through differential interactions. We explored the role of loop E tyrosines in mediating the effects of full and partial agonists through biochemical assays. Our results indicate that both Y143 and Y153 are involved in mediating the gating of the *m*5-HT<sub>3A</sub>R although Y153 is more specific to the structural class of agonist. While Y143 appears to participate in gating for all agonists tested, Y153 is involved only in mediating the effects of hydroxytryptamines (5-HT and 2-methyl 5-hydroxytryptamine [2-Me5HT]) and not phenylbiguanides (phenylbiguanide [PBG] and *mCPBG*

### 4.3 Materials and Methods

#### 4.3.1 Materials:

*Xenopus laevis* frogs and frog food were purchased from Xenopus Express (FL, US). Sigma type II collagenase was purchased from Sigma-Aldrich (MO, US). [<sup>3</sup>H]granisetron was purchased from New England Nuclear, 5-HT, 2-Me5HT from Spectrum, and *m*CPBG and *d*-TC from Research Biochemical International. All other chemicals were obtained from Fisher Scientific (TX, US).

#### 4.3.2 Receptor modeling:

Extracellular regions of the homopentameric murine 5-HT<sub>3</sub>R were built based on the crystal structure of AChBP from the snail *Lymnaea stagnalis* (PDB entry: 1I9B). The sequence of 5-HT<sub>3</sub>R A subunit was taken from the Protein Information Resource (Wu et al., 2002) with an entry code of NF00508262. Multiple sequence alignments of their extracellular regions and AChBP were performed by 'ClustalW' using default parameters (Thompson et al., 1994). Based on this alignment, homology-model building of 5-HT<sub>3A</sub>R subunit was carried out using the 'Nest' and 'Loopy' facility of the Jackal protein structure modeling package. 'Nest' predicts the experimental dihedral angles chi1 within an error range of 20 degrees for 94 % of protein side chains (Xiang and Honig, 2001). Protein loop predictions for amino acid insertions and deletion were done by 'Loopy' (Xiang et al., 2002). Homodimeric units of the pentamer were built on the basis of crystal structure data to reach minimal root mean standard deviation (RMSD) between the matched monomers. Further refinements of the resulting dimers were carried out by

Sybyl 6.6 program (Tripos Inc., St. Louis, MO) on a Silicon Graphics Octane workstation under Irix 6.5 operation system. First, the all-atom model was allowed to relax during a short molecular dynamics run (2000 fs) using constrains for backbone atoms, not allowing distortions of the backbone. Finally, the entire structures were fully minimized without any restriction using Powell conjugate gradient method until the maximum derivative was less than 0.050 kcal/molÅ. Gasteiger-Huckel partial charges were applied during the calculations. The quality of the model was verified using 'Procheck', as compared with well-refined structures at the same resolution ((Laskowski, 1993). Intra- and interface H-bonds were analysed by HBPLUS v 3.0, an hydrogen bond calculation program (McDonald and Thornton, 1994). Homology model for the ground state receptor was constructed based on the same alignment as for the ligand-bound receptor model. Chain F of AChBP (Celie et al., 2004) taken from RCSB Protein Bank entry 1UV6 was used as a template for ground state receptor model. The loop C conformation of this ligand-free subunit is strikingly different from the conformation of the other crystallized chains with bound ligands. Side chain prediction, dimer building and structural minimization of the ground state receptor were carried out using the same workflow described above for the ligand-bound receptor model.

'AutoDock 3.0' was applied for docking calculations, using the Lamarckian genetic algorithm (LGA) and the 'pseudo-Solis and Wets' (pSW) methods. The ligand docking calculations were performed independent of experimental data. The parameters included in Autodock are based on the 'Assisted Model Building with Energy Refinement' (AMBER) force field (Cornell, 1995). Gasteiger-Huckel partial charges

were applied both for ligands and proteins. Solvation parameters were added to the protein coordinate file and the ligand torsions were defined using the 'Addsol' and 'Autotors' utilities, respectively, in Autodock 3.0. The atomic affinity grids were prepared with 0.375 Å spacing using the Autogrid program for a 15 x 15 x 22.5 Å box around the interface of subunits. No constraints based on experimental data were employed to carry out ligand docking. Random starting positions, orientations and torsions (for flexible bonds) were used for the ligands. Each docking run consisted of 100 cycles. The number of evaluations was set to 1.5 million. Final structures with RMSD less than 1.5 Å were considered to belong to the same cluster. The structures with low energies and high frequencies of docking were subjected to a further minimization by Sybyl and were examined.

#### **4.3.3 Site-directed Mutagenesis:**

Wild type m5-HT<sub>3A</sub>S receptor cDNA was derived from N1E-115 neuroblastoma cells as previously described (Yan et al., 1999). All mutant receptors were constructed using the pAlter *altered sites* mutagenesis kit (Promega, CA) as described earlier (Venkataraman et al., 2002a). All mutations were confirmed by restriction digests and DNA sequencing (UC Davis, CA).

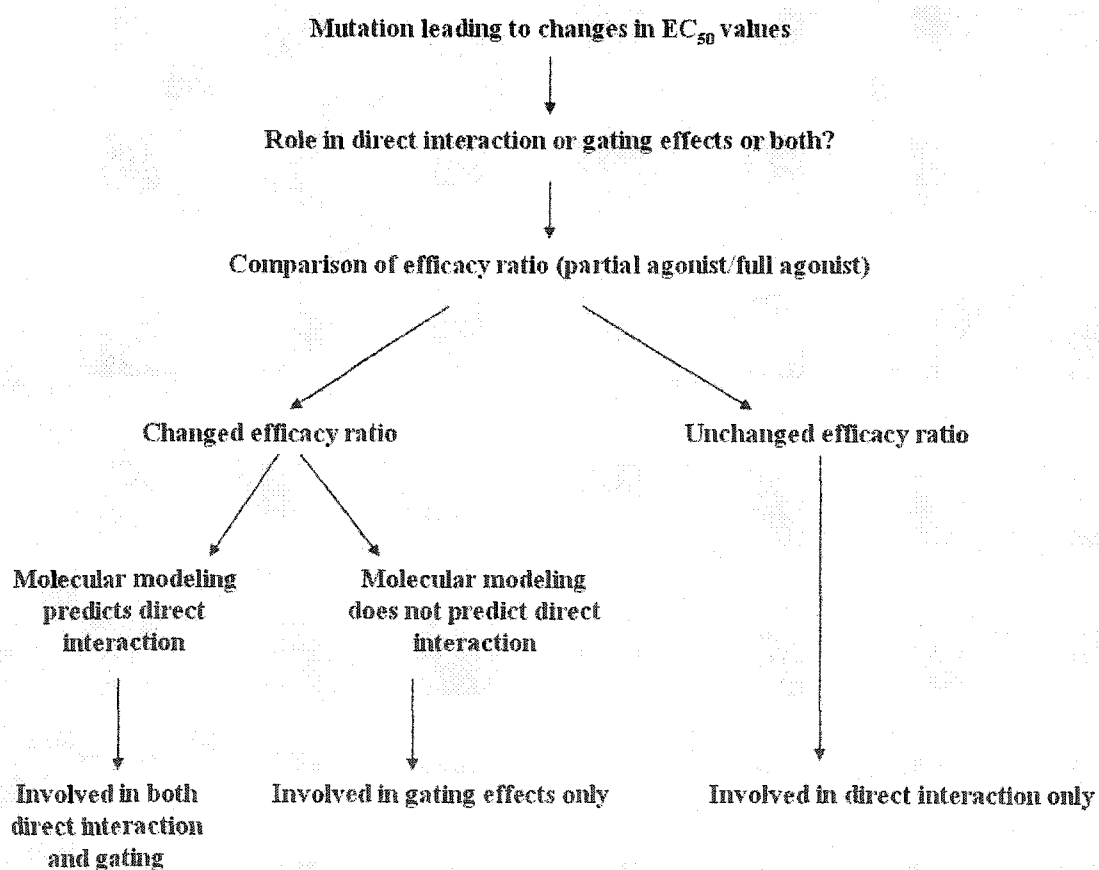
#### **4.3.4 Cell culture and transient transfection:**

tSA201 cells (a derivative of HEK 293 cells) were cultured in Dulbecco's modified Eagle medium (DMEM, New Life Technologies, NY) supplemented with 10 % fetal bovine serum and 100 units/ml penicillin/streptomycin in a humidified 5% CO<sub>2</sub> atmosphere at 37



<sup>0</sup>C. For radio-ligand binding studies, tSA201 cells were plated on 90 mm culture dishes at a density of  $5 \times 10^6$  cells/dish and grown for 9 hours prior to transfection. Cells were transfected with 20  $\mu$ g/ dish wt or mutant plasmid DNA using a calcium phosphate transfection kit (New life technologies, NY). Transfected cells were supplemented with fresh DMEM 12-15 hours later and harvested 48 hours after transfection. For whole-cell patch-clamp assays, tSA201 cells were transfected using Superfect transfection reagent (Qiagen, CA) as described earlier (Venkataraman et al., 2002b).

The following flow-chart summarizes the use of partial agonist approach to determine binding vs. gating effects as a result of a mutation.



#### 4.3.5 *Xenopus laevis* oocyte two-electrode voltage-clamp assay

Details of the methodology employed for electrophysiological assays have been described earlier (Joshi et al., 2004). Ovarian lobes were surgically removed from *Xenopus laevis* frogs and washed twice in Ca<sup>+2</sup> free Barth's buffer [82.5 mM NaCl / 2.5 mM KCl / 1mM MgCl<sub>2</sub> / 5 mM HEPES, pH 7.4], then gently shaken with 1.5mg/ml collagenase (Sigma type II, Sigma-Aldrich) for 1hour at 20-25 °C. Stage IV oocytes were selected for microinjection. Synthetic cRNAs for wt and mutant m5-HT<sub>3A</sub>Rs were prepared using an mMESSAGING mMACHINE™ High Yield Capped RNA Transcription Kit (Ambion, TX). Each oocyte was injected with 50 nl cRNA at a concentration of 0.2 ng/nl. Oocytes were incubated at 19°C for 2 to 4 days before electrophysiological recording. Electrical recordings were made using conventional two-electrode voltage-clamp at -60 mV employing an OC-725C oocyte clamp amplifier (Warner Instruments, CT) coupled to an online, computerized data acquisition system (DataPac 2000, RUN technologies). Recording and current electrodes were filled with 3M KCl and had resistances of 1-2 MΩ. Oocytes were held in a chamber of 400 μl volume and perfused with ND-96 recording buffer (96 mM NaCl / 2 mM KCl / 1.8 mM CaCl<sub>2</sub> / 1 mM MgCl<sub>2</sub> / 5 mM HEPES, pH 7.4) at a rate of 15 ml/min. All agonists and antagonists were prepared in ND-96 buffer and applied at a rate of 25 ml/min using an electrical pump. For competition assays involving *d*-TC, oocytes expressing Wt or mutant receptors were pre-exposed to varying concentrations of *d*-TC for a period of 30 seconds. After 30 seconds, the oocyte was co-exposed to a mixture of 5-HT and *d*-TC. The 5-HT concentration in each case corresponded to the EC<sub>50</sub> value for the receptor under consideration.

#### 4.3.5.1 Comparison of efficacy values for various agonists on wild type and mutant receptors:

Maximal currents were measured using supra-maximal concentrations of agonists (10-40 X the EC<sub>50</sub> value). I<sub>Max</sub> values were compared to those obtained using the endogenous agonist 5-HT. Relative efficacies for *m*CPBG, PBG and 2-Me5HT were calculated using the equation  $I_{Max}(\text{Agonist})/I_{Max} \text{ 5-HT} \times 100\%$  (Eq. 1). Each value is indicated in the text as mean  $\pm$  S.E and *n* denotes the number of experiments for each agonist. For each experiment, maximal currents elicited by each agonist (*m*CPBG, PBG and 2-Me5HT) were directly compared to those elicited by 5-HT on the same oocyte. Values were normalized separately for each experiment and the results were combined.

#### 4.3.6 Whole-cell Patch-clamp assay:

Whole-cell patch-clamp assays were performed as described earlier (Venkataraman et al., 2002a). Briefly, transfected cells were transferred to a recording chamber containing extracellular solution (140 mM NaCl, 1.7 mM MgCl<sub>2</sub>, 5 mM KCl, 1.8 mM CaCl<sub>2</sub>, 25 mM HEPES pH 7.4). Patch electrodes of resistance 2.5-3.0 M $\Omega$  were filled with filtered intracellular solution containing 145 mM KCl, 2 mM MgCl<sub>2</sub>, 1 mM EGTA, 25 mM HEPES (pH 7.4). Cells were clamped in whole-cell configuration at a holding potential of -60 mV. A continuous extracellular solution flow (0.8 ml/min) was maintained throughout the recording procedure. 5-HT was dissolved in extracellular solution and delivered to cells using a rapid perfusion system (Warner Instruments, CT) at a rate matching the extracellular solution flow rate. The drug perfusions lasted for a period

varying from 4 to 8 seconds. Currents elicited by agonist application were measured using an Axopatch 200 B amplifier (Axon Instruments, CA).

#### *Radio-ligand Binding Assays:*

Radio-ligand binding assays was performed as described earlier (Venkataraman et al., 2002b). Briefly, transfected cells were scraped from the dishes, washed twice with PBS (New Life Technologies, NY), then resuspended in 1.0 ml PBS with protease inhibitor cocktail /100mm dish. (*Complete*<sup>™</sup> protease inhibitor cocktail, Roche, Mannheim, Germany). Cells were either used fresh or frozen at this step until needed. Immediately prior to use, cells were homogenized in PBS (with protease inhibitor) using a glass tissue homogenizer then centrifuged at 35000 X g for 30 minutes in a Beckman JA20 rotor. Membranes were washed once more with PBS and resuspended in 1ml PBS/100 mm dish. Protein content was determined using Lowry assay (Sigma Diagnostics, MO). Binding assays were performed in PBS with protease inhibitors. For  $K_d$  determinations, 50  $\mu$ l of homogenate was incubated at 37°C for 1 hour with varying concentrations of [<sup>3</sup>H]granisetron. Specific binding of [<sup>3</sup>H] granisetron was determined as bound [<sup>3</sup>H] granisetron not displaced by a saturating concentration of a competing ligand (typically 10  $\mu$ M Tropicsetron). For  $K_i$  determinations, 50  $\mu$ l of homogenate was incubated at 37°C for 2 hours with varying concentrations of inhibitor and [<sup>3</sup>H]granisetron. Binding was terminated by rapid filtration onto a GF/B filters.

#### **4.3.7 Data analysis:**

Data obtained from radio-ligand binding assays was analyzed as follows.  $K_d$  values were determined by fitting the binding data to the following equation using GraphPad PRISM

(San Diego, CA):  $B = B_{\text{Max}} [L]^n / ([L]^n + K^n)$  (Eq.2), where B is bound ligand,  $B_{\text{Max}}$  is the maximum binding at equilibrium, L is the free ligand concentration, K is the equilibrium dissociation constant and  $n$  is the Hill coefficient. Statistical analysis of concentration-response data from electrophysiological assays was performed using the equation  $I = I_{\text{Max}} / (1 + EC_{50} / [A]^n)$  (Eq.3), where I is the peak current,  $I_{\text{Max}}$  is the maximal response at a given concentration of agonist A,  $EC_{50}$  is the half-maximal concentration of the agonist A and  $n$  describes apparent Hill slope. Data from competition assays involving *d*-TC was analyzed using the equation  $\theta = [(1 + EC_{50} / [A])^n]^{-1}$  (Eq.4) as previously described (Yan et al., 1999), where  $\theta$  is the normalized current at 5-HT concentration [A],  $EC_{50}$  is the concentration of 5-HT required to obtain half-maximal current, and  $n$  is the apparent Hill slope. Concentration-Response curves were obtained by non-linear regression analysis using GraphPad PRISM. Data were compared for significant differences using student's *t* test.

## 4.4 Results

### 4.4.1 Results from molecular modeling studies:

Ligand-docking studies were performed using the ligand-bound model of the 5-HT<sub>3A</sub>R (Table 4.1, Figure 4.1). This model is based on the crystal structure of AChBP and probably indicates the activated/desensitized state of the receptor (Le Novere et al., 2002; Maksay et al., 2003; Reeves et al., 2003). The ligand-docking studies were originally performed to explore the role of loop C region in ligand-interactions. A part of the results from the ligand docking studies have been presented earlier (Suryanarayanan et al., 2004). 5-HT docked model suggests that the side chain of Y153 is positioned within less than 4Å of the hydroxyl group of 5-HT. The O-H group of 5-HT forms a hydrogen bridge with Y153, interfering with the H-bonding network of the receptor. In case of *m*CPBG-docked model of the receptor, the side chain or the backbone of Y153 are not within 4Å of the docked *m*CPBG. There is no strong hydrogen bonding interaction possible between the ligand and loop E tyrosine residues, since the chloro group of *m*CPBG points toward the loop E. In case of both 5-HT and *m*CPBG docked models, both Y141 and Y143 are positioned more than 4Å from the docked ligands. Both 5-HT and *m*CPBG seem to interact with Y234 through a cation-pi interaction.

Molecular modeling studies were performed to investigate interactions of the loop E tyrosine residues in the ligand-free and ligand-bound state (Table 4.2, Figure 4.1). To this purpose, hydrogen bonding pattern of the tyrosine residues was examined using the ground state model and the ligand-bound model of the murine 5-HT<sub>3A</sub> receptor. Movement of loop C apparently influences the inter-subunit hydrogen bonding pattern of

the molecule. Y141 possess only intrasubunit interactions, which remain unchanged during the conformational change. In the closed form model, Y234 forms an intersubunit hydrogen bond only with Y143. In ligand-bound state, the position of Y234 is shifted closer to Y153, and forms a dual hydrogen bond with Y143 and Y153. Y234 also gets closer to the W183, however this distance is still more than 4Å even in open form. A reduction in the distance between Y153 main chain and W183 side chain is also observed. These calculations also suggest that residues Y141, Y143, Y153 and W183 form various intra-subunit contacts with other residues. These intra-subunit contacts are not altered significantly by agonist binding and may indicate structural features. The main finding of these protein modeling results that while Y143 seems to form intermolecular hydrogen bonds both in closed and open state, Y153 is hydrogen bonded with Y234 only in 5-HT-bound form model of the receptor.

#### **4.4.2 Results from biochemical assays:**

Site directed mutagenesis studies of LGICs have been used extensively to identify amino acids participating in receptor-ligand interactions. Electrophysiological assays are regularly employed to assess the possible role played by an amino acid in such interactions.  $EC_{50}$  measurements from electrophysiological assays can demarcate an amino acid as potentially important. However, these data alone cannot unequivocally determine whether a residue plays a role in a direct binding interaction or is involved in the transduction of the binding signal that leads to channel opening; i.e. gating (Colquhoun, 1998). A simplest form of mechanism for receptor activation (Del Castillo and Katz mechanism) is given as:



where the agonist A binds to the vacant closed receptor R. This interaction is governed by the equilibrium binding rate constant  $KA$ . The receptor-agonist complex AR then isomerizes to the open state  $AR^*$ . The activation step is governed by equilibrium gating constant  $E$ . Measurement of  $EC_{50}$  value for the receptor R will be influenced both by the changes to  $KA$  and  $E$ . To address this issue of 'binding vs. gating' we have employed the "traditional partial agonist approach" (Downie et al., 1996; Downie et al., 1995; O'Shea and Harrison, 2000; O'Shea et al., 2000; Rajendra et al., 1995). This approach compares the fractional maximal currents ( $I_{Max}$ ) of full and partial agonist on a single receptor preparation for both the wild type and mutant receptors. Changes to fractional  $I_{Max}$  ratios can be qualitatively correlated with changes in  $E$  value (Lynch, 2004).  $I_{Max}$  is described by the equation  $I_{Max} = inPO_{Max}$ , where  $i$  is the single channel conductance,  $n$  is the receptor number and  $PO_{Max}$  is the maximum fraction of activated receptors. The maximum fraction of activated receptors ( $PO_{Max}$ ) is described by the equation,  $PO_{Max} = E/(1+E)$  (Lynch, 2004). Since the  $I_{Max}$  values for all the agonists are being measured on single preparation, the receptor number  $n$  will be a constant value. Assuming that the single channel conductance ( $i$ ) and the desensitization rates remain unchanged, measurement of fractional  $I_{Max}$  ratios (relative efficacies) can be correlated with changes in  $E$  (Lynch, 2004).

To compare fractional maximal currents (relative efficacies) for all four agonists (5-HT, *m*CPBG, PBG and 2-Me5HT), the fractional  $I_{Max}$  value obtained for 5-HT was



assumed to be 100% or 1 for each of the receptor. This assumption is being solely used as a reference for all the  $I_{Max}$  comparisons. We do not assume that the fractional  $I_{Max}$  for 5-HT is unchanged for any of the mutant receptors.

*Xenopus* oocytes expressing wt receptors produced characteristic inward currents when rapidly exposed to 5-HT or *mCPBG* (Figure 4.2A). Iterative curve fitting of the data yielded  $EC_{50}$  values that corroborate well with the published results (Figure 4.2, Table 4.4). 5-HT was the most efficacious agonist on wt receptors, producing maximal currents ( $I_{Max}$ ) of  $14.8 \pm 1.58 \mu A$  ( $n=12$ ) at supra-maximal concentrations (Table 4.5). To accurately record  $I_{Max}$  values, drug concentrations were limited to 10-40 X  $EC_{50}$ . Higher concentrations can produce erroneously low  $I_{Max}$  values due to rapid receptor desensitization. To avoid such effects on maximal currents, an optimal concentration of each agonist for each receptor type was chosen after assaying a range of supra-maximal concentrations. Maximal concentration was defined using the doses-response curve. An optimal supra-maximal concentration was determined to be that which caused less than 5% reduction compared to the maximal concentration. In addition, a specially designed perfusion chamber was employed in order to achieve faster rise times and faster solution changes compared to conventional perfusion chambers (Joshi et al., 2004). At such concentrations, *mCPBG* elicited only 92 ( $\pm 1$ ) % of the current produced by 5-HT. The ligands 2-Me5HT and PBG also behaved as partial agonists; producing only 12 ( $\pm 1$ ) and 87 ( $\pm 7$ ) % of 5-HT induced currents (Figure 4.2B & C). These data are in agreement with previously published results (Downie et al., 1994; Hope et al., 1993) and suggest that the open conformation of the wild type 5-HT<sub>3A</sub>SR channel is most efficiently stabilized by

the endogenous agonist 5-HT, followed by *m*CPBG, PBG and least efficiently by 2-Me5HT.

A homogeneous population of receptors was labeled when membrane preparations of *t*SA201 mammalian cells transiently transfected with m5-HT<sub>3A</sub>S cDNA were employed in a saturation ligand-binding assay. [<sup>3</sup>H] granisetron bound to wt receptors with high affinity ( $K_d = 0.98 \pm 0.18$  nM) and a Hill slope greater than one ( $n_H = 1.6 \pm 0.08$ ).

Oocytes expressing Y141A mutant receptors exhibited inward currents on exposure to 5-HT. Response characteristics, including rapid rise times and fast desensitization, were indistinguishable from those of wt receptor (Figure 4.3A). Exposure to *m*CPBG and PBG produced similar results. The EC<sub>50</sub> for 5-HT was unaltered while a 4-fold increase for *m*CPBG was observed (Figure 4.3B, Table 4.4). Only a 2-fold change was observed in the EC<sub>50</sub> value for PBG.

5-HT was the most efficacious agonist for the Y141A receptor, producing an I<sub>Max</sub> of  $0.54 \pm 0.04$   $\mu$ A ( $n = 9$ ) at supra maximal concentrations. Among mutant receptors, Y141A produced the lowest I<sub>Max</sub> values. At supra-maximal concentrations, *m*CPBG produced approximately 90 ( $\pm 2$ ) %, ( $n = 5$ ) while PBG produces 85.4 ( $\pm 2.8$ ) % ( $n = 6$ ) of currents produced by 5-HT; results that are similar to those obtained with the wild type receptor (Figure 4.2C). The substantially lower I<sub>Max</sub> of 5-HT induced responses impeded our attempts at fully characterizing the actions of the partial agonist 2-Me5HT. We have previously reported that the Y141A mutation produces a 50-fold reduction in the K<sub>i</sub> for *d*-TC on the 5-HT<sub>3A</sub> receptor, measured as a function of [<sup>3</sup>H]granisetron displacement

(Venkataraman et al., 2002b), suggesting an altered interaction of *d*-TC with the 5-HT<sub>3A</sub> binding domain. In the present study, we performed electrophysiological competition assays involving 5-HT and *d*-TC to assess the effects of Y141A on *d*-TC inhibition of 5-HT induced responses (Figure 4.2D). *d*-TC inhibited 5-HT induced currents at the wt receptor with a high potency ( $2.57 \pm 0.37$  nM,  $n=3$ ). Unexpectedly, the Y141A mutation led to only a 2.5 fold increase in the apparent IC<sub>50</sub> for *d*-TC (Y141A *d*-TC IC<sub>50</sub> =  $5.9 \pm 1.8$  nM,  $n=3$ ). Although the value for Y141A receptor was significantly different (\*\* $p<0.01$ ) from that obtained for wt receptors, the fold change was minor and was substantially less than the change in K<sub>i</sub> observed for inhibition of [<sup>3</sup>H]granisetron binding by *d*-TC (Venkataraman et al., 2002b)

Minor increase in K<sub>d</sub> for [<sup>3</sup>H] granisetron was observed with Y141A mutation. However, a significant reduction in the receptor expression in tSA 201 cells was observed (Table 4.1). The low I<sub>Max</sub> values for 5-HT obtained from oocytes can be explained by low levels of receptor number, an assumption supported by low expression levels in mammalian system.

No inward currents could be elicited from oocytes injected with Y143A mutant cRNA in response to 1 mM of either 5-HT, *m*CPBG or PBG (data not shown). These experiments were repeated multiple times ( $n=27$ ) using at least six different batches of oocytes with identical results. In contrast, oocytes expressing Y143F mutant receptors produced rapid inward currents with rapid desensitization on exposure to both 5-HT and *m*CPBG. The response characteristics of Y143F receptors were thus indistinguishable from wt receptors (Figure 4.4A). Compared to wt receptors, the EC<sub>50</sub> for 5-HT on Y143F

receptors increased by 61 fold ( $207 \pm 22.8 \mu\text{M}$ ). A large increase in the  $\text{EC}_{50}$  value was also observed for 2-Me5HT (170 fold,  $2.77 \pm 0.13 \text{ mM}$ ), while a relatively minor increase was seen for both *m*CPBG (6 fold,  $5.33 \pm 0.19 \mu\text{M}$ ,  $**p < 0.01$ ) and PBG (16 fold,  $337 \pm 14.2 \mu\text{M}$ ) (Table 4.4). Only a minor change in Hill slopes was apparent (Table 4.4). Efficacies of all four agonists were compared using the protocol described earlier. *m*CPBG was the most efficacious agonist for the Y143F receptors, inducing maximal currents of  $1.29 \pm 0.43 \mu\text{A}$  ( $n = 10$ ); a value substantially lower than the  $I_{\text{Max}}$  values obtained for wt receptors (Table 4.5). The maximum current induced by application of  $100 \mu\text{M}$  *m*CPBG was significantly different than that produced by  $3 \text{ mM}$  5HT ( $115 \pm 5.3\%$  of 5-HT current,  $n = 9$ ,  $**p < 0.01$ ). Although average  $I_{\text{Max}}$  values produced were in the range of 1 to  $2 \mu\text{A}$ , some of the oocytes tested produced currents up to  $3.6 \mu\text{A}$  at supra-maximal *m*CPBG concentrations, allowing us to characterize action of partial agonists. Maximal currents induced by  $3 \text{ mM}$  PBG were  $31.1 \pm 3\%$  ( $n = 5$ ), while maximal current induced by  $10 \text{ mM}$  of 2-Me5HT were only  $1.8 \pm 0.27\%$  ( $n = 4$ ) of those induced by 5-HT. The Y143F mutation thus resulted in significantly altered  $I_{\text{Max}} \text{ PBG} / I_{\text{Max}} \text{ 5-HT}$  and  $I_{\text{Max}} \text{ 2-Me5HT} / I_{\text{Max}} \text{ 5-HT}$  ratios (Figure 4.4C).

Both Y143A and Y143F mutations produced minor changes in  $K_d$  for [ $^3\text{H}$ ] granisetron. While receptor expression levels of Y143A in mammalian cells was moderately reduced, Y143F mutation did not cause any significant changes to receptor expression (Table 4.3).

A shift of  $\sim 40$  fold ( $136 \pm 8.1 \text{ mM}$ ) was observed in the  $\text{EC}_{50}$  value for the agonist 5-HT, on Y153A mutant receptors expressed in *Xenopus* oocytes (Table 4.4). In addition,

responses obtained from these receptors following perfusion with 5-HT show drastically different characteristics when compared to wt responses. 5-HT induced responses on Y153A receptors were marked by both very slow rise times and very slow desensitization (Figure 4.5A), even at supra-maximal concentrations. The Y153A mutation produced a five-fold increase ( $\sim 2000$  msec. Vs. 400 msec.  $n=7$ ) in the rise time to the peak inward current as compared to the wt receptor, measured at supra-maximal 5-HT concentration (3 mM for Y153A and 100  $\mu$ M for the wt receptor). We have earlier reported similar results for Y153A mutant receptors expressed in *tSA201* cells (Venkataraman et al., 2002b). These findings confirm and further supplement those results.

In contrast to 5-HT, the  $EC_{50}$  value for *mCPBG* on Y153A receptor increased only by  $\sim 9.5$  fold compared to the wt receptor (Figure 4.5C). Surprisingly, *mCPBG* induced responses obtained from Y153A receptors were identical in characteristics to those obtained from wt receptors, with rapid rise times and fast desensitization (Figure 4.5B). *mCPBG* was the most efficacious agonist at Y153A receptors with maximal currents of  $13.8 \pm 2.2$   $\mu$ A ( $n=7$ ). In addition *mCPBG* elicited a  $\sim 33$  fold larger  $I_{Max}$  compared to that obtained with 5-HT ( $3284 \pm 192\%$  of 5-HT current,  $n=7$ ) at supra maximal concentrations (Figure 4.5D). To confirm that these results were not unique to receptor proteins expressed in *Xenopus laevis* oocytes, *mCPBG*'s effects on Y153A receptors expressed in mammalian cells (*tSA 201*) were characterized using whole-cell patch-clamp assay. Figure 4.6 shows a comparison of currents elicited from wild type and Y153A receptors using 5-HT and *mCPBG* at maximal concentrations. Results were similar to those obtained from oocytes expressing Y153A receptors (Figure 4.6).

An  $EC_{50}$  of  $243 \pm 17.1 \mu\text{M}$  was determined for PBG activation of Y153A receptors expressed in oocytes, a rightward shift of  $\sim 12$  fold compared to wt receptors. PBG currents were similar to those observed for *mCPBG* displaying rapid rise times and fast desensitization. Currents elicited by 3 mM PBG were  $\sim 31$  fold greater than those elicited by 5-HT ( $3148 \pm 714$  % of 5-HT current,  $n=7$ ) and slightly less than those obtained with *mCPBG*. Thus, the rank efficacy of *mCPBG* compared to PBG is unchanged by the Y153A mutation (Figure 4.5D). Maximal currents obtained with 5-HT produced average currents of only  $0.5 \mu\text{A}$ ; however, some oocytes produced up to  $1.6 \mu\text{A}$  currents in response to 3 mM 5-HT. On these oocytes, 2-Me5HT would be expected to produce an  $I_{\text{Max}}$  of  $\sim 0.19 \mu\text{A}$  if the Y153A mutation did not alter its efficacy relative to 5-HT. However, no currents could be elicited with 2-Me5HT up to a concentration of 10 mM suggesting a change in the  $I_{\text{Max}} 2\text{-Me5HT} / I_{\text{Max}} 5\text{-HT}$  (efficacy) ratio. This conclusion is also supported by data obtained for 2-Me5-HT on Y153F receptors (described below). The rank efficacy of the four agonists tested on wt receptor was 5-HT > *mCPBG*  $\geq$  PBG  $\gg$  2-Me5HT. This rank of efficacy was drastically altered for Y153A receptor (Figure 4.5D). For Y153A receptor, the rank efficacy was: *mCPBG*  $\geq$  PBG  $\gg$  5-HT  $\gg$  2-Me5HT.

Mutation of Y153 to phenylalanine led to a relatively minor increase in  $EC_{50}$  values for all four agonists. While a  $\sim 14.5$  fold increase was observed in the  $EC_{50}$  value for 5-HT, the  $EC_{50}$  for *mCPBG* increased only  $\sim 3$  fold (Table 4.4). Similarly, a  $\sim 2$  fold increase in the  $EC_{50}$  value for 2-Me5HT and  $\sim 3$  fold increase in the  $EC_{50}$  for PBG were observed. The Y153F mutation also produced normal kinetics for the 5-HT induced

response, with rapid onset and rapid desensitization (Figure 4.7A). Similar to the Y153A mutation, *m*CPBG was the most efficacious agonist. Oocytes expressing Y153F receptors produced  $I_{Max}$  values in response to supra-maximal concentrations of *m*CPBG that were significantly less than those expressing Y153A receptors (Table 4.5). The low  $I_{Max}$  values are in agreement with reduced receptor protein expression levels observed for the Y153F mutation in *t*SA201 cells.

A comparison of efficacies of all four agonists reveals changes in rank efficacy similar to the Y153A mutation. Although moderate, changes in efficacies were nonetheless significant. While exposure of Y153F mutant receptor to *m*CPBG yielded 177 ( $\pm 11$ ) % of  $I_{Max}$  compared to 5-HT induced maximal current (assumed 100% in each case,  $n=22$ ), exposure to PBG resulted in 138 ( $\pm 2$ ) % of 5-HT  $I_{Max}$  ( $n=8$ ). Most importantly, 2-Me5HT produced 0.7 ( $\pm 0.2$ ) % of maximal current ( $n=7$ ), compared to 5-HT (Figure 4.7 B and C). Thus, even for the subtle Tyr to Phe mutation, the change in rank of efficacy observed for the Y153A mutation was preserved, i.e.,  $mCPBG \geq PBG > 5-HT \gg 2-Me5HT$ .

Both Y153A and Y153F mutations produced minor changes in  $K_d$  for [ $^3H$ ] granisetron. While receptor expression level of Y153A in mammalian cells was unaltered, Y153F mutation produced moderate changes in receptor expression level (Table 4.3).

#### 4.5 Discussion

This study was primarily conducted to determine whether tyrosine residues of loop E region play a role in mediating gating of the 5-HT<sub>3A</sub>R channel. The theoretical framework for the mutagenesis experiments was provided by the molecular modeling studies. These studies indicated that Y143 hydroxyl forms inter-subunit contacts residues from the principal face of the binding domain. These studies also suggested that H-bonding partner for the Y153 hydroxyl group differs depending on the class of the agonist bound. While 5-HT hydrogen bonds with Y153, *m*CPBG does not. In case of bound *m*CPBG, Y153 forms the H-bond with Y234.

The majority of the biochemical data presented here has been obtained from two-electrode voltage-clamping of *Xenopus* oocytes, although whole-cell recording was employed in a limited manner. To overcome limitations on slow solution exchange rates inherent to oocyte electrophysiology, we employed a specially designed small-volume oocyte chamber (Joshi et al., 2004). The method of oocytes electrophysiology was validated by reproduction of a complete pharmacological profile of the murine 5-HT<sub>3AS</sub> including relative efficacies. In case of Y153, we were able to reproduce the results obtained from *Xenopus* oocytes using whole-cell recordings. Other studies have noted the difficulties associated with mammalian expression of loop E mutant receptors (Price and Lummis, 2004; Venkataraman et al., 2002b). Although oocyte based assays cannot replace whole-cell assays in terms of resolution and accuracy, they provide a viable alternative in cases where mammalian cell whole-cell recording is difficult to obtain.



Previous competition binding studies of Y141A mutants resulted in largely unaltered  $K_i$  values for both agonists and antagonists, suggesting a lack of any major interaction between Y141 and 5-HT<sub>3A</sub>R ligands. We observed no significant change in  $EC_{50}$  values, Hill slopes or relative efficacies on Y141A receptors, thus further supporting this conclusion. Our results also rule out involvement of Y141 in mediating conformational changes related to gating. The results from the molecular modeling studies presented here also suggest that Y141 does not interact with either 5-HT or *m*CPBG.

In contrast, expression levels of Y141A receptors appeared to decrease.  $B_{Max}$  values observed in mammalian cells were consistent with very low  $I_{Max}$  values for most efficacious agonist 5-HT, obtained in oocytes. The reduced  $I_{Max}$  values from oocytes could be a result of drastic changes to channel gating (E) mediated by 5-HT. However, such changes to gating would also result in drastic changes to  $EC_{50}$  value for 5-HT. Since no change to 5-HT  $EC_{50}$  resulted from Y141A mutation, low  $I_{Max}$  values cannot be explained by assuming a disruption in 5-HT induced gating. These results suggest a role for Y141 in receptor assembly. Although caution should be exercised while comparing  $I_{Max}$  and  $B_{Max}$  values from two different expression systems, such a comparison may provide useful correlations between measurements of receptor expression and efficacy changes. Our results thus predict a structural role for Y141. Molecular models of the 5-HT<sub>3A</sub>R predict that Y141 forms a static intra-subunits hydrogen bond with T117. Such a hydrogen bond may play a role in either protein assembly or in maintaining proper receptor structure.

Docking studies of *d*-TC do not predict an interaction with Y141 of the m5-HT<sub>3A</sub>R (Maksay et al., 2003). Consistent with this prediction, only a small increase in IC<sub>50</sub> value was observed for *d*-TC inhibition of 5-HT induced currents on Y141A receptors compared to wt. We previously reported a 50-fold increase in K<sub>i</sub> values for *d*-TC in competition binding assays on tSA201 cells. The basis for this discrepancy is unclear although a more recent study supports this finding (Price and Lummis, 2004). Due to differences in cell type, competing ligands and reaction conditions, binding and functional data cannot be directly compared. The shift of both IC<sub>50</sub> and K<sub>i</sub> in the same direction, however, suggests a minor interaction of Y141 with *d*-TC.

Y143F mutation produced significant changes in efficacy ratios for partial agonists PBG and 2-Me5HT and 5-HT (i.e., I<sub>Max</sub> PBG/I<sub>Max</sub> 5-HT and I<sub>Max</sub> 2-Me5HT/I<sub>Max</sub> 5-HT). These results strongly support a central role for Y143 in gating. Other observations also support the role of Y143 in channel gating. I<sub>Max</sub> values for 5-HT induced responses on Y143F receptors were reduced in comparison to those obtained from wt receptors indicating a possible decrease in 5-HT efficacy. While it is possible that the low I<sub>Max</sub> values obtained in oocytes were actually as a result of low receptor number, B<sub>Max</sub> values for Y143F receptors expressed in mammalian cells were comparable to those of wt receptors. Based on expression levels obtained in mammalian cells, a more parsimonious explanation for low I<sub>Max</sub> values obtained in *Xenopus* oocytes would be an alteration in gating constant for agonists in Y143F mutant receptors. Competition binding studies of Y143A receptors have reported large changes in K<sub>i</sub> values for both 5-HT and *m*CPBG (Venkataraman et al., 2002b). In the present study, no responses could be

elicited from oocytes or mammalian cells expressing Y143A receptors, although  $B_{Max}$  values obtained from *tSA201* cells (Table 4.3) were 40% of the wt values. These results again suggest that Y143 plays a role in channel gating and/or ligand binding in addition to proper receptor assembly. The results from the molecular modeling studies suggest that Y143 forms several inter-subunit H-bonds during the ground- as well as the agonist-bound state. The combined results from biochemical and modeling studies suggest that the involvement of Y143 in the formation of the static and probably the dynamic H-bonding network is responsible for its role in both maintaining the structural integrity and mediation of the gating effects. The results from the molecular modeling studies presented here also suggest that Y143 does not interact with either 5-HT or *mCPBG*. Previous studies have demonstrated the importance Y234 in mediating agonist action (Beene et al., 2004; Price and Lummis, 2004; Suryanarayanan et al., 2004). Y143 may be playing a role in mediating gating through H-bonding interactions with side chain hydroxyl group of Y234. Presence of such interactions in the activated state probably explains the severe effects of even a subtle mutation at Y143 and Y234 positions. These data also indicate that Y143 exerts its effect via interacting with other amino acids of the binding domain rather than the bound ligand.

Y143 may also be playing a role in agonist specificity. Rank efficacies of full agonists were altered for Y143F receptors compared to wt. Changes in efficacy parallel the shifts in  $EC_{50}$  value with the most efficacious agonist *mCPBG* showing the least change in  $EC_{50}$  and the least efficacious agonists 2-Me5HT showing the largest change in  $EC_{50}$ . These results suggest that *mCPBG* induced channel gating is more tolerant to

disruption at Y143 as compared to 5-HT induced channel gating. Although the efficacy of *m*CPBG appeared to increase relative to 5-HT, the drastically reduced  $I_{Max}$  value associated with *m*CPBG responses may indicate that *m*CPBG efficacy was also decreased.

Along with a large reduction in  $EC_{50}$  value, Y153A receptors have drastically altered 5-HT induced response characteristics, showing peculiar currents with increased rise times. These response characteristics suggest a major alteration in the gating mechanism. 2-Me5HT, an analog of 5-HT failed to produce any currents in oocytes expressing Y153A receptors, again reflecting a possible change in gating. At supra-maximal concentrations, currents induced by 5-HT on Y153A receptors are strikingly similar in characteristics to those induced by 2-Me5HT on wt receptors, further suggesting that 5-HT acts in a manner similar to a low efficacy partial agonist on the Y153A receptor. On the other hand, the partial agonist action of 2-Me5HT on wt cannot be linked to a lack of involvement of Y153 since mutations at Y153 also severely alter the efficacy of 2-Me5HT. Mutation of Y153 to phenylalanine produced normal response characteristics and produced currents in response to 2-Me5HT. The efficacy profiles for Y153A and Y153F receptors were identical: *m*CPBG >> PBG >> 5-HT >> 2-Me5HT. Compared to 5-HT and 2-Me5HT,  $EC_{50}$  values for *m*CPBG and PBG increased only moderately on Y153A receptors and both phenylbiguanides displayed response characteristics indistinguishable from wt receptors. *m*CPBG and PBG, produced  $I_{Max}$  amplitudes that were not significantly different than those obtained for wt receptors (Table 4.3). The differences in efficacy for *m*CPBG and PBG were also similar to wt

receptors while  $EC_{50}$  values increased slightly. Expression levels of Y153A mutant receptor in *t*SA201 cells are also very similar to those of the wt receptor.  $I_{Max}$  values identical to wt and moderate *increase* in the  $EC_{50}$  for *m*CPBG and PBG, suggest that the efficacy of these phenylbiguanides on Y153A has not increased compared to wt. The data for both Y153A and Y153F receptors suggest that Y153 may be differentially modulating the gating of the 5-HT<sub>3A</sub>R according to structural class of the agonist. Thus, mutations at Y153 specifically alter responses to hydroxytryptamine and not phenylbiguanide agonists. Although substituting alanine with a phenylalanine restored the normal characteristics of 5-HT induced response, the effects on gating could not be completely reversed indicating that both the aromatic ring and the hydroxyl group may be involved in a complex interaction mediating 5-HT induced channel gating. While the effects of Y153 mutations appear specific for 5-HT type agonists, it should be pointed out that the slight increase in  $EC_{50}$  values for *m*CPBG and PBG may also indicate a minor role for Y153 in mediating the interaction of these agonists.

The role played by the loop E tyrosine residues in the differential modulation of the gating mechanism may indicate a conserved feature of the LGIC superfamily. The apparent lack of conservation in this region of the protein among various members of this family supports such a contention (Figure 4.8). The amino acid homologous to Y153 in the  $\gamma_2$  GABA<sub>A</sub> R ( $\gamma_2$ T142; Figure 4.8) is involved in differentially modulating the efficacy of benzodiazepines (Mihic et al., 1994). T142 presumably mediates these effects through a hydrogen bond with Y160 (homologous to W183 of 5-HT<sub>3A</sub>R) of  $\alpha$ GABA<sub>A</sub> on the (+) face of the binding site (Cromer et al., 2002). Available data on the nicotinic

acetylcholine receptors suggests that nicotine and acetylcholine interact differentially with the amino acids in the ligand-binding domain (Beene et al., 2002; Petersson et al., 2002). Crystallographic studies of AChBP show a hydrophobic interaction between R104 (homologous to Y143) and carbamylcholine, but not nicotine (Celie et al., 2004). M114 (homologous to Y153) on the other hand, is involved in hydrophobic contact both with nicotine and carbamylcholine. In addition, main chains of L102 (homologous to Y141) and M114 (homologous to Y153) interact with nicotine but not carbamylcholine by virtue of a hydrogen bond. These studies provide evidence for the role of loop E region in mediating agonist specificity. These results also provide the most explicit evidence of direct interaction of agonists with the amino acids under consideration. Crystallographic studies can thus provide immense amount of details about protein structure. While such information cannot be easily obtained from electrophysiological assessment of mutant receptors, such assessment provides information about the dynamics of conformational changes and receptor gating.

Our data suggests that in the activated state, Y234 of the loop C region moves closer to the loop E region. Results from studies on the AChBP indicate that loop C as well as the other regions of the ligand-binding domain close in on the bound agonist upon activation (Celie et al., 2004). Modeling studies described here show that Y143 and Y153 play a role in forming hydrogen-bonding contacts during activation. The biochemical data supports such a role for Y143 and Y153. Both Y143 and Y153 form H-bonds with Y234, although the mode of bond formation differs according to the state of the receptor (ligand-free vs. ligand-bound) and the type of agonist (5-HT vs. *m*CPBG). While the

Y143-Y234 hydrogen bond exists both in closed and open state, the Y153-Y234 hydrogen bond is only seen in our *m*CPBG-docked open state model. Thus, Y143 apparently forms a hydrogen bonding interaction with Y234 in the case of both 5-HT and *m*CPBG binding. The results of our modeling studies also suggest that the specific role played by Y153 in 5-HT mediated gating could be the result of a direct interaction of the Y153 side chain with the hydroxyl group of 5-HT. This conclusion is well supported by the biochemical data. The lack of an interaction between Y153 and *m*CPBG may explain why mutations at Y153 are better tolerated by *m*CPBG-mediated agonism. The biochemical data obtained from phenylbiguanides also suggest that the Y153-Y234 H-bond may not be critical to proper channel gating. Similar profile of the results for *m*CPBG and PBG for mutations at Y153 suggests a similar mode of action for all phenylbiguanide agonists. These data thus suggest that amino acids Y143 and Y153 are involved in stabilization of the open state of the receptor through different mechanisms.

In the case of the nicotinic acetylcholine receptor, mutation of amino acids and around the purported ligand binding domain destabilizes the open state of the receptor (Chakrapani et al., 2004). It is conceivable that the Y153-5-HT interaction at least partially stabilizes the open state of the receptor. On the other hand, H-bonding interactions of Y143 seem to be involved in mediating agonist action in general.

The role of loop E tyrosine residues in receptor mechanism is probably not restricted to inter-subunit interactions. Several other lines of evidence suggest that both Y143 and Y153 could both be involved in direct interactions with 5-HT<sub>3A</sub>R antagonists (Maksay et al., 2003; Venkataraman et al., 2002a; Venkataraman et al., 2002b). The

results of previous and present studies thus indicate a dual role for Y143 and Y153. As part of the ligand-binding domain these residues may be involved in binding interactions with competitive antagonists. Agonists on the other hand probably mediate channel gating by bringing about the local rearrangement of the H-bond network formed by these tyrosine residues. Our results indicate that subtle changes in this rearrangement could be at least partially responsible for the differential action of two structurally distinct agonists, 5-HT and *m*CPBG.



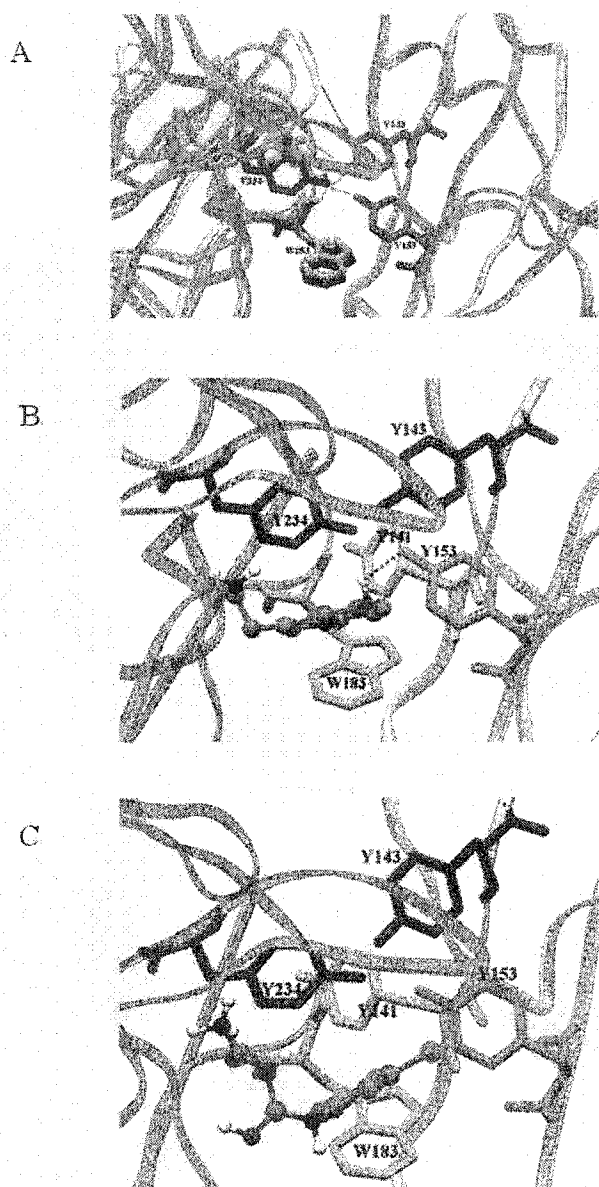


**Figure 4.1 Results from molecular modeling and ligand-docking studies**

**4.1.A Movements of the 5-HT<sub>3A</sub>R regions surrounding the ligand-binding domain associated with activation:**

Structures of 5-HT<sub>3A</sub> dimer units with open (ligand-free, green) and closed (ligand-bound, blue) binding clefts. The conformational change causes a shift in Y234 position, which alters its inter-subunit hydrogen bonding partners, forming a Y234-Y153 bond.

**4.1.B Docking of 5-HT to ligand-bound 5-HT<sub>3A</sub>R receptor model:**

The O-H group of 5-HT forms a hydrogen bridge with Y153, interfering with the H-bonding network of the receptor.

**4.1.C Docking of *m*CPBG to ligand-bound 5-HT<sub>3A</sub>R receptor model:**

There is no strong hydrogen bonding interaction possible between the ligand and loop E tyrosine residues, since the chloro- group of *m*CPBG points toward the loop E.

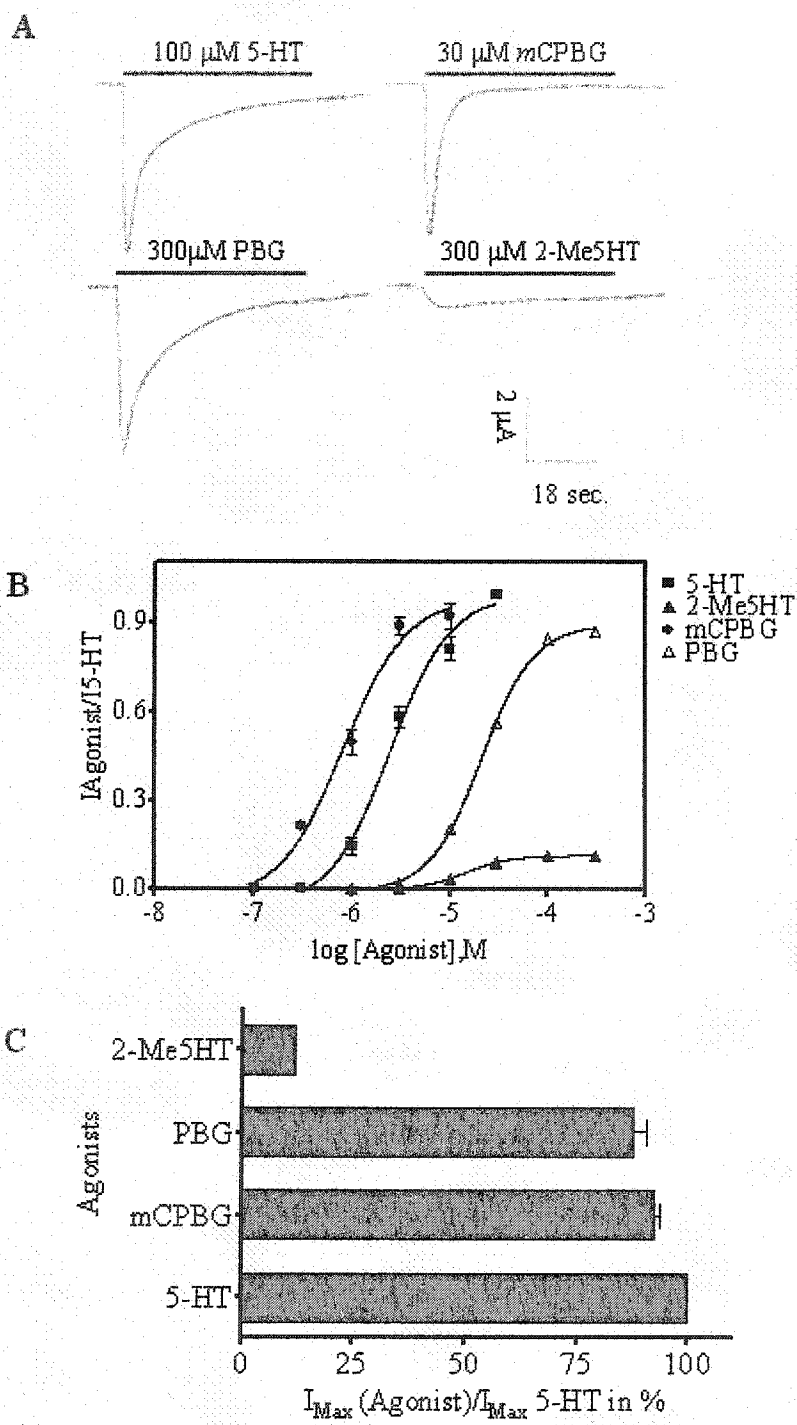


**Figure 4.2 Electrophysiological characterization of wt 5-HT<sub>3A</sub>S receptors expressed in *Xenopus laevis* oocytes**

**4.2.A Characteristics of inward currents elicited by application of agonists at supra-maximal concentration.**

The set of traces shown was obtained from a single oocyte. Traces shown are representative of multiple experiments. The solid bar on the top of each trace denotes time of drug exposure, type of agonist used and its concentration.

**4.2.B Concentration-response curves for four agonists**

Data obtained for each agonist, i.e., 2-Me5HT, *m*CPBG and PBG were normalized to those obtained for 5-HT for each experiment separately using equation 1. Concentration-Response curves were obtained as described in the methods and materials section. Error bars indicate  $\pm$  S.E.

**4.2.C A comparison of efficacy values for agonists**

Currents for *m*CPBG, PBG and 2-Me5HT were normalized to those obtained for 5-HT as described in methods section. Values are reported as percentages. Results from multiple experiments were combined to plot the bar graph. Error bars indicate S.E. Values obtained were 5-HT = 100% (n=9), *m*CPBG=  $92.6 \pm 0.97\%$  (n=6), PBG= $87.6 \pm 3\%$  (n=6), 2-Me5HT=  $11.8 \pm 0.2\%$  (n=6).

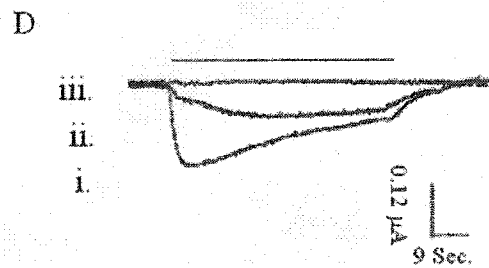
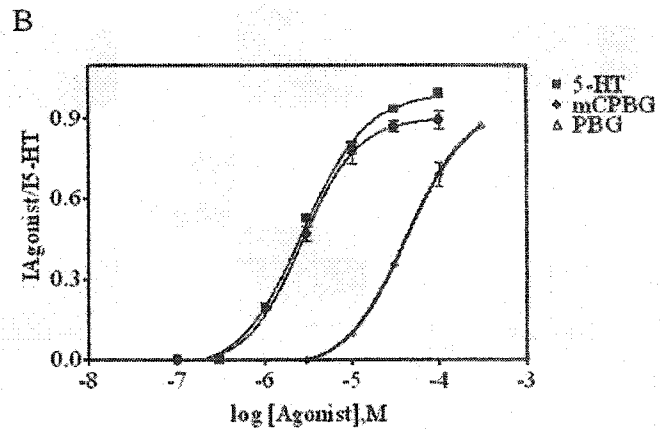
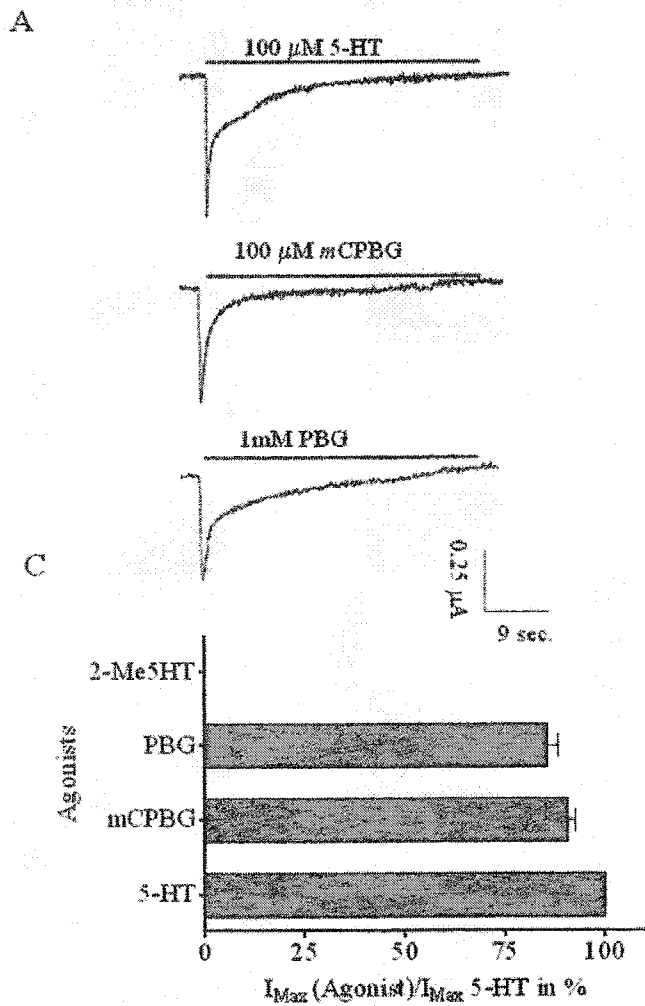


**Figure 4.3 Electrophysiological characterization of Y141A 5-HT<sub>3AS</sub> receptors expressed in *Xenopus laevis* oocytes**

**4.3.A Characteristics of inward currents elicited by application of agonists at supra-maximal concentration.**

The set of traces shown was obtained from a single oocyte. Traces shown are representative of multiple experiments. The solid bar on the top of each trace denotes time of drug exposure, along with the type of agonist used and its concentration.

**4.3.B Concentration-response curves for four agonists**

Data obtained for each agonist, i.e., 2-Me5HT, *m*CPBG and PBG were normalized to those obtained for 5-HT for each experiment separately using equation 1. Concentration-Response curves were obtained as described in the methods and materials section. Changes both to EC50 values as well as efficacies (relative to 5-HT) are evident from the concentration-response curves. Refer to Table 4.2 for Hill slope values. Error bars indicate S.E.

**4.3.C A comparison of efficacy values for agonists 5-HT, *m*CPBG and PBG**

For each experiment, the maximal currents elicited by each agonist (*m*CPBG, PBG and 2-Me5HT) were directly compared to those elicited by 5-HT on a single oocyte. Results from multiple experiments were combined to plot the bar graph comparing efficacy values. Error bars indicate S.E. produced approximately 5-HT= 100% (n=9), *m*CPBG= 90±2 %, (n=5) PBG= 85.4±2.8% (n=6). 2-Me5HT currents could not be recorded due to very low *I*<sub>max</sub> values.

**4.3.D Inhibition of 5-HT induced responses by co-application of *d*-TC.**

Application of *d*-TC was initiated 30 sec prior to co-application of 5-HT and *d*-TC. (i) 3 μM 5-HT (ii) 3 μM 5-HT + 3 nM *d*-TC (iii) 3 μM 5-HT + 30 nM *d*-TC

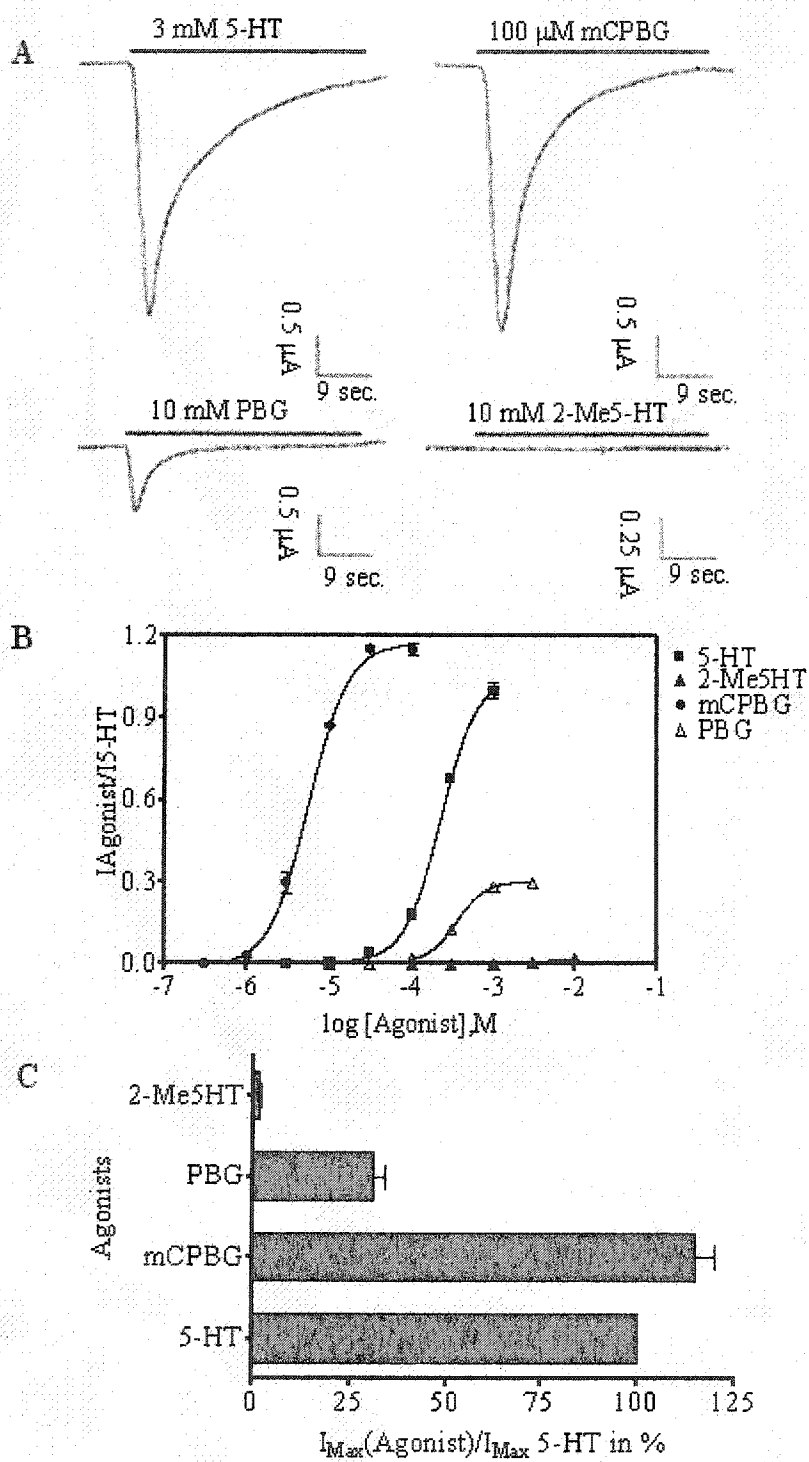


**Figure 4.4 Electrophysiological characterization of Y143F 5-HT<sub>3AS</sub> receptors expressed in *Xenopus laevis* oocytes.**

**4.4.A Characteristics of inward currents elicited by application of agonists at supra-maximal concentration.**

The set of traces shown was obtained from a single oocyte. Traces shown are representative of multiple experiments. The solid bar on the top of each trace denotes time of drug exposure, along with the type of agonist used and its concentration.

**4.4.B Concentration-response curves for four agonists**

Data obtained for each agonist, i.e., 2-Me5HT, *m*CPBG and PBG were normalized to those obtained for 5-HT for each experiment separately using equation 1. Concentration-Response curves were obtained as described in the methods and materials section. Changes both to EC<sub>50</sub> values as well as efficacies (relative to 5-HT) are evident from the concentration-response curves. Refer to Table 4.2 for Hill slope values. Error bars indicate S.E.

**4.4.C Comparison of efficacies of 5-HT, *m*CPBG, PBG and 2-Me5HT**

For each experiment, the maximal currents elicited by each agonist (*m*CPBG, PBG and 2-Me5HT) were directly compared to those elicited by 5-HT on a single oocyte. Results from multiple experiments were combined to plot the bar graph comparing efficacy values. Error bars indicate S.E. Values obtained were 5-HT = 100% (n=10), *m*CPBG= 115 ± 5.34 % (n=9), PBG= 31.1 ± 3.96 % (n=5), 2-Me5HT= 1.87 ± 0.27% (n=4).



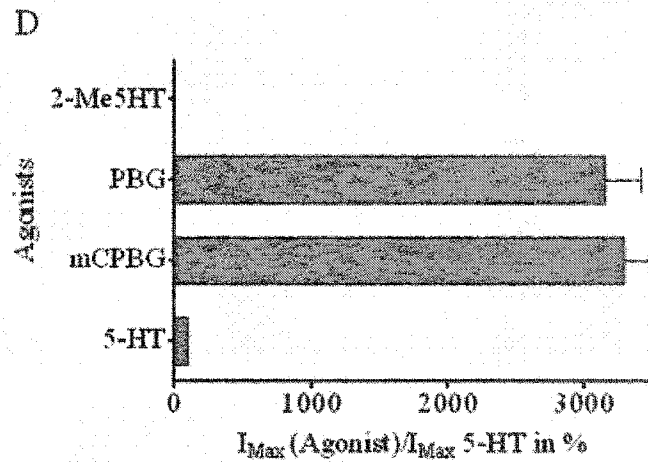
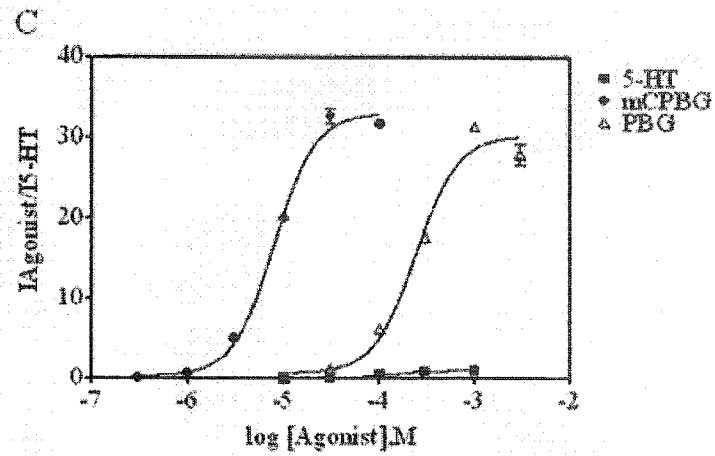
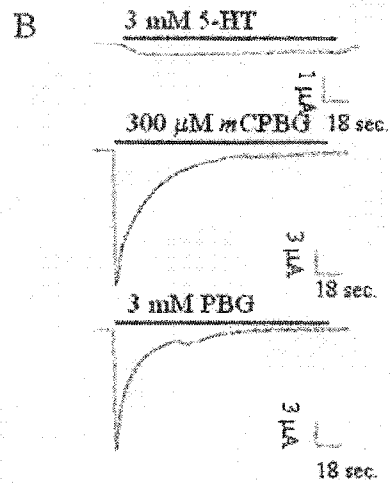
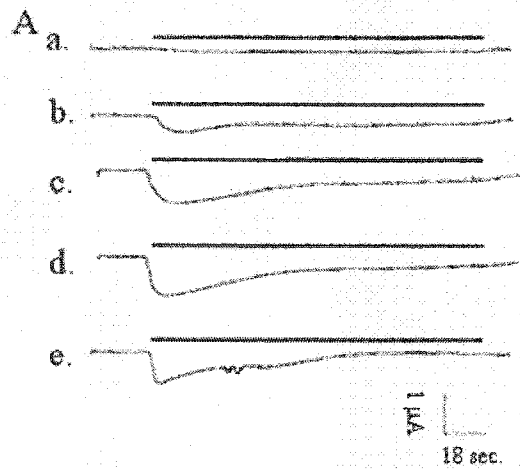


**Figure 4.5 Electrophysiological characterization of Y153A 5-HT<sub>3A</sub> receptors expressed in *Xenopus laevis* oocytes.**

**4.5.A Currents elicited by application of increasing concentrations of 5-HT to oocytes expressing Y153A mutant receptors.**

Note that the time scale is different as compared to other traces shown in the Figure. All the traces are characterized by increased rise times and slow desensitization rates. The rise times do not increase significantly with increasing concentrations.

**4.5.B Characteristics of inward currents elicited by application of agonists at supra-maximal concentration**

The set of traces shown was obtained from a single oocyte. Traces shown are representative of multiple experiments. The solid bar on the top of each trace denotes time of drug exposure, along with the type of agonist used and its concentration. Concentration-response curves for four agonists. Data obtained for each agonist, i.e., 2-Me5HT, *m*CPBG and PBG were normalized to those obtained for 5-HT for each experiment separately using equation 1. Concentration-Response curves were obtained as described in the methods and materials section. Changes both to EC<sub>50</sub> values as well as efficacies (relative to 5-HT) are evident from the concentration-response curves. Refer to Table 4.2 for Hill slope values. Error bars indicate S.E.

**4.5.C Comparison of efficacies of 5-HT, *m*CPBG, PBG and 2-Me5HT.**

For each experiment, the maximal currents elicited by each agonist (*m*CPBG, PBG and 2-Me5HT) were directly compared to those elicited by 5-HT on a single oocyte. Results from multiple experiments were combined to plot the bar graph comparing efficacy values. Error bars indicate S.E. Values obtained were 5-HT = 100% (n=7), *m*CPBG= 3284 ± 192% (n=7), PBG= 3148 ± 270% (n=7), 2-Me5HT= 0% (n=7).

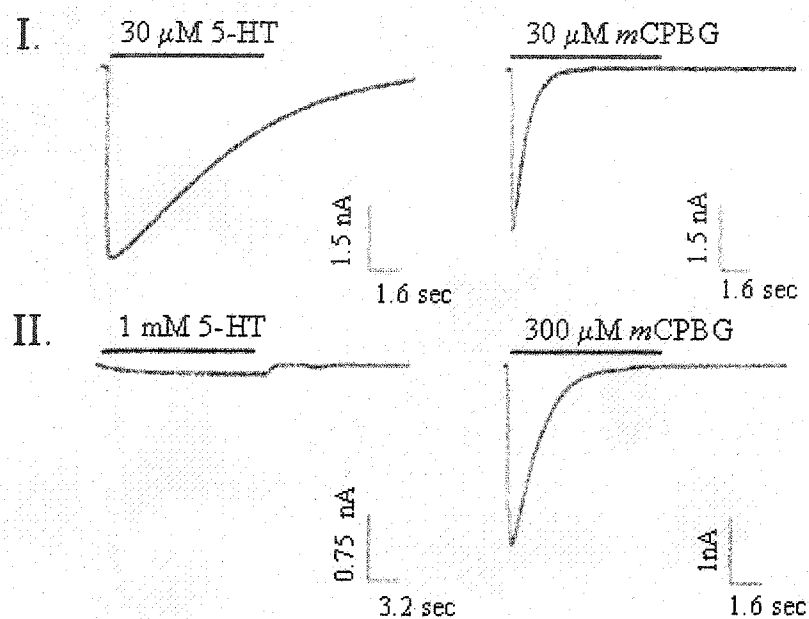


**Figure 4.6** Whole-cell patch-clamp recording from tSA 201 cells transfected with wt and Y153A cDNA.

Data were obtained using whole-cell patch-clamp on tSA201 cells transfected with wt or Y153A mutant 5-HT<sub>3ASR</sub> cDNA as described in methods section. The solid bar on the top of each trace denotes time of drug exposure, along with the type of agonist used and its concentration. The responses indicated in A and B are representative examples of at least 3 sets of experiments.

**I. wt 5-HT<sub>3ASR</sub>:** Agonists were applied for 4 s duration.

**II. Y153A mutant receptors:** Agonists were applied for 8 s duration.

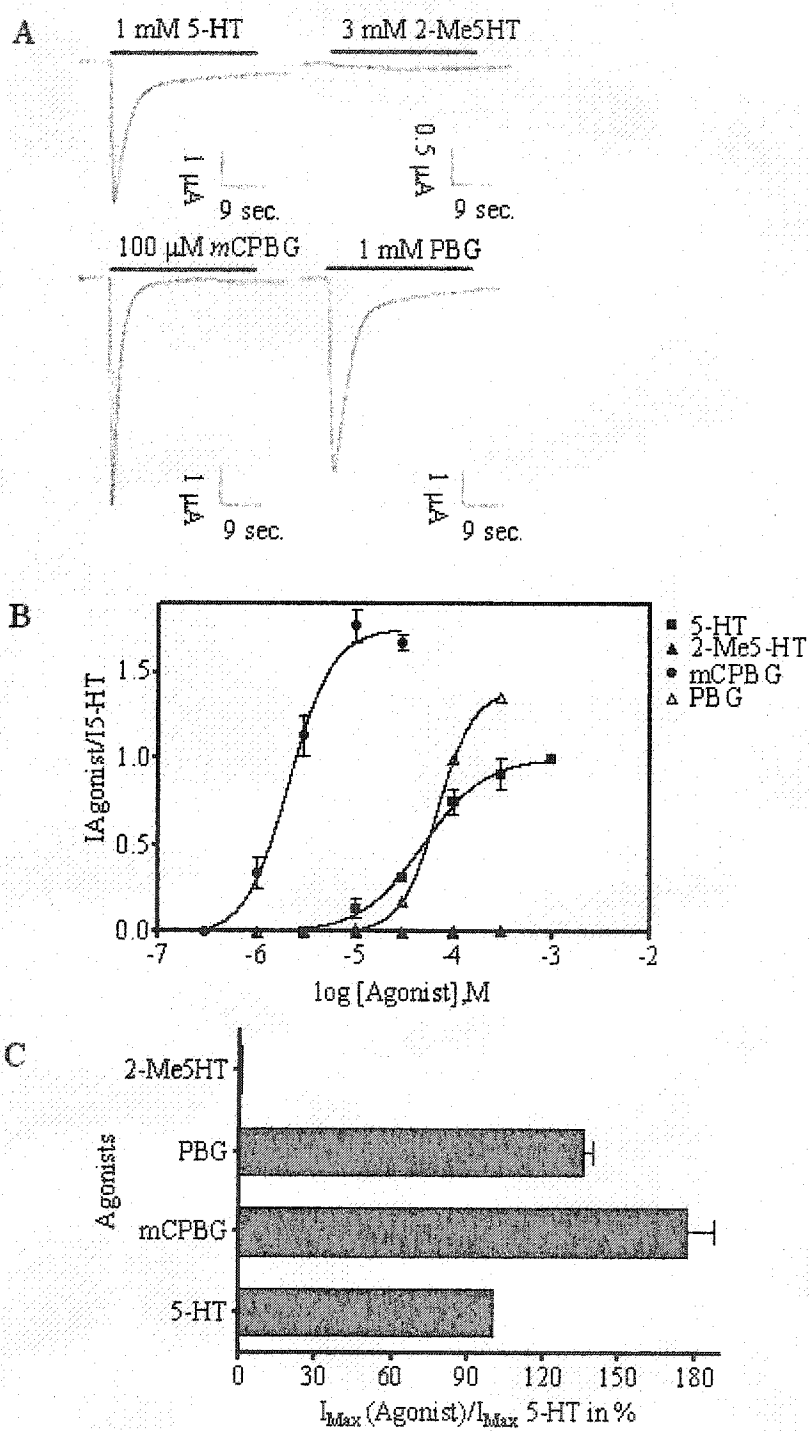


**Figure 4.7 Electrophysiological characterization of Y153F 5-HT<sub>3AS</sub> receptors expressed in *Xenopus laevis* oocytes.**

**4.7.A Characteristics of inward currents elicited by application of agonists at supra-maximal concentration.**

The set of traces shown was obtained from a single oocyte. Traces shown are representative of multiple experiments. The solid bar on the top of each trace denotes time of drug exposure, along with the type of agonist used and its concentration.

**4.7.B Concentration-response curves for four agonists.**

Data obtained for each agonist, i.e., 2-Me5HT, *m*CPBG and PBG were normalized to those obtained for 5-HT for each experiment separately using equation 1. Concentration-Response curves were obtained as described in the methods and materials section. Changes both to EC<sub>50</sub> values as well as efficacies (relative to 5-HT) are evident from the concentration-response curves. Refer to Table 4.2 for Hill slope values. Error bars indicate S.E.

**4.7.C Comparison of efficacies of 5-HT, *m*CPBG, PBG and 2-Me5HT.**

For each experiment, the maximal currents elicited by each agonist (*m*CPBG, PBG and 2-Me5HT) were directly compared to those elicited by 5-HT on a single oocyte. Results from multiple experiments were combined to plot the bar graph comparing efficacy values. Error bars indicate S.E. 5-HT = 100% (n=22), *m*CPBG= 178 ± 11% (n=18), PBG= 136 ± 3.2% (n=8), 2-Me5HT= 0.7 ± 0.19% (n=7).

	140	155
<b>m 5-HT3 AS</b>	PYVY VHH--R	GEVQ NYKP
<b>m 5-HT3 B</b>	PYVY VNS--S	GTIR NHKP
<b>h 5-HT3 A</b>	PYVY IRH--Q	GEVQ NYKP
<b>h 5-HT3 B</b>	PYVY VNS--S	GTIE NYKP
<b>Torpedo nACh alpha</b>	TKLL LDY--T	GKIM WTPP
<b>m nACh alpha</b>	TKVL LDY--T	GKIT WTPP
<b>m nACh alpha 7</b>	TNVL VNA--S	GHCQ YLPP
<b>h nACh alpha7</b>	TNVL VNS--S	GHCQ YLPP
<b>AChBP</b>	TPQL ARVVS	DGEVL YMPS
<b>m GABAA alpha 1</b>	PNKL LRITD	GTLT YTMR
<b>m GABAA beta 1</b>	KNRM IRLHP	DGTVL YGLR
<b>m GABAA delta</b>	ENKL IRLQP	DGVIL YSIR
<b>m GABAA gamma 2</b>	PNRM LRIWN	DGRVL YTLR

**Figure 4.8** Sequence alignment of the purported loop E region of the 5HT3A receptor.

*Murine* 5-HT<sub>3AS</sub>R receptor's deduced amino acid sequence was aligned with members of the LGIC superfamily as well as acetylcholine binding protein sequences by employing multi-sequence ClustalX alignment method. Conserved residue(s) are shaded gray.

Residues discussed in the text are marked bold. The numbers at the end indicate position as measured from the N-terminal of *murine* 5-HT<sub>3AS</sub>R.

**Table 4.1 Results from ligand-docking studies**

Modeling of the extracellular domain of the *murine* 5-HT<sub>3A</sub>R and ligand docking were performed as described in “Methods”. Interactions predicted for 5-HT, 2-Me5HT and *m*CPBG are shown in the table.

Ligand	5-HT <sub>3A</sub> Amino Acids												
	N128	T181	W183	F226	I228	D229	I230	S231	Y234	E236	W90	Y153	I207
5-HT	+	+	PP	CP	+	HB		+	CP	SB	+	+	+
2-Me5HT	+	+	PP	CP	+	HB	+	+	HB	SB	+	HB	+
<i>m</i> CPBG	+		PP	CP	+			+	CP	SB	+		

+ Within 4 Å  
 PP Pi-pi  
 CP Cation- Pi  
 HB Hydrogen bond  
 SB Salt Bridge



**Table 4.2 Heteroatomic distances (Y141, Y143, Y153, W183 and their H-bonding partners) in ligand-bound and ligand-free receptor models**

These values indicate distances in Å.

Intra-subunit								
Number	Amino Acid		Number	Amino Acid		Distance		Type
						Ligand-bound	Ligand-free	
141	TYR	N	117	THR	OG1	3.14	3.12	MS
143	TYR	OH	153	TYR	OH	2.66	3.04	SS
183	TRP	N	124	ASP	O	3.68	2.94	MM
183	TRP	N	124	ASP	OD2	2.82	3.40	MS
Inter-subunit								
Number	Amino Acid		Number	Amino Acid		Distance		Type
						Ligand-bound	Ligand-free	
143	TYR	OH	183	TRP	O	2.96	3.25	SM
143	TYR	OH	184	LEU	O	3.86	3.06	SM
143	TYR	OH	185	HIS	N	3.74	4.26	SM
143	TYR	OH	234	TYR	OH	3.24	3.00	SS
153	TYR	O	183	TRP	NE1	3.26	3.60	MS
153	TYR	OH	183	TRP	O	3.71	3.83	SM
153	TYR	OH	234	TRP	OH	2.62	4.79	SS

M: main chain

S: side chain

**Table 4.3 Characteristics of wt and mutant receptors expressed in tSA201 cells.**

Receptors were expressed transiently in mammalian tSA201 cells and receptor protein expression measured as described in the methods section. Radio-ligand binding assays were carried out to measure the affinity of [<sup>3</sup>H]granisetron for wt and mutant receptors. Each experiment was repeated 5-8 times. All values are expressed as mean ± S.E.  $K_d$  values for all mutant receptors were significantly different compared to wt receptors (\*\* $p < 0.01$ ) although changes were minor.

Receptor	$B_{Max}$ <i>pmol/mg of total protein</i>	[ <sup>3</sup> H]granisetron binding		
		$K_d$ (nM)	$n_H$	Fold change in $K_d$
WT	12.6 ± 0.23	0.98 ± 0.18	1.17 ± 0.08	-
Y141A	3.5 ± 0.14	2.4 ± 0.17	1.54 ± 0.15	2.5
Y143A	5.2 ± 0.08	3.89 ± 0.42	1.62 ± 0.24	4.0
Y143F	12 ± 0.51	3.46 ± 0.31	1.34 ± 0.17	3.5
Y153A	13 ± 0.37	6.73 ± 0.71	1.12 ± 0.12	6.9
Y153F	7.04 ± 0.53	5.98 ± 0.33	1.79 ± 0.14	6.1

**Table 4.4 Electrophysiological characterization of wt and mutant receptors expressed in *Xenopus laevis* oocytes.**

Wt and mutant receptors expressed in *X. laevis* oocytes were assayed using two-electrode voltage-clamp. Each value is expressed as mean  $\pm$  S.E. and is obtained from combined data sets of at least 4 separate experiments. With the exception of the EC<sub>50</sub> value for 5-HT on Y141A receptors, all values determined for mutant receptors, were significantly different (\*\* $p < 0.01$ ) from wt values. The extent of change however, varied. N.D. indicates that no currents were detected.

Receptor	5-HT		2-Me5HT		<i>m</i> CPBG		PBG	
	EC <sub>50</sub> (μM)	<i>n</i> <sub>H</sub>	EC <sub>50</sub> (μM)	<i>n</i> <sub>H</sub>	EC <sub>50</sub> (μM)	<i>n</i> <sub>H</sub>	EC <sub>50</sub> (μM)	<i>n</i> <sub>H</sub>
WT	3.4 ± 0.3	1.4 ± 0.2	16.4 ± 1.1	1.77 ± 0.18	0.8 ± 0.07	1.6 ± 0.2	20.5 ± 0.44	1.75 ± 0.06
Y141A	2.99 ± 0.17	1.28 ± 0.08	N.D	N.D	2.76 ± 0.17	1.46 ± 0.17	36.5 ± 1.2	1.66 ± 0.08
Y143A	N.D	N.D	N.D	N.D	N.D	N.D	N.D	N.D
Y143F	207 ± 22.8	1.95 ± 0.36	2773 ± 134	2.01 ± 0.2	5.33 ± 0.19	1.93 ± 0.1	337 ± 14.2	2.3 ± 0.26
Y153A	136 ± 8.08	2.02 ± 0.22	N.D	N.D	7.62 ± 0.27	2.03 ± 0.13	243 ± 17.1	1.75 ± 0.2
Y153F	49.2 ± 5.2	1.46 ± 0.18	38 ± 3.7	1.74 ± 0.26	2.2 ± 0.2	1.99 ± 0.3	65.7 ± 2.95	2.4 ± 0.19

**Table 4.5  $I_{MAX}$  values measured from oocytes expressing wt and mutant receptors**

Reported values indicate currents in  $\mu A$  obtained for the most efficacious of the four agonists assayed (indicated in the last column).  $n$  indicates the number of experiments. Each value is expressed as mean  $\pm$  S.E.

	$I_{MAX} (\mu A)$	$n$	Agonist
WT	$14.8 \pm 1.58$	12	5-HT
Y141A	$0.54 \pm 0.04$	6	5-HT
Y143A	0	27	-
Y143F	$1.29 \pm 0.43$	10	<i>m</i> CPBG
Y153A	$13.8 \pm 2.2$	7	<i>m</i> CPBG
Y153F	$7.8 \pm 0.5$	12	<i>m</i> CPBG

## References

- Bartrup JT and Newberry NR (1996) Electrophysiological consequences of ligand binding to the desensitized 5-HT<sub>3</sub> receptor in mammalian NG108-15 cells. *J Physiol* **490** (Pt 3):679-690.
- Beene DL, Brandt GS, Zhong W, Zacharias NM, Lester HA and Dougherty DA (2002) Cation- $\pi$  interactions in ligand recognition by serotonergic (5-HT<sub>3A</sub>) and nicotinic acetylcholine receptors: the anomalous binding properties of nicotine. *Biochemistry* **41**(32):10262-10269.
- Beene DL, Price KL, Lester HA, Dougherty DA and Lummis SC (2004) Tyrosine residues that control binding and gating in the 5-hydroxytryptamine<sub>3</sub> receptor revealed by unnatural amino acid mutagenesis. *J Neurosci* **24**(41):9097-9104.
- Boess FG, Steward LJ, Steele JA, Liu D, Reid J, Glencorse TA and Martin IL (1997) Analysis of the ligand binding site of the 5-HT<sub>3</sub> receptor using site directed mutagenesis: importance of glutamate 106. *Neuropharmacology* **36**(4-5):637-647.
- Brejč K, van Dijk WJ, Klaassen RV, Schuurmans M, van Der Oost J, Smit AB and Sixma TK (2001) Crystal structure of an ACh-binding protein reveals the ligand-binding domain of nicotinic receptors. *Nature* **411**(6835):269-276.
- Celie PH, van Rossum-Fikkert SE, van Dijk WJ, Brejč K, Smit AB and Sixma TK (2004) Nicotine and carbamylcholine binding to nicotinic acetylcholine receptors as studied in AChBP crystal structures. *Neuron* **41**(6):907-914.
- Chakrapani S, Bailey TD and Auerbach A (2004) Gating dynamics of the acetylcholine receptor extracellular domain. *J Gen Physiol* **123**(4):341-356.
- Colquhoun D (1998) Binding, gating, affinity and efficacy: the interpretation of structure-activity relationships for agonists and of the effects of mutating receptors. *Br J Pharmacol* **125**(5):924-947.
- Cornell WD, Cieplak, P., Bayly, C.I., Gould, I.R., Merz, K.M. Jr., Ferguson, D.M., Spellmeyer, D.C.; Fox, T., Caldwell, J.W. and Kollman, P.A. A Second Generation Force Field for the Simulation of Proteins, Nucleic Acids, and Organic Molecules (1995) *J Am Chem Soc* **117**:5179-5197.
- Cromer BA, Morton CJ and Parker MW (2002) Anxiety over GABA(A) receptor structure relieved by AChBP. *Trends Biochem Sci* **27**(6):280-287.
- Davies PA, Pistis M, Hanna MC, Peters JA, Lambert JJ, Hales TG and Kirkness EF (1999) The 5-HT<sub>3B</sub> subunit is a major determinant of serotonin-receptor function. *Nature* **397**(6717):359-363.

- Derkach V, Surprenant A and North RA (1989) 5-HT<sub>3</sub> receptors are membrane ion channels. *Nature* **339**(6227):706-709.
- Downie DL, Hall AC, Lieb WR and Franks NP (1996) Effects of inhalational general anaesthetics on native glycine receptors in rat medullary neurones and recombinant glycine receptors in *Xenopus* oocytes. *Br J Pharmacol* **118**(3):493-502.
- Downie DL, Hope AG, Belelli D, Lambert JJ, Peters JA, Bentley KR, Steward LJ, Chen CY and Barnes NM (1995) The interaction of trichloroethanol with murine recombinant 5-HT<sub>3</sub> receptors. *Br J Pharmacol* **114**(8):1641-1651.
- Downie DL, Hope AG, Lambert JJ, Peters JA, Blackburn TP and Jones BJ (1994) Pharmacological characterization of the apparent splice variants of the murine 5-HT<sub>3</sub> R-A subunit expressed in *Xenopus laevis* oocytes. *Neuropharmacology* **33**(3-4):473-482.
- Hanna MC, Davies PA, Hales TG and Kirkness EF (2000) Evidence for expression of heteromeric serotonin 5-HT<sub>3</sub> receptors in rodents. *J Neurochem* **75**(1):240-247.
- Hope AG, Downie DL, Sutherland L, Lambert JJ, Peters JA and Burchell B (1993) Cloning and functional expression of an apparent splice variant of the murine 5-HT<sub>3</sub> receptor A subunit. *Eur J Pharmacol* **245**(2):187-192.
- Joshi PR, Suryanarayanan A and Schulte MK (2004) A vertical flow chamber for *Xenopus* oocyte electrophysiology and automated drug screening. *J Neurosci Methods* **132**(1):69-79.
- Lankiewicz S, Lobitz N, Wetzel CH, Rupprecht R, Gisselmann G and Hatt H (1998) Molecular cloning, functional expression, and pharmacological characterization of 5-hydroxytryptamine<sub>3</sub> receptor cDNA and its splice variants from guinea pig. *Mol Pharmacol* **53**(2):202-212.
- Laskowski RA, MacArthur, M.W., Moss, D.S., and Thornton, J.M. Main-chain bond lengths and bond angles in protein structures. (1993) *J Mol Biol.* **231**(4):1049-67.
- Le Novere N, Grutter T and Changeux JP (2002) Models of the extracellular domain of the nicotinic receptors and of agonist- and Ca<sup>2+</sup>-binding sites. *Proc Natl Acad Sci USA* **99**(5):3210-3215.
- Lynch JW (2004) Molecular structure and function of the glycine receptor chloride channel. *Physiol Rev* **84**(4):1051-1095.

- Maksay G, Bikadi Z and Simonyi M (2003) Binding interactions of antagonists with 5-hydroxytryptamine<sub>3A</sub> receptor models. *J Recept Signal Transduct Res* **23**(2-3):255-270.
- Maricq AV, Peterson AS, Brake AJ, Myers RM and Julius D (1991) Primary structure and functional expression of the 5HT<sub>3</sub> receptor, a serotonin-gated ion channel. *Science* **254**(5030):432-437.
- McDonald IK and Thornton JM (1994) Satisfying hydrogen bonding potential in proteins. *J Mol Biol* **238**(5):777-793.
- Mott DD, Erreger K, Banke TG and Traynelis SF (2001) Open probability of homomeric murine 5-HT<sub>3A</sub> serotonin receptors depends on subunit occupancy. *J Physiol* **535**(Pt 2):427-443.
- Niemeyer MI and Lummis SC (1998) Different efficacy of specific agonists at 5-HT<sub>3</sub> receptor splice variants: the role of the extra six amino acid segment. *Br J Pharmacol* **123**(4):661-666.
- Niesler B, Frank B, Kapeller J and Rappold GA (2003) Cloning, physical mapping and expression analysis of the human 5-HT<sub>3</sub> serotonin receptor-like genes HTR3C, HTR3D and HTR3E. *Gene* **310**:101-111.
- O'Shea SM and Harrison NL (2000) Arg-274 and Leu-277 of the gamma-aminobutyric acid type A receptor alpha 2 subunit define agonist efficacy and potency. *J Biol Chem* **275**(30):22764-22768.
- O'Shea SM, Wong LC and Harrison NL (2000) Propofol increases agonist efficacy at the GABA(A) receptor. *Brain Res* **852**(2):344-348.
- Petersson EJ, Choi A, Dahan DS, Lester HA and Dougherty DA (2002) A perturbed pK(a) at the binding site of the nicotinic acetylcholine receptor: implications for nicotine binding. *J Am Chem Soc* **124**(43):12662-12663.
- Price KL and Lummis SC (2004) The role of tyrosine residues in the extracellular domain of the 5-hydroxytryptamine-3 receptor. *J Biol Chem* **279**(22):23294-23301.
- Rajendra S, Lynch JW, Pierce KD, French CR, Barry PH and Schofield PR (1995) Mutation of an arginine residue in the human glycine receptor transforms beta-alanine and taurine from agonists into competitive antagonists. *Neuron* **14**(1):169-175.
- Reeves DC and Lummis SC (2002) The molecular basis of the structure and function of the 5-HT<sub>3</sub> receptor: a model ligand-gated ion channel (review). *Mol Membr Biol* **19**(1):11-26.



- Reeves DC, Sayed MF, Chau PL, Price KL and Lummis SC (2003) Prediction of 5-HT<sub>3</sub> receptor agonist-binding residues using homology modeling. *Biophys J* **84**(4):2338-2344.
- Schreiter C, Hovius R, Costioli M, Pick H, Kellenberger S, Schild L and Vogel H (2003) Characterization of the ligand-binding site of the serotonin 5-HT<sub>3</sub> receptor: the role of glutamate residues 97, 224, AND 235. *J Biol Chem* **278**(25):22709-22716.
- Spier AD and Lummis SC (2000) The role of tryptophan residues in the 5-Hydroxytryptamine(3) receptor ligand binding domain. *J Biol Chem* **275**(8):5620-5625.
- Steward LJ, Boess FG, Steele JA, Liu D, Wong N and Martin IL (2000) Importance of phenylalanine 107 in agonist recognition by the 5-hydroxytryptamine(3A) receptor. *Mol Pharmacol* **57**(6):1249-1255.
- Suryanarayanan A, Joshi PR, Bikadi Z, Muthalagi M, Kulkarni TR, Gaines C and Schulte MK (2004) Characterization of Residues in the Loop C Region of Murine 5-HT<sub>3</sub>AR by Alanine Scanning Mutagenesis. *Society for Neuroscience Abstracts*(34th annual meeting):626.621.
- Thompson JD, Higgins DG and Gibson TJ (1994) CLUSTAL W: improving the sensitivity of progressive multiple sequence alignment through sequence weighting, position-specific gap penalties and weight matrix choice. *Nucleic Acids Res* **22**(22):4673-4680.
- van Hooft JA, Spier AD, Yakel JL, Lummis SC and Vijverberg HP (1998) Promiscuous coassembly of serotonin 5-HT<sub>3</sub> and nicotinic alpha4 receptor subunits into Ca(2+)-permeable ion channels. *Proc Natl Acad Sci U S A* **95**(19):11456-11461.
- Venkataraman P, Joshi P, Venkatachalan SP, Muthalagi M, Parihar HS, Kirschbaum KS and Schulte MK (2002a) Functional group interactions of a 5-HT<sub>3</sub>R antagonist. *BMC Biochem* **3**(1):16.
- Venkataraman P, Venkatachalan SP, Joshi PR, Muthalagi M and Schulte MK (2002b) Identification of critical residues in loop E in the 5-HT<sub>3</sub>ASR binding site. *BMC Biochem* **3**(1):15.
- Wu CH, Huang H, Arminski L, Castro-Alvear J, Chen Y, Hu ZZ, Ledley RS, Lewis KC, Mewes HW, Orcutt BC, Suzek BE, Tsugita A, Vinayaka CR, Yeh LS, Zhang J and Barker WC (2002) The Protein Information Resource: an integrated public resource of functional annotation of proteins. *Nucleic Acids Res* **30**(1):35-37.
- Xiang Z and Honig B (2001) Extending the accuracy limits of prediction for side-chain conformations. *J Mol Biol* **311**(2):421-430.

Xiang Z, Soto CS and Honig B (2002) Evaluating conformational free energies: the colony energy and its application to the problem of loop prediction. *Proc Natl Acad Sci USA* **99**(11):7432-7437.

Yan D, Schulte MK, Bloom KE and White MM (1999) Structural features of the ligand-binding domain of the serotonin 5HT<sub>3</sub> receptor. *J Biol Chem* **274**(9):5537-5541.

**Appendix**

Acknowledgements: This work is supported by the National Science Foundation (NSF CAREER 9985077) and the American Heart Association (AHA 0151065B).

PRJ and AS are both Alaska INBRE pre-doctoral research fellows.

## Chapter 5: The role of loop B amino acid residues in the structure and function of the 5-HT<sub>3A</sub>R<sup>4</sup>

### 5.1 Summary

5-HT<sub>3</sub> receptors are pentameric membrane bound receptors that belong to the ligand-gated ion channel (LGIC) superfamily. The ligand-binding site of these receptors is located in the extracellular domain. Results from previous studies on nicotinic acetylcholine receptors and structural homology with the Acetylcholine Binding Protein (AChBP) suggest that the binding site of the 5-HT<sub>3A</sub>R is composed of six loops; A-F. Using site directed mutagenesis, we investigated the role of amino acid residues in the putative loop B region of the mouse 5-HT<sub>3A</sub>R in receptor function. To this end, twelve amino acids (T179-I190) of the mouse 5-HT<sub>3A</sub>R loop B region were sequentially mutated to alanine. Each mutant was characterized using radio-ligand binding and electrophysiological assays. In order to further investigate the roles of mutants that showed altered binding and/or function, secondary mutations were constructed and similarly characterized. The results were correlated with the results of ligand-docking studies using both ligand-free and ligand bound models of the *murine* 5-HT<sub>3A</sub>R, based on AChBP. These studies indicate that T181 and W183 are located in the ligand binding domain and interact directly with ligands. Intra-subunit and inter-subunit interactions of loop B residues on either side of ligand-binding residues seem to be involved in mediating conformational changes associated with receptor activation. Our studies also

---

<sup>4</sup> Manuscript in preparation for submission to *Neuropharmacology* (Elsevier publication).

indicate that the intra-subunit and inter-subunit contacts formed by loop B residues are involved in proper receptor expression.

## 5.2 Introduction

The 5-HT<sub>3</sub>R belongs to a superfamily of ligand-gated ion channel coupled receptors and shares several structural and functional features with other members, including the nAChR, GABA and Gly receptors. An understanding of ligand-gated ion channel function contributes significantly to the improvement of drug development and treatment options. In particular, studies involving the ligand-binding site contribute tremendously to the development of potent and specific ligands and aid in rational drug design. The ligand-binding site of the 5-HT<sub>3A</sub>R is located in the extracellular N-terminal domain. Based on sequence homology with the nACh receptor and acetylcholine binding protein (AChBP), it is assumed that the ligand binding site is located in the inter-subunit interface and is formed by at least 6 loop structures designated A to F. Results from site-directed mutagenesis studies support this assumption. Studies of 5-HT<sub>3A</sub>R involving the loop B region have focused on W183. This amino acid is thought to interact with the quaternary ammonium group of serotonergic ligands in a cation- $\pi$  interaction. The homologous residue is conserved as an aromatic amino acid in all LGIC receptor subunits (W149 of the nAChR  $\alpha$ -subunit, Glycine – F159, GABA<sub>A</sub>  $\alpha$ 1 – Y159) (Figure 5.1). Spier et al utilized site-directed mutagenesis in combination with radio-ligand binding assays and whole-cell patch-clamp to decipher the role of W183 in ligand-binding (Spier and Lummis, 2000). According to this study, mutation of tryptophan 183 to either tyrosine or phenylalanine results in ablation of radio-ligand binding. Although agonists can bind to

and activate the mutant receptors, large changes in  $EC_{50}$  values for both serotonin and *mCPBG* are observed. Using unnatural amino acid substitutions, it has been postulated that this tryptophan residue forms a cation- $\pi$  interaction with the amino group of 5-HT (Beene et al., 2002). In such an interaction, the charged amino group of the ligand interacts with the  $\pi$  cloud of the aromatic ring. Using the non-sense suppression method, various unnatural amino acids (modified forms of tryptophan) with substitutions on the aromatic ring of tryptophan, were introduced at position 183. The mutant protein was expressed in *Xenopus* oocytes and assayed with two-voltage electrode clamp using endogenous agonist serotonin. This technique provides a unique approach for examining the structure-activity relationship of a particular amino acid while maintaining the biologically active form of the protein. The homologous residue in the nAChR has been shown to form a cation-  $\pi$  interaction with acetylcholine, but not nicotine (Beene et al., 2002; Zhong et al., 1998).

With the exception of W183, the structural and functional role of the purported loop B region remains unexplored. In the present study, we have systematically examined each amino acid of the purported loop B region of the *murine* 5-HT<sub>3A</sub>R. These studies indicate that amino acids T181 and W183 probably interact directly with agonists 5-HT and *mCPBG*, while W183, H185 and D189 seem to be involved in granisetron binding. Amino acids T179, F180, H185, I187, and D189 probably mediate agonist-induced conformational changes. Our studies also indicate that intra-subunit and inter-subunit contacts formed by loop B residues are involved in proper receptor expression.

## 5.3 Materials and Methods

### 5.3.1 Materials:

*Xenopus laevis* frogs and frog food were purchased from Xenopus Express (FL, US). Sigma type II collagenase was purchased from Sigma-Aldrich (MO, US). [<sup>3</sup>H]granisetron was purchased from New England Nuclear, 5-HT, 2-Me5HT from Spectrum, and *m*CPBG and *d*-TC from Research Biochemical International. All other chemicals were obtained from Fisher Scientific (TX, US).

### 5.3.2 Methods:

#### 5.3.2.1 Site-directed Mutagenesis

Wild type m5-HT<sub>3A</sub>S receptor *c*DNA was derived from N1E-115 neuroblastoma cells as previously described (Yan et al., 1999). All mutant receptors were constructed using the pAlter *altered sites* mutagenesis kit (Promega, CA) as described earlier (Venkataraman et al., 2002a). All mutations were confirmed by restriction digests and DNA sequencing (UC Davis, CA).

#### 5.3.2.2 Cell culture and transient transfection

*t*SA201 cells (a derivative of HEK 293 cells) were cultured in Dulbecco's modified Eagle medium (DMEM, New Life Technologies, NY) supplemented with 10 % fetal bovine serum and 100 units/ml penicillin/streptomycin in a humidified 5% CO<sub>2</sub> atmosphere at 37 °C. For radio-ligand binding studies, *t*SA201 cells were plated on 90 mm culture dishes at a density of 5 x 10<sup>6</sup> cells/dish and grown for 9 hours prior to transfection. Cells were

transfected with 20 µg/ dish wt or mutant plasmid DNA using a calcium phosphate transfection kit (New life technologies, NY). Transfected cells were supplemented with fresh DMEM 12-15 hours later and harvested 48 hours after transfection. For whole-cell patch-clamp assays, tSA201 cells were transfected using Superfect transfection reagent (Qiagen, CA) as described earlier (Venkataraman et al., 2002)

### 5.3.2.3 *Xenopus laevis* oocyte two-electrode voltage-clamp assay

Details of the methodology employed for electrophysiological assays have been described earlier (Joshi et al., 2004). Ovarian lobes were surgically removed from *Xenopus laevis* frogs and washed twice in Ca<sup>+2</sup> free Barth's buffer [82.5 mM NaCl / 2.5 mM KCl / 1mM MgCl<sub>2</sub> / 5 mM HEPES, pH 7.4], then gently shaken with 1.5mg/ml collagenase (Sigma type II, Sigma-Aldrich) for 1hour at 20-25 °C. Stage IV oocytes were selected for microinjection. Synthetic cRNAs for wt and mutant m5-HT<sub>3A</sub>Rs were prepared using an mMMESSAGE mMACHINE™ High Yield Capped RNA Transcription Kit (Ambion, TX). Each oocyte was injected with 50 nl cRNA at a concentration of 0.2 ng/nl. Oocytes were incubated at 19°C for 2 to 4 days before electrophysiological recording. Electrical recordings were made using conventional two-electrode voltage-clamp at -60 mV employing an OC-725C oocyte clamp amplifier (Warner Instruments, CT) coupled to an online, computerized data acquisition system (DataPac 2000, RUN technologies). Recording and current electrodes were filled with 3M KCl and had resistances of 1-2 MΩ. Oocytes were held in a chamber of 400 µl volume and perfused with ND-96 recording buffer (96 mM NaCl / 2 mM KCl / 1.8 mM CaCl<sub>2</sub> / 1 mM MgCl<sub>2</sub> / 5 mM HEPES, pH 7.4) at a rate of 15 ml/min. All agonists and antagonists were prepared



in ND-96 buffer and applied at a rate of 25 ml/min using an electrical pump. For competition assays involving *d*-TC, oocytes expressing Wt or mutant receptors were pre-exposed to varying concentrations of *d*-TC for a period of 30 seconds. After 30 seconds, the oocyte was co-exposed to a mixture of 5-HT and *d*-TC. The 5-HT concentration in each case corresponded to the EC<sub>50</sub> value for the receptor under consideration.

#### 5.3.2.4 Radio-ligand Binding Assays

Radio-ligand binding assays were performed as described earlier (Venkataraman et al., 2002). Briefly, transfected cells were scraped from the dishes, washed twice with PBS (New Life Technologies, NY), then re-suspended in 1.0 ml PBS with protease inhibitor cocktail /100mm dish. (*Complete*<sup>TM</sup> protease inhibitor cocktail, Roche, Mannheim, Germany). Cells were either used fresh or frozen at this step until needed. Immediately prior to use, cells were homogenized in PBS (with protease inhibitor) using a glass tissue homogenizer then centrifuged at 35000 X g for 30 minutes in a Beckman JA20 rotor. Membranes were washed once more with PBS and re-suspended in 1ml PBS/100 mm dish. Protein content was determined using Lowry assay (Sigma Diagnostics, MO). Binding assays were performed in PBS with protease inhibitors. For K<sub>d</sub> determinations, 50 µl of homogenate was incubated at 37°C for 1 hour with varying concentrations of [<sup>3</sup>H]granisetron. Non-specific binding of [<sup>3</sup>H] granisetron was determined as bound [<sup>3</sup>H] granisetron not displaced by a saturating concentration of a competing ligand (typically 10 µM Tropicsetron). For K<sub>i</sub> determinations, 50 µl of homogenate was incubated at 37°C for 2 hours with varying concentrations of inhibitor and [<sup>3</sup>H]granisetron. Binding was terminated by rapid filtration onto a GF/B filters.

### 5.3.3 Data analysis

Data obtained from radio-ligand binding assays was analyzed as follows.  $K_d$  values were determined by fitting the binding data to the following equation using GraphPad PRISM (San Diego, CA):  $B = B_{Max} [L]^n / ([L]^n + K^n)$  (Eq.2), where  $B$  is bound ligand,  $B_{Max}$  is the maximum binding at equilibrium,  $L$  is the free ligand concentration,  $K$  is the equilibrium dissociation constant and  $n$  is the Hill coefficient. Statistical analysis of concentration-response data from electrophysiological assays was performed using the equation  $I = I_{Max} / (1 + EC_{50} / [A]^n)$  (Eq.3), where  $I$  is the peak current,  $I_{Max}$  is the maximal response at a given concentration of agonist  $A$ ,  $EC_{50}$  is the half-maximal concentration of the agonist  $A$  and  $n$  describes apparent Hill slope. Data from competition assays involving  $d$ -TC was analyzed using the equation  $\theta = [(1 + EC_{50} / [A])^n]^{-1}$  as previously described (Yan et al., 1999), where  $\theta$  is the normalized current at 5-HT concentration  $[A]$ ,  $EC_{50}$  is the concentration of 5-HT required to obtain half-maximal current, and  $n$  is the apparent Hill slope. Concentration-Response curves were obtained by non-linear regression analysis using GraphPad PRISM. Data were compared for significant differences using student's  $t$  test.

### 5.3.4 Receptor modeling

Extracellular regions of the homopentameric murine 5-HT<sub>3</sub>R were built based on the crystal structure of the AChBP from the snail *Lymnaea stagnalis* (PDB entry: 1I9B). The sequence of 5-HT<sub>3</sub>R A subunit was taken from the Protein Information Resource (Wu et al., 2002) with an entry code of NF00508262. Multiple sequence alignments of their

extracellular regions and AChBP were performed by 'ClustalW' using default parameters (Thompson et al., 1994). Based on this alignment, homology-model building of the 5-HT<sub>3</sub>A subunit was carried out using the 'Nest' and 'Loopy' facility of the Jackal protein structure modeling package. 'Nest' predicts the experimental dihedral angles  $\chi_1$  within an error range of 20 degrees for 94 % of protein side chains (Xiang and Honig, 2001). Protein loop predictions for amino acid insertions and deletion were done by 'Loopy'(Xiang et al., 2002). Homodimeric units of the pentamer were built on the basis of crystal structure data to reach minimal root mean standard deviation (RMSD) between the matched monomers. Further refinements of the resulting dimers were carried out by Sybyl 6.6 program (Tripos Inc., St. Louis, MO) on a Silicon Graphics Octane workstation under Irix 6.5 operation system. First, the all-atom model was allowed to relax during a short molecular dynamics run (2000 fs) using constrains for backbone atoms, not allowing distortions of the backbone. Finally, the entire structures were fully minimized without any restriction using Powell conjugate gradient method until the maximum derivative was less than 0.050 kcal/molÅ. Gasteiger-Huckel partial charges were applied during the calculations. The quality of the model was verified using 'Procheck', as compared with well-refined structures at the same resolution ((Laskowski, 1993). Intra- and interface H-bonds were analysed by HBPLUS v 3.0, an hydrogen bond calculation program (McDonald and Thornton, 1994). Homology model for the ground state receptor was constructed based on the same alignment as for the ligand-bound receptor model. Chain F of AChBP (Celie et al., 2004) taken from RCSB Protein Bank entry 1UV6 was used as a template for ground state receptor model. The loop C conformation of this

ligand-free subunit is strikingly different from the conformation of the other crystallized chains with bound ligands. Side chain prediction, dimer building and structural minimization of the ground state receptor were carried out using the same workflow described above for the ligand-bound receptor model.

'AutoDock 3.0' was applied for docking calculations, using the Lamarckian genetic algorithm (LGA) and the 'pseudo-Solis and Wets' (pSW) methods. The ligand docking calculations were performed independent of experimental data. The parameters included in Autodock are based on the 'Assisted Model Building with Energy Refinement' (AMBER) force field (Cornell, 1995). Gasteiger-Huckel partial charges were applied both for ligands and proteins. Solvation parameters were added to the protein coordinate file and the ligand torsions were defined using the 'Addsol' and 'Autotors' utilities, respectively, in Autodock 3.0. The atomic affinity grids were prepared with 0.375 Å spacing using the Autogrid program for a 15 x 15 x 22.5 Å box around the interface of subunits. No constraints based on experimental data were employed to carry out ligand docking. Random starting positions, orientations and torsions (for flexible bonds) were used for the ligands. Each docking run consisted of 100 cycles. The number of evaluations was set to 1.5 million. Final structures with RMSD less than 1.5 Å were considered to belong to the same cluster. The structures with low energies and high frequencies of docking were subjected to a further minimization by Sybyl and were examined.

## 5.4 Results

The primary objective of alanine scanning mutagenesis is to rapidly identify functional and/or structural importance of each amino acid in a pre-defined region of the protein. Alanine substitution of both surface and buried residues is tolerated equally well. The structure of the protein backbone formed with the alanine substitution is similar to that formed with the native amino acid. Therefore a single alanine substitution is expected to produce little backbone distortion. Alanine substitutions on the other hand can quickly identify amino acids of potential importance, since the R-group of the substituted amino acid is replaced with a methyl group.

Wild type and mutant 5-HT<sub>3A</sub>R receptors were expressed in two expression systems; mammalian *tSA* cells and *Xenopus laevis* oocytes. The mammalian system was primarily used to characterize antagonist interaction with mutant receptors, while *Xenopus laevis* oocytes used to determine functional characteristics of the mutant receptors.

### 5.4.1 Electrophysiological characterization of loop B mutant receptors

*Xenopus* oocytes expressing wt receptors produced characteristic inward currents when rapidly exposed to 5-HT or *mCPBG*. Iterative curve fitting of the data yielded an EC<sub>50</sub> value of  $3.4 \pm 0.3 \mu\text{M}$  with a Hill slope of  $1.4 \pm 0.2$  for 5-HT. Similar experiments involving *mCPBG* produced an EC<sub>50</sub> value of  $0.8 \pm 0.07 \mu\text{M}$  and a Hill slope of  $1.6 \pm 0.2$  (Table 5.2). Hill slopes greater than unity indicate the cooperative nature of agonist induced channel opening. No inward currents could be detected when non-injected or mock-injected oocytes were exposed to 5-HT or *mCPBG*.

Loop B mutant receptors were similarly expressed in *Xenopus* oocytes and characterized using agonists 5-HT and *m*CPBG. No inward currents could be elicited on application of either 5-HT or *m*CPBG from oocytes expressing T179A, F180A, L184A, H185A, D189 or I190 mutant receptors. These data suggest that these amino acids influence agonist mediated channel opening at the wt 5-HT<sub>3A</sub>R. However, such an assumption would be valid only if the mutant receptors are expressing on the cell surface. It is possible that mutation at each of these positions alters the ability of the receptor to be expressed on the cell surface, which would result in the lack of detectable response from these oocytes. Secondary mutations at positions L184 (L184V), H185 (H185F and Y) and I190 (I190V) resulted in detectable inward currents from the oocytes expressing these proteins, allowing EC<sub>50</sub> values to be recorded. Secondary mutants at T179, F180 and D189 are currently being evaluated in our laboratory.

#### **5.4.1.1 Electrophysiological profile of loop B mutant receptors: 5-HT**

Among loop B mutant receptors, mutations W183F and I187A resulted in large changes (50 and 27 fold respectively) to 5-HT EC<sub>50</sub> (Table 5.1). The W183F mutation caused the largest increase in EC<sub>50</sub>. Results obtained for the W183F mutation are in tandem with previously reported values for 5-HT EC<sub>50</sub> values on receptors with natural and unnatural substitutions at the W183 position. The L184V mutation, a subtle mutation, resulted in ten-fold increase in 5-HT EC<sub>50</sub> value. Subtle mutations at position H185 (H185F and H185Y) also resulted in a moderate (~6 fold) increase in the EC<sub>50</sub> value. These results indicate that amino acids W183, L184, H185 and I187 play a role in mediating the action of the natural agonist 5-HT.

The T181A mutation produced a modest 7-fold increase in 5-HT  $EC_{50}$ , suggesting a minor role for this amino acid in 5-HT mediated action. S182A, T186A and Q188A mutant receptors displayed only minor changes to 5-HT  $EC_{50}$  (Table 5.1). These data suggest that amino acids S182, T186 and Q188 may not be playing any role in mediating 5-HT induced channel opening.

An alanine mutation at the I190 position resulted in mutant receptors that did not respond to 5-HT or *mCPBG*. A subtle mutation at I190 (I190V) not only restored function to the 5-HT<sub>3A</sub>R, but the  $EC_{50}$  value recorded for 5-HT was almost identical to that for the wild type receptor.

Minor but statistically significant increases in Hill number value were noted for mutant receptors S182A, W183F, L184V and H185Y ( $p < 0.05$ ). However, the H185F mutation did not produce any significant change in Hill number. Similarly, reduction in Hill number was observed for I190V mutant receptors.

#### **5.4.1.2 Electrophysiological profile of loop B mutant receptors: *mCPBG***

Large changes in  $EC_{50}$  for *mCPBG* were noted for S182A, W183F and I187A mutant receptors (Table 5.1). The I187A mutation led to the largest increase in  $EC_{50}$  (64 fold), while the S182A mutation resulted in a 34-fold increase. The W183F mutation also produced 20-fold change. All of the remaining mutations caused only minor changes to *mCPBG*  $EC_{50}$  (Table 5.1). These results suggest that S182, W183 and I187 amino acids play a role either in the direct interaction of *mCPBG* with the ligand-binding domain or *mCPBG* mediated channel gating.

Statistically significant increase ( $p < 0.05$ ) in Hill number was recorded for mutations T181A and H185F, while mutations S182A, H185Y and T186A led to a statistically significant decrease ( $p < 0.05$ ) in Hill number (Figure 5.3). The Hill number remained unchanged for all other mutant receptors.

#### 5.4.1.3 Differential effects of the loop B mutations on action of 5-HT and *m*CPBG

Figures 5.2 and 5.3 show a comparison of  $EC_{50}$  and Hill numbers for agonists 5-HT and *m*CPBG on loop B mutant receptors. The T181A mutation led to a 5-HT specific effect on  $EC_{50}$ , with *m*CPBG related parameters remaining almost unaffected (Table 5.2). These results suggest that T181 is involved in specifically mediating the action of 5-HT and not *m*CPBG. Although the W183F mutation causes an increase in  $EC_{50}$  for both 5-HT and *m*CPBG, the value for 5-HT seems to be much more affected (50-fold for 5-HT vs. 20-fold for *m*CPBG; Table 5.2). L184V caused changes similar to W183F, although the magnitude of change was smaller (11-fold for 5-HT vs. 6-fold for *m*CPBG; Table 5.2). These results suggest that both W183 and L184 influence 5-HT and *m*CPBG induced channel opening. However, both amino acids may be more important for action of 5-HT compared to *m*CPBG.

The S182A mutation led to a specific effect on  $EC_{50}$  for *m*CPBG while parameters for 5-HT remained unchanged (no change for 5-HT vs. 30-fold change for *m*CPBG; Table 5.2). These results suggest that S182A is involved in specifically mediating the action of *m*CPBG and not 5-HT.

The waveform of inward currents induced from S182A expressing oocytes by supra-maximal concentrations of 5-HT were compared to those obtained from the wild



type receptors (Figure 5.4B). Although the first (rapid) phase of the desensitization appeared to be slower in case of the S182A mutant receptor, other differences in the waveform were not observed.

The waveform of inward currents induced from S182A expressing oocytes by supra-maximal concentrations of *m*CPBG were compared to those obtained from the wild type receptors (Figure 5.4C). In the case of the wild type receptor, the waveform clearly shows the presence of a non-desensitizing phase on continued application of *m*CPBG (marked with a circle in figure 5.4 C). A similar phase in continued presence of *m*CPBG is conspicuously absent in the current waveform of S182A (marked with a circle in figure 5.7C). The recovery phase for S182A mutant receptors from desensitization also appears to be prolonged. The wild type receptors completely recover from the state of desensitization induced by supra-maximal concentration of *m*CPBG after a period of  $7 \pm 2$  ( $n = 3$ ) minutes. For S182A receptors, the recovery is complete only at the end of a  $30 \pm 3$  ( $n = 3$ ) minute period.

The I187A mutation led to an increase in  $EC_{50}$  for both 5-HT and *m*CPBG. However, the value for *m*CPBG was affected to a greater extent compared to 5-HT (25-fold for 5-HT vs. 65-fold for *m*CPBG; Table 5.2).

Mutations at position H185 (H185Y and H185F) produced changes of equal magnitude for both 5-HT and *m*CPBG  $EC_{50}$  (Table 5.2), suggesting that H185 plays a general role in agonist induced channel opening.

#### 5.4.2 Granisetron binding to loop B mutant receptors

[<sup>3</sup>H] granisetron, a 5-HT<sub>3</sub>R specific competitive antagonist, bound with a high affinity to wild type receptors expressed in *t*SA cells ( $K_d$  0.96 nM, Table 5.2, Figure 5.5). Untransfected and mock-transfected cells did not show specific binding to the radio-ligand (data not shown). All mutations (alanine, tyrosine and phenylalanine) at W183 position and the alanine mutation at H185 position resulted in receptors lacking detectable binding to [<sup>3</sup>H] granisetron. These results suggest that W183 and H185 are critical to ligand-binding and/or receptor assembly. Although a subtle mutation at H185 (H185Y) restored binding to [<sup>3</sup>H] granisetron, a 6-fold reduction in binding affinity was noted.

An alanine mutation at position D189 (D189A) resulted in a 23 fold reduction in the affinity of the [<sup>3</sup>H] granisetron, suggesting that an acidic residue at this position may be important for antagonist binding. Alanine mutation at positions T179, F180, T181 caused moderate changes (from 4-8) in affinity of the receptor for [<sup>3</sup>H] granisetron (Table 5.2, Figure 5.5), while alanine mutation at positions T186, I187 and Q188 resulted in minor (1.5 to 3 fold) changes in [<sup>3</sup>H] granisetron binding.

#### 5.4.3 Maximal binding ( $B_{Max}$ ) values for the loop B mutant receptors

Mutations at all positions in the loop B region except L184 resulted in large scale changes in  $B_{Max}$  values obtained from [<sup>3</sup>H] granisetron binding assay (Figure 5.6). T179A, T180, H185Y, D189A and I190A mutations each resulted in drastic reduction (5-7 % compared to the wild type receptor) in receptor expression, as suggested by  $B_{Max}$  values (Figure 5.6). Mutations T181, S182, T186 and I187 also resulted in significant changes (10-30 % compared to the wild type receptor) in  $B_{Max}$  values. The Q188A

mutation resulted in a 50% decline in  $B_{Max}$ . Thus, most loop B amino acid residues appear critical for proper expression of the 5-HT<sub>3A</sub>R.

#### **5.4.4 Displacement of granisetron binding to loop B mutant receptors by 5-HT and *m*CPBG**

[<sup>3</sup>H] granisetron binding to the wild type receptor was displaced by both non-selective endogenous agonist 5-HT and selective synthetic agonist *m*CPBG with apparent affinity of 0.16  $\mu$ M and 0.072  $\mu$ M respectively (Table 5.2, Figure 5.7.1 and 5.7.2). Since competition binding assays for agonists were performed under equilibrium conditions, the  $K_i$  values obtained probably reflect the affinity of these agonists for the desensitized state of the 5-HT<sub>3R</sub>.

Since W183A, W183F and H185A mutant receptors did not bind [<sup>3</sup>H] granisetron; competition binding assays involving these receptors could not be performed. [<sup>3</sup>H] granisetron binding to mutations T179A, T180, H185Y, and D189A could not be displaced by either 5-HT or *m*CPBG. These data suggest that mutation at these positions specifically alter the ability of agonists to mediate binding and/or gating. However, mutations T179A, T180, H185Y, and D189A also resulted in drastic reduction in receptor expression (5-7 % compared to the wild type receptor), as suggested by the  $B_{Max}$  values (Figure 5.6). Such low levels of  $B_{Max}$  values place limitations on the precision of data obtained from competition assays and results obtained need to be interpreted with caution. In case of I190A mutant receptor, very low receptor expression prevented complete characterization of [<sup>3</sup>H] granisetron displacement.

The L184A mutation resulted in a large decrease in apparent affinity of the receptor for 5-HT, resulting in a 141-fold increase in  $K_i$ . Mutation T181A also resulted in a 70-fold increase in  $K_i$ . On the other hand, S182A, T186A, I187A and Q188A mutations produced only 2-4 fold change in apparent affinity for 5-HT (Figure 5.7.1).

The T181A and I187A mutations resulted in a moderate (~14-15 fold) reduction in apparent affinity for *m*CPBG. Each of S182A, T186A and Q188A mutations resulted in small but significant *increase* in the apparent affinity (2 to 5 fold,  $p < 0.05$ ), while values for L184A show a small decrease. The S182A mutation resulted in the largest (5-fold) increase in the affinity for *m*CPBG.

#### **5.4.5 Results of the molecular modeling studies**

Molecular modeling studies were performed according to the protocol described in materials and methods section. No constraints based on experimental data were applied while conducting these studies. The ligand-docking studies were performed using the homology model of the *murine* 5-HT<sub>3A</sub>R. This model was built using crystal structure of AChBP which is presumably in the open/desensitized state. The prepared models of the ligand-free and ligand-bound 5-HT<sub>3A</sub>R in dimeric form were optimized in Sybyl 7.0 molecular modeling software (Tripos Inc., St. Louise, MO). The H-bonding interactions of loop B residues were also calculated using Sybyl 7.0 software.

##### **5.4.5.1 Results from the ligand-docking studies using 5-HT<sub>3A</sub>R homology model.**

Docking studies of 5-HT and *m*CPBG predict that 5-HT but not *m*CPBG interacts with amino acid T181. Amino acid T181 is located within 4Å of the docked 5-HT molecule.

Amino acid W183 interacts with each of the docked ligands. W183 apparently interacts with various ligands either through cation-pi or pi-pi interaction (Table 5.3). Other amino acids of the purported loop B region do not seem to be involved directly in receptor-ligand interaction(s). These amino acids probably play a role in mediating either a purely structural role or a role in mediating conformational changes in the protein associated with channel gating.

#### **5.4.5.2 Results form structural predictions obtained from 5-HT<sub>3A</sub>R homology models.**

Comparison of predicted structural features of the loop B region from the ligand-free and ligand (agonist)-bound state models of the 5-HT<sub>3A</sub>R were obtained. The pattern of H-bonding is strikingly different in both these models of the receptor. These differences have been tabulated in Table 5.4.1 and 5.4.2. Figure 5.8 summarizes the hydrogen bonding pattern observed in the agonist-bound state.

**Following bonds remain unchanged indicating their role in maintenance of structural rigidity**

- 1) T179 backbone amide - E129 (E106) side chain oxygen
- 2) T179 backbone carbonyl - N128 backbone amide
- 3) Q188 forms no H-bonds at any time
- 4) D189 carbonyl backbone-T64 amide backbone

**Following H-bonds form during open/desensitized state:** Formation of these bonds during the activated state suggests that these interactions are at least partially responsible for stabilization of distinct confirmation(s) associated with activation/desensitization.

- 1) F180 backbone carbonyl and amide -M237 backbone carbonyl and amide
- 2) W183 side chain nitrogen -Y153 backbone carbonyl
- 3) I187 backbone amide-S232 backbone carbonyl
- 4) I192 amide backbone-T186 carbonyl backbone

**Complex rearrangements:** These complex re-arrangements during the activated state suggest that these interactions are at least partially responsible for stabilization of distinct confirmation(s) associated with activation/desensitization.

- 1) T179 backbone carbonyl - N128 side chain amino group becomes T179 side chain hydroxyl-N128 side chain amino group.
- 2) T181 side chain carbonyl-S182 backbone amide becomes T181 backbone carbonyl and amide -I125 backbone carbonyl and amide and S182 backbone carbonyl -H185 backbone amide.
- 3) L184 carbonyl backbone- H185 side chain nitrogen becomes W183 backbone carbonyl -H185 backbone amide. L184 forms no H-bonds during open/desensitized state.
- 4) In ground state T186 backbone carbonyl H bonds with both D189 backbone amide and I190 backbone amide. In open/desensitized state T186 backbone carbonyl shifts H bond from D189/I190 amide backbone to I192 amide backbone and T186 hydroxyl side chain H bonds with D189 amide backbone (left free by the shift of T186 carbonyl backbone).

## 5.5 Discussion

Our studies identified several novel amino acid residues of the loop B region. This region probably constitutes the area around the ligand-binding domain of the 5-HT<sub>3A</sub>R. Amino acids T179, F180, T181, S182, H185, I187 as well as D189 were identified as contributing to either direct interaction with ligands or transduction of agonist-induced conformational changes.

### 5.5.1 Loop B region plays a role in proper receptor expression

In the ground state of the receptor, T179 and F180 probably maintain the integrity of the protein structure. In this state, the T181 side-chain may form an important stabilizing interaction with the backbone of S182. Loss of such an interaction probably leads to altered protein stability and results in reduction in receptor expression. The L184A mutation does not cause any change in receptor expression. H185Y causes a severe change to the receptor number. A receptor model of the ground state of the 5-HT<sub>3A</sub>R suggests that the protein backbone at L184 forms a H-bond with the side chain nitrogen of H185 in the ground state of the receptor. If such a bond does exist, any alteration in the characteristics of the histidine side-chain would not be tolerated. Mutations at H185, I187 and D189 also affect receptor expression. While I190A mutation results in lack of demonstrable responses to 5-HT or *m*CPBG, I190V mutation yields EC<sub>50</sub> values comparable to that of the wild type receptor. These results from I190A and I190V mutant receptors suggest that amino acid I190 may be important only in maintaining the proper receptor expression. In ligand-docked models, I190 appears to be distant from the general ligand-binding domain and may not be involved in interactions with ligands.

### 5.5.2 Ligand-receptor interactions

Electrophysiological studies indicate that T181A mutation disrupts 5-HT induced binding and/or gating, while minor changes in *m*CPBG action are observed. Results from radioligand competition assays also suggest that T181 interacts strongly with 5-HT. Taken together, these data suggest that T181 specifically interacts with 5-HT in the activated/desensitized state of the receptor. Results from the docking studies also suggest that 5-HT and not *m*CPBG interact with T181 in open/desensitized state of the receptor.

Effects of mutation at W183 have been well characterized. We were able to reproduce these results using the W183F mutation. Mutation at W183 causes a 50-fold change in  $EC_{50}$  for 5-HT and a relatively smaller 20-fold change for *m*CPBG, suggesting that 5-HT and *m*CPBG may be interacting differentially with W183. W183 probably also plays a role in initiating/mediating conformational changes that lead to channel opening and desensitization. According to modeling studies, W183 does not form any hydrogen-bonding interaction at the ground state of the receptor while in the activated state; its side chain forms an H-bond with the side chain of Y153. In addition, backbone carbonyl groups of both W183 and S182 share an H-bond with the backbone amide of H185. W183 may also form either a cation-pi or pi-pi interaction with all 5-HT<sub>3</sub> receptor ligands. Thus, W183 seems to be critical for proper functioning of 5-HT<sub>3A</sub>R.

The principle interaction of granisetron is probably with W183. The ligand-docking studies also predict the interaction of W183 with granisetron. It is likely that H185 and S182 share a minor interaction with granisetron. Mutations at T179, F180 and D189 severely affect granisetron binding. However, given their distance from the



purported ligand-binding site (marked by position of W183), it is unlikely that these residues interact directly with granisetron. It is more likely that these residues are merely involved in maintaining the proper positioning of W183. In such a scenario, mutations at these positions will cause disruption of granisetron interaction through alteration of W183 position.

### **5.5.3 Ligand-specific mechanisms mediated through loop B region**

From the loop B region, amino acids T181A, L184, and I187 mediate the action of the endogenous agonist 5-HT. Available biochemical and molecular modeling data suggests that T181 is involved in direct interaction with 5-HT, but not *mCPBG*. The L184A mutation causes a large decrease in the apparent affinity for 5-HT (140 fold), but not *mCPBG*. It is likely that the selectivity of changes observed with L184 mutations is the result of a minor alteration in the position of adjacent W183. Amino acids S182 and I187 are *mCPBG* specific and probably play a lesser role in 5-HT mediated action. A mutation at S182 leads to *mCPBG*-specific changes to receptor desensitization while I187 probably mediates *mCPBG*-specific channel gating. Thus, *mCPBG* and 5-HT seem to mediate agonist action through distinct domains of the 5-HT<sub>3A</sub>R.

### **5.5.4 Desensitization**

Amino acid S182 is specifically involved in defining affinity of *mCPBG* for the desensitized state of 5-HT<sub>3A</sub>R. Loss of the non-desensitizing phase of *mCPBG*-induced response as well as delayed recovery from desensitization suggests that *mCPBG* induces a desensitization state of heightened affinity. However, this phenomenon is not observed

with 5-HT. Increased affinity of *m*CPBG for the desensitized state is also reflected in decrease in the *m*CPBG  $K_i$ . However, ligand-docking studies do not predict a direct interaction of granisetron, 5-HT or *m*CPBG with this amino acid, suggesting a possible role in mediating agonist-induced gating of the 5-HT<sub>3A</sub>R, possibly by altering post-opening receptor mechanisms.

### 5.5.5 Gating mechanism of the 5-HT<sub>3A</sub>R

Biochemical data from the loop B studies suggests that the loop B region plays a critical role in initiating the conformational changes that lead to channel opening (see Figure 5.8). Several mutations in the loop B region lead to loss of function or severely altered function. T179, F180, T181, W183, L184, H185, I187 and D189 mutants display such characteristics. These effects on function suggest that residues T179, F180, T181, W183, L184, H185, I187 and D189 are involved in direct interaction with agonists or in mediating receptor gating. Ligand-docking studies, however, predict direct interaction of agonists only with residues T181 and W183. Molecular modeling studies also suggest that all the loop B residues except T181 and W183 are positioned outside the purported ligand-binding domain. These data suggest that T179, F180, L184, H185, I187 and D189 mediate receptor gating.

Molecular modeling data suggests that in the activated state of the receptor, early part of loop B interacts with the pre-M1 region of the 5-HT<sub>3A</sub>R through F180-M237 interaction. On activation, the side chain of T179 possibly undergoes a complex rearrangement. This rearrangement may indicate a conformational change associated with activation. In the activated state, the H185 backbone shares an H-bond with both the

W183 and S182 backbone. These data suggest that the triad of S182 W183 and H185 is involved in mediating changes associated with activation/desensitization. Comparison of ground and active state model of the receptor reveals that I187 backbone forms an H-bonding interaction with the backbone of S232, an amino acid in the C loop region of the receptor. Crystallographic studies on AChBP indicate that the C loop region is drawn closer to the ligand binding domain on activation. Such a movement would be aided by interaction between I187 and S232. The movement of the C loop probably plays an important role in mediating conformational changes associated with gating. Data obtained from comparison of models of the ground and activated state 5-HT<sub>3</sub> receptor suggests that H-bonds between D189 and T186 undergo certain modifications during receptor activation. However, H-bonds between D189 and T64 remain unaltered. Thus, D189 seems to be playing a complex role in maintaining structural integrity and mediating agonist action.

Biochemical and molecular modeling data collectively suggests that amino acids T179, F180, L184, H185, I187, and D189 probably play a role only in mediating receptor gating. It is also possible that the changes to EC<sub>50</sub> values observed with mutations at these positions are a result of alteration in the protein backbone leading to alterations in the position of W183 side chain. Based on the data currently present, such a distinction cannot be easily made.

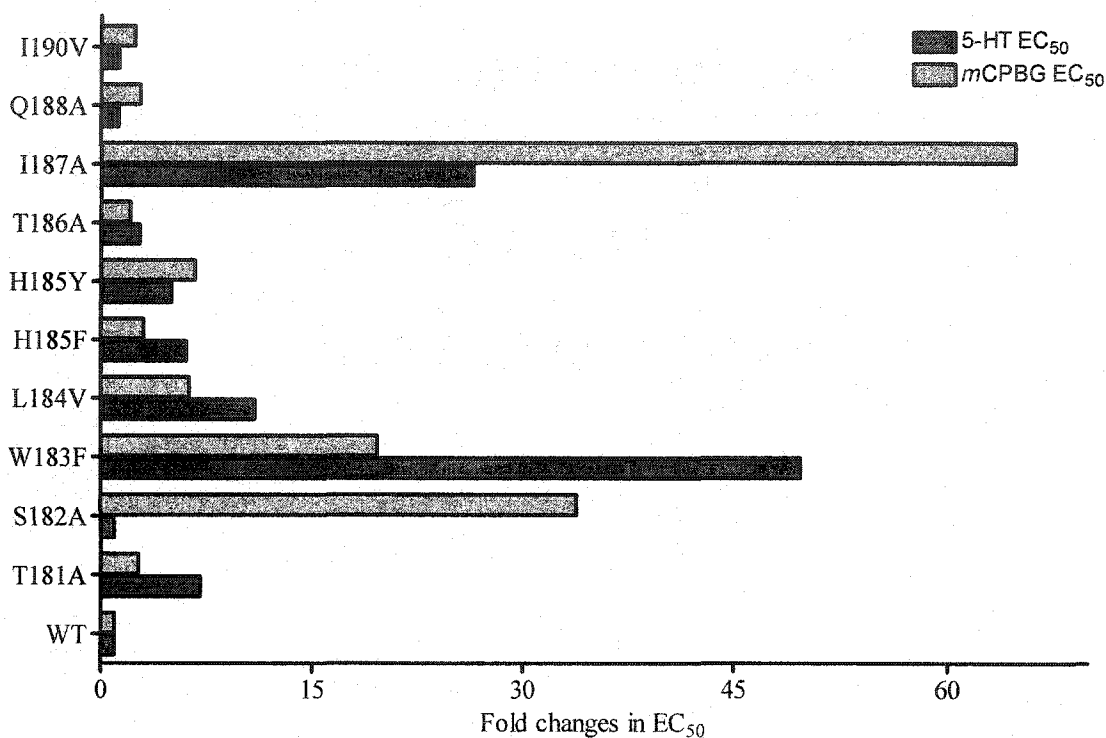
We have utilized molecular models of the 5-HT<sub>3A</sub>R in both ground and activate state to predict interactions that may be mediating conformational changes associated with gating. These changes have been summarized in Figure 5.8. The major interaction

at the ligand binding domain is mediated through W183, which is located almost at the center of the loop B region. Molecular modeling data suggests that agonist binding leads to rearrangement of hydrogen bonds between loop B region and other regions from the same subunit such as loop A region, loop C region, pre-loop D region and pre-M1 region. Agonist binding at the binding cleft between two subunits also leads to formation of hydrogen bonds between loop B on the principal face and loop E on the complimentary face. The rearrangement of hydrogen bonds occurs in the regions on both sides of W183. All of these connections are probably associated with the conformational changes mediating channel opening. In case of other members of ligand-gated ion channel superfamily, it has been suggested earlier that the 'conformational wave' that accompanies channel opening travels from the ligand binding domain to the channel (M2) region. Our data suggests that following its initiation in the ligand binding domain, the conformational wave travels to all the regions surrounding the loop B region with W183 forming the central reference point.

m	5-HT3	AS	LTFT <b>S</b> WLHTIQDI
m	5-HT3	B	LTFN <b>S</b> ILHTVEDI
h	5-HT3	A	LTFT <b>S</b> WLHTIQDI
h	5-HT3	B	LTFK <b>S</b> ILHTVEDV
m	nACh	a7	LKFG <b>S</b> WSYGGWSL
h	nACh	a7	LKFG <b>S</b> WSYGGWSL
	AChBP		IKIG <b>S</b> WTHHSREI
m	GABAA	a1	LKFG <b>S</b> YAYTRAEV
m	GABAA	b1	LEIE <b>S</b> YGYTTDDI
m	GABAA	d	LDLE <b>S</b> YGYSSEDI
m	GABAA	g	LEF <b>S</b> YGYPREEI

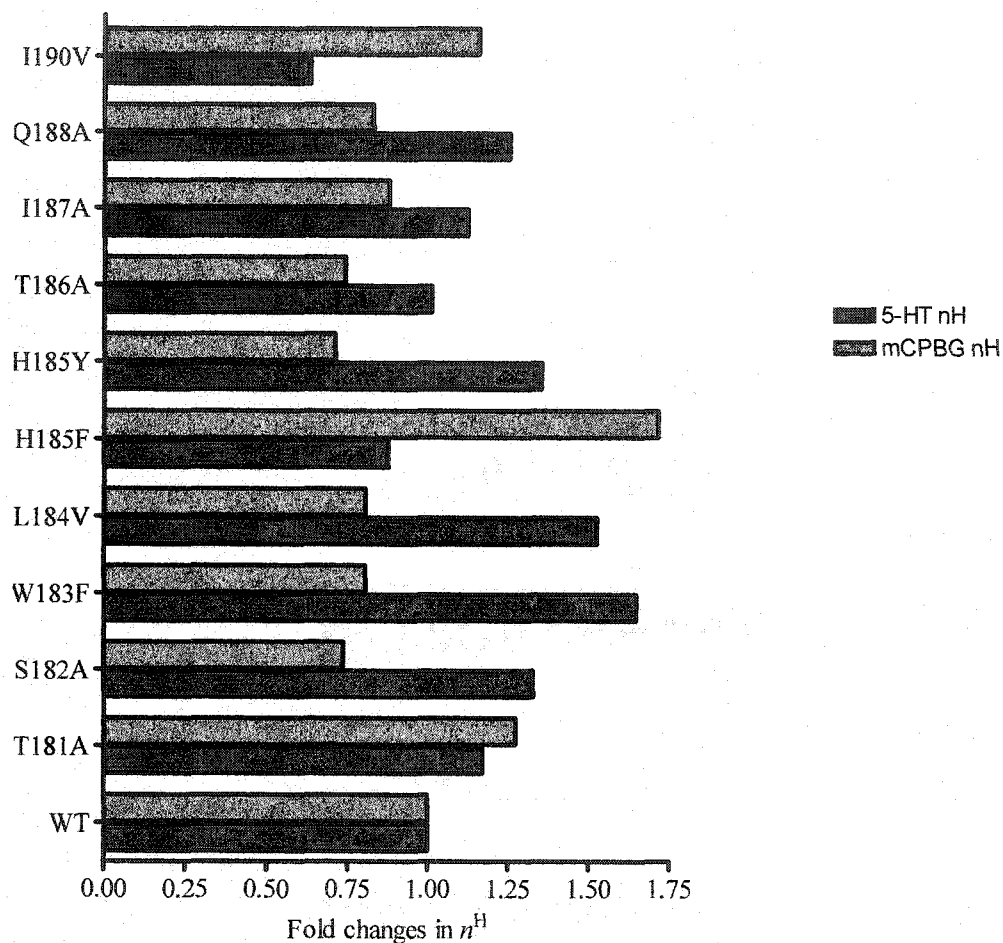
**Figure 5.1** Amino acid sequence alignment of *murine* 5-HT<sub>3A</sub>R with other members of the superfamily, with a focus on the predicted loop B region.

Primary sequences of the members of the LGIC superfamily were aligned using Clustal X algorithm. The conserved amino acids are marked in grey. The amino acid positions with conserved side chain characteristics are marked in bold.



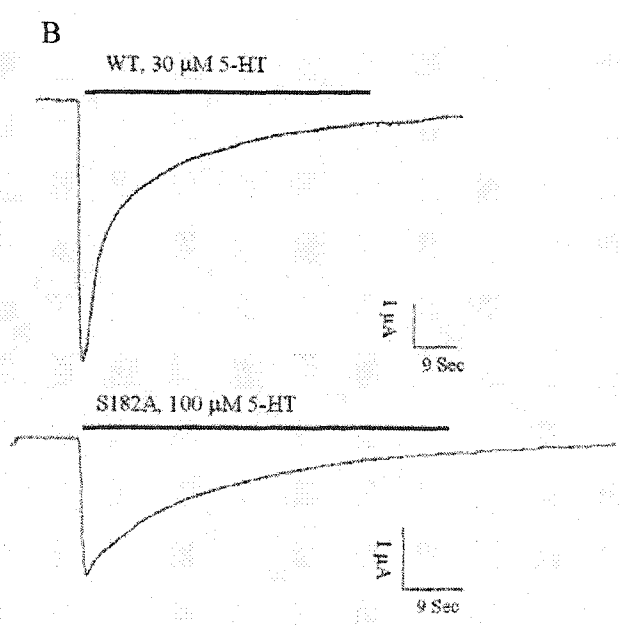
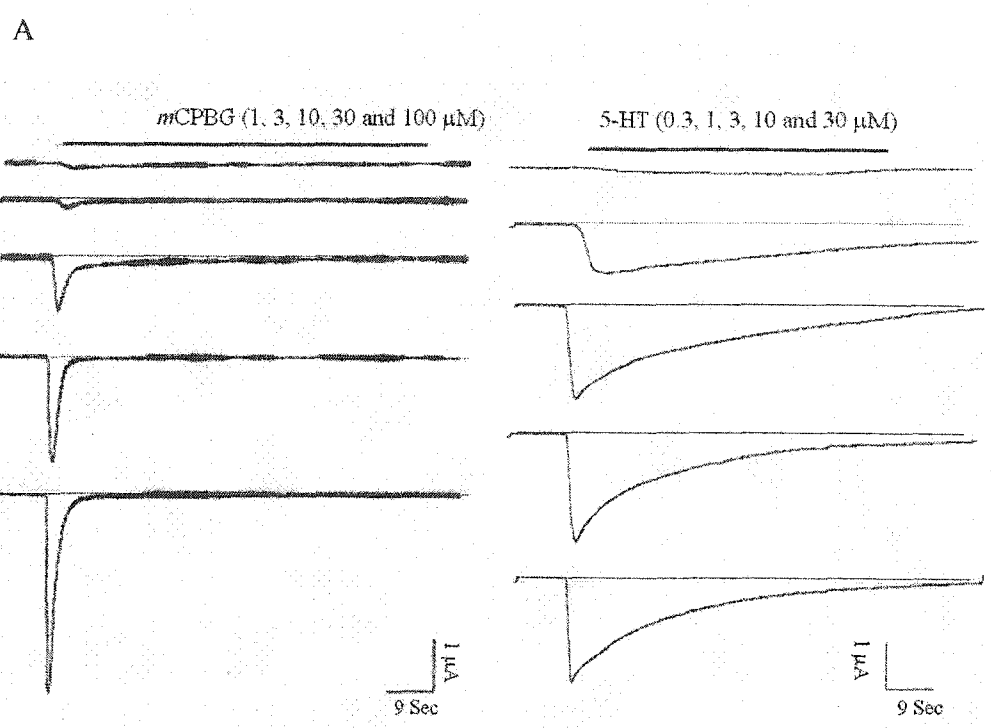
**Figure 5.2: A comparison of EC<sub>50</sub> values for 5-HT and *mCPBG***

Bar graph shows comparison of fold changes in 5-HT and *mCPBG* EC<sub>50</sub> values for the mutant receptors compared to the WT values. The WT fold-change values have been normalized to 1. Each fold change value was calculated based on at least 4 separate experiments. The error bars indicate standard error. Bars indicating 5-HT EC<sub>50</sub> fold change are marked with black while those indicating *mCPBG* EC<sub>50</sub> fold change are marked grey. The fold change values are approximations. The bars lack error bars since fold changes and not actual data values are displayed.



**Figure 5.3: A comparison of Hill number values for 5-HT and *m*CPBG**

Bar graph shows comparison of fold changes in 5-HT and *m*CPBG  $n^H$  values for the mutant receptors compared to the WT values. The WT fold-change values have been normalized to 1. Each fold change value was calculated based on at least 4 separate experiments. The error bars indicate standard error. Bars indicating 5-HT  $n^H$  fold change are marked with black while those indicating *m*CPBG  $n^H$  fold change are marked grey. The fold change values are approximations. The bars lack error bars since fold changes and not actual data values are displayed.





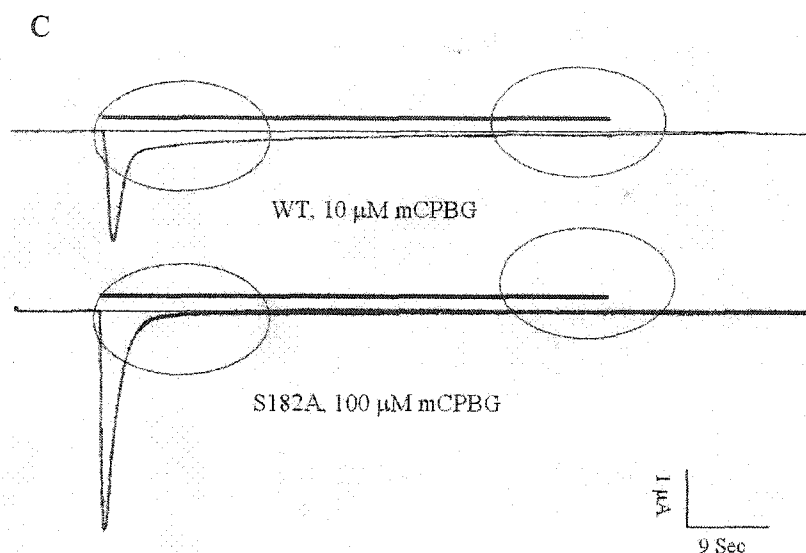


**Figure 5.4: Electrophysiological characterization of S182A mutation**

#### 5.4.A Comparison of 5-HT and *mCPBG* induced responses from S182A mutant receptor

The right and left hand column of the figure shows responses elicited by a range of *mCPBG* and 5-HT concentrations recorded from separate oocyte expressing S182A mutant receptors respectively. The concentrations of respective agonist utilized are indicated at the top of each column. The responses displayed are representative of at least 4 separate experiments. In case of *mCPBG* induced responses, the return to the baseline following the second phase of the desensitization is rapid, while no such change is observed in 5-HT induced responses. The characteristics of the responses induced by either agonist otherwise appear normal.

#### 5.4.B Comparison of 5-HT induced responses from WT and S182A mutant receptor

A comparison of responses induced by supra maximal concentration of 5-HT from WT (top trace) and S182A mutant receptor (bottom trace) suggests that the second phase of the desensitization of 5-HT induced response from S182A receptor is slower as compared to that of the WT receptor.

#### 5.4.C Comparison of *mCPBG* induced responses from WT and S182A mutant receptor

A comparison of responses induced by supra maximal concentration of *mCPBG* from WT (top trace) and S182A mutant receptor (bottom trace). The WT trace clearly shows second, slower phase of desensitization (marked by the first circle) followed by the third,

non-desensitizing phase (marked by the second circle). The comparison suggests that the third, non-desensitizing phase of *m*CPBG induced response WT receptor is missing in the *m*CPBG induced response from the S18A mutant receptor. The response returns to baseline following the second phase of desensitization (marked by two circles). The traces shown here are representative of at least 4 experiments.

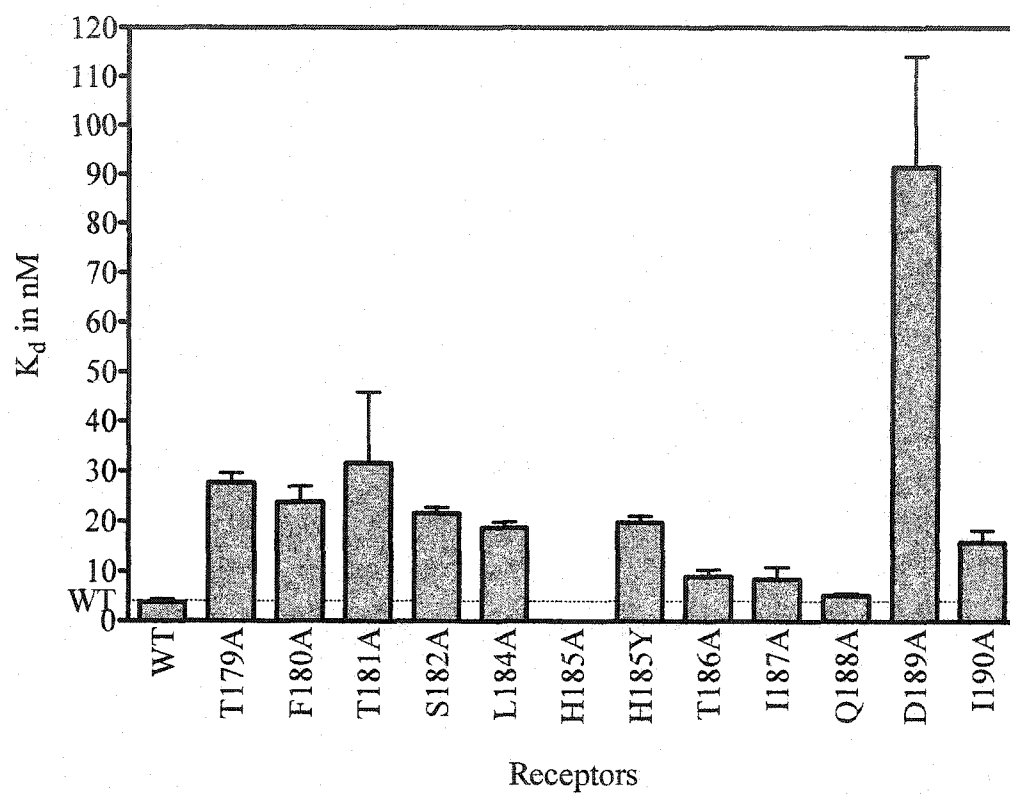


**Figure 5.5 [3H] granisetron binding to loop B mutant receptors**

Bar graph shows comparison of [3H] granisetron  $K_d$  values for each of the loop B mutant receptors. The Y axis shows  $K_d$  in nanomolar (nM). Each value was calculated based on at least 4 separate experiments. The error bars indicate standard error. Granisetron binding to the H185A mutant receptor could not be detected.

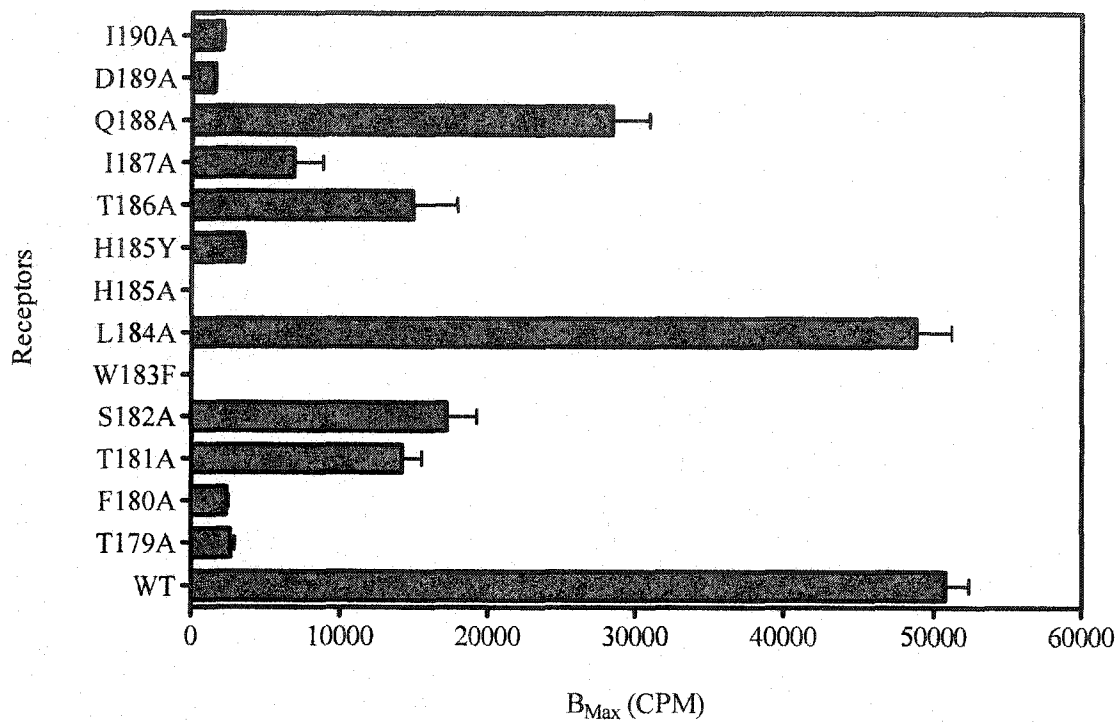
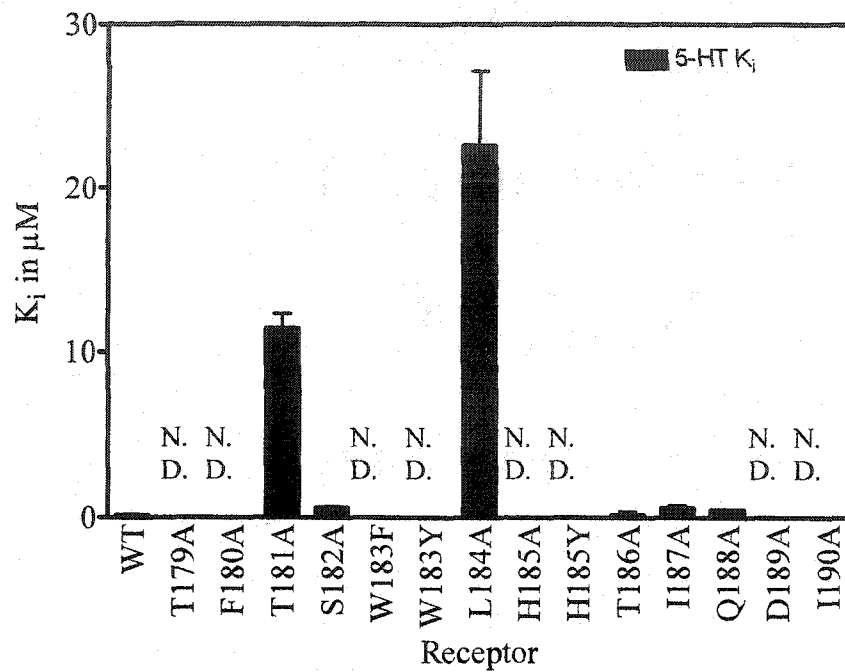


**Figure 5.6 A comparison of B<sub>Max</sub> values of loop B mutant receptors**

Bar graph shows comparison of B<sub>Max</sub> values for each of the loop B mutant receptors. The Y-axis shows B<sub>Max</sub> measured as Counts Per Minute (CPM). The CPM for each preparation is comparable since same number of cells were seeded for every experiment (250,000 cells/ 100 mm Petri dish). Each value was calculated based on at least 4 separate experiments. The error bars indicate standard error. Granisetron binding to the H185A mutant receptor could not be detected.

A



B

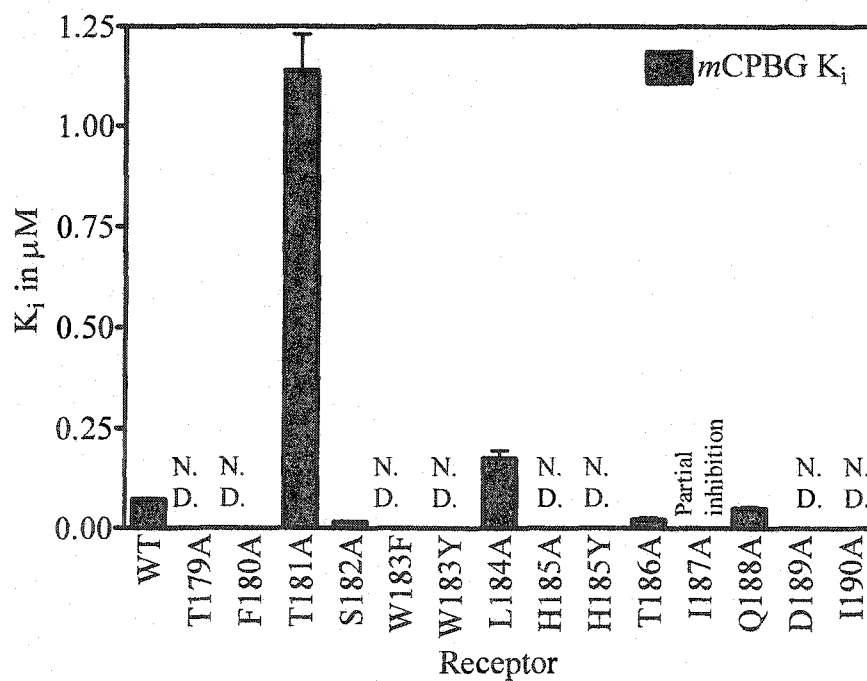


**Figure 5.7 Displacement of bound radio-ligand by 5-HT<sub>3A</sub>R agonists****5.7.A Displacement of [<sup>3</sup>H] granisetron binding to loop B mutant receptors by 5-HT**

Bar graph shows comparison of 5-HT K<sub>i</sub> values for each of the loop B mutant receptors. The Y axis shows K<sub>i</sub> in micromolar (μM). Each value was calculated based on at least 4 separate experiments. The error bars indicate standard error. N.D. denotes 'Not Detected'.

**5.7.B Displacement of [<sup>3</sup>H] granisetron binding to loop B mutant receptors by *m*CPBG**

Bar graph shows comparison of *m*CPBG K<sub>i</sub> values for each of the loop B mutant receptors. The Y axis shows K<sub>i</sub> in micromolar (μM). Each value was calculated based on at least 4 separate experiments. The error bars indicate standard error. N.D. denotes 'Not Detected'.

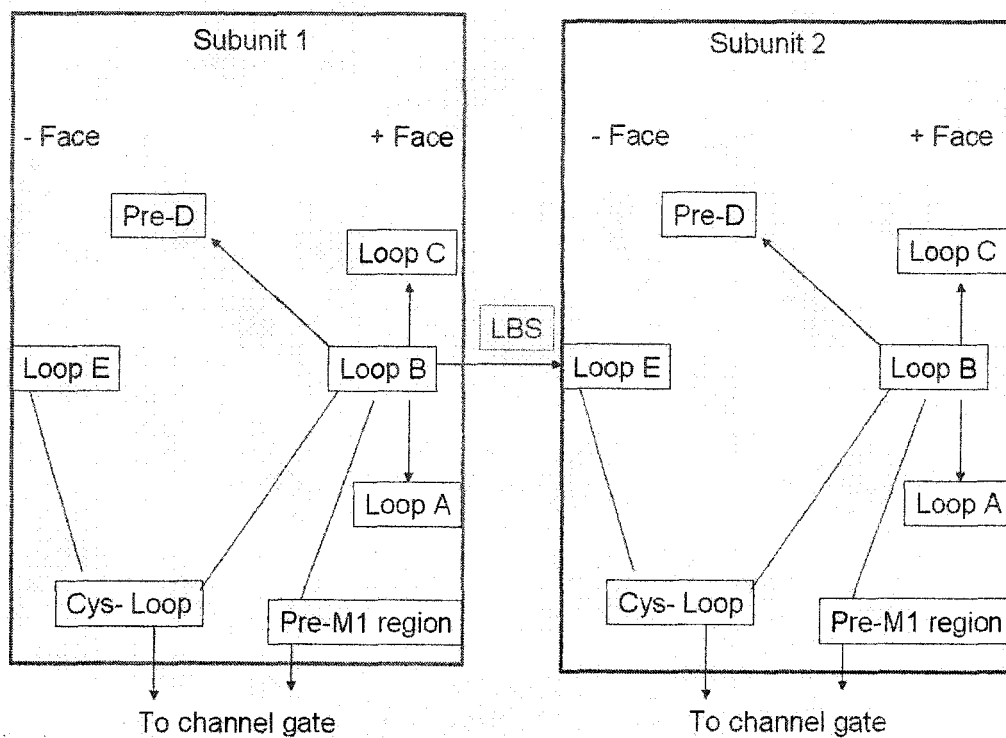


**Figure 5.8 Intra-subunit and inter-subunit contacts of the loop B region formed in the agonist-bound state of the receptor**

Two squares represent amino terminal domains of adjacent subunits (named subunit 1 and subunit 2). The arrows indicate probable intra-subunit and inter-subunit interactions of loop B amino acids formed after agonist binds to the binding domain.

**Table 5.1 Electrophysiological characterization of loop B receptors, data obtained using agonists 5-HT and *m*CPBG.**

5-HT and *m*CPBG EC<sub>50</sub> and *n*<sup>H</sup> values in  $\mu$ M for each of the loop B mutant receptors. Each value was calculated based on at least 4 separate experiments. The standard error is indicated by the ' $\pm$ ' sign. N.D. denotes 'Not Detected'.

	<i>Receptor</i>		<i>5-HT</i>	<i>mCPBG</i>
	EC <sub>50</sub> ( $\mu$ M)	<i>n</i> <sub>H</sub>	EC <sub>50</sub> ( $\mu$ M)	<i>n</i> <sub>H</sub>
WT	3.4 $\pm$ 0.3	1.4 $\pm$ 0.2	0.8 $\pm$ 0.07	1.6 $\pm$ 0.2
T179A	N.D	N.D	N.D	N.D
F180A	N.D	N.D	N.D	N.D
T181A	24.2 $\pm$ 0.91	1.64 $\pm$ 0.09	2.18 $\pm$ 0.09	2.04 $\pm$ 0.16
S182A	3.33 $\pm$ 0.18	1.86 $\pm$ 0.19	27.1 $\pm$ 3.7	1.18 $\pm$ 0.17
W183F	169 $\pm$ 9.29	2.31 $\pm$ 0.22	15.7 $\pm$ 1.51	1.29 $\pm$ 0.14
L184A	N.D	N.D	N.D	N.D
L184V	37.3 $\pm$ 1.6	2.14 $\pm$ 0.18	5.09 $\pm$ 0.19	1.6 $\pm$ 0.08
H185A	N.D	N.D	N.D	N.D
H185F	20.9 $\pm$ 1.57	1.23 $\pm$ 0.10	2.49 $\pm$ 0.04	2.75 $\pm$ 0.13
H185Y	17.24 $\pm$ 0.83	1.9 $\pm$ 0.15	5.4 $\pm$ 0.42	1.14 $\pm$ 0.08
T186A	9.56 $\pm$ 0.63	1.42 $\pm$ 0.12	1.70 $\pm$ 0.10	1.19 $\pm$ 0.08
I187A	90 $\pm$ 6.18	1.58 $\pm$ 0.16	51.9 $\pm$ 4.08	1.41 $\pm$ 0.13
Q188A	4.38 $\pm$ 0.28	1.76 $\pm$ 0.17	2.28 $\pm$ 0.19	1.33 $\pm$ 0.13
D189A	N.D	N.D	N.D	N.D
I190A	N.D	N.D	N.D	N.D
I190V	4.42 $\pm$ 0.58	0.89 $\pm$ 0.09	1.953 $\pm$ 0.09	1.86 $\pm$ 0.15



**Table 5.2 Radio-ligand binding to loop B receptors, data from saturation and competition assays**

[<sup>3</sup>H] granisetron  $K_d$  values in nanomolar (nM), as well as 5-HT and mCPBG  $K_i$  values in micromolar ( $\mu$ M) for each of the loop B mutant receptors. Each value was calculated based on at least 4 separate experiments. The standard error is indicated by the ' $\pm$ ' sign. N.D. denotes 'Not Detected'.

<i>Receptor</i>	<i>[<sup>3</sup>H] granisetron</i>		<i>5-HT</i>	<i>mCPBG</i>
	$K_d$ (nM)	$n_H$	$K_i$ ( $\mu$ M)	$K_i$ ( $\mu$ M)
WT	0.96 $\pm$ 0.16	1.02 $\pm$ 0.07	0.16 $\pm$ 0.04	0.072 $\pm$ 0.003
T179A	6.9 $\pm$ 0.49	1.26 $\pm$ 0.13	N.D	N.D
F180A	5.9 $\pm$ 0.78	1.5 $\pm$ 0.22	N.D	N.D
T181A	3.35 $\pm$ 0.35	1.19 $\pm$ 0.14	11.4 $\pm$ 0.91	1.14 $\pm$ 0.09
S182A	5.4 $\pm$ 0.31	1.68 $\pm$ 0.15	0.61 $\pm$ 0.07	0.016 $\pm$ 0.001
W183F	N.D	N.D	N.D	N.D
W183Y	N.D	N.D	N.D	N.D
L184A	4.7 $\pm$ 0.28	1.52 $\pm$ 0.12	22.6 $\pm$ 4.57	0.175 $\pm$ 0.02
H185A	N.D	N.D	N.D	N.D
H185Y	4.9 $\pm$ 0.32	1.25 $\pm$ 0.09	ND up to 300 $\mu$ M	ND up to 300 $\mu$ M
T186A	2.25 $\pm$ 0.34	1.2 $\pm$ 0.2	0.176 $\pm$ 0.20	0.022 $\pm$ 0.005
I187A	3.4 $\pm$ 0.46	1.25 $\pm$ 0.19	0.60 $\pm$ 0.15*	0.94 $\pm$ 0.17*
Q188A	1.37 $\pm$ 0.1	1.19 $\pm$ 0.08	0.48 $\pm$ 0.03	0.05 $\pm$ 0.004
D189A	N.D	N.D	N.D	N.D
I190A	N.D	N.D	N.D	N.D

**Table 5.3 Results from the ligand-docking studies using 5-HT<sub>3A</sub>R homology model**

Modeling of the extracellular domain of the *murine* 5-HT<sub>3A</sub>R and ligand docking were performed as described in "Experimental procedures". The results are also represented in Figure 1. Interactions predicted for 5-HT, 2-Me 5-HT, granisetron and *m*CPBG (model '1' and model '2') are shown in the table. HB: Hydrogen bond, SB: Salt bridge, CP: Cation-interaction, PP: interaction +: Within 4 Å of docked ligand.

	N128	T179	T181	W183	F226	I228	D229	I230	S231	Y234	E236	W90	R92	Y153	I207
5HT	*		*	PP	CP	+	HB		+	CP	SB	+		+	+
2ME5HT	*		*	PP	CP	+	HB	+	+	HB	SB	+		+	+
CPBG1	*			CP	PP	+	SB	+	+	HB	+	+		HB	+
CPBG2	+			PP	CP	+			+	CP	SB	+			
GRANI	+	+		+	CP	+	+	+	+	HB		+	+	+	

HB hydrogen bond  
 SB salt bridge  
 CP cation-pi interaction  
 PP pi-pi interaction

**Table 5.4 A comparison of the H-bonding interactions of the loop B region in molecular models of the relaxed and ligand bound state of 5-HT<sub>3A</sub>R.**

The molecular models for the relaxed and ligand bound state of 5-HT<sub>3A</sub>R were provided by Dr. Zsolt Bikadi, National Academy of Sciences, Hungary. The PDB files of the molecular models were imported in to Sybyl version 7.0 (Tripos Inc., St. Louise, MO). The PDB files were checked for irregularities such as incorrect molecular assignment, incorrect bond angles and missing amino acid side chains. All essential water molecules, hydrogen atoms and charges were added. The comparisons in H-bonding in relaxed and ligand bound state were made using these corrected models.

**Table 5.4.1: Loop B H-Bonds in the ground state**

<b>H-Bonds formed by residues of Loop B in the ground state model of the m5-HT<sub>3A</sub>R</b>	
T179	T179 amide backbone- side chain carbonyl of E129 (E106) T179 carbonyl backbone- N128 amide backbone-N128 side chain carbonyl
F180	No H bond
T181	T181 side chain carbonyl-S182 backbone amide
S182	T181 side chain carbonyl-S182 backbone amide
W183	No H bond
L184	L184 carbonyl backbone- H185 nitrogen
H185	L184 carbonyl backbone- H185 nitrogen
H185	Q188 No bonds
T186	T186 backbone carbonyl H bonds with both D189 backbone amide and I190 backbone amide
I187	No H bonds
Q188	No H bonds
D189	D189 carbonyl backbone-T64 amide backbone D189 backbone amide-T186 backbone carbonyl
I190	I190 backbone amide -T186 backbone carbonyl
N191	T64 carbonyl backbone-N191 amide backbone
I192	No H bonds

**Table 5.4.2: Loop B H-Bonds in the ligand-bound open/desensitized state**

<b>H-Bonds formed by residues of Loop B in the open/desensitized state model of the 5-HT<sub>3A</sub>R</b>	
T179	T179 side chain carbonyl-N128 side chain amino H bond T179 backbone carbonyl -N128 backbone amide T179 backbone amide -E129 side chain carbonyl
F180	F180 backbone carbonyl and amide -M237 backbone carbonyl and amide
T181	T181 backbone carbonyl and amide -I125 backbone carbonyl and amide
S182	S182 backbone carbonyl -W183 backbone carbonyl -H185 backbone amide
W183	W183 side chain nitrogen -Y153 backbone carbonyl S182 backbone carbonyl -W183 backbone carbonyl -H185 backbone amide
L184	No H bonds
H185	W183 side chain nitrogen -Y153 backbone carbonyl S182 backbone carbonyl -W183 backbone carbonyl -H185 backbone amide
T186	T186 carbonyl side chain -D189 amide backbone T186 carbonyl backbone -I192 amide backbone
I187	I187 backbone amide-S232 backbone carbonyl
Q188	No H-bonds
D189	D189 carbonyl backbone -T64 amide backbone
I190	No H-bonds
N191	No H-bonds
I192	I192 amide backbone-T186 carbonyl backbone

## References

- Beene DL, Brandt GS, Zhong W, Zacharias NM, Lester HA and Dougherty DA (2002) Cation-pi interactions in ligand recognition by serotonergic (5-HT<sub>3A</sub>) and nicotinic acetylcholine receptors: the anomalous binding properties of nicotine. *Biochemistry* **41**(32):10262-10269.
- Celie PH, van Rossum-Fikkert SE, van Dijk WJ, Brejc K, Smit AB and Sixma TK (2004) Nicotine and carbamylcholine binding to nicotinic acetylcholine receptors as studied in AChBP crystal structures. *Neuron* **41**(6):907-914.
- Cornell WD, Cieplak, P., Bayly, C.I., Gould, I.R., Merz, K.M. Jr., Ferguson, D.M., Spellmeyer, D.C.; Fox, T., Caldwell, J.W. and Kollman, P.A. (1995) *J Am Chem Soc* **117**:5179-5197.
- Joshi PR, Suryanarayanan A and Schulte MK (2004) A vertical flow chamber for *Xenopus* oocyte electrophysiology and automated drug screening. *J Neurosci Methods* **132**(1):69-79.
- Laskowski RA, MacArthur, M.W., Moss, D.S., and Thornton, J.M. Main-chain bond lengths and bond angles in protein structures. (1993) *J Mol Biol.* **231**(4):1049-67.
- McDonald IK and Thornton JM (1994) Satisfying hydrogen bonding potential in proteins. *J Mol Biol* **238**(5):777-793.
- Spier AD and Lummis SC (2000) The role of tryptophan residues in the 5-Hydroxytryptamine(3) receptor ligand binding domain. *J Biol Chem* **275**(8):5620-5625.
- Thompson JD, Higgins DG and Gibson TJ (1994) CLUSTAL W: improving the sensitivity of progressive multiple sequence alignment through sequence weighting, position-specific gap penalties and weight matrix choice. *Nucleic Acids Res* **22**(22):4673-4680.
- Venkataraman P, Venkatachalan SP, Joshi PR, Muthalagi M and Schulte MK (2002) Identification of critical residues in loop E in the 5-HT<sub>3ASR</sub> binding site. *BMC Biochem* **3**(1):15.
- Wu CH, Huang H, Arminski L, Castro-Alvear J, Chen Y, Hu ZZ, Ledley RS, Lewis KC, Mewes HW, Orcutt BC, Suzek BE, Tsugita A, Vinayaka CR, Yeh LS, Zhang J and Barker WC (2002) The Protein Information Resource: an integrated public resource of functional annotation of proteins. *Nucleic Acids Res* **30**(1):35-37.

- Xiang Z and Honig B (2001) Extending the accuracy limits of prediction for side-chain conformations. *J Mol Biol* **311**(2):421-430.
- Xiang Z, Soto CS and Honig B (2002) Evaluating conformational free energies: the colony energy and its application to the problem of loop prediction. *Proc Natl Acad Sci U S A* **99**(11):7432-7437.
- Yan D, Schulte MK, Bloom KE and White MM (1999) Structural features of the ligand-binding domain of the serotonin 5HT3 receptor. *J Biol Chem* **274**(9):5537-5541.
- Zhong W, Gallivan JP, Zhang Y, Li L, Lester HA and Dougherty DA (1998) From *ab initio* quantum mechanics to molecular neurobiology: a cation-pi binding site in the nicotinic receptor. *Proc Natl Acad Sci U S A* **95**(21):12088-12093.

**Appendix**

**Acknowledgements:** This work is supported by the National Science Foundation (NSF CAREER 9985077) and the American Heart Association (AHA 0151065B).

PRJ and AS are both Alaska INBRE pre-doctoral research fellows.



## Chapter 6: Conclusions

### 6.1 An overview

5-HT<sub>3A</sub>R is a widely distributed ion channel in peripheral and central nervous system, and plays a major role in mediating physiological processes in cardiovascular, nervous and digestive systems. Studies directed at the ligand-binding domain and dynamics of 5-HT<sub>3A</sub>R function at the molecular level described here serve a three-fold purpose.

Members of the LGIC superfamily include nACh, GABA<sub>A</sub>, GABA<sub>C</sub> and Gly receptors. These ion channels are widely distributed the nervous system and mediate physiological (such as neuro-muscular neurotransmission, autonomic neurotransmission, excitatory and inhibitory neurotransmission, sleep), pharmacological (anesthesia) and pathological processes (myasthenia gravis, convulsions, cerebrovascular accidents). The studies described here increase the understanding of how complex multi-meric membrane bound ion channel coupled receptors coordinate agonist binding and conformational changes associated with the resulting functional response (i.e.; channel opening). Despite all the advances in molecular biology and molecular biochemistry, detailed knowledge of mechanisms governing functioning of membrane bound ion channel coupled receptors is unavailable. Advances in the understanding of 5-HT<sub>3A</sub>R structure and function will definitely aid studies of other LGIC receptors.

5-HT<sub>3A</sub>R antagonists have been used clinically for the last 15 years and recent studies have suggested that 5-HT<sub>3A</sub>R agonists can also be employed in clinical conditions such as gastro-esophageal reflux disease (GED) and constipation associated with irritable

bowel syndrome. Based on the studies of 5-HT<sub>3A</sub>R described here, we are beginning to understand how agonists, partial agonists or antagonists use distinct features of the ligand-binding domain to bring about specific changes. This knowledge can be used to create ligands that modulate specific aspects of receptor function. For example, it may be possible to synthesize agonists that specifically affect the desensitization state or the open state stability. Such ligands can be used clinically to fine-tune 5-HT<sub>3A</sub>R function.

The 5-HT<sub>3A</sub>R is modulated by non-specific endogenous (cations, glucocorticoids, gonadal steroids) and exogenous (alcohols, anesthetics, neuroleptic drugs) agents (See Chapter 1 for details). These agents interact with the 5-HT<sub>3A</sub>R in competitive or non-competitive manner and modulate agonist action. These interactions with non-specific agents probably influence various aspects of 5-HT<sub>3R</sub> physiology and pathophysiology. The influence of these agents on 5-HT<sub>3R</sub> physiology and pathophysiology is clinically relevant in conditions such as alcoholism, surgical anesthesia and certain drug interactions (e.g. with steroids). To better understand how 5-HT<sub>3R</sub> function is modulated by non-specific agents at the molecular level, we need to understand the molecular mechanism of agonist and antagonist action on the 5-HT<sub>3R</sub>.

## **6.2 Methodological advancement**

The vertical flow chamber developed for these studies provides an improved platform for *Xenopus* electrophysiology (see Appendix 2). This chamber offers both a stable environment for long term recording and rapid solution exchange rates that result in reliable, reproducible data. This system has proved invaluable for the evaluation of mutant receptors with very low  $I_{Max}$  values, since it enables the use of rapid solution

exchange rates. The use of a novel vertical perfusion system has also allowed us to perform accurate evaluation of relative efficacy values for various agonists and partial agonists. These measurements aid in the identification of changes in the gating mechanism that result from mutation of some amino acids. Certain mutations lead to changes in 'gating'. This approach has been successfully applied for GABA<sub>A</sub> receptor, to decipher changes in gating mechanism as a result of point mutations. Studies involving full and partial agonists described here are unique and have not been conducted for the 5-HT<sub>3A</sub>R previously. While other laboratories have suggested involvement of certain amino acids residues in the gating mechanism, biochemical evidence supporting such assertions has been presented solely in the studies described here. While such studies can also be performed using conventional perfusion chambers, the vertical perfusion confers the ability to accurately measure peak heights. It is also imperative that measurements for all agonists be carried out on the same oocyte when comparing relative efficacies. Our method of perfusion allows recording from a single oocyte for an extended period of time (10-12 hours); whereas such stability is not usually obtained using conventional perfusion chambers.

### **6.3 The ligand binding domain**

Studies described here have identified a number of novel amino acids affecting ligand-binding and channel opening (T179, F180, T181, S182, H185, I187 and D189); while detailed analyses of amino acids identified earlier have been performed (Y141, Y143 and Y153). These results suggest that various ligands (agonists, partial agonists and

antagonists) produce specific effects on receptor function by utilizing specific features of the ligand binding domain.

Alanine scanning mutagenesis study of the loop B region was based on the hypothesis that homologous regions of related proteins share structural and functional features. Previous studies of the nAChR, GABA<sub>A</sub>R and AChBP suggested that a conserved aromatic residue in the loop B region (homologous to W143 of AChBP) interacts with the amino group of interacting ligands. Our studies indicate that T181 also interacts directly with 5-HT and granisetron, but not *m*CPBG. We have also shown that the loop B region transduces conformational changes associated with agonist induced channel opening.

The role of Y143 and Y153 in direct ligand interaction is less clear. Available data from lerisetron and its analogs suggests that Y143 and Y153 are involved in direct interaction with competitive antagonists. Molecular modeling data supports a direct interaction of 5-HT with Y153 but not with Y143. The model does not support any interaction between *m*CPBG and either of these two tyrosine residues. It is possible that agonists interact with Y143 in a conformational state that is different than the one modeled. The ligand-bound homology model represents either the open or the desensitized state of the receptor. If agonists interact with Y143 as a part of early events in ligand-receptor interaction (i.e., the pre-open state), ligand-bound models will not predict such interactions. However, the role of Y143 in mediating gating by all the agonists is well supported.

#### 6.4 5-HT<sub>3A</sub>R ligand specificities

We performed studies focusing on the role played by various parts of the ligand-binding domain in ligand specificity. Based on the results of previous studies involving the loop E region, we formed the hypothesis that structurally distinct agonists mediate specific actions through differential interactions with ligand binding domain. Results from studies of the loop E and loop B region indicate that structurally distinct agonists utilize distinct regions of the ligand binding domain to mediate distinct conformational changes.

Y153 appears to be selectively involved in mediating gating events promoted by 5-HT but not *m*CPBG. We have utilized biochemical data in combination with molecular modeling to obtain insights into the dynamics of the interactions of amino acid Y143 and Y153. Biochemical data indicates that the hydroxyl group of Y143 is critical to both 5-HT and *m*CPBG promoted channel opening, while the hydroxyl group of Y153 is critical to only 5-HT promoted channel opening. Molecular models of the agonist-bound state suggest that the side chain of Y153 apparently interacts with 5-HT, while it interacts with Y234 when *m*CPBG is bound. Therefore, interaction with Y153 is critical to the channel opening promoted by 5-HT, but not *m*CPBG. Taken together, these data indicate that the direct interaction 5-HT with Y153 specifically mediates 5-HT promoted channel opening. T181A, W183, L184, H185 and I187 and D189 all affect agonist induced channel opening. Available biochemical and molecular modeling data suggests that T181 is involved in direct interaction with 5-HT, but not *m*CPBG. T181A, W183, L184, H185 and I187 are more important for gating induced by 5-HT. Amino acids S182 and I187 are *m*CPBG specific and play a lesser role in 5-HT mediated action. Thus, *m*CPBG and 5-HT

mediate agonist action through distinct interactions at the binding domain of the 5-HT<sub>3A</sub>R.

### **6.5 Mechanism of activation and desensitization.**

Our studies involving loops E and B suggest that mutations in and around the ligand binding domain decrease the open channel stability. These data are consistent with the results obtained for other members of the superfamily. In case of nicotinic acetylcholine receptor, mutation of amino acids in and around the purported ligand binding domain leads to the destabilization of open state of the receptor. Similarly in case of the 5-HT<sub>3A</sub>R, amino acids Y143 and Y153 may be involved in stabilization of the open state of the receptor. Interestingly, the selective effect of Y153 mutations on 5-HT induced gating suggests that structurally distinct agonists mediate channel opening by stabilizing distinct open states. Such differential mechanisms for agonist action have not been yet proposed or demonstrated for any other member of the Cys loop LGIC family. The mechanism proposed here could also be evaluated in other members of the LGIC family.

Examination of the 5-HT<sub>3A</sub>R homology model suggests a mechanism by which both Y143 and Y153 could mediate channel gating (Figure 6.1). A direct link between the E-loop region and the critical Cys loop structure is clearly evident in all models of LGIC receptors. It has been speculated that agonist interaction with E-loop tyrosines causes a conformation change in the Cys loop that is involved in channel opening of the 5-HT<sub>3A</sub>R. Emerging evidence suggests that the Cys loop region of ligand-gated ion channels plays a critical role in gating mechanism. Previous studies have implicated W149 of  $\alpha$ AChR in a cation- $\pi$  interaction with the quaternary ammonium of

acetylcholine. Based on the crystal structure of the AChBP, it has been suggested that W149 of  $\alpha$ AChR mediates its effects by the virtue of its direct connection to the Cys loop region through  $\beta$ -strand 6, which may interact with the ion channel through M2-M3 linker region. While W183 of the 5-HT<sub>3A</sub>R, homologous to W149 of the  $\alpha$ AChR, is directly connected to the Cys loop region, so are residues Y143 and Y153. Interestingly, molecular dynamic simulation studies of an  $\alpha$ 7 homology model indicate that the side chain of residue L118; homologous to Y153 of 5-HT<sub>3A</sub>R undergoes conformational change during ligand binding. The same study also indicates that ligand binding leads to a dynamic interaction of the Cys loop with the M2-M3 linker. It can therefore be proposed that both Y143 and Y153 exert their effects by influencing direct ligand interaction with the ligand-binding domain on one hand and by effecting gating through their connection with the Cys loop structure. Thus E-loop tyrosines may be providing a connection between the ligand-binding domain of agonists and conformational changes in the Cys loop that subsequently induce channel opening via M2-M3 interactions. The connection between loop E and the Cys loop on one hand as well as the Cys loop and loop B on the other hand may form the basis of a functional link between adjacent binding sites (Figure 6.1). Such a link may be important in mediating co-operativity between adjacent binding sites; i.e. occupancy of one binding site with agonist may lead to conformational changes in the adjacent binding site. Such a change in turn may lead to co-operative channel opening.

Data from the loop B studies suggests that this region plays a critical role in initiating the conformational changes that lead to channel opening (see Figure 2). These

data suggest that amino acids T179, F180, L184, H185, I187 and D189 play a role in mediating receptor gating. We have utilized molecular models of the 5-HT<sub>3A</sub>R in both ground and activate state to predict interactions that may be mediating conformational changes associated with gating. The results from molecular modeling suggest that loop B region forms a 'point of reference' around which a multitude of changes takes place. Our data suggests that agonist binding leads to formation of hydrogen bonds between loop B region and other regions of the same subunit, including loop A loop C, pre-loop D and pre-M1 regions. Agonist binding at the binding cleft between two subunits also leads to formation of hydrogen bonds between loop B on the principal face and loop E on the complimentary face. These changes have been detailed in chapter 6 (see Table 6.4) and are summarized in Figure 6.2 (reproduced from chapter 6). A central role played by loop B is not surprising since the major interaction at the ligand-binding domain is mediated through W183, which is located almost at the center of the loop B region. It has been suggested that the interaction of agonist with W183 probably triggers the conformational wave that eventually results in opening of the channel gate. In case of other members of ligand-gated ion channel superfamily, it has been previously suggested that a "conformational wave" accompanying channel opening travels from the ligand binding domain to the channel (M2) region. In the 5-HT<sub>3A</sub>R, amino acid residue R222 in the pre-M1 region is critical in maintaining the stability of the closed state of the receptor. This observation suggests that the 'conformational wave' could also travel down to the M2 region through the pre-M1 region. Our data suggests that the initiation of the signal in the ligand-binding domain may travel down to the pre-M1 region through formation of F180-



M237 interaction. Another route for the conformational wave may be through the Cys loop-M2 connection. The conformational wave could also down the Cys loop region through its direct connection with loops B and E. Data presented here regarding amino acids Y143, Y153 and W183 supports this assertion. Thus, our data suggests that the conformational wave that triggers the channel opening travels from the ligand-binding domain to the M2 region through both the Cys loop and the pre-M1 region.

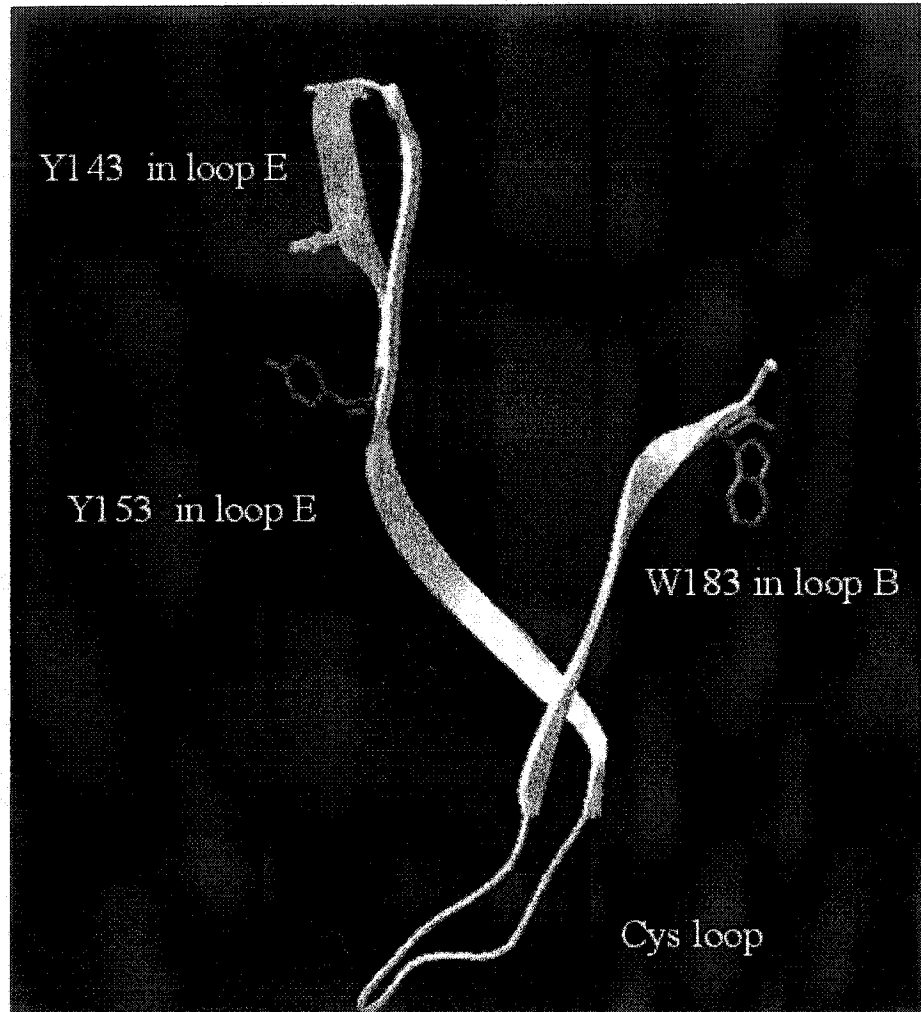


**Figure 6.1: Loop B-Cys loop-loop E connection**

The backbone structure connecting loops E and B through the Cys loop is displayed in white. This connection may be playing a role in signal transduction leading to channel opening.

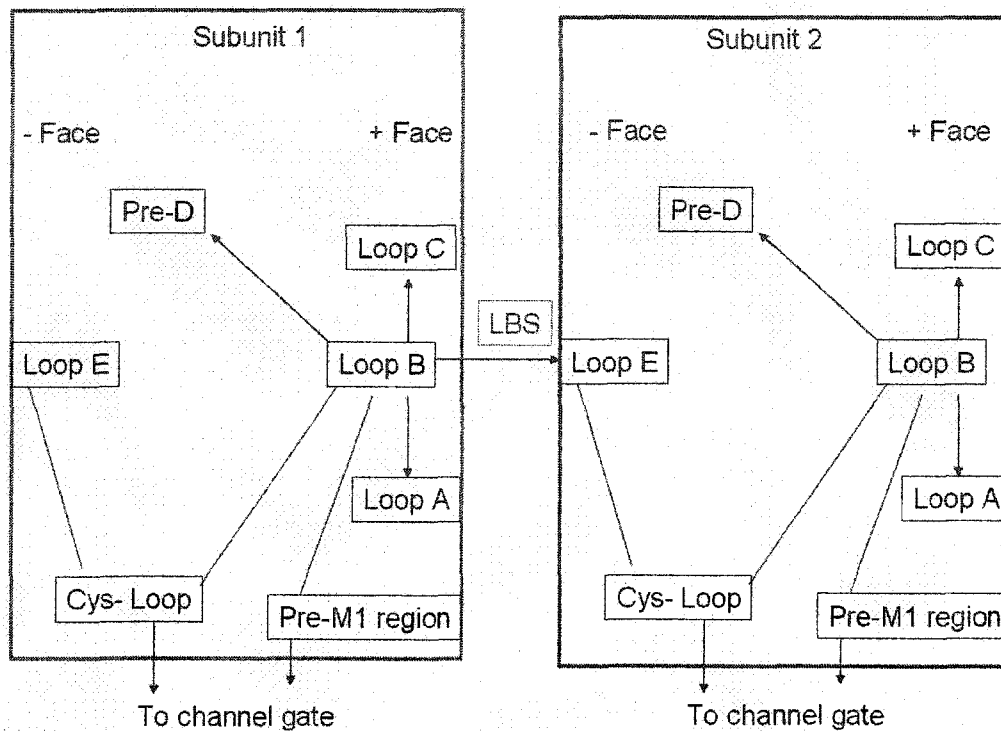


**Figure 6.2: Interactions formed during activation of the homomeric 5-HT<sub>3</sub>AR.**

These interactions are supported by both biochemical as well as molecular modeling data.

## **Appendix 1: Mechanistic models of the 5-HT<sub>3</sub> receptor function**

Multi-subunit proteins with more than one binding sites require involvement of more than one subunit in their functioning. The site of action that causes biological activity (such as channel opening) is located far from the binding site. Such proteins are called allosteric proteins. Allosteric proteins are multimeric proteins that demonstrate symmetry. In case of nicotinic-acetylcholine receptor, the pentameric structure demonstrates pseudo-symmetry, which is also the case with 5-HT<sub>3</sub>R. For allosteric proteins, two major theories of receptor function have been proposed.

1. Concerted model of receptor action and
2. Sequential model of receptor action.

### **A1.1 Concerted model of receptor action**

Nicotinic acetylcholine receptor binds two agonist molecules before it opens. Involvement of at least two binding sites is thus required for the opening to occur. Thus a mechanistic model that applies to multiple binding sites was developed based on a similar scheme proposed for enzyme action. This model, which is called the concerted model of the receptor function was originally proposed by Monod-Wyman-Changeux, and was adapted to describe receptor mechanisms by Karlin (Karlin, 1967), Jackson (Jackson, 1994) and Colquhoun (Colquhoun and Hawkes, 1977). This model can also be applied to the 5-HT<sub>3</sub>R. The concerted model makes following assumptions.

- A) The model assumes presence of only three distinct states for the 5-HT<sub>3</sub>R; namely open, closed and desensitized. No intermediate states are assumed.
- B) In the absence of agonist at equilibrium, the receptor can exist all three states, although the closed state is preferred as it is energetically most favored. Such an equilibrium can be shifted by addition of agonists
- C) Agonists preferentially bind with higher affinity to the active or the desensitized state of the receptor.
- D) Addition of agonist shifts the equilibrium towards the active state/desensitized state depending on the equilibrium constants of the reaction.
- E) Symmetry in the protein molecule is maintained at all conformations.

The receptor exists in an equilibrium condition in resting conditions with no contact with agonist molecules. In such conditions, the energy barriers that oppose transformation into the open state cannot be easily overcome, and the protein can only rarely venture into the open state. 5-HT<sub>3</sub>R protein is designed to carry out multiple functions. The multimeric protein with a total of 2400 amino acids (480 X 5) held together of thousands of chemical bonds. These bonds are in constantly being stretched, rotated, broken and newly formed on a picoseconds time-scale. The collective energy change that leads to a lower and more stable energy state as a result of these changes results in passage of the protein from one conformation to another. Each conformation may not be greatly different than the previous one or the one following. A protein may thus pass through literally hundreds of conformations with very small amounts of change in energy, and it is sometimes difficult to experimentally detect such conformations. Certain conformations are however

associated with major changes in the energy landscape and associated alteration in physical state. Such confirmations are also associated with distinct states of functional importance, and can be usually detected. In case of ligand-gated ion channels, the opening of the ion channel is greatly facilitated by presence of agonist molecules. The binding of agonist molecule(s) probably helps overcome the energy barrier propelling the channel into open and subsequent confirmations.

Certain observations about nicotinic acetylcholine receptor are in tandem with the concerted model. At single channel level a clear open and closed state of the receptor with unitary conductance is observed. Although no experimental evidence exists that indicates that 5-HT<sub>3</sub>R opens in absence of agonist, studies of nicotinic acetylcholine receptor indicate such to be the case. Opening of the nicotinic acetylcholine receptor in absence of agonist can again be observed using single-channel recording, although the frequency of such openings is very low (1 in 10<sup>7</sup> receptors open/ sec) (Jackson, 1994). In case of the 5-HT<sub>3</sub>R, spontaneous opening of mutant receptors has been observed (Zhang et al., 2002). The mutation in such a case presumably lowers the energy of 'activation', allowing spontaneous openings.

Also, both in the case of nicotinic and 5-HT<sub>3</sub>R, there exists a (pseudo) symmetry around the central axis. Taken together, these observations suggest that concerted model of receptor action may be suitable for the ligand-gated ion channels in general and 5-HT<sub>3</sub>R in particular.

Methods used for analysis of the electrophysiological and radio-ligand binding data (obtained from studies described here) are based on mathematical expressions of

concerted model. Various parameters of the drug-ligand interactions for a protein with multiple binding sites can be derived from Hill equation. This equation can be used to calculate both receptor saturation as well as maximal response with agonist.

$$B = (B_{\max} [L]^n) / ([L]^n + K_n)$$

Where,  $B$  is the occupancy at ligand concentration  $L$ ,  $B_{\max}$  is the maximum receptor occupancy,  $L$  is the ligand concentration.  $K$  is the dissociation constant or the apparent affinity,  $n$  indicates the Hill coefficient. Hill coefficient puts a lower limit on the number of binding steps. Thus  $n$  value of 2.1 indicated that there are at least two agonist molecules bound, but the actual number could be higher.

Three models, all based on the concerted mechanism of receptor action, have been published to date.

#### **A1.2 A concerted model of 5-HT<sub>3</sub>R function**

Mott et al. used data obtained from kinetic experiments to generate a kinetic model of *murine* 5-HT<sub>3A</sub>R function. The kinetic model suggested is based on cyclic model of receptor function originally proposed by Katz and Thesleff (Katz and Thesleff, 1957). This model is shown in figure above.

This model predicts 3 different open states, and three different desensitized states. The model also predicts that the ion channel opens when there are at least three agonist molecules occupying the 3 out of 5 5-HT<sub>3A</sub>R binding sites. The probability of being in open state increases when 4 agonists are bound. With binding of 5 agonist molecules, the probability of being in the desensitized state increases, which in turn results in reduced probability of opening.

### **A1.2.1 Alternate model of 5-HT<sub>3</sub>R function-1**

Zhou et al. proposed a sequential kinetic model, which was built using a kinetic model for the nicotinic acetylcholine receptor (Zhou et al., 1998). The model assumes that two agonist molecules needed to open the channel.

This model was proposed in an attempt to explain the potentiation of 5-HT<sub>3</sub>R currents by trichloroethanol (TCEt) at low concentrations and channel blockade at higher concentrations. The model suggests that TCEt, at lower concentrations, potentiates 5-HT induced currents by altering the stability of the open state. This stabilization of the open state is achieved both by decreasing dissociation and desensitization rates and increasing activation rates. The kinetic model suggested by authors successfully simulated experimental data from studies using 1  $\mu$ M 5-HT and TCEt, and represents a simple model for receptor action. However, it is not known whether such a model can successfully simulate receptor behavior at all concentrations of 5-HT, especially supra-maximal concentrations. Such models on the other hand provide a starting point for development of more complex models of receptor action.

### **A1.2.3 Alternate model of 5-HT<sub>3</sub>R function-2**

Based on Hill number obtained from dose-response curves, Hapfelmeier et al. and others have predicted that 2 (Hapfelmeier et al., 2003) and not 3 molecules of agonist are required to open the channel. When a specially designed solution exchange system is used to record 5-H or *m*CPBG induced responses from 5-HT<sub>3A</sub>R, rapid removal of agonist induces tail currents. These tail currents probably result from removal of 5-HT



molecules causing channel blockade. Thus, 5-HT induced channel blockade may be at least partially responsible for 5-HT<sub>3A</sub>R desensitization. Hapfelmeier et al. have proposed sequential kinetic model for 5-HT<sub>3A</sub> receptor based on their findings. The authors predict that the biphasic desensitization waveform is a result of channel block resulting from binding of 5-HT to a combination of high or low affinity binding sites in the channel region producing high and low affinity block. According to this model, 3<sup>rd</sup> agonist molecule actually induces desensitization by binding to either high or low channel blocking site.

The authors report experimental findings suggestive of multiple desensitization states, while their reported kinetic model supports single final desensitization state for both 5-HT<sub>3A</sub> and 5-HT<sub>3AB</sub> receptors.

On the other hand, currents induced from 5-HT<sub>3AB</sub> receptors using 5-HT do not show tail currents, based on which it was suggested that 5-HT<sub>3AB</sub> receptor follows a more standard model of receptor function. The kinetic model suggested is based on cyclic model of receptor function originally proposed by Katz and Thesleff (Katz and Thesleff, 1957).

Interestingly, *m*CPBG was able to induce tail currents even in 5-HT<sub>3AB</sub> receptors, suggesting a complex mechanism of desensitization for these heteromeric receptors. Co-expression of B subunit also confers biophysical parameters to the heteromers, which are not observed with homomers. The deactivation rate of the 5-HT induced currents becomes significantly faster than the desensitization rate. This feature is also evident in recordings from neural cells natively expressing 5-HT<sub>3R</sub>, suggesting that most of 5-HT<sub>3R</sub> is expressed in neural tissues as a heteromer and not homomer.

While the models proposed by Hapfelmeier et al. for 5-HT and *m*CPBG action on 5-HT<sub>3A</sub> and 5-HT<sub>3AB</sub> receptors are simplistic, the suggestion that 5-HT and *m*CPBG induce desensitization in 5-HT<sub>3AB</sub> receptor through different mechanisms is intriguing. *m*CPBG is also unusual in demonstrating high apparent affinity ( $EC_{50}$ ) for the receptor, and still have almost 8% lower efficacy compared to 5-HT. *m*CPBG also shows delayed recovery from desensitization, which probably accounts for the lower efficacy. Other studies have proposed that structurally diverse agonists induce distinct desensitization states and recognize distinct conformations of receptors recovering from desensitization. These data are in agreement with the suggestion that 5-HT and *m*CPBG follow different paths in and out of desensitization for the heteromeric 5-HT<sub>3AB</sub> receptor.

### **A1.3 Sequential model of receptor action**

The sequential model assumes that

- 1) Intermediate states between closed and open are possible.
- 2) The successive binding of agonist molecules drives the conformational change.
- 3) Cooperatively emanates from sequential conformational changes in subunits. Conformational change in one subunit affects its subunit contact with neighbouring subunit and changes binding characteristics of the neighboring subunit.
- 4) Symmetry in the protein molecule is not necessarily maintained. The protein goes through sequential changes in confirmation as a result of gradual changes in quaternary structure.

Although a sequential model of the receptor function appears simple, in terms of kinetic measurements, it presents with several complexities. These complexities arise from the assumption of multiple intermediate states between several functionally recognizable conformations of the protein; i.e., closed open and desensitized. In case of membrane bound receptors (as opposed to soluble enzymes), it is exceedingly difficult to experimentally detect the assumed intermediate conformations and their associated kinetic rates.

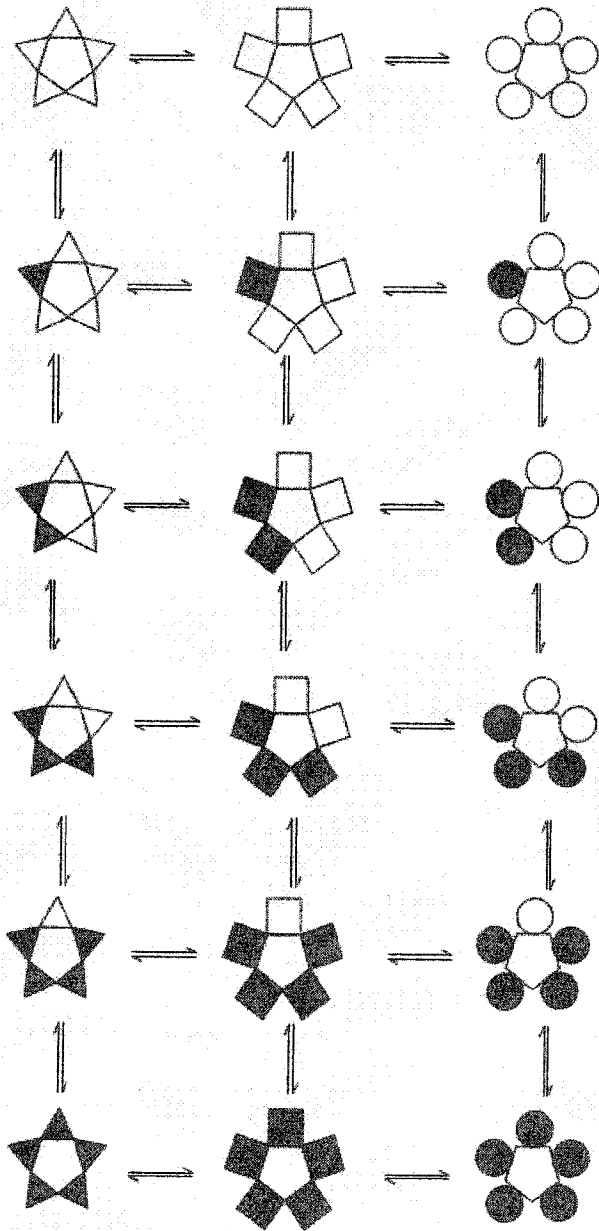
Membrane bound receptors cannot be easily crystallized. For the same reason, various conformations of these receptors cannot be easily 'trapped'. The intermediate conformational changes assumed by the sequential model possibly occur at a very fast rate, further complicating any possible measurement of kinetic rates. For these reasons, sequential models of receptor action can be less easily validated compared to concerted models of receptor behavior.

There are no published sequential models of 5-HT<sub>3</sub>R function.

**References**

- Colquhoun D and Hawkes AG (1977) Relaxation and fluctuations of membrane currents that flow through drug-operated channels. *Proc R Soc Lond B Biol Sci* **199**(1135):231-262.
- Hapfelmeier G, Tredt C, Haseneder R, Zieglgansberger W, Eisensamer B, Rupprecht R and Rammes G (2003) Co-expression of the 5-HT<sub>3B</sub> serotonin receptor subunit alters the biophysics of the 5-HT<sub>3</sub> receptor. *Biophys J* **84**(3):1720-1733.
- Jackson MB (1994) Single channel currents in the nicotinic acetylcholine receptor: a direct demonstration of allosteric transitions. *Trends Biochem Sci* **19**(10):396-399.
- Karlin A (1967) On the application of "a plausible model" of allosteric proteins to the receptor for acetylcholine. *J Theor Biol* **16**(2):306-320.
- Katz B and Thesleff S (1957) A study of the desensitization produced by acetylcholine at the motor end-plate. *J Physiol* **138**(1):63-80.
- Zhang L, Hosoi M, Fukuzawa M, Sun H, Rawlings RR and Weight FF (2002) Distinct molecular basis for differential sensitivity of the serotonin type <sub>3A</sub> receptor to ethanol in the absence and presence of agonist. *J Biol Chem* **277**(48):46256-46264.
- Zhou Q, Verdoorn TA and Lovinger DM (1998) Alcohols potentiate the function of 5-HT<sub>3</sub> receptor-channels on NCB-20 neuroblastoma cells by favouring and stabilizing the open channel state. *J Physiol* **507** (Pt 2):335-352.

A.



B.



**Figure A1.1: Mechanistic models of 5-HT<sub>3</sub>R function****A1.1.A A Concerted model for cooperative behavior of pentameric 5-HT<sub>3</sub>R**

Five subunits of the 5-HT<sub>3A</sub>R are depicted in a pseudo-symmetric arrangement. Various reversible transitions between states are indicated by double arrows. Squares indicate basal closed state. Triangles indicate desensitized state, while circles indicate open state. Color indicates presence of ligand, while lack of color indicates absence thereof. According to this model, all five subunits can exist either in closed, open or desensitized state.

**A1.2.B Sequential model for cooperative behavior of pentameric 5-HT<sub>3</sub>R**

Five subunits of the 5-HT<sub>3A</sub>R are depicted in a pseudo-symmetric arrangement. Various reversible transitions between states are indicated by double arrows. Squares indicate basal closed state. Triangles indicate desensitized state, while circles indicate open state. Color indicates presence of ligand, while lack of color indicates absence thereof. According to this model, five sequentially pass from closed to the open and from open to the desensitized state

## Appendix 2: A vertical flow chamber for *Xenopus* oocyte electrophysiology and automated drug screening<sup>5</sup>

### A2.1 Abstract

*Xenopus laevis* oocytes are used extensively in the study of ion channel coupled receptors. Efficient use of oocytes for ion channel characterization requires a system that is inherently stable, reproducible, minimizes drug volumes, and maximizes of oocyte longevity. We have constructed a vertical flow oocyte recording chamber to address the aforesaid issues, where the oocyte is placed in a funnel-shaped chamber and perfused from the bottom of the funnel. The vertical rather than horizontal flow of perfusate results in an unusually stable environment for oocyte recording. Two-electrode voltage-clamp recordings from a single oocyte are acquired easily and routinely over several hours while maintaining stable baseline currents and reproducible response profiles. Chamber characteristics were tested using a serotonin ligand-gated ion channel receptor (5-HT<sub>3</sub>R). Data obtained from this system corresponds well with published data. To further test the stability and reliability of this perfusion chamber, we constructed an automated oocyte perfusion system utilizing a commonly available HPLC autosampler. We were able to obtain dose response curves for various 5-HT<sub>3A</sub> R ligands using the automated perfusion system with minimal user intervention. Such a system can easily satisfy need for

---

<sup>5</sup> Published in the *Journal of Neuroscience Methods*. (Citation: Joshi PR, Suryanarayanan A and Schulte MK (2004) A vertical flow chamber for *Xenopus* oocyte electrophysiology and automated drug screening. *J Neurosci Methods* 132(1):69-79.)

automated oocyte electrophysiology in academic settings, especially small to medium sized laboratories.



## A2.2 Introduction

The *Xenopus laevis* oocyte, a heterologous expression system, has been successfully used to study various biological systems and ion channels including ligand-gated ion channels such as the nicotinic acetylcholine and serotonin type three receptors (5-HT<sub>3</sub>R) (Bertrand et al, 1997; Maricq et al 1991). The functional aspects of these receptors can be studied electrophysiologically using two-electrode voltage-clamp. In this technique, oocytes are injected with cRNA (cytoplasmic) or cDNA (nuclear) coding for the ion channel receptor under study. After incubation at 19°C to 21°C for an appropriate length of time (usually 24-48 hours), an oocyte expressing ion channel receptors is placed in a perfusion chamber and voltage-clamped. Rapid exposure of such an oocyte to an agonist results in inward currents with characteristic shapes and distinct desensitization characteristics.

In the conventional perfusion method, an oocyte is placed in a circular or elongated depression, with perfusion inlet from one end and drainage from the other end. Depending on specific requirements, the chamber volume can vary from small (~50-250 µl) to large (~1ml). Most of the conventional perfusion chambers involve a solution flow across the oocyte and the electrodes (fig.A2.1D). Such a flow results in a constant application of force to the oocyte at a direction that is perpendicular to its points of anchorage (base and the recording electrodes). Minute vibrations of the electrodes impaled in the oocyte may damage the oocyte membrane and increase the leak of electrode filling solution (usually 3M KCL). These effects may not be obvious in short term studies although may contribute towards oocyte mortality on a long-term basis.

Additionally, many of the standard oocyte chambers, oocyte may not be exposed to the drug rapidly from all the sides, thus limiting rise times.

Oocyte electrophysiology is commonly employed in high throughput drug screening assays. These assay systems must meet certain requirements in order to produce reliable and reproducible data. Simplicity and rapidity of operation are important considerations, in addition to low drug volumes, rapid drug exchange rates, and stability. Among the various factors, stability appears to be of paramount importance to the successful execution of automation. An increase in the longevity of the oocyte will result in a highly productive system; where as reduced longevity will necessitate constant monitoring and intervention.

We describe a novel oocyte perfusion chamber where the oocyte is placed in a small volume funnel-shaped chamber on top of a wire mesh and perfused from an inlet at the bottom of the funnel. We have utilized ligand-gated ion channel coupled receptors, the 5-HT<sub>3A</sub> and 5-HT<sub>3AB</sub> receptors (Maricq et al 1991; Davies et al 1999), to demonstrate various features of the funnel shaped chamber. A vertical flow as opposed to a sideways flow is expected to provide a stable environment to the oocyte. We show that an oocyte is stable for an extended period in the vertical flow chamber. The stability and reliability of the perfusion chamber have allowed us to construct an automated oocyte perfusion system utilizing a commonly available HPLC autosampler. We were able to obtain dose response curves for various 5-HT<sub>3A</sub> R ligands using the automated perfusion system with minimal user intervention.

## **A2.3 Materials and Methods**

### **A2.3.1 Materials:**

Sigma type II collagenase was purchased from Sigma-Aldrich (MO, US). mMESSAGE mMACHINE™ High Yield Capped RNA Transcription Kit was purchased from Ambion (TX, US). The OC-725C oocyte clamp and 7.5-150GT glass electrodes were purchased from Warner Instruments (CT, US). Datapac 2000 data acquisition software was purchased from RUN technologies (CA, US). *Xenopus laevis* frogs and frog food were purchased from Xenopus Express (FL, US). All other chemicals were obtained from Fisher Scientific (TX, US).

### **A2.3.2 Methods**

#### **A2.3.2.1 Chamber construction**

Figure A2.1 provides with line diagrams of the chamber; a photograph is shown in figure A2.2A. We constructed the chamber apparatus using blocks of clear acrylic material. It consists of three parts: 1) A funnel shaped perfusion chamber 2) Chamber holding apparatus and 3) Fluid inlet and drainage system (Figure A2.1). The scheme shown in figure A2.1 refers to the manual operation of the system.

##### **1) Funnel shaped perfusion chamber**

The funnel shaped perfusion chamber (Figure A2.1C, Fc in Figure A2.1B) is a *separable* part of the perfusion system. Externally, it is cylindrical in shape with a funnel shaped interior at an angle of 30 degrees. The cylinder is 19 mm in diameter and 10 mm in height, with a 7 mm diameter circular inlet at the bottom, through which the fluid enters.

The uppermost edge is the broadest part of the funnel with a diameter of 17 mm. Six drainage tubes are present in the funnel wall (Ex in Figure A2.1B). These tubes are arranged equidistant, tangentially to the perimeter of the funnel at a height of 2.1 mm from the top of the chamber. Each tube is 1 mm in diameter providing outlet for the perfusate. On the right side, an oblique tunnel (T) extends from the outer wall 1.5 mm from the upper rim, to a level 3 mm above the lower rim at the inner wall (Figure A2.1C). This oblique tunnel allows placement of an agar bridge that in turn is placed in a well containing the sense reference electrode (R2) in 3 M KCl. Another well contains a second reference electrode (R1). The perfusion chamber holds a volume of 250  $\mu$ l.

## 2) The chamber holding apparatus

The chamber holding apparatus consists of three concentric wells designated as 'A', 'B' and 'C' in Figure A2.1B. The outermost well 'A' is largest with a diameter of 30 mm and a depth of 4.5 mm and functions as the overflow drainage well. The volume in this well is maintained at  $\sim$ 200  $\mu$ l. The middle well 'B' functions as the perfusion chamber holder with a diameter 0.01 mm greater than the diameter of the perfusion chamber and a depth of 4.2 mm. A no. 40, 250 micron stainless mesh ( Small Parts Inc., Miami Lakes, FL) (M in Figure A2.1) is placed at the bottom of well 'B' and the perfusion chamber is pressed in place on top of the mesh. The innermost well 'C' is 8 mm in diameter and 2.1 mm in depth with an inlet connected from the bottom. The main inlet tube 'D' is 3.2 mm in diameter and runs down from well C for 4 mm before making a right angle turn and running parallel to the bottom of the chamber where it assumes a diameter of 1.3 mm.

The two inlet tubes 'E' and 'F' (1.3 mm diameter) run from the top of the chamber and join tube 'D' at right angles. 'E' acts as drug inlet while 'F' acts as buffer inlet.

### 3) Fluid inlet and drainage system

All of the tubing used in the perfusion system is clear polyethylene PE 50 tubing. Since some drugs stick to the polyethylene tubing, a non-stick Teflon material can also be used. Drug inlet 'E' is connected via a 15 cm T tube to an 18-gauge syringe needle, which in turn can be connected to varying sizes of syringes to carry out drug perfusions. Drug perfusions are accomplished by using a perfusion pump. Buffer inlet 'F' is connected to the buffer reservoir and the flow adjusted to a rate of 20 ml /min. A flow rate of ~ 20 ml/min is faster than commonly reported (6-10 ml/min). However, other authors (e.g. Vijverberg et al, 1997) have previously reported such rates. The oocyte is exposed to the drug dissolved in ND96 recording buffer [96 mM NaCl / 2 mM KCl / 1.8 mM CaCl<sub>2</sub> / 1 mM MgCl<sub>2</sub> / 5 mM HEPES, titrated with NaOH to pH 7.4] at the rate of 25 ml/min; this flow rate is used only during sample injection. The buffer flow need not be stopped during the sample injection. The drainage tube ('P' in Figure A2.1), placed in the holder, is positioned on the outermost well 'A' at a height 1mm below the level of exit tubes. Drainage is achieved with help of vacuum suction. All the described features can be identified in the photograph (figure A2.2A).

### 4) Automated perfusion system

The automated oocyte perfusion system utilizes a Gilson 231XL auto sampling HPLC injector coupled with a keypad controller and a Gilson 401 dilutor. In order to minimize drug requirements the volume of the conical chamber was reduced to an effective

chamber volume of 200  $\mu\text{l}$ . Figure A2.3 shows the schematic arrangement of elements comprising the automated oocyte perfusion system. The autosampler injection valve (V) controls the traffic of fluids to the oocyte chamber (C). A 5ml syringe (S) mounted on the 401 dilutor draws ND96 from either a reservoir (R1) or the drug sample tube in the sample rack (SR). The injection port (IP) is connected to an injection loop (IL), which holds 2000  $\mu\text{l}$  of fluid. The other end of the injection loop is attached to port 4 of the injection valve (V). Reservoir 2 (R2) is the default supplier of the ND96 buffer to the oocyte chamber, and is connected to port 2 of the injection valve. In the load position, the buffer from reservoir 1 flows through the valve then out port 3 to the chamber. The load position of the valve thus provides for a continuous flow of buffer to the chamber and is the default valve position. The contents of the injection loop are directed through port 5 to the drain when the valve is in the load position. After withdrawing the sample from the tube in the sample rack, 2000  $\mu\text{l}$  of the sample is injected through the injection loop. The valve is then switched to inject and 1000  $\mu\text{l}$  of the buffer in reservoir 1 (R1) is injected through the injection loop. In the inject position, the contents of the sample loop are injected through port 3 to the chamber and the buffer flow from R2 is stopped; thus directing the sample to the chamber. The flow rate during sample injection is set to 20 ml/min. After the 1000  $\mu\text{l}$  sample is injected into the chamber, the flow is stopped for a predetermined exposure time. Directly following drug exposure, the valve is switched back to load position and the buffer begins to flow to the chamber to wash out the sample. After washing the injection port and needle, the autosampler then draws up the next sample and the process repeats.

### **A2.3.2.2 Harvesting and maintenance of *Xenopus laevis* oocytes**

*Xenopus laevis* ovarian lobes were surgically removed using sterile techniques. Ovarian lobes were washed twice in Ca<sup>+2</sup> free Barth's buffer [82.5 mM NaCl / 2.5 mM KCl / 1 mM MgCl<sub>2</sub> / 5 mM HEPES, pH 7.4] under sterile conditions and gently shaken with 1.5 mg/ml collagenase (Sigma type II, Sigma-Aldrich) for 1 hour at 20-25 °C. Stage IV and V oocytes were selected and prepared for microinjection. Selected oocytes were maintained at 10°C in Ca<sup>+2</sup> free Barth's medium.

cRNA synthesis and microinjection: Synthetic cRNAs for the mouse/ 5-HT<sub>3A</sub> and human 5-HT<sub>3A</sub> / 5-HT<sub>3AB</sub> receptors were prepared (mMESSAGE mMACHINE™ High Yield Capped RNA Transcription Kit). Approximately 50 nl cRNA solution injected into oocytes at a concentration of 0.2 mg/ml. Oocytes were incubated at 19°C for 24 to 48 hrs. At the end of the incubation period, healthy oocytes were selected for electrophysiological recording.

### **A2.3.2.3 Electrophysiological recordings**

Data were acquired using an OC-725C oocyte clamp amplifier (Warner Instruments) coupled to online, computerized data acquisition system (Datapac 2000, RUN technologies). Data collection rates of 20 msec were used for all the recordings. The recording setup was prepared as follows. An agar bridge was placed in well 'A' connecting it to the well containing a reference electrode (R1 in figure A2.1) in 3M KCl. A second agar bridge was placed in the wall of the perfusion chamber (T in Figure A2.1) connecting the interior of the perfusion chamber to the 'sense' reference electrode in 3M KCl (R2 in Figure A2.1). An even flow of ND96, the recording buffer, was established.

An oocyte was placed in the center of the perfusion chamber on the stainless mesh after stopping the buffer flow. Two Glass(7.5-150GT, Warner instruments, CT, US) electrodes('current' and 'voltage') with resistance of 1-2 M $\Omega$  were filled with 3M KCl and lowered until they converged on the oocyte placed on the mesh. The oocyte was thus held in place with three points of contact; two electrodes at the 10 and 2 o'clock positions and the mesh at the 6 o'clock position. The oocyte was voltage-clamped only if the resting membrane potential was  $-15$  mV and above. The holding potential was  $-60$  mV for all experiments unless stated otherwise.

The voltage-clamped oocyte was perfused with ND96 buffer solution at a constant rate of 20 ml/min by gravity feed through inlet 'F' and tube Ft. All the recordings involved switching from buffer perfusion to drug perfusion

The manual operation of the recording system is described first. Drugs (5-HT and *m*CPBG) constituted in ND96 buffer were applied through inlet 'E' connected to a syringe containing drug through tubing Et, using a motor driven pump (Harvard Apparatus) at a flow rate of 25 ml/min. Each drug application was followed by a buffer wash for 3 minutes. The duration of the drug application was four to five seconds at which time the perfusion was stopped ( $\sim 1.6$  ml drug per exposure) and the drug retained in the chamber until the desired washout time. No difference in the characteristics of 5-HT elicited currents was observed when longer drug exposures were performed. The drug was washed out of the chamber at the end of 108 seconds and the buffer flow continued for three additional minutes. At the end of each drug perfusion and after initiation of wash buffer, tubing Et is disconnected from the syringe containing the drug and lowered



into a receptacle at a level lower than that of the chamber. This allows the running wash-buffer to purge tube Et resulting in complete clearance of the drug from the drug inlet tube Et.

To compare data generated from conventional side-flow chamber with that generated from the vertical-flow chamber, following protocol was followed. First, a conventional side-flow oocyte perfusion chamber (RC-1Z Oocyte Recording Chamber, Warner Instruments, Hamden, CT, approximate chamber volume 225  $\mu$ l, with minor differences) was employed to elicit inward currents from oocytes expressing mouse 5-HT<sub>3A</sub>R. The perfusion system was set up exactly as described for the vertical-flow system, including two separate in-flows for drug and buffer. The voltage-clamped oocyte was perfused with ND96 buffer solution at a constant rate of 20 ml/min by gravity feed through inlet 'F' and tube Ft. The clamped oocyte was exposed to 30  $\mu$ M 5-HT dissolved in the ND-96 buffer at a rate of 25 ml/min using the motor driven pump, and the inward currents were recorded. The procedure was repeated at least four times with the oocyte being used; at the end of which period the oocyte was removed from the side-flow chamber and stored for the future use. The side-flow chamber was then replaced with the vertical-flow chamber, while preserving the tubing, the recording electrodes, the agar bridges being used as well as rest of the recording setup. The agonist solution in use was also preserved. The entire operation of switching recording chambers was completed within 15 minutes. The oocyte used earlier was then placed in the vertical-flow chamber and was exposed to the agonist (30  $\mu$ M 5-HT). The wash buffer as well as the agonist was perfused at rates 20 and 25 ml/min respectively. The whole experiment was repeated

3 times, using three different oocytes. Figure A2.2C shows representative results obtained from these experiments.

To obtain IV curves, voltage was stepped up +10 mV at a time before agonist application, starting from -80 mV up to +30 mV. All the currents were normalized to the value obtained at -80 mV. Data represents a combination of three data sets obtained from three different oocytes.

A program written for the sampler keypad controller achieves automated perfusion. The sequence of events leading to a single drug exposure is as follows. Buffer from reservoir two (R2) is continuously flowing through the chamber (C) at a constant rate of 20 ml /min. When the sequence is initialized, the 5ml syringe (S) first draws 300  $\mu$ l of buffer from reservoir 1. This buffer is then used to rinse the inside and outside of the injection needle (N). The syringe then draws 4500  $\mu$ l of buffer and injects it into the injection port (IP) and the injection loop (IL) which drains out of the drain tube, thus rinsing the injection port and the injection loop. Drug sample (1 ml), stored in a 1.7 ml eppendorf tube is then collected by the syringe and injected into the injection loop. The next step involves loading of 1000  $\mu$ l of buffer in the syringe from reservoir 1 and initiation of recording trace in the data acquisition software (DataPac 2000), through an external pulse generated by the autosampler. This step is accompanied by a change in the default valve position, which shuts off the buffer flow from reservoir 2 and directs the contents of the injection loop to the chamber. The injection of 1000  $\mu$ l of buffer into the injection loop injects 1000  $\mu$ l of the drug sample into the chamber. This step is followed by a waiting period of 36 seconds, which ensures appropriate exposure of the oocyte to

the drug. At the end of the waiting period, the valve shifts to its default position, reinitializing buffer flow from reservoir 2. Another waiting period of 1.5 minutes then commences before the cycle is repeated. The sampler has been programmed to collect samples from sequentially arranged eppendorf tubes in the sample rack.

## A2.4 Results

We utilized oocytes expressing 5-HT<sub>3A</sub> receptors to assess the functionality of the newly designed chamber. The characteristics of 5-HT<sub>3A</sub> mediated inward currents recorded from microinjected oocytes are well established. (Davies et al, 1999; Dubin et al 1999; Yakel et al, 1996). Application of 5-HT to oocytes expressing 5-HT<sub>3AB</sub> receptors resulted in characteristic inward currents. Figure A2.4A shows representative responses obtained from application of 0.3, 3, 10 and 30  $\mu$ M 5-HT to such an oocyte. The inward currents show all critical parameters of 5-HT<sub>3AB</sub> receptor-mediated currents. The onset of response corresponds with onset of drug application. The onset of inward current is rapid (10 to 90% of peak current within  $\sim$ 400 msec), with a sharp 'peak'. Drug exposure is terminated in five seconds, when the response is in the slow phase of desensitization. The chamber then functions as a static chamber. To rule out occurrence of artifacts due to shorter perfusions, we performed longer perfusions of 5-HT (from 24 to 36 seconds, data not shown). Recordings obtained with varying perfusion times were essentially identical. The slow phase of desensitization is evident even in the continued presence of agonist. Wash buffer is started at 108 seconds when the trace has almost returned to the baseline during the non-desensitizing phase. Figure A2.4B shows the dose-response curve of 5-HT for the 5-HT<sub>3</sub> AB receptor, with an EC<sub>50</sub> value of  $7.6 \pm 0.46$   $\mu$ M. These results agree well with previously published data (Davies et al, 1999).

To compare the functionality of the vertical-flow chamber with the side-flow chamber, we compared data obtained from the two systems using a single oocyte expressing mouse 5-HT<sub>3A</sub> R. We used a small volume conventional side-flow chamber,

which was identical to the vertical-flow chamber in all the other aspects. However, dramatic differences were observed in the data obtained from the two chambers, an example of which is shown in figure A2.2C. The traces marked as (a) were obtained from the vertical flow chamber while those marked with (b) were obtained with the conventional side-flow chamber. The average rise time obtained using the side-flow chamber was 850 ms, while an average rise time of 400 ms was obtained using the vertical-flow. The response amplitudes also differed proportionately, with almost a double amount of current elicited when using the vertical-flow chamber. Differences were also observed in the characteristics of the desensitization. These results suggest that vertical flow results in better exposure of the oocyte to the drug solution, as compared to the side flow.

To further test the validity of the novel perfusion system, a current-voltage analysis was undertaken. Oocytes expressing 5-HT<sub>3A</sub> receptor were clamped at holding potentials ranging from -80 mV to +30 mV (increments of 10 mV) and currents induced by application of 30  $\mu$ M 5-HT were recorded for each holding potential. Currents were normalized to value obtained at -80 mV. The plot of normalized inward currents vs. holding potential is shown in Figure A2.4C (n=3). The current-voltage relationship is typical of an inwardly rectifying ion channel with a reversal potential near zero mV. These data agree well with reported values for the human 5-HT<sub>3A</sub> receptor ((Davies et al, 1999).

To demonstrate the considerable stability achieved in oocyte perfusions, an oocyte expressing the mouse 5-HT<sub>3A</sub> receptor was maintained in a funnel shaped chamber

for 10 hours and perfused with a fixed concentration of 5-HT every 45 minutes by following the protocol described above (Figure A2.5). The traces shown in figure A2.5 are representative of two separate experiments. The oocyte was superfused with wash buffer at a constant rate of 2ml/min in intervals between two complete manual recording procedures. Over the 10-hour period, the baseline current (at approximately 0.4 pA) being injected into the oocyte showed no demonstrable change. Only minor changes in the maximum amplitude of the responses were observed. Gradual changes in the characteristics of the slow phase of desensitization were observed over the 10-hour period (see figure A2.5, traces D - O). The exact mechanism of these changes remains unknown. This decrease in desensitization rates is similar to the well-characterized "deceleration" phenomena commonly observed in whole-cell patch-clamp studies of 5-HT<sub>3</sub>Rs (Yakel et al, 1991). While these effects are not commonly observed in *Xenopus* oocytes, it is possible that the prolonged recording time in these experiments produces a similar alteration in desensitization. Changes in levels of intracellular calcium or changes in second messenger systems are among the myriad of potential causes of these effects (Davies et al, 1999).

Automated oocyte recording systems are receiving attention due to their potential use in high throughput drug screening. The automated perfusion system described here was set up using a commonly available Gilson HPLC autosampler and injector. Continuous traces of inward currents elicited from an oocyte expressing human 5-HT<sub>3A</sub> receptors by exposure to agonists 5-HT and *m*CPBG are shown in Figure A2.6A. Data obtained from the same traces was utilized for calculation of EC<sub>50</sub> values for both

agonists (Figure A2.6B). The characteristics of the responses as well as the  $EC_{50}$  values obtained (5-HT,  $3.4 \pm 0.39 \mu\text{M}$  and *m*CPBG,  $4.0 \pm 0.2 \mu\text{M}$ ) agree well with previously published results (Davies et al, 1999). The use of a 200  $\mu\text{l}$  chamber in these experiments resulted in faster response onrates (10 to 90% of peak current within  $\sim 250$  msec) when compared to the 450 ml chamber used in the manual perfusion system ( $\sim 400$  msec). As a result of the automation provided by this system, the recording procedure described above was completed in approximately 40 minutes without any user intervention.

### A2.5 Discussion

A reproduction of the established pharmacological profile for the 5-HT<sub>3</sub> receptor using the vertical flow apparatus validates our novel drug exposure method. Ligand affinities as well as other physiological characteristics (desensitization, voltage dependence) are in close agreement with previously reported values. The oocyte in a vertical flow chamber is suspended in the path of drug flow, achieving exposure to the complete oocyte surface area. This is akin to certain whole-cell patch-clamp techniques, where a mammalian cell is lifted up and then perfused to achieve maximum exposure. A similar chamber design was utilized for bath perfusion of brain slices (Koerner and Cotman, 1983). In a vertical flow system, drug solution flows over most of the oocyte surface before encountering the recording electrodes, thus minimizing turbulence. The decrease in turbulence even at high flow rates is apparently responsible for the high level of stability of this system. Multiple exit points at a fixed level above the oocyte hold the buffer level constant at all flow rates, avoiding cyclic rise and drop in solution levels. Lack of electrode movement as well as changes in the bath level at drug application, avoids agonist-application related artifacts, either at the onset of drug perfusion or at the onset of wash buffer. The solution exchange rates measured as a function of 5-HT induced response on-rates (~ 250- to 400 msec) were adequately rapid, although faster rates have been obtained (200 msec) with other chambers, using mouse 5-HT<sub>3A</sub>R (Yakel, J.L 1993). Fast flow rate of 25 ml/min was necessary to obtain fast exchange rates. The flow rate was not altered due to the presence of the stainless steel mesh. A stainless steel mesh provides a solid support to the oocyte and hence is preferred to a nylon mesh. The mesh also plays an important role in



redistributing the flow of the drug around the oocyte. Despite fast flow rates, drug requirement was limited to 1.6 ml/exposure (up to 1 ml in case of the smaller chamber), as a result of the static exposure system. Although we could obtain faster onrates and lower drug requirements by further reducing the chamber volume ( $> 200 \mu\text{l}$ ), it undermined the stability of the system.

Although data presented here consists mostly of relatively large currents, we have expressed and successfully characterized various mutant 5-HT<sub>3</sub>Rs that generate small currents using the described system. Although we cannot specifically comment about other receptors or transporters, the relatively rapid drug exchange rates as well as low dead volume may result in increased sensitivity for detecting smaller currents.

Experiments involving the comparison of the vertical with the side-flow chamber clearly show that vertical flow system offers a distinct advantage over the conventional systems. Such a comparison at times could be misleading, since a number of minor differences collectively could result in large differences in the data obtained. We exercised utmost precaution in making such a comparison. To avoid any bias, the general setup was carefully preserved while changing only the perfusion chambers during these experiments. Since vertical flow results in half the rise times and double the current amplitudes, a strong argument could be made for the much improved drug exposure, in case of the vertical-flow perfusion system.

The stability of the perfusion system was demonstrated by the ability to record electrophysiological traces from single oocyte for more than ten hours. Although we see changes in the desensitization characteristics over a period of 10 hours, these changes

only manifest prominently at the beginning of 4<sup>th</sup> hour of recording (trace marked "E" in Figure A2.5). In addition, the changes seen are very specific to the slower phase of desensitization, where as the base line current, the rise time as well as the fast phase of the desensitization remains largely unchanged. The slower phase of desensitization shows gradual changes (traces marked E to O in figure A2.5), where a progressive deceleration is observed over time. Moreover, these results could be reproduced in a second identical experiment. These changes could result from a variety of causes including effects introduced by the prolonged oocyte use. The specific nature of the changes however speaks against a generalized trauma to the oocyte as a cause. Any such trauma will result in increased baseline leak current, which did not change at all. To explain this phenomenon, an in-depth analysis of many possible causative factors needs to be undertaken.

The ability to a single oocyte over a period of ten and half hours represents regularly obtainable operational ability of the recording apparatus rather than specially designed and controlled conditions. We routinely record for a single oocyte over a period of 7-8 hours, with drug flow rates of 25 ml/min without any qualitative loss. The stability of the system actually permits recording from a single oocyte for as long as the operator wishes to use it. Similar studies may be employed that allow long-term measurement of receptor function, desensitization, modulation of receptor function by second messengers and receptor turnover. The design of the chamber also allows for placement of various probes (such as temperature, pH) very close to the oocyte without obstruction to the flow of buffer.

A simple experiment amply demonstrates stability offered by the vertical flow. The oocyte is placed at the centre of the mesh without the recording electrodes and perfused sequentially with wash buffer at 20ml/min and a dye at 25 ml/min. The oocyte retains its position on the mesh in the rapid buffer/dye flow even in absence of the recording electrodes. Serial images captured of such an experiment are shown in figure A2.2B. No such phenomenon was observed with a sideways buffer flow using a conventional chamber, where an oocyte cannot be retained in the recording chamber without being anchored by the recording electrodes. These experiments suggest that the vertical flow system provides a non-turbulent environment to the oocyte.

The automated system was primarily developed to assess the utility of the vertical flow chamber in automated settings. It should however be noted that any type of chamber can be adapted to the described automated perfusion system. The automated system described here uses a relatively inexpensive HPLC auto injector to provide a highly reproducible system requiring only small quantities of test compounds, low maintenance, and minimal human intervention. A number of automated oocyte recording systems have been recently introduced. OpusXpress™ (Axon Instruments, CA), offers many advanced features such as automated impalement, perfusion and data acquisition from up to eight *Xenopus* oocytes simultaneously. ALA Scientific offers Roboocyte™; a 96 well plate based automated system that allows both automated cRNA injections as well as recording. Automated system described here can only record from a single oocyte at a time and does not allow automatic impalement. Commercially available systems are primarily designed for industrial applications and are not easily available for academic

laboratories. While it lacks certain advanced features present in the commercially available systems, the HPLC pump based automated system offers a viable alternative, particularly for medium to small sized operations. HPLC based system is a relatively simple system requiring very little training. During the past two years, students at all levels of expertise were successful in obtaining excellent quality recordings using this system.

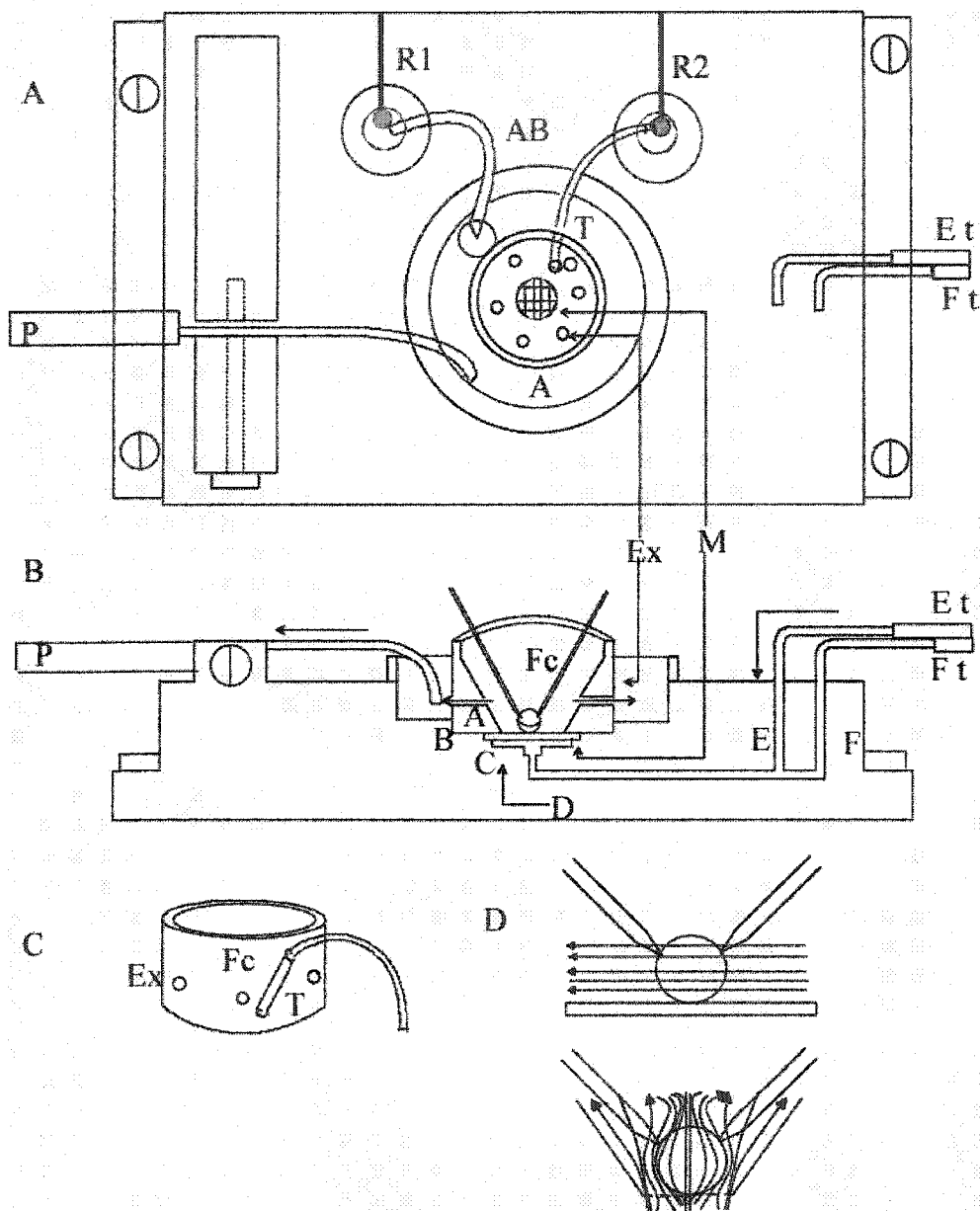


**Figure A2.1: A schematic diagram of *X. laevis* oocyte perfusion chamber.**

A-Top view, B- side view.

Fc: Funnel shaped chamber, Ex: Exit tube(s), T: Tunnel in the wall of funnel shaped chamber for the placement of Agar bridge, A: Outermost well, B: Middle well, C: Innermost well, M: Stainless mesh, D: Main inlet tube, E: Drug Inlet tube, F: Buffer inlet tube, Et: Tube connected to drug inlet, Ft: Tube connected to Buffer inlet, P: Drainage tube connected to vacuum suction, R1 and R2: Reference electrodes.

C- Funnel shaped inner chamber with an agar bridge in tunnel T is shown. AB: Agar bridge.

D- Solution flow in sideways vs. vertical flow chamber. Sideways solution flow is perpendicular to the placement of the electrodes; vertical flow follows the same direction as electrodes.

These connections are used for the manual operation of the system.

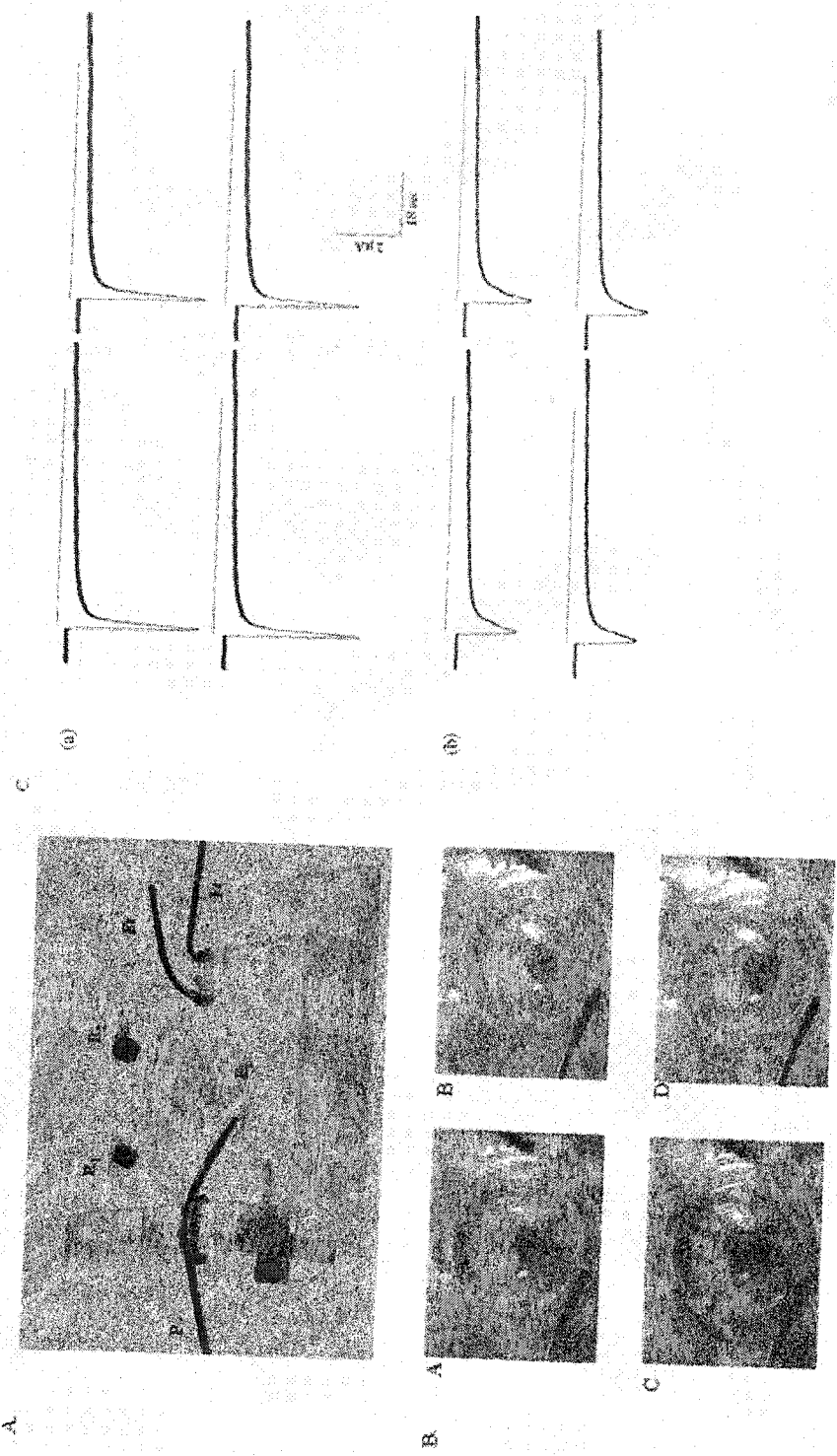


**Figure A2.2: The chamber design****A2.2.A The vertical flow chamber**

A photograph of the conical oocyte chamber with the agar bridges in position. Et: Tube connected to drug inlet, Ft: Tube connected to Buffer inlet, P: Drainage tube connected to vacuum suction, R1 and R2: Reference electrodes.

**A2.2.B An experiment demonstrating non-turbulent flow in the vertical flow system**

An oocyte was placed in the chamber without recording electrodes and sequentially perfused with buffer at a flow rate of 20 ml/min and with blue-dyed buffer at 25 ml/min (to simulate plain buffer and drug with buffer exposure). The sequential images were captured from a video recording of the experiment. All images clearly show an oocyte placed at the center of the recording chamber without recording electrodes. These sequential images are marked from A to D; A. Buffer flow at 20 ml/min B. No buffer flow C. Dyed buffer being perfused at 25ml/min D. Wash buffer being perfused at 20 ml/min after the dyed buffer flow. During the entire experiment, the oocyte absolutely retains its position.

**A2.2.C Inward currents elicited from a single oocyte using (a) the conventional chamber and (b) vertical-flow chamber, using 30 micromolar 5-HT.**

Results shown are representative of four different experiments. The traces marked as (a) were obtained from the vertical flow chamber while those marked with (b) were obtained with the conventional side-flow chamber. Experimental conditions including the chamber fluid volume, perfusion apparatus, recording buffer preparation, 5-HT solution, buffer, and drug flow rates, electrodes, agar bridges, 3M KCl solution, as well as the rest of the recording conditions were identical during use of both the conventional as well as the vertical flow chamber. Approximately half the rise times and double the maximal current amplitudes were obtained from the use of the vertical flow chamber as compared to the conventional side-flow chamber.



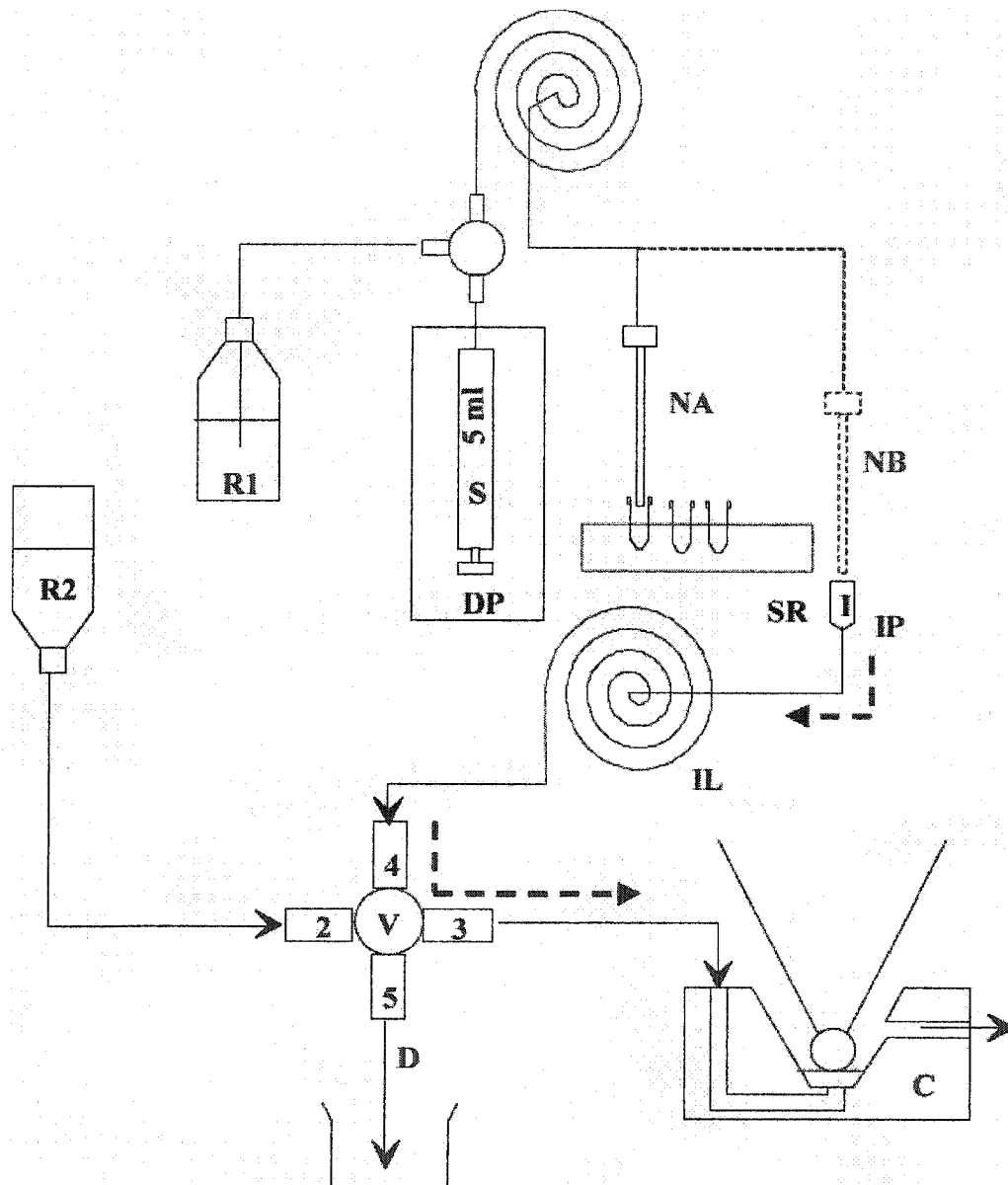


**Figure A2.3: The schematic arrangement of elements comprising the automated oocyte perfusion system.**

V: The injection valve of the sampler (controls the traffic of fluids), C: oocyte chamber with an oocyte impaled by two electrodes, S: A 5ml syringe mounted on the dilutor pump, DP: dilutor pump, R1: reservoir one, SR: sample rack, IP: injection port, N: needle, NA: needle position in default position (needle with solid line), NB: needle in load position (needle with dotted line), IL: injection loop, R2: Reservoir 2, D: drain tube draining into the waste receptacle. . Ports 2, 3, 4 and 5 of the valve V are also marked.

The solid arrows indicate flow of fluids when the injection valve is in the default position. Needle marked with dotted lines indicates its position during drug perfusion. Dotted arrows indicate the pathway of drug flow through the valves 4 and 3 in load position.

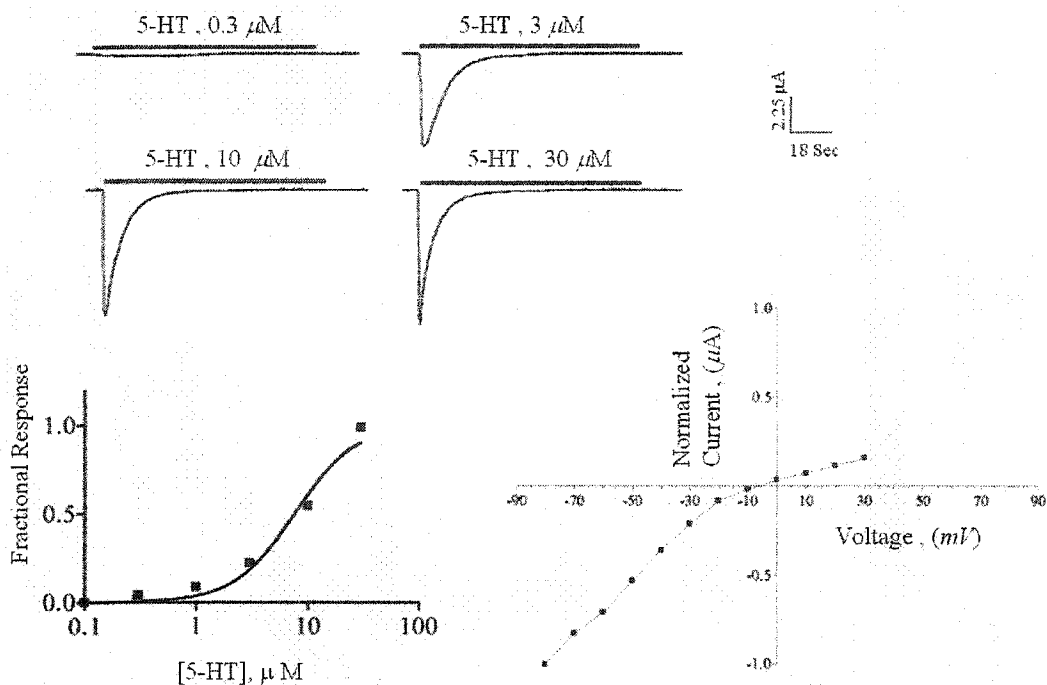


**Figure A2.4: Validation of the apparatus**

**A2.4.A Currents elicited by rapid application of various concentrations of 5-HT to *Xenopus laevis* oocytes expressing human 5-HT<sub>3AB</sub> receptors.**

The bar above each trace indicates the period of drug exposure. The traces recorded at higher concentrations (10 and 30  $\mu\text{M}$ ) characteristically show rapid onset with a sharp peak (10 to 90% of peak current within  $\sim 400\text{msec}$ ,  $n=6$ ), as well as multiphasic desensitization. The membrane potential was kept constant at  $-60\text{ mV}$ . Use of a smaller volume inner chamber (225  $\mu\text{l}$ ) leads to an rise time of 10-90% current in 250msec (data not shown).

**A2.4. B. Dose-response curves for 5-HT<sub>3AB</sub> R obtained from exposure to agonist 5-HT.**

Normalized current amplitudes were plotted against concentrations of serotonin (5-HT). Experiments were performed in triplicate. Error bars indicate  $\pm S.E.$  An  $EC_{50}$  value of  $7.6 \pm 0.46\ \mu\text{M}$  was obtained.

**A2.4.C. Current-voltage (I-V) relationship curve generated from oocytes expressing human 5-HT<sub>3A</sub> receptor.**

Currents were obtained by exposure of oocytes to 30  $\mu\text{M}$  5-HT at holding potentials ranging from  $-80$  to  $+30\text{ mV}$  in increments of  $+10\text{ mV}$ . The voltage steps were applied before the application of the agonist. The data shown is a composite of three experiments at each holding potential.

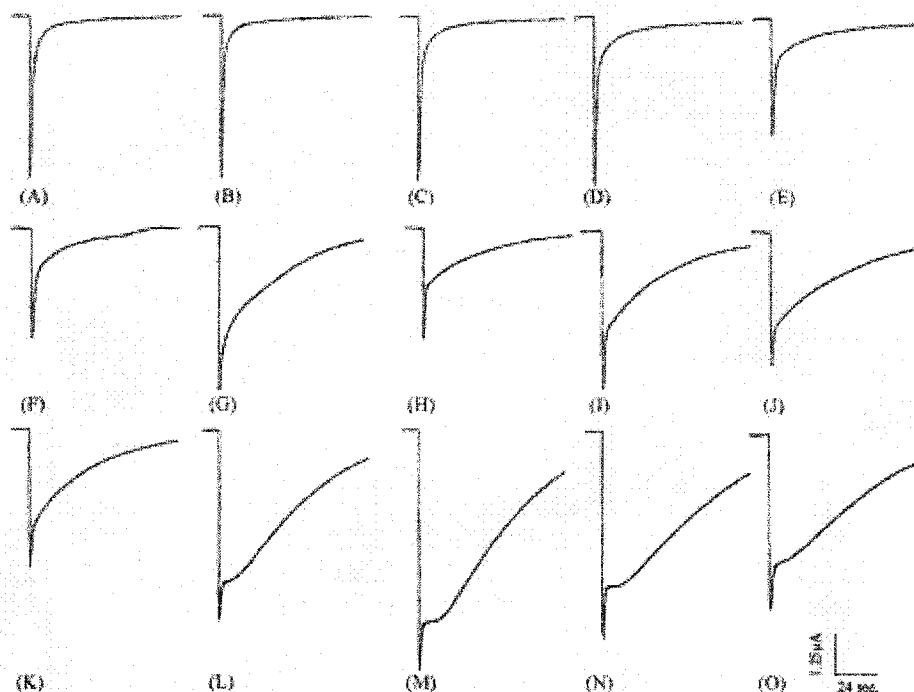


**Figure A2.5: 5-HT induced traces recorded from single oocyte expressing human 5-HT<sub>3A</sub>R, over a period of 10.5 hours.**

Traces were recorded by application of 30  $\mu$ M 5-HT to an oocyte expressing human 5-HT<sub>3A</sub>R, clamped at a holding potential of -60 mV. Traces are labeled from A to O (0 - 10.5 hrs). Traces shown are representative of two separate experiments. The oocyte was washed for 43 min (2 ml/min) between sequential 5-HT exposures. Gradual changes in the slow phase of desensitization can be observed beginning with trace D (at 135 minutes). The fast phase of desensitization in all the traces shows little change in characteristics. No changes in baseline current as well as response rise times were observed during the course of the 10.5 hours experiment.

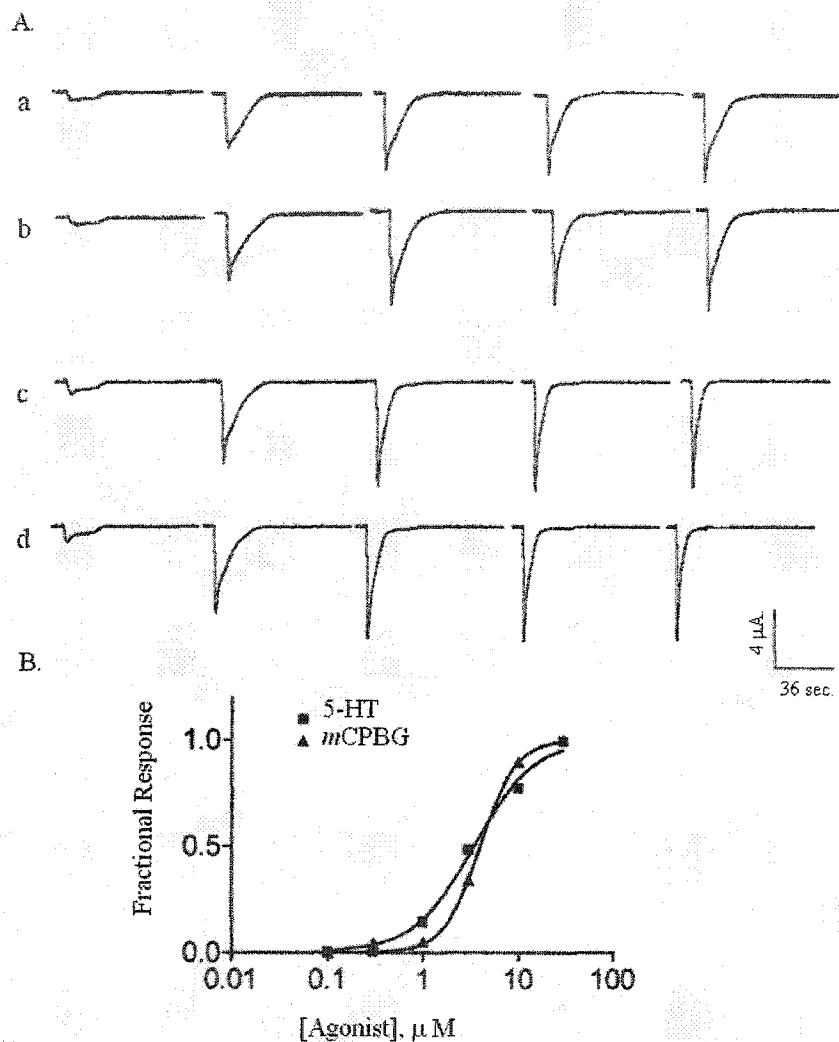


**Figure A2.6: Validation of the automated drug perfusion system**

**A2.6. A** Currents elicited from an oocyte expressing human 5-HT<sub>3A</sub> receptors by exposure to agonists 5-HT and mCPBG utilizing the automated oocyte perfusion system.

The traces show sequential exposure of increasing concentrations of 5-HT (1, 3, 10, 30, 100 μM). A and B represent traces recorded in that order. C and D show similar recordings performed utilizing increasing concentrations of mCPBG (1, 3, 10, 30, 100 μM). All the recordings were obtained from a single oocyte.

**A2.6. B Dose response relationship curves obtained from automated drug perfusion experiments (human 5-HT<sub>3A</sub>R).**

Data obtained from two different experiments was combined (n=4). EC<sub>50</sub> values: 5-HT;  $3.4 \pm 0.39 \mu\text{M}$ , *m*CPBG;  $4.0 \pm 0.2 \mu\text{M}$ . Hill coefficients: 5-HT; 1.4, *m*CPBG; 2.3.

## References

- Bertrand, D., B Buisson, R.M. Krause, H.Y Hu and S. Bertrand. Electrophysiology: a method to investigate the functional properties of ligand-gated channels., *J Recept Signal Transduct Res* 1997, *17*: 227-42.
- Davies, P.A., M. Pistis, M.C. Hanna, J.A. Peters, J.J. Lambert, T.G. Hales and E.F. Kirkness. The 5-HT<sub>3B</sub> subunit is a major determinant of serotonin-receptor function., *Nature* 1999, *397*: 359-63.
- Dubin, A.E., R. Huvar, M.R. D'Andrea, J. Pyati, J.Y. Zhu, K.C. Joy, S.J. Wilson, J.E. Galindo, C.A. Glass, L. Luo, M.R. Jackson, T.W. Lovenberg and M.G. Erlander. The pharmacological and functional characteristics of the serotonin 5-HT (3A) receptor are specifically modified by a 5-HT (3B) receptor subunit., 1999, *J Biol. Chem.* *274*: 30799-810.
- Jackson, M.B. and J.L. Yakel The 5-HT<sub>3</sub>-receptor channel., *Annu Rev Physiol* 1995, *57*:447-68.
- Koerner, J.F. and C.W Cotman. A microperfusion chamber for brain slice pharmacology. *J Neurosci. Methods* 1983, *7*: 243-51.
- Maricq, A.V, A.S Peterson, A.J. Brake, R.M. Myers and D Julius. Primary structure and functional expression of the 5HT<sub>3</sub> receptor, a serotonin-gated ion channel. 1991, *Science* *254*: 432-437.
- Yakel, J.L, Single amino acid substitution affects desensitization of the 5-hydroxytryptamin type 3 receptor expressed in *Xenopus* oocytes *Proc. Natl. Acad. Sci. USA*, 1993, vol. 90. pp. 5030-50338.
- Yakel JL, X.M. Shao, M.B. Jackson. Activation and desensitization of the 5-HT<sub>3</sub> receptor in a rat glioma x mouse neuroblastoma hybrid cell., *J Physiol* 1991, *436*: 293-308 .
- van Hooft JA, Kreikamp AP, Vijverberg HP. Native serotonin 5-HT<sub>3</sub> receptors expressed in *Xenopus* oocytes differ from homopentameric 5-HT<sub>3</sub> receptors. *J Neurochem.* 1997 Sep; *69*(3):1318-21.

**Appendix**

Acknowledgements: This work is supported by the National Science Foundation (NSF CAREER 9985077) and the American Heart Association (AHA 0151065B).